TR 94-106

THE DISSOCIATION OF AMMONIUM SALTS AND THEIR EFFECT ON THE PHYSIOLOGY AND BIOCHEMISTRY OF L-LYSINE SYNTHESIS BY *CORYNEBACTERIUM GLUTAMICUM* FP6

THESIS

Submitted in fulfilment of the
requirements for the Degree of
DOCTOR OF PHILOSOPHY
of RHODES UNIVERSITY

by

COLIN PETER KENYON

Department of Biochemistry and Microbiology
Rhodes University

January 1994

ABSTRACT

The availability and assimilation of NH_4^+ plays an integral role in the growth of microorganisms and the production of amino acids by these organisms. This study investigated the dissociation of NH_4^+ in aqueous solution, its availability and effect on the enzymes of NH_4^+ assimilation and its influence on lysine production by *Corynebacterium glutamicum*.

In aqueous solution the extent of dissociation of NH_4Cl, $(NH_4)_2SO_4$ and $(NH_4)_2HPO_4$ increases with decreasing concentration. A model is proposed for the dissociation of these molecules. It is believed that at very low concentrations, dissociation to NH_3 plus the respective counter-ions occurs. At these low concentrations the NH_3 acts as the substrate for glutamine synthetase. At the higher concentrations the dissociation is to NH_4^+ which is the substrate for glutamate dehydrogenase. At these higher concentrations the enzyme activities obtained for glutamate dehydrogenase, at equivalent concentrations of the above ammonium salts, were different when based on the total concentration of NH_4^+, and similar when based on the concentration of free NH_4^+.

L-lysine occurs in the +1 ionic form, at pH 7,2. The lysine which is produced during fermentation associates with the anionic counter-ion of the ammonium salt used. The concentration of the free NH_4^+ in the media appears to affect both the rate of lysine synthesis as well as the yield.

The lysine fermentation occurs in two stages; a growth (or replicative) phase, during which very little lysine is produced, and a lysine synthesis (or maturation) phase. During the lysine synthesis phase there is no cell replication, however an increase in the mass of the biomass produced is apparent. Evidence is provided for the possible concomitant synthesis of the of the cell wall polymer, glycerol teichoic acid, and lysine. On the basis of this evidence, a nucleotide balance is proposed for lysine and teichoic acid synthesis.

The replicative phase and the maturation phase have to be effectively separated to obtain optimal lysine yields and titres. It is believed that teichoic acid synthesis during the replicative phase must be kept to a minimum for optimal yields and titres to be obtained, and on completion of the cell wall and therefore teichoic acid synthesis, lysine synthesis ceases.

As the production of lysine appears to be affected by the NH_4^+ concentration in the culture media, it is proposed that a futile cycle may exist around the transport and assimilation of the NH_4^+. If the fermentations are run at low free NH_4^+ concentrations, it was shown that lysine yields of 0,66, on the glucose utilised, are attainable during the fermentation.

INDEX

		Page Nº
CHAPTER 1	GENERAL INTRODUCTION	
1.1	GENERAL INTRODUCTION	1
CHAPTER 2	DISSOCIATION OF $(NH_4)Cl$, $(NH_4)_2SO_4$ AND $(NH_4)_2HPO_4$, AND ITS IMPLICATION IN FERMENTATION CULTURE MEDIA AND THE AVAILABILITY OF NH_4^+ FOR BACTERIAL METABOLISM	
2.1	SUMMARY	5
2.2	INTRODUCTION	5
2.2.1	Theory of dissociation of electrolytes	5
2.2.2	Aspartokinase Enzyme	9
2.3	MATERIALS AND METHODS	10
2.3.1	Determination of pH	10
2.3.2	Determination of specific conductivity	10
2.3.3	Determination of aspartokinase activity	10
2.3.4	Effect of $(NH_4)_2SO_4$ on L-lysine fermentations	11
2.3.5	Analytical techniques	11
2.3.5.1	Biomass determination	11
2.3.5.2	Lysine determination	12
2.3.5.3	Glucose determination	12

2.4	RESULTS AND DISCUSSION	12
2.4.1	Dissociation of $(NH_4)_2SO_4$	12
2.4.2	Dissociation of $(NH_4)_2HPO_4$	27
2.4.3	Effect of NH_4^+ on aspartokinase activity	34
2.4.4	Effect of $(NH_4)_2SO_4$ concentration on fed-batch fermentation	39
2.5	CONCLUSION	41
CHAPTER 3	THE EFFECT OF THE FREE NH_4^+ AND ANIONIC COUNTER-ION CONCENTRATION ON LYSINE SYNTHESIS BY *CORYNEBACTERIUM GLUTAMICUM* FP6	
3.1	SUMMARY	45
3.2	INTRODUCTION	45
3.3	MATERIALS AND METHODS	46
3.3.1	Effect of NH_4Cl and $(NH_4)_2HPO_4$ on L-lysine fermentation	46
3.3.2	Analytical techniques	47
3.3.3	Dissociation of NH_4Cl and $(NH_4)_2HPO_4$	47
3.4	RESULTS AND DISCUSSION	48
3.4.1	Effect of NH_4Cl concentration on L-lysine synthesis	48
3.4.2	Effect of the $(NH_4)_2HPO_4$ concentration on lysine synthesis	53

3.5	CONCLUSION	66
CHAPTER 4	*CORYNEBACTERIUM GLUTAMICUM* CARBON MASS BALANCE TO LYSINE, BIOMASS AND CO_2: THE PROPOSED INFLUENCE OF CELL WALL SYNTHESIS	
4.1	SUMMARY	69
4.2	INTRODUCTION	69
4.2.1	Peptidoglycans	70
4.2.2	Polyolphosphate polymers (teichoic acids)	73
4.2.3	Synthesis of cell wall precursors	77
4.2.4	Peptidoglycan and teichoic acid synthesis	78
4.3	MATERIALS AND METHODS	81
4.3.1	Organism	81
4.3.2	Media and culture conditions	81
4.3.3	Analyses	82
4.3.3.1	Cell counts	82
4.3.3.2	Biomass	83
4.3.3.3	L-lysine	83
4.3.3.4	Glucose	83
4.3.3.5	Scanning electron microscopy	83
4.3.3.6	Transmission electron microscopy	84

4.3.4	Isolation and extraction of cell wall components	84
4.3.4.1	Isolation of soluble biomass fraction	84
4.3.4.2	Isolation and characterization of teichoic acid	84
4.4	RESULTS AND DISCUSSION	86
4.4.1	The possible existence of two distinct phases making up a cell cycle	86
4.4.2	Effect of the yeast extract concentration and the initial sugar feed rate on cell replication, maturation and lysine synthesis	91
4.4.2.1	Fermentation conditions	91
4.4.2.2	Data analysis	91
4.4.2.3	The effect of the glucose feed rate on fermentation	93
4.4.3	The identification of the storage material produced during the maturation phase	103
4.4.3.1	Soluble fraction of biomass	103
4.4.3.2	Characterization of the soluble fraction of biomass	105
4.4.3.3	Theoretical lysine yield taking cell wall synthesis into account	114
4.5	CONCLUSION	116

v/...

CHAPTER 5	AMMONIA ASSIMILATION, AMMONIA TRANSPORT, AMINO ACID METABOLISM AND FUTILE CYCLES	
5.1	SUMMARY	121
5.2	INTRODUCTION	121
5.2.1	Glutamine synthetase (GS)	122
5.2.2	Glutamate synthase enzyme	126
5.2.3	Amino acid utilization	127
5.2.4	Genetic regulation of glutamine synthetase, nitrogen regulation and the gln ALG operon	129
5.2.5	Transcription of glnALG operon	134
5.2.6	Regulation of the transport of amino acids and ammonia	137
5.2.6.1	Amino acid transport	137
5.2.6.2	Ammonia Transport	138
5.3	MATERIALS AND METHODS	142
5.3.1	Organism	142
5.3.2	Media and culture conditions	142
5.3.3	Enzyme assays	143
5.3.3.1	Glutamate dehydrogenase	143
5.3.3.2	Glutamine synthetase assay: (Determination of the iso activity point)	144

5.3.3.3	Glutamine synthetase: (Determination of the kinetic constants)	145
5.3.3.4	Glutamine synthetase: The effect of ammonia on the extent of adenylation of the enzyme	146
5.3.4	Analyses	146
5.3.4.1	Biomass	146
5.3.4.2	L-lysine	147
5.3.4.3	Glucose	147
5.3.4.4	Phosphate	148
5.4	RESULTS AND DISCUSSION	148
5.4.1.	Enzymes involved in ammonia assimilation	148
5.4.1.1	Glutamate dehydrogenase: coenzyme and substrate specificity	148
5.4.1.2	The effect of the ammonium salt and ammonium ion concentration on the activity of glutamate dehydrogenase	149
5.4.1.3	Glutamine synthetase: γ-glutamyl transferase and synthesis reaction activity	152
5.4.1.4	Kinetic constants of glutamine synthetase for its substrates	152
5.4.2	The effect of a limiting free NH_4^+ ion concentration on fermentation and L-lysine synthesis	155
5.4.3	The utilization of amino acids during fermentation	178

5.4.4 Phosphate utilization during fermentation 178

5.5 CONCLUSION 186

CHAPTER 6 GENERAL DISCUSSION

6.1 GENERAL DISCUSSION 189

LIST OF FIGURES

		Page Nº
1.1	The biosynthesis of L-lysine by bacteria	2
2.1	The effect of the $(NH_4)_2SO_4$ concentration on the on the conductivity in aqueous solution	13
2.2	Plot of molar conductivity versus the square root of the concentration	13
2.3	The effect of the $(NH_4)_2SO_4$ concentration on the pH and the change in the H^+ ion concentration	15
2.4	Effect of the $(NH_4)_2SO_4$ concentration on the specific conductivity arising from the H^+ ions and the "normal" dissociation at 20 deg C	17
2.5	Effect of the $(NH_4)_2SO_4$ concentration on the specific conductivity arising from the H^+ ions and the "normal" dissociation at 20 deg C and pH 7,0	17
2.6	Effect of the $(NH_4)_2SO_4$ concentration on the specific conductivity arising from the H^+ ions and the "normal" dissociation at 30 deg C	18
2.7	Effect of the $(NH_4)_2SO_4$ concentration on the specific conductivity arising from the H^+ ions and the "normal" dissociation at 30 deg C and pH 7,0	18
2.8	Effect of the $(NH_4)_2SO_4$ concentration on the fraction associated bivalent ion at 20 deg C and unadjusted pH. Data of Banks *et al* at 18 deg C	19
2.9	Effect of the $(NH_4)_2SO_4$ concentration on the fraction associated bivalent ion at 20 deg C and pH 7,0. Data	

of Banks *et al* at 18 deg C 19

2.10 Effect of the $(NH_4)_2SO_4$ concentration on the fraction associated bivalent ion at 30 deg C and unadjusted pH. Banks *et al* data at 18 deg C 20

2.11 Effect of the $(NH_4)_2SO_4$ concentration on the fraction associated bivalent ion at 30 deg C and pH 7,0. Banks *et al* data at 18 deg C 20

2.12 The effect of the $(NH_4)_2SO_4$ concentration on the molar conductivity at pH 7,0 and in an unadjusted solution at 20 deg C 21

2.13 The effect of the $(NH_4)_2SO_4$ concentration on the molar conductivity at pH 7,0 and in an unadjusted solution at 30 deg C 21

2.14 The effect of the $(NH_4)_2SO_4$ concentration on the molar conductivity at pH 7,0 and in an unadjusted solution at 20 deg C 22

2.15 The effect of the $(NH_4)_2SO_4$ concentration on the molar conductivity at pH 7,0 and in an unadjusted solution at 30 deg C 22

2.16 Debye-Hückel plot. Experimental data at 20 deg C and unadjusted pH and the data of Banks *et al* 1931 24

2.17 Debye-Hückel plot. Experimental data at 20 deg C and pH 7,0 and the data of Banks *et al* 1931 24

2.18 Debye-Hückel plot. Experimental data at 30 deg C and unadjusted pH and data of Banks *et al* 1931 25

2.19 Debye-Hückel plot. Experimental data at 30 deg C and pH 7,0 and data of Banks *et al* 1931 25

2.20	Effect of $(NH_4)_2SO_4$ concentration on the H ion concentration at 22,2 deg C	26
2.21	Effect of $(NH_4)_2SO_4$ concentration on the free NH_4 concentration and % of total NH_4 as unassociated NH_4 at 20 deg C and unadjusted pH	28
2.22	Effect of $(NH_4)_2SO_4$ concentration on the free NH_4 concentration and % of total NH_4 as unassociated NH_4 at 20 deg C and pH 7,0	28
2.23	Effect of $(NH_4)_2SO_4$ concentration on the free NH_4 concentration and % of total NH_4 as unassociated NH_4 at 30 deg C and unadjusted pH	29
2.24	Effect of $(NH_4)_2SO_4$ concentration on the free NH_4 concentration and % of total NH_4 as unassociated NH_4 at 30 deg C and pH 7,0	29
2.25	The effect of the $(NH_4)_2HPO_4$ concentration on pH	30
2.26	Effect of $(NH_4)_2HPO_4$ concentration on the specific conductivity arising from the H ions and the "normal" dissociation at 30 deg C	30
2.27	The effect of the $(NH_4)_2HPO_4$ concentration on the molar conductivity at 30 deg C	32
2.28	Effect of the $(NH_4)_2HPO_4$ concentration on the fraction associated bivalent ion at 30 deg C and unadjusted pH	32
2.29	Debye-Hückel plot for $(NH_4)_2HPO_4$	33
2.30	Effect of $(NH_4)_2HPO_4$ concentration on the free NH_4 concentration and % of total NH_4 as unassociated NH_4 at 30 deg C	33

2.31A	Effect of NH_4Cl and NH_4 concentration on the aspartokinase activity	35
2.31B	Lineweaver-Burk plot of the effect of NH_4 on aspartokinase activity	35
2.32	Effect of the NH_4Cl concentration on the specific conductivity arising from the H ions and the "normal" dissociation at 20 deg C	36
2.33	Effect of the NH_4Cl concentration on the specific conductivity arising from the H ions and the "normal" dissociation at 30 deg C	36
2.34	Effect of the NH_4Cl concentration on the pH and the change in H ion concentration with a change in NH_4Cl concentration at 20 deg C	37
2.35	Effect of the NH_4Cl concentration on the pH and the change in H ion concentration with a change in NH_4Cl concentration at 30 deg C	37
2.36	Effect of the NH_4Cl concentration on the free NH_4 concentration and the % of total NH_4 as unassociated NH_4 at 20 deg C	38
2.37	Effect of the NH_4Cl concentration on the free NH_4 concentration and the % of total NH_4 as unassociated NH_4 at 30 deg C	38
2.38	Effect of the NH_4Cl concentration on the molar conductivity at 20 deg C and unadjusted pH	40
2.39	Effect of the NH_4Cl concentration on the molar conductivity at 30 deg C and unadjusted pH	40
2.40	Effect of the $(NH_4)_2SO_4$ concentration on the	

xii/...

	fermentation by *C. glutamicum*. Initial $(NH_4)_2SO_4$ concentration 40g/l ending at 28,4g/l	42
2.41	Effect of the $(NH_4)_2SO_4$ concentration on the fermentation by C. glutamicum. $(NH_4)_2SO_4$ concentration maintained at 40 (g/l)	42
3.1	The effect of the NH_4Cl concentration on the lysine and biomass production. Final NH_4Cl concentration 9,45g/l	49
3.2	Sugar profiles during fermentation. Final NH_4Cl concentration 9,45g/l	49
3.3	The effect of the NH_4Cl concentration on the lysine and biomass production. Final NH_4Cl concentration 14,91g/l	50
3.4	Sugar profiles during fermentation. Final NH_4Cl concentration 14,91g/l	50
3.5	The effect of the total and free NH_4 concentration on lysine synthesis. Final NH_4Cl concentration 9,45g/l	51
3.6	The effect of the total and free NH_4 concentration on lysine synthesis. Final NH_4Cl concentration 14,91g/l	51
3.7	The effect of the $(NH_4)_2HPO_4$ concentration on the lysine and biomass production. Final $(NH_4)_2HPO_4$ concentration 0,0g/l	54
3.8	The effect of the total, residual and free NH_4 concentrations on lysine and biomass production. Final $(NH_4)_2HPO_4$ concentration 0,0g/l	54
3.9	Sugar profiles during fermentation. Final $(NH_4)_2HPO_4$ concentration 0,0g/l	55

3.10	The effect of the $(NH_4)_2HPO_4$ concentration on the lysine and biomass production. Final $(NH_4)_2HPO_4$ concentration 14,7g/l	56
3.11	The effect of the total, residual and free NH_4 concentrations on lysine and biomass production. Final $(NH_4)_2HPO_4$ concentration 14,7g/l	56
3.12	Sugar profiles during fermentation. Final $(NH_4)_2HPO_4$ concentration 14,7g/l	57
3.13	The effect of the $(NH_4)_2HPO_4$ concentration on the lysine and biomass production. Final $(NH_4)_2HPO_4$ concentration 17,0g/l	58
3.14	The effect of the total, residual and free NH_4 concentrations on lysine and biomass production. Final $(NH_4)_2HPO_4$ concentration 17,0g/l	58
3.15	Sugar profiles during fermentation. Final $(NH_4)_2HPO_4$ concentration 17,0g/l	59
3.16	The effect of the $(NH_4)_2HPO_4$ concentration on the lysine and biomass production. Final $(NH_4)_2HPO_4$ concentration 22,0g/l	60
3.17	The effect of the total, residual and free NH_4 concentrations on lysine and biomass production. Final $(NH_4)_2HPO_4$ concentration 22,0g/l	60
3.18	Sugar profiles during fermentation. Final $(NH_4)_2HPO_4$ concentration 22,0g/l	61
3.19	The effect of the $(NH_4)_2HPO_4$ concentration on the lysine and biomass production. Final $(NH_4)_2HPO_4$ concentration 25,6g/l	62

3.20	The effect of the total, residual and free NH_4 concentrations on lysine and biomass production. Final $(NH_4)_2HPO_4$ concentration 25,6g/l	62
3.21	Sugar profiles during fermentation. Final $(NH_4)_2HPO_4$ concentration 25,6g/l	63
3.22	The effect of the $(NH_4)_2HPO_4$ concentration on the lysine and biomass production. Final $(NH_4)_2HPO_4$ concentration 40,0g/l	64
3.23	The effect of the total, residual and free NH_4 concentrations on lysine and biomass production. Final $(NH_4)_2HPO_4$ concentration 40,0g/l	64
3.24	Sugar profiles during fermentation. Final $(NH_4)_2HPO_4$ concentration 40,0g/l	65
4.1	Model of Gram-positive cell wall	71
4.2	General structure of peptidoglycan	72
4.3	Glycerol and ribitol teichoic acids	74
4.4	Alanylglucosylribitol-5-phosphate of *Bacillus subtilis*	76
4.5	Biosynthesis of peptidoglycan in *B. subtilis* and *E. coli*	79
4.6	Change in the biomass, lysine and cell count during fermentation	87
4.7	Change in the total reactor biomass and cell count during fermentation	87
4.8A	The change in the cell wall morphology of	

xv/...

Corynebacterium glutamicum during fermentation as shown by transmission electron microscopy 88

4.8B The change in cell wall morphology of *Corynebacterium glutamicum* during fermentation as shown by scanning electron microscopy 89

4.9A The effect of the glucose feed rate during the replication phase on the biomass yield at the end of the replication phase 94

4.9A The effect of the glucose utilization rate during the replication phase on the biomass yield at the end of the replication phase 94

4.10A The effect of the glucose feed rate during the replication phase on the biomass titre at the end of the replication phase 95

4.10B The effect of the glucose utilization rate during the replication phase on the biomass titre at the end of the replication phase 95

4.11A The effect of the initial glucose feed rate on the lysine "yield", i.e. the lysine per glucose used during the replication phase. 96

4.11B The effect of the specific glucose utilization rate on the lysine "yield", i.e. the lysine per glucose used during the replication phase. 96

4.12A The effect of the initial glucose feed rate on the lysine yield during the maturation phase 97

4.12B The effect of the specific glucose utilization rate on the lysine yield during the maturation phase 97

4.13A	The effect of the initial glucose feed rate on the lysine titre	98
4.13B	The effect of the specific glucose utilization rate on the lysine titre	98
4.14A	The effect of the glucose feed rate on the biomass titre during the maturation phase	100
4.14B	The effect of the specific glucose utilization rate on the biomass titre during the maturation phase	100
4.15A	The effect of the glucose feed rate on the biomass yield during the maturation phase	101
4.15B	The effect of the initial glucose utilization rate on the biomass yield during the maturation phase	101
4.16	The effect of the specific glucose utilization rate on the "biomass" produced per mass of lysine during the maturation phase	102
4.17	The effect of the yeast extract concentration on the specific lysine yield and the lysine titre	102
4.18	Infrared spectrum of the CTAB extract	106
4.19	FAB mass spectrum of the CTAB extract	108
4.20	Hydrolysis of the CTAB extract with 0,05M NaOH at 65 deg C	109
4.21	Hydrolysis of the residual cell mass with 0,05M NaOH at 100 deg C	109
4.22	The effect of NaOH on the ethanol precipitable material from water washed cells	112

4.23	The structure of lysylglycerolphosphate	113
4.24	The biochemical pathways involved in lysine synthesis. Included is the proposed nucleotide balance, assuming that the process starts with 3 moles of glucose resulting in the synthesis of 2 moles of lysine	115
4.25	Fermentation profile indicating the change in the biomass, lysine and glucose concentration with time	117
4.26	The change in respiratory quotient and lysine yield during fermentation	117
4.27	The change in the moles CO_2 produced per mole lysine during the course of the fermentation	118
4.28	The change in biomass as teichoic acid) per mole of lysine produced and the lysine yield on glucose during fermentation	118
5.1	Plan view of the hexagonal arrangement of the subunits of a glutamine synthetase molecule from *Salmonella typhimurium*.	123
5.2A	Covalent modification of glutamine synthetase	125
5.3	Pathways by which the carbon skeletons of amino acids enter into the tricarboxylic acid cycle	128
5.5	Cyclic NH_3/NH_4^+ retention	140
5.6	Effect of the NH_4 arising from NH_4Cl, $(NH_4)_2SO_4$ and $(NH_4)_2HPO_4$ on the specific activity of glutamate dehydrogenase	150
5.7	Effect of the free NH_4 concentration arising from	

	NH_4Cl, $(NH_4)_2SO_4$ and $(NH_4)_2HPO_4$ on the specific activity of glutamate dehydrogenase	150
5.8	Lineweaver-Burk plot of the total NH_4 concentration versus activity	151
5.9	Lineweaver-Burk plot of the free NH_4 concentration versus activity	151
5.10	The isoactivity point of glutamine synthetase	153
5.11	The inhibition of the glutamyl transferase reaction of glutamine synthetase by magnesium	153
5.12	Activity of glutamine synthetase and its activation by the removal of NH_4 in whole cells	154
5.13A	The change in the concentration of biomass, lysine and glucose during fermentation	159
5.13B	Change in the lysine yield, the instantaneous yield and the free NH_4 concentration taken from the onset of the high glucose feed	159
5.14A	The change in the concentration of biomass, lysine and glucose during fermentation	160
5.14B	Change in the lysine yield, the instantaneous yield and the free NH_4 concentration taken from the onset of the high glucose feed	160
5.15A	The change in the concentration of biomass, lysine and glucose during fermentation	162
5.15B	Change in the lysine yield, the instantaneous yield and the free NH_4 concentration taken from the onset of the high glucose feed	162

5.15C	Change in the lysine yield, the instantaneous yield and the free NH_4 concentration taken from the onset of the second base pH control	163
5.16A	The change in the concentration of biomass, lysine and glucose during fermentation	164
5.16B	Change in the lysine yield, the instantaneous yield and the free NH_4 concentration taken from the onset of the high glucose feed	164
5.16C	Change in the lysine yield, the instantaneous yield and the free NH_4 concentration taken from the onset of the second base pH control	164
5.17A	The change in the concentration of biomass, lysine and glucose during fermentation	166
5.17B	Change in the lysine yield, the instantaneous yield and the free NH_4 concentration taken from the onset of the high glucose feed	166
5.17C	Change in the lysine yield, the instantaneous yield and the free NH_4 concentration taken from the onset of the second base pH control	167
5.18A	The change in the concentration of biomass, lysine and glucose during fermentation	169
5.18B	Change in the lysine yield, the instantaneous yield and the free NH_4 concentration taken from the onset of the high glucose feed	169
5.18C	Change in the lysine yield, the instantaneous yield and the free NH_4 concentration taken from the onset of the second base pH control	170

5.19A	The change in the concentration of biomass, lysine and glucose during fermentation	171
5.19B	Change in the lysine yield, the instantaneous yield and the free NH_4 concentration taken from the onset of the high glucose feed	171
5.19C	Change in the lysine yield, the instantaneous yield and the free NH_4 concentration taken from the onset of the second base pH control	172
5.19D	Change in the percent deadenylation of glutamine synthetase during fermentation	172
5.20A	The change in the concentration of biomass, lysine and glucose during fermentation	173
5.20B	Change in the lysine yield, the instantaneous yield and the free NH_4 concentration taken from the onset of the high glucose feed	173
5.20C	Change in the lysine yield, the instantaneous yield and the free NH_4 concentration taken from the onset of the second base pH control	174
5.20D	Change in the percent deadenylation of glutamine synthetase during fermentation'	174
5.21A	The change in the concentration of biomass, lysine and glucose during fermentation	176
5.21B	Change in the lysine yield, the instantaneous yield and the free NH_4 concentration taken from the onset of the high glucose feed	176
5.21C	Change in the lysine yield, the instantaneous yield and the free NH_4 concentration taken from the onset	

xxi/...

	of the second base pH control	177
5.21D	Change in the percent deadenylation of glutamine synthetase during fermentation	177
5.22A	The change in the concentration of biomass, lysine and glucose during fermentation	179
5.22B	Change in the lysine yield, the instantaneous yield and the free NH_4 concentration taken from the onset of the high glucose feed	179
5.22C	Change in the lysine yield, the instantaneous yield and the free NH_4 concentration taken from the onset of the second base pH control	180
5.22D	The change in the oxygen utilization rate, carbon dioxide evolution rate and the respiratory quotient during fermentation	180
5.23A	The change in the concentration of biomass, lysine and glucose during fermentation	181
5.23B	Amino acid profile during fermentation H	181
5.23C	Amino acid profile during fermentation H	182
5.23D	Amino acid profile during fermentation	182
5.24A	The change in the concentration of biomass, lysine and glucose during fermentation	183
5.24B	Amino acid profile during fermentation I	183
5.24C	Amino acid profile during fermentation I	184
5.24D	Amino acid profile during fermentation	184

5.25	The change in the concentration of the biomass, lysine, phosphate and glucose during fermentation	185
5.26	The effect of the free NH_4^+ concentration on lysine synthesis and subsequent transfer to the culture media	187
6.1	The model for lysine synthesis	192
6.2	The effect of the free NH_4^+ concentration on lysine synthesis and subsequent transfer to the culture media	194
6.3	Model of the induction of glutamine synthetase at various concentrations of NH_4^+ and glucose	196
6.4	Model of the induction of glutamine synthetase under conditions of NH_4^+ and glucose limitation	198

xxiii/.

ACKNOWLEDGEMENTS

My sincere appreciation and gratitude are expressed to the members of Process Biochemistry Group, AECI, for their support and assistance.

I would like to thank Mr Frank Fisher and Dr Roger Jones for their encouragement over the years.

My sincere thanks go to Professor John Duncan for his support and encouragement.

I am grateful to Mrs Sue Warren for her assistance and patience with the word processing.

To my wife Carol, your support and understanding over the years was invaluable. I would like to thank my family, Carol, Amy, Monique and David, for the time they gave to allow me to do this thesis.

CHAPTER 1

GENERAL INTRODUCTION

1.1 GENERAL INTRODUCTION

Since the discovery of monosodium glutamate as a seasoning agent by Kikunae Ikeda in 1908 there has been a steady increase in the demand for monosodium glutamate as well as an expansion into the manufacture of other amino acids (Aida, 1986). Initially all amino acids were obtained by the acid hydrolysis of proteins obtained from grain, such as gluten, or by the hydrolysis of soybean protein. In 1957 two groups reported that L-glutamate could be synthesized into the culture broth by bacteria. The groups were those of Kinishita *et al* and Asai *et al*. Surprisingly both groups found that the monosodium glutamate was produced by microorganisms of the genus *Micrococcus*. During the 1960s basic and applied research was carried out on the biochemistry and regulation of the synthesis of not only monosodium glutamate, but all the other amino acids.

Since poultry and pigs are unable to synthesize a number of amino acids, including L-lysine (lysine), these must be added to their foodstuffs to provide an adequate diet. This is usually done by using grain, fish meal and defatted oil seeds. However one of the first limiting nutrients in a typical diet remains lysine, and to balance the feed additional lysine is added. This is produced commercially via two biotechnology processes. These employ either direct fermentation using bacteria, or the enzymatic conversion of DL-α-amino-ϵ-caprolactam into L-lysine (Tosaka *et al*, 1983). The direct fermentation processes, using various carbohydrate sources such as starch hydrolysates, molasses or various sugar syrups as the substrates, have become firmly established as the major methods for producing lysine. The development of better strains of microbe by mutant selection programmes has had a major impact on the economics of the fermentation process. The two types of mutants produced which had the most significant impact on the overproduction of lysine are the auxotrophic mutants and the regulatory mutants.

The pathway for the biosynthesis of lysine in bacteria was first reported by Gilvarg *et al* (1963) using a coliform bacteria from the genus *Enterobacteriaciae* (Figure 1.1). Misano and Soda (1980) showed the presence of diaminopimelate dehydrogenase as an alternative route to

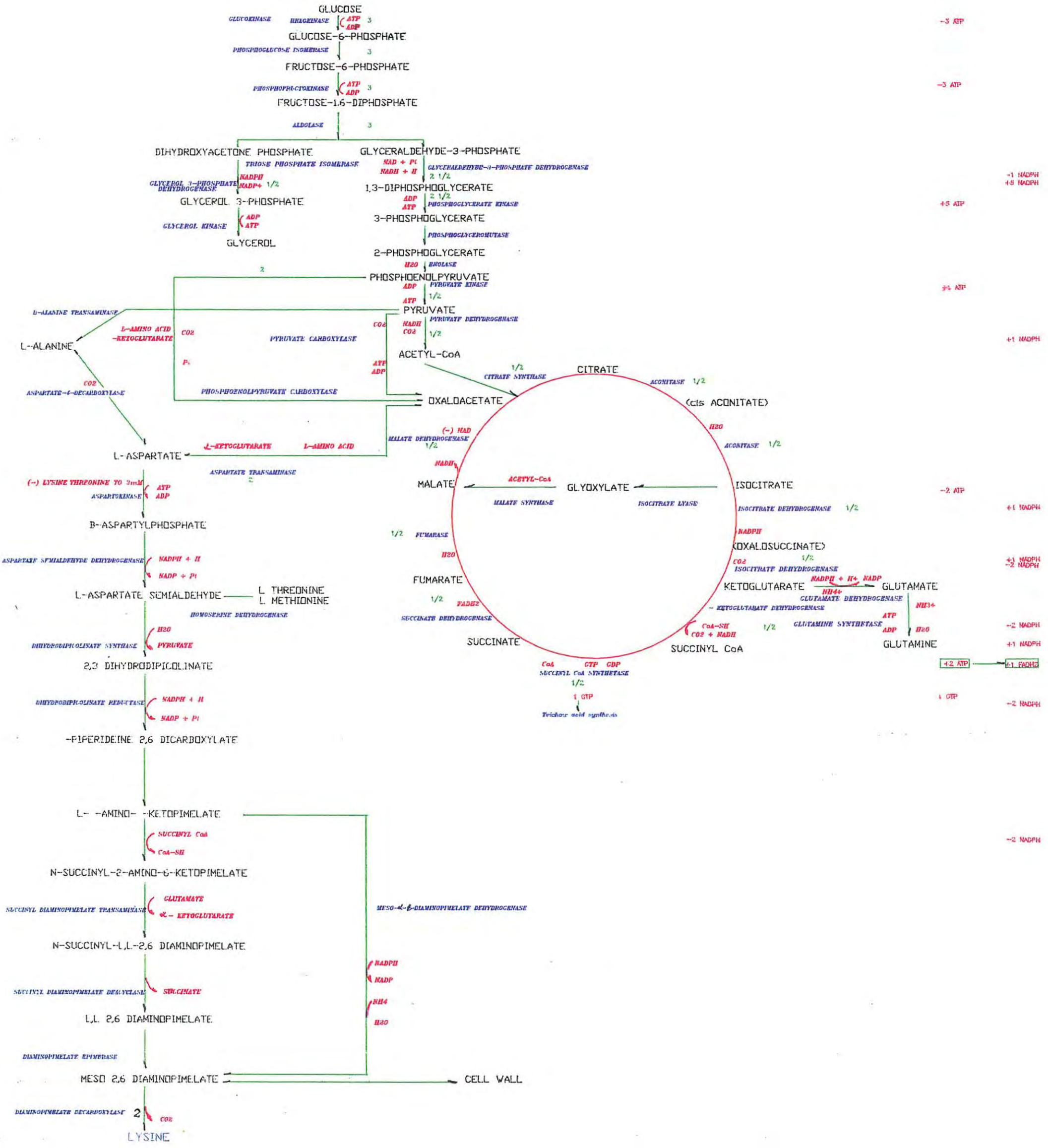

FIGURE 1.1 The biosynthesis of L-lysine by bacteria.

meso-diaminopimelate. This was also found to be the case in *Corynebacterium glutamicum* (Ishino *et al*, 1984).

Lysine was the first amino acid to be produced on an industrial scale with the aid of auxotrophic mutants, when the homoserine-requiring auxotrophic mutant of *Corynebacterium glutamicum* was derived (Kinoshita *et al*, 1958). The *Micrococcus* which was originally used for the production of monosodium glutamate was subsequently renamed *Corynebacterium glutamicum*. It was found that in both *Corynebacterium* and *Brevibacterium* the enzyme aspartokinase catalyses the first step in the synthesis of lysine and threonine from aspartic acid. It was also shown that this reaction is subject to concerted feedback inhibition by lysine plus threonine. The isolation of a threonine-methionine double auxotroph of *Brevibacterium flavum* gave an organism producing similar amounts of lysine (Shiio and Sano, 1969). However unlike *Escherichia coli* which may have as many as 3 isoenzymes of aspartokinase (Cohen, 1969), the *Corynebacteria* and *Brevibacteria* have no isoenzymes (Tosaka and Takinami, 1986).

Another effective technique in the isolation of mutants for the overproduction of lysine is the selection of regulatory mutants which are insensitive to feedback inhibition or repression. With the *Corynebacteriaceae* only having one enzyme catalysing the phosphorylation of aspartate, and therefore no isoenzymes, the selection of regulatory mutants of aspartokinase with no concerted feedback inhibition was thus simpler than it would have been had *Escherichia coli* been used. These aspartokinase regulatory mutants in aspartokinase were obtained by the selection for resistance to inhibition of growth by compounds such as the lysine analogue, *S*-(2-aminoethyl) L-cysteine (AEC) (Sano and Shiio, 1970). Other analogues used were α-chlorocaprolactam (Kubota *et al*, 1976) and γ-methyl-L-lysine (Tosaka *et al*, 1981).

Alternative regulatory mutants which were selected for, could be categorised as mutants with an altered carbon flux through the various pathways. During lysine synthesis there are other metabolic pathways which are functional. The selection of these regulatory mutants supposedly ensures that there is optimum carbon flux to lysine and all

the other pathways which will ensure cell viability. The β-fluoropyruvate sensitive mutants fall into this category (Tosaka *et al*, 1981). In these mutants the pyruvate dehydrogenase is more sensitive to inhibition by the pyruvate analogue, β-fluoropyruvate. The carbon flux in these mutants is supposedly redirected towards oxaloacetate, which is then transaminated to give aspartate and therefore lysine. This however does not take account of the nucleotide balance required for lysine synthesis.

A fact which becomes increasingly evident on reviewing all the literature on lysine synthesis for commercial purposes, is the lack of research which has been reported on the assimilation of ammonia to enable lysine synthesis to occur. This includes research both on the fundamental biochemistry of ammonia assimilation in the *Corynebacteriaciae*, as well as on the cell physiology during lysine synthesis via fermentation. This study was therefore undertaken to determine some of the aspects of ammonia assimilation in the physiology of *Corynebacterium glutamicum* FP6 during fermentation. Some of the fundamentals of the biochemistry of ammonia assimilation were also investigated to ascertain which possible mechanisms are used by the organism. The organism used was *Corynebacterium glutamicum* FP6 obtained from the Council for Scientific and Industrial Research, Pretoria, Republic of South Africa (Watson, 1989). The genetic characteristics of the organism are *Corynebacterium glutamicum* Hse^- Leu^- FP^S.

CHAPTER 2

DISSOCIATION OF NH_4Cl, $(NH_4)_2SO_4$ AND $(NH_4)_2HPO_4$, AND ITS IMPLICATION IN FERMENTATION CULTURE MEDIA AND THE AVAILABILITY OF NH_4^+ FOR BACTERIAL METABOLISM

2.1 SUMMARY

Using the Debye-Hückel theory and conductivity analysis, the dissociation of $(NH_4)_2SO_4$ was determined in aqueous solution and it was proposed that as the concentration of $(NH_4)SO_4$ tends towards infinite dilution, the dissociation may be expressed by the following model:

$$2NH_3 + 2H^+ + SO_4^{--}:NH_3 + NH_4^+ + HSO_4^-:2NH_4^+ + SO_4^{--}:NH_4^+ + NH_4SO^-_4:(NH_4)_2\ SO_4$$

Infinite dilution

This was compared to the dissociation of $(NH_4)_2HPO_4$ and NH_4Cl. On determining the effect of the NH_4^+ concentration on activity of the enzyme aspartokinase, maximal activity was found to occur at a concentration of 150mM. By determining the degree of dissociation of $(NH_4)_2SO_4$, a concentration of 40g/l $(NH_4)_2SO_4$ yields a free NH_4^+ concentration of approximately 150mM. This is the standard fermentation concentration for $(NH_4)_2SO_4$ for *Corynebacterium glutamicum*. The low free NH_4^+ concentration is as a result of more than 60% of the bivalent ion being associated at this concentration. A reduction in the NH_4^+ concentration as a result of the dilution of the broth by the fed-batch fermentation feed pattern was found to significantly affect the productivity of the fermentation. As the NH_4^+ is taken up in bacterial cells by active transport the maximum intracellular concentration which is attainable can exceed the extracellular dissociated concentration. However at low concentrations the NH_3 may not be available for assimilation.

2.2 INTRODUCTION

2.2.1 Theory of dissociation of electrolytes

The dissociation of salts in aqueous culture media is of interest, as it affects not only the water activity of the culture media, but also the availability of ions for metabolism and the concentration of ions which act in association with most enzymes. Many of these ions are stimulatory to enzyme activity. They also have the effect of being thermoprotective to enzymes and protecting the enzyme from changes in water activity.

Of concern in this study is that during the manufacture of L-lysine by fermentation, a major constituent of the culture media is $(NH_4)_2SO_4$. The extent of dissociation of the $(NH_4)_2SO_4$ is of interest as it not only acts as the source of NH_4^+ for lysine synthesis, but the NH_4^+ has a stimulatory effect on key enzymes in the synthesis of L-lysine, namely aspartokinase, glutamate dehydrogenase and glutamate synthetase.

The association of the ions of a uni-bivalent salt takes place in two stages (Righellato and Davies, 1930):

$$M^+ + A^{--} \rightleftarrows MA^- \; ; \; M^+ + MA^- \rightleftarrows M_2A$$

At low concentrations where the extent of the association is small, the second stage may be disregarded and the solution contains only three species, M^+, A^{--} and MA^-.

According to Kohlrausch's law, the relationship between the molar conductivity of a solution and the concentration of a completely dissociated salt is given by the equation (Glasstone and Lewis,1978):

$$\Lambda = \Lambda o - a\sqrt{c} \qquad 1.$$

where Λ = molar conductivity, $\Omega^{-1}.cm^2.mol^{-1}$
Λo = limiting equivalent conductivity
a = constant for the salt
c = concentration

This equation only applies to very dilute solutions, as at higher concentrations the linearity in the relationship between molar conductivity and the square root of the concentration is lost. In these cases the conductance is less than required by the theory, and it appears that not all the ions are available for the carrying of current. This is the fraction α, called the degree of dissociation of the electrolyte, which is defined as "the fraction of solution which is dissociated into ions that are free to carry current at a given concentration" (Glasstone and Lewis, 1978).

According to Debye-Hückel-Onsager theory equation 1 then becomes:

$$\Lambda = \alpha[\Lambda o - (A + B\Lambda o)\sqrt{\alpha C}] \qquad 2.$$

where A and B are constants for a given solvent that depend only on the temperature. For water at 25°C, A is 60,20 and B is 0,229.

It was therefore decided to use the theory of electrolytic conduction as a means of determining the degree of dissociation of $(NH_4)_2SO_4$ in aqueous solution and consequently the concentration of free NH_4^+ in solution and its possible effect on fermentation and lysine synthesis. However to use the theory of electrolytic conduction one should be capable of:

a) predicting the value of the limiting molar conductivity, Λ_o
b) predicting the value of the constants
c) accounting for the deviations from equation 1 at the higher concentrations (Robinson and Stokes, 1970)

In the state of infinite dilution to which Λ_o refers, the motion of an ion is limited by its interactions with the surrounding solvent molecules and not by any other ions within a finite distance (Robinson and Stokes, 1970). In other words, at infinite dilution each species of ion present contributes a definite amount to the total molar conductivity, regardless of the nature of the other ions present. Thus for an electrolyte having two ions:

$$\Lambda_o = \lambda^+ + \lambda^- \qquad 3.$$

when λ^+ and λ^- are the limiting molar conductivities of the ions. These values are calculated by the measurement of transport numbers.

On this basis, the limiting equivalent conductivity of an $(NH_4)_2SO_4$ solution dissociates into its various ions as follows:

$$(NH_4)_2SO_4 \rightarrow NH_4SO_4^- + NH_4^+ \quad 4.$$

$$NH_4SO_4^- \rightarrow NH_4^+ + SO_4^{--} \quad 5.$$

Therefore the total molar conductivity may be calculated from:

$$\Lambda_o = 2\lambda_{NH_4^+} + \lambda_{SO_4^{--}} + \lambda_{NH_4SO_4^-} \quad 6.$$

The data for the NH_4^+ and SO_4^{--} ions are obtained from the literature (Robinson and Stokes, 1970). Righellato and Davies (1930) claim that the value for the intermediate ion should be taken to be 60% of the anion. The following limiting molar conductivity was therefore obtained at 30°C:

$$2 \times 77{,}051 + 80{,}342 + 48{,}205 = 282{,}65 \Omega^{-1}.cm^2.mol^{-1} \text{ at } 30°C$$

At 20°C the limiting molar conductivity is $237{,}07 \Omega^{-1}.cm^2.mol^{-1}$.

These values are calculated from the data of Robinson and Stokes (1970) (Appendix 1). To calculate the fraction of bivalent radical, namely α, which exists in solution as the intermediate ion at different concentrations of $(NH_4)_2SO_4$, and assuming the dissociation as in equations 4 and 5, the following equation is used:

$$\Lambda = \alpha\lambda NH_4SO_4^- + (1 - \alpha)\lambda SO_4^{--} + (2 - \alpha)\lambda NH_4^+ \quad 7.$$

The values of Λ are obtained experimentally by determining the specific conductivity of various concentrations of $(NH_4)_2SO_4$ in aqueous solution and then determining the molar conductivity.

The ionic strength (μ) of the solution is calculated from (Gladstone and Lewis, 1978):

$$\mu = {}^1/_2(m_+Z^2 + m_-Z^2) \quad 8.$$

where m = concentration of the ion (moles)
Z = corresponding valency

9/...

The "Ostwald" constant k' was obtained from:

$$k' = \frac{m_{SO_4^{2-}} \times m_{NH_4^+}}{m_{NH_4SO_4^-}} \qquad 9.$$

This is incorporated into the Debye-Hückel equation:

$$\log K = \log k' - 2\sqrt{\mu} + \Sigma B\mu \qquad 10.$$

to become:

$$\log K = (\log \frac{m_{SO_4^{2-}} \times m_{NH_4^+}}{m_{NH_4SO_4^-}} - 2\sqrt{\mu}) + \Sigma B\mu \qquad 11.$$

A plot of the expression in parentheses against μ should give a straight line of slope ΣB. This is provided that no further dissociation occurs as this should be linear.

2.2.2 Aspartokinase enzyme

The first enzyme in the synthesis of the aspartate family of amino acids is aspartokinase [ATP:L-aspartate 4-phosphotransferase, EC 2.7.2.4], (Black and Wright, 1955), which catalyses the reaction:

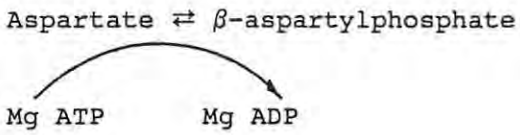

Many enzymes catalysing phosphoryl transfer and elimination reactions are activated by monovalent cations. This catalytic activity is often markedly specific for the cation used (Shaw *et al*, 1983). Shaw *et al* (1983) found that the aspartokinase in *E. coli* B is highly specific and absolutely dependent on K^+ or NH_4^+ for the ADP-ATP exchange reaction.

2.3 MATERIALS AND METHODS

2.3.1 Determination of pH

The pH of aqueous solutions of varying concentrations of $(NH_4)_2SO_4$, $(NH_4)_2HPO_4$ and NH_4Cl was determined using a Jenway 3020 pH meter.

2.3.2 Determination of specific conductivity

Conductivity measurements were determined for solutions of varying concentrations of $(NH_4)_2SO_4$, $(NH_4)HPO_4$ and NH_4Cl using a Metrohm 660 conductometer. The specific conductivity was then converted to the molar conductivity by dividing by the equivalent molar concentration. The conductivities were measured at 20°C and 30°C at pH 7,0 and at the same temperatures in solutions with unadjusted pH levels.

All solutions were prepared in nano-pure water using a Milli-Q^R water system (Millipore, Inc).

2.3.3 Determination of aspartokinase activity

The aspartokinase activity was determined by a modified method of Black and Wright (1955). All the reagents were prepared in 0,05M Tris base (pH 7,5) containing 30mM mercaptoethanol to the following concentrations (mmoles/l): ATP 8mmoles; MgSO4 8mmoles; aspartic acid 8mmoles; and hydroxylamine hydrochloride to the same molar concentration as the NH_4Cl requirement. The hydroxylamine hydrochloride solution was then neutralized with NH_4OH to get the required NH_4Cl concentration. The assay was carried out at 25°C and pH 7,5 using duplicate samples. The enzyme solution was prepared from *Corynebacterium glutamicum* FP6. Cultures were aerobically grown in TNIY media (Appendix I) for 24 hours. The cells were harvested by centrifugation (35 000 x g, 10 minutes) and then washed twice in phosphate buffer (0,1M, pH 6,8). After the final wash, the cells were resuspended in phosphate buffer with 0,001M mercaptoethanol.

The partial purification of the enzyme was carried out at 4°C. The harvested cells were disrupted by sonic oscillation using a Branson

Sonicator at the highest intensity for twenty cycles of 480 seconds each with cooling between cycles. The suspension of broken cells was centrifuged (35 000 x 5, 20 minutes). The nucleic acids were removed from the supernatant (crude extract) by the slow addition of streptomycin sulphate (10% of an 11% w/v solution). After 30 minutes of continual stirring on ice, the suspension was centrifuged (35 000 x g, 20 minutes). The supernatant was adjusted to a 50% level of saturation with ammonium sulphate. The extract was then centrifuged (35 000 x g, 20 minutes) and the pellet was resuspended in phosphate buffer (0,1M, pH 6,8) containing 0,001M mercaptoethanol. This cycle was repeated for the 60% and 70% levels of saturation of ammonium sulphate.

The assay was run on two separate enzyme preparations and similar results were obtained from both. The reaction was stopped by the addition of 3ml of 0,7N HCl containing 3,3% trichloroacetic acid and 16,66% $FeCl_3.6H_2O$. After centrifugation the resulting ferric hydroxamate complex was measured spectrophotometrically at 540nm. The activity was then expressed as µmoles ferric hydroxamate complex formed per minute per mg protein, using a molar extinction coefficient of 600.

2.3.4 Effect of $(NH_4)_2SO_4$ on L-lysine fermentations

Fermentations were carried out to produce L-lysine using *Corynebacterium glutamicum* FP6 using the culture media as outlined in Appendix I. The inoculum for the fermentation was initiated on LM agar and then transferred to TNIY inoculum broth, containing sucrose of the same constituents as outlined in Appendix I. This inoculum was then transferred to the prefermenter stage of media composition as outlined in Appendix I. The inocula volumes were all 10% of the subsequent stage.

2.3.5 Analytical techniques

2.3.5.1 Biomass determination

The biomass was determined gravimetrically by centrifuging 10ml of sample at 1 000 x g and drying the biomass to constant mass at 105°C. Biomass samples were not washed due to the loss of key constituents such as

proline and teichoic acid. This will become clearly evident in all subsequent chapters.

2.3.5.2 Lysine determination

The L-lysine was determined during the fermentation by the modified Autotag method of Millipore Corporation (Waters Technical Bulletin, 1989), as outlined in Appendix II. The fermentation broth was centrifuged at 10 000 x g and the supernatant used for analysis.

2.3.5.3 Glucose determination

The glucose was determined in the fermentation broth by HPLC as outlined in Appendix II. The samples were centrifuged as in section 3.4.1.2.

2.4 RESULTS AND DISCUSSION

2.4.1 Dissociation of $(NH_4)_2SO_4$

The data obtained for the effect of $(NH_4)_2SO_4$ concentration on the molar conductivity at 20°C was similar to that of Banks *et al* (1937) at 25°C (Figure 2.1). The data does not however fit the Debye-Hückel theory, as the relationship between the molar conductivity and the square-root of the concentration is not linear as defined by equation 1 (Figure 2.2).

It is also evident from the experimental data that at the low concentrations, high molar conductivities are obtained. To account for this a further dissociation of the $(NH_4)_2SO_4$ is therefore proposed:

$$2NH_3 + H^+ + HSO_4^- \rightarrow 2NH_4^+ + SO_4^{--} \rightarrow (NH_4)_2SO_4$$

In other words, as the $(NH_4)_2SO_4$ concentration tends towards infinite dilution the degree of dissociation increases and the high equivalent conductivities which are not accounted for by the theory, as outlined by the dissociation (equations 4 and 5), may be accounted for by the higher mobility and equivalent conductivity of the H^+ ion. This should also account for the higher limiting molar conductivity at infinite dilution,

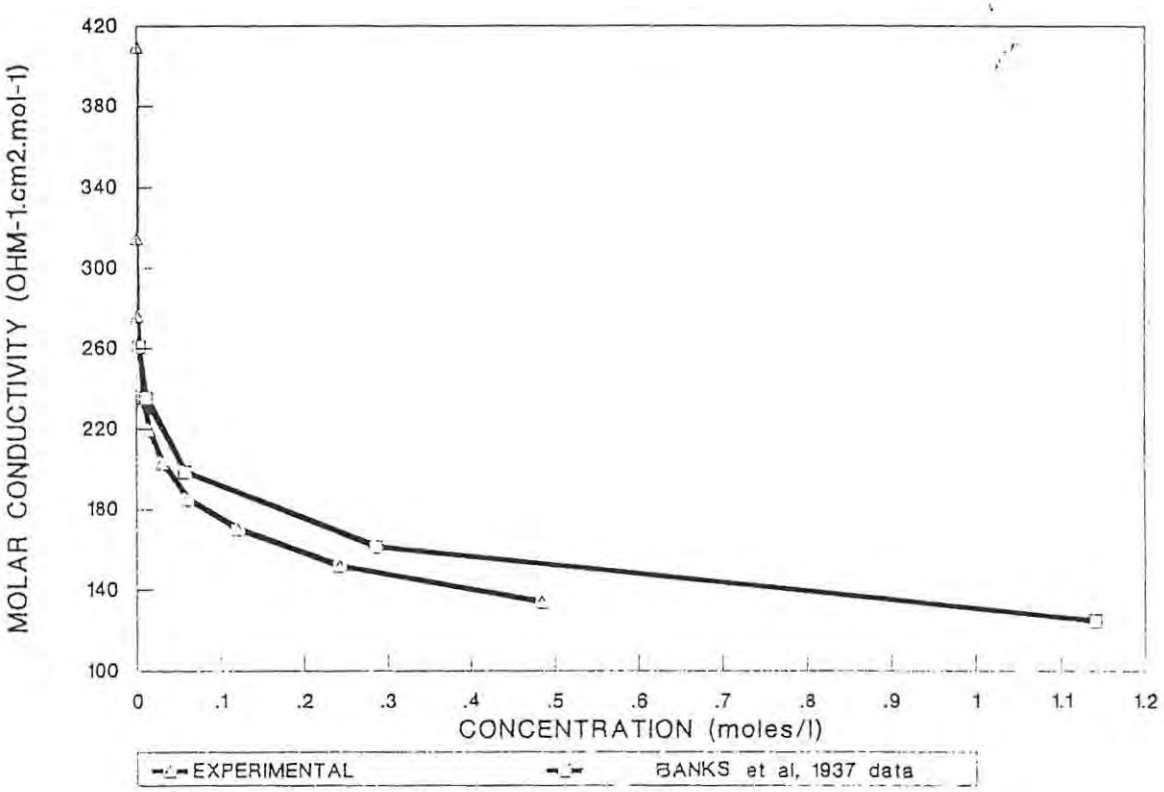

FIGURE 2.1 The effect of the (NH4)2SO4 concentration on the conductivity in aqueous solution.

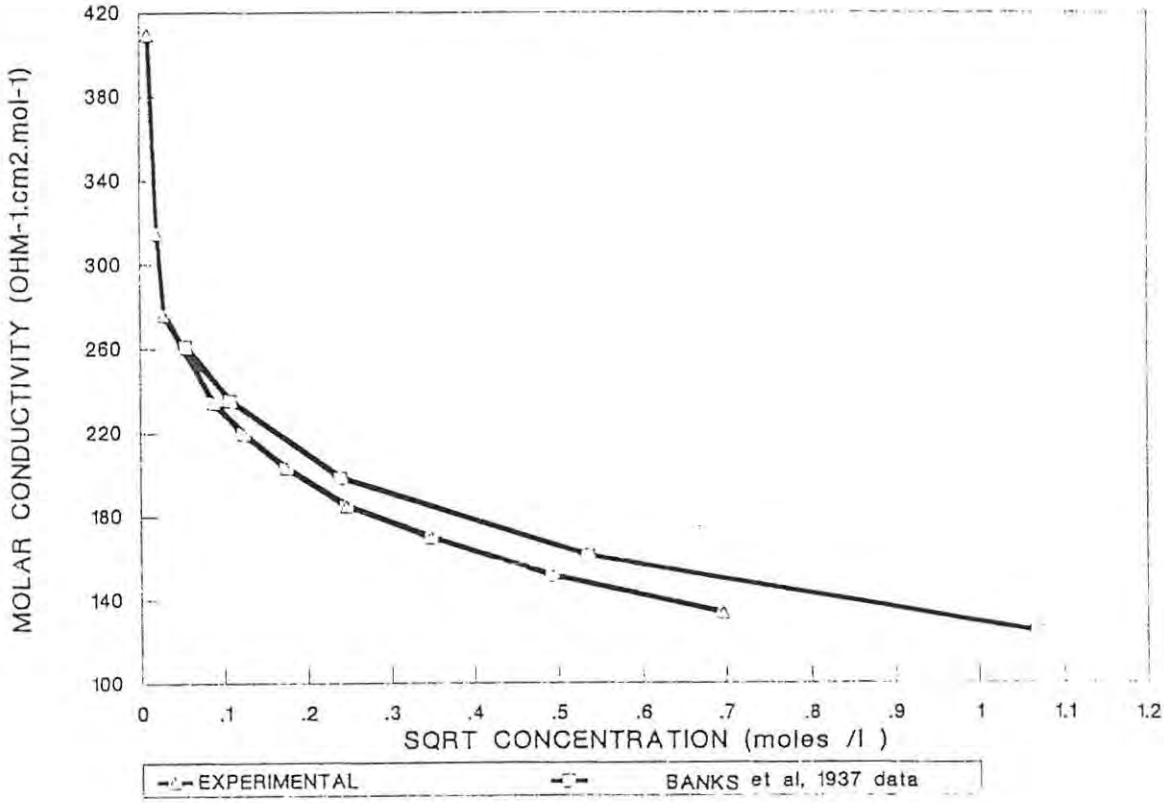

FIGURE 2.2 Plot of molar conductivity versus the square root of the concentration.

14/...

i.e. higher than 237,07 $\Omega^{-1}.cm^2.mol^{-1}$ at 20°C and 282,65 $\Omega^{-1}.cm^2.mol^{-1}$ at 30°C (Figures 2.1 and 2.2).

It would also appear that as the $(NH_4)_2SO_4$ concentration increases, the degree of association of NH_4^+ increases, with a concomitant increase in association of the bivalent ion, to the intermediate ion $NH_4SO_4^-$. If the effect of $(NH_4)_2SO_4$ concentration on the pH is determined (Figure 2.3), at the lower concentrations a greater dissociation of the NH_4^+ ion is found. A similar trend was observed by Cranston and Brown (1937). If the change in H^+ ion concentration with change in the $(NH_4)_2SO_4$ concentration is plotted against the $(NH_4)_2SO_4$ concentration (Figure 2.3), it is in fact found that the major change in H^+ ion concentration does occur at very low $(NH_4)_2SO_4$ concentrations.

By using the values for the 3 molar conductivities at infinite dilution as outlined by Robinson and Stokes (1970) for H^+ and HSO_4^-, i.e. 323,446 and 43,026 respectively, and calculating the H^+ concentration from the pH using both the experimental data and that of Cranston and Brown (1937), a regression analysis was set up which allowed the specific conductivity to be calculated at the different concentrations of $(NH_4)_2SO_4$, which was as a result of the "free" H^+ ions. Also calculated was the specific conductivity which resulted from the dissociation of the $(NH_4)_2SO_4$ as outlined in equations 4 and 5. For ease of reference this will be termed the conductivity arising from the "normal" dissociation of $(NH_4)_2SO_4$. The specific conductivity obtained as a result of increasing the $(NH_4)_2SO_4$ concentration was determined analytically. By using this data the proportion of the conductivity resulting from the H^+ ions was calculated. The conductivity which arises from the H^+ ions is a result of the further dissociation of $(NH_4)_2SO_4$ at the lower concentrations. The experiments were carried out at 20°C and 30°C in solutions with unadjusted pH, and then compared at the same temperatures after adjusting the pH to 7,00 with NH_4OH. The use of NH_4OH to adjust the pH did not significantly affect the concentration of NH_4^+ due to the low concentrations of H^+ ions at pH 6,0 and 5,0. Due to problems in maintaining the temperatures, the exact temperatures were 21,7°C and 28,8°C at pH 7,0. The molar equivalent conductivities used at infinite dilution at the different temperatures were obtained by regression analysis of data of Robinson and Stokes (1970) and are outlined in Appendix III and Figure 1, Appendix III.

15/...

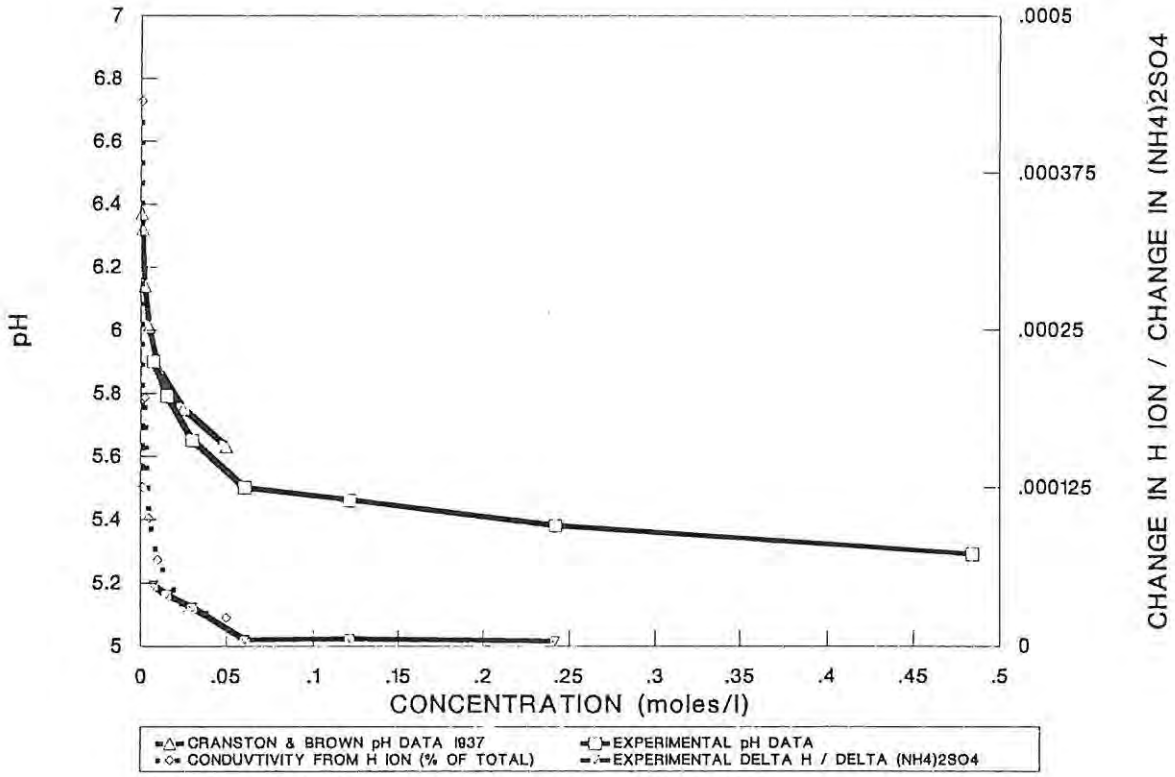

FIGURE 2.3 The effect of the (NH4)2SO4 concentration on the pH and the change in the H Ion concentration.

16...

The data on the effect of $(NH_4)_2SO_4$ concentration on the specific conductivity arising from the H^+ ions and that arising from the "normal" dissociation at the different temperatures and pH values are depicted in: Figure 2.4, 20°C and unadjusted pH; Figure 2.5, 21,7°C and pH 7,00; Figure 2.6, 30°C and unadjusted pH; and Figure 2.7, 28,8°C and pH 7,00. In Figures 2.4 and 2.6 it is evident that at the lower concentrations the bulk of the conductivity arises as a result of the mobility of the H^+ ion, and at the higher concentrations from the association of the bivalent ion to the intermediate ion $NH_4SO_4^-$ and NH_4^+. Similar specific conductivities were obtained in the solutions where the pH was adjusted to pH 7,0, indicating that the increased conductivity at the lower concentrations was as a result of the dissociation of the NH_4^+ to NH_3 and H^+ (Figures 2.5 and 2.7).

With these data the molar conductivity arising from the intermediate ion $NH_4SO_4^-$ and NH_4^+ was calculated allowing the determination of α, the fraction of the bivalent ion which exists in solution as the intermediate ion. The data are plotted in: Figure 2.8, 20°C and unadjusted pH; Figure 2.9, 20°C and pH 7,0; Figure 2.10, 30°C and unadjusted pH; and Figure 2.11, 30°C and pH 7,0. It is evident from these graphs that as the $(NH_4)_2SO_4$ concentration increases, the extent of dissociation of the molecule decreases. Similar data was obtained by Banks *et al* (1931).

At the very low concentrations in solutions with unadjusted levels of pH, there is an increase in association of the bivalent ion with increasing $(NH_4)_2SO_4$ concentration. This increase results from the bivalent radical existing in the associated form as HSO_4^-. A comparison of the molar conductivities of the solutions with unadjusted pH levels, with the solutions at pH 7,0, at both temperatures, indicates that the conductivities are lower at pH 7,0, especially at the lower concentrations (Figures 2.12 to 2.15). The very high molar conductivities obtained at the low $(NH_4)_2SO_4$ concentrations are a result of the high molar conductivities of the H^+ ions.

The pH adjustment did not significantly affect the conductivities as, at these low concentrations tending towards infinite dilution, the H^+ ions are still available to transfer current.

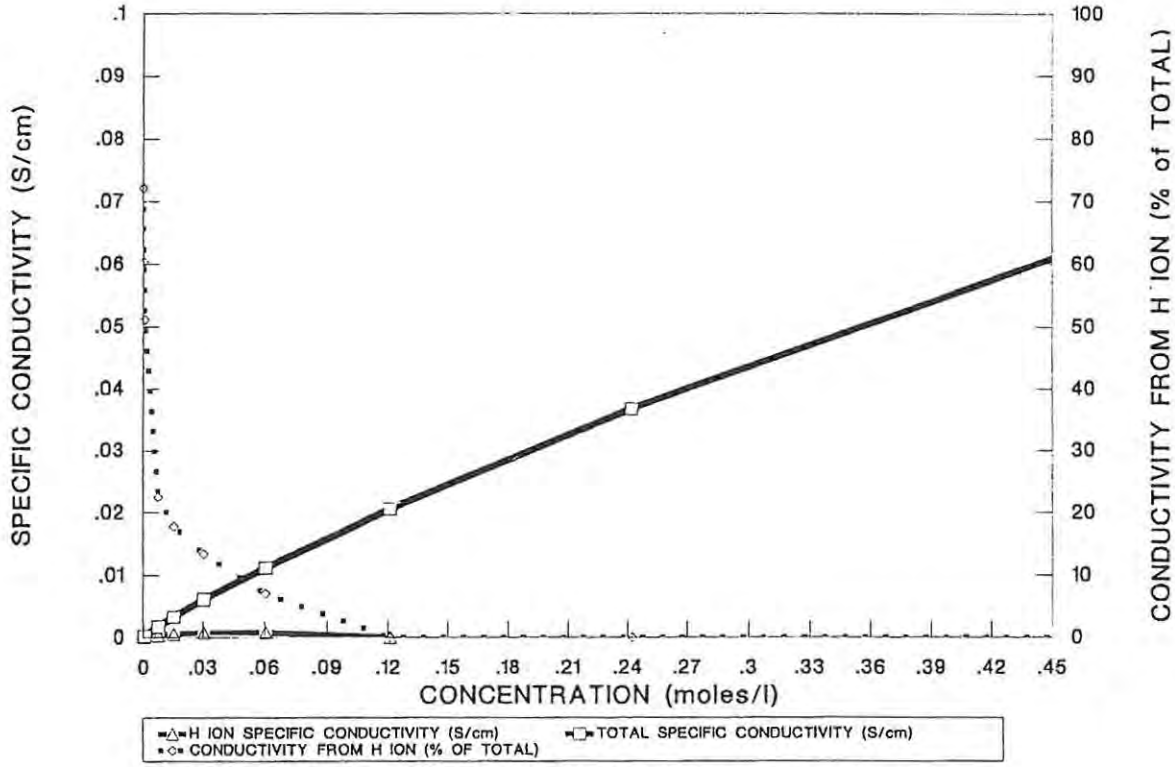

FIGURE 2.4 Effect of (NH4)2SO4 concentration on the specific conductivity arising from the H ions and the "normal" dissociation at 20 deg C.

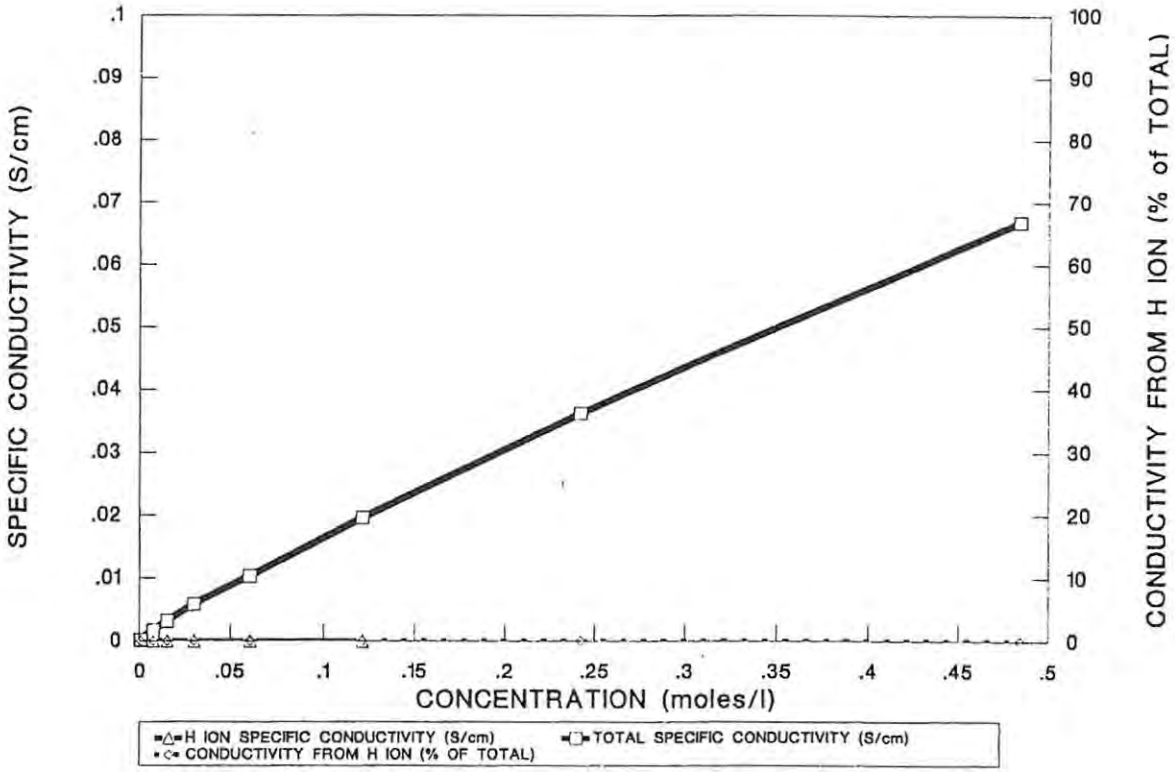

FIGURE 2.5 Effect of (NH4)2SO4 concentration on the specific conductivity arising from the H ions and the "normal" dissociation at 20 deg C and pH 7.00

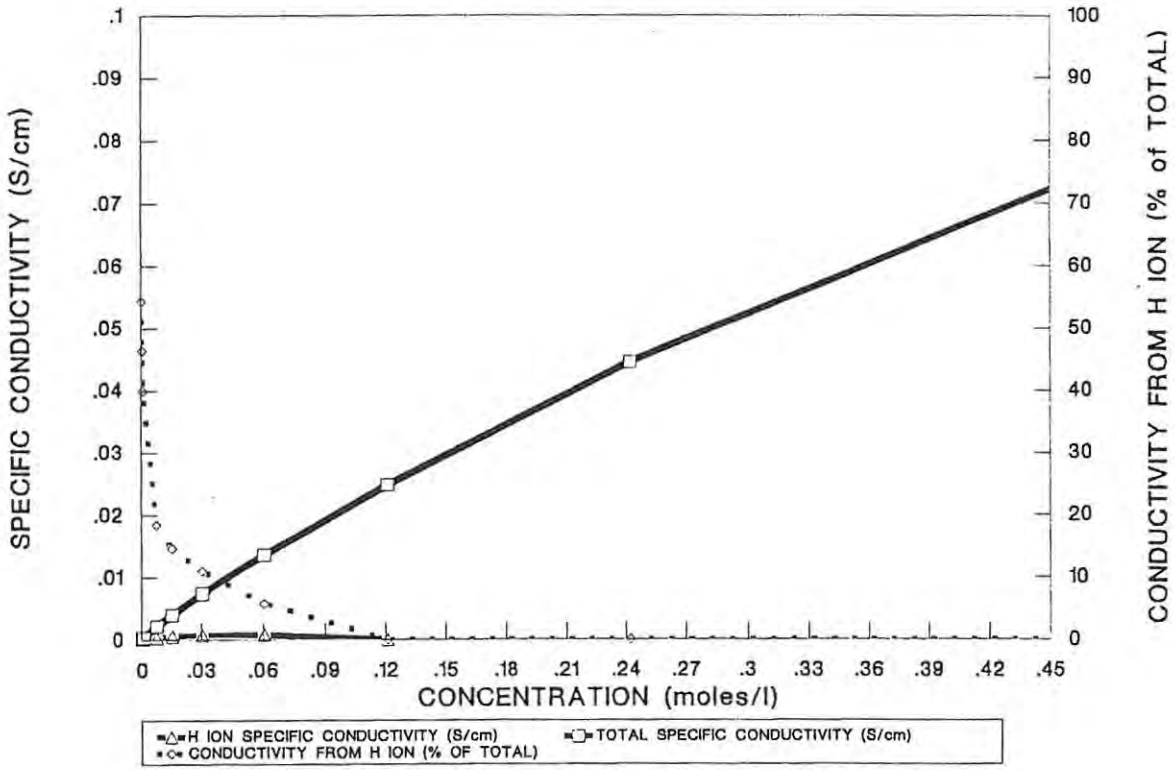

FIGURE 2.6 Effect of (NH4)2SO4 concentration on the specific conductivity arising from the H ions and the "normal" dissociation at 30 deg C.

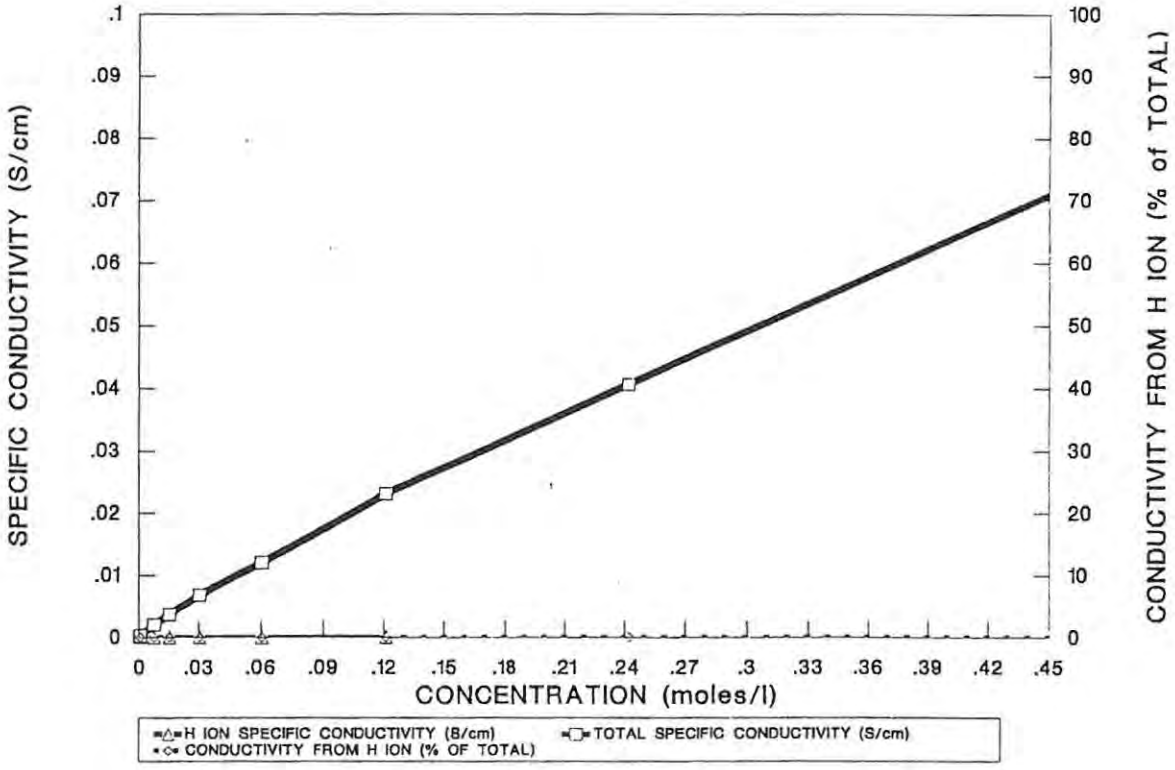

FIGURE 2.7 Effect of (NH4)2SO4 concentration on the specific conductivity arising from the H ions and the "normal" dissociation at 30 deg C and pH 7.0

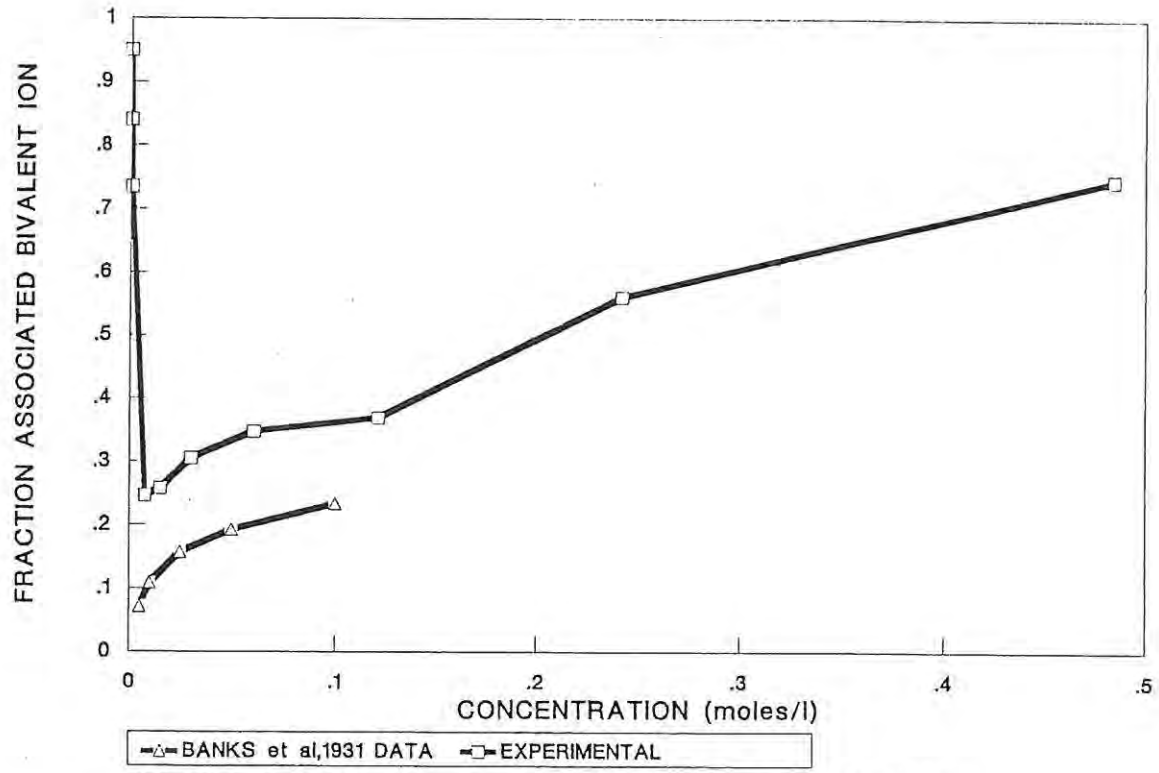

FIGURE 2.8 Effect of the (NH4)2SO4 concentration on the fraction associated bivalent ion at 20 degC and unadjusted pH. Data of Banks et al at 18 deg C.

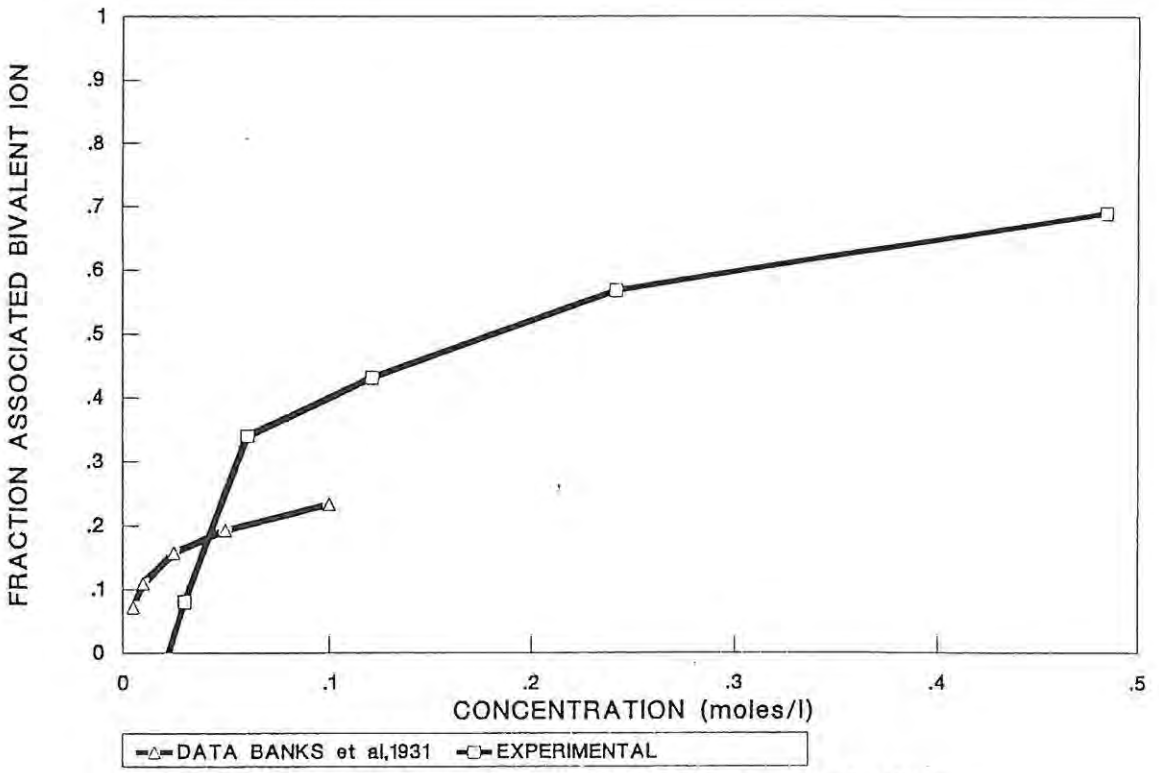

FIGURE 2.9 Effect of the (NH4)2SO4 concentration on the fraction associated bivalent ion at 20 degC and pH 7.0. Data of Banks et al at 18 degC.

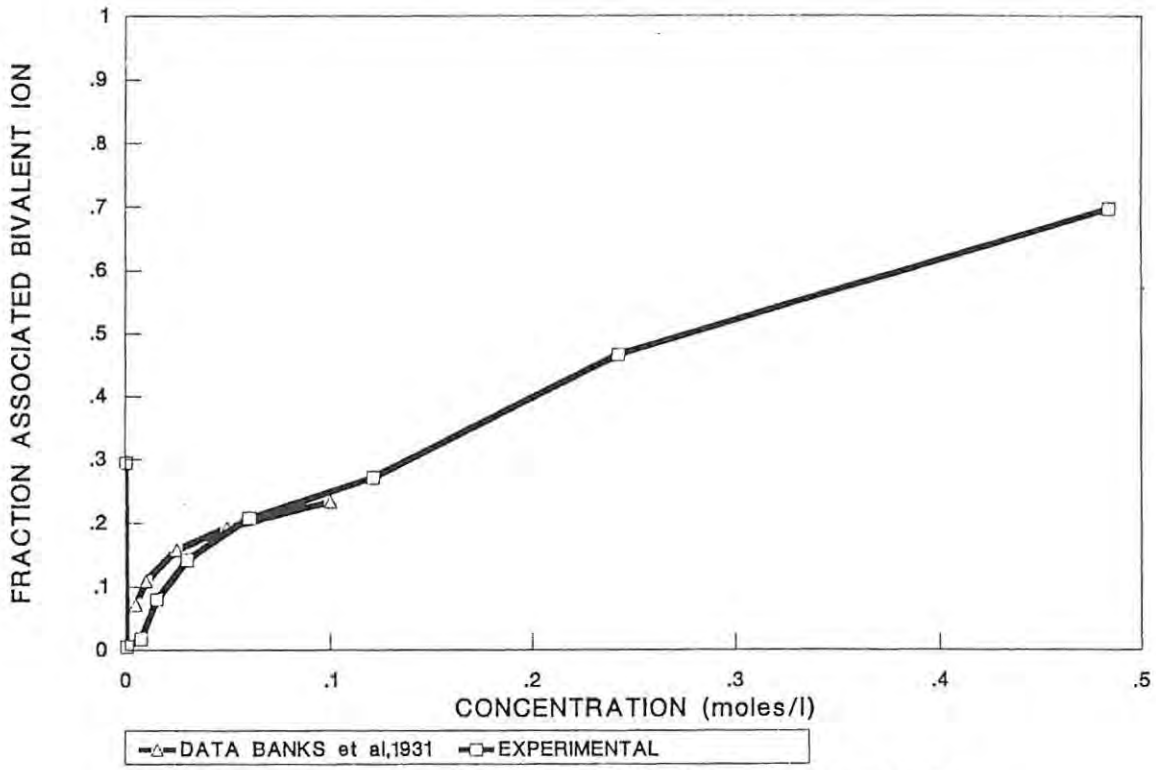

FIGURE 2.10 Effect of the (NH4)2SO4 concentration on the fraction associated bivalent ion at 30 degC and unadjusted pH. Banks et al data at 18 degC.

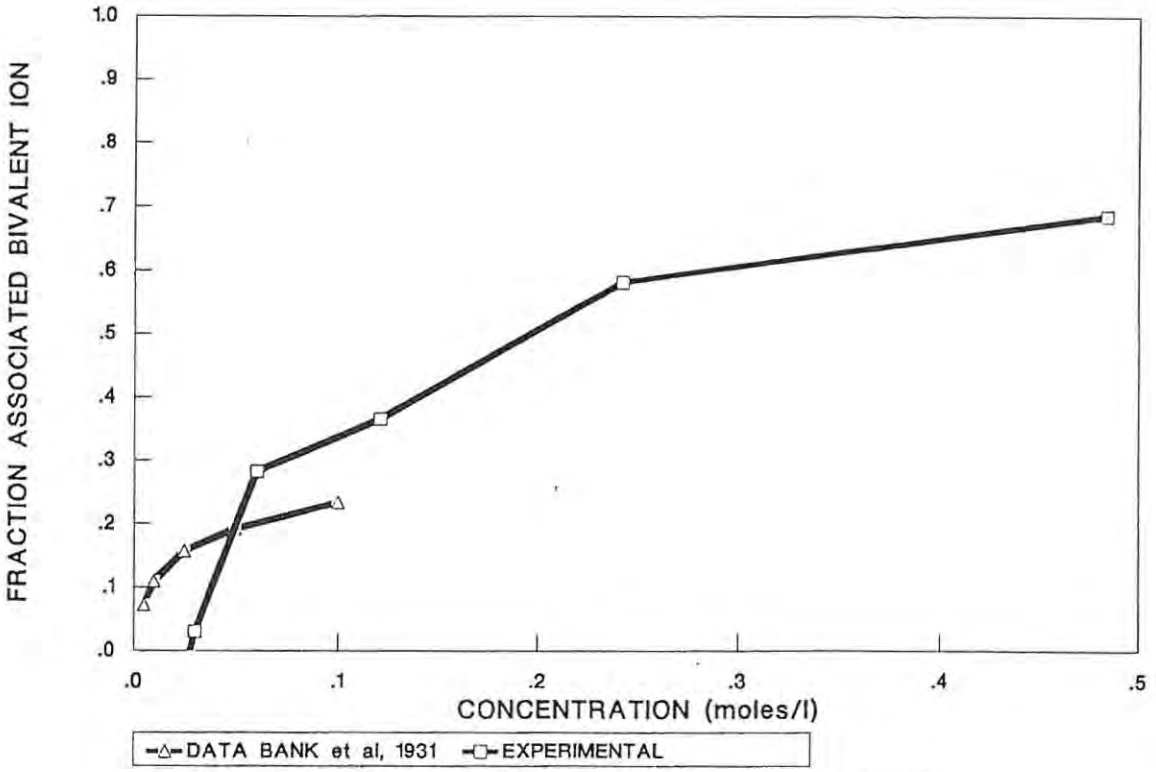

FIGURE 2.11 Effect of the (NH4)2SO4 concentration on the fraction associated bivalent ion at 30 degC and pH 7.0. Banks et al data at 18 degC.

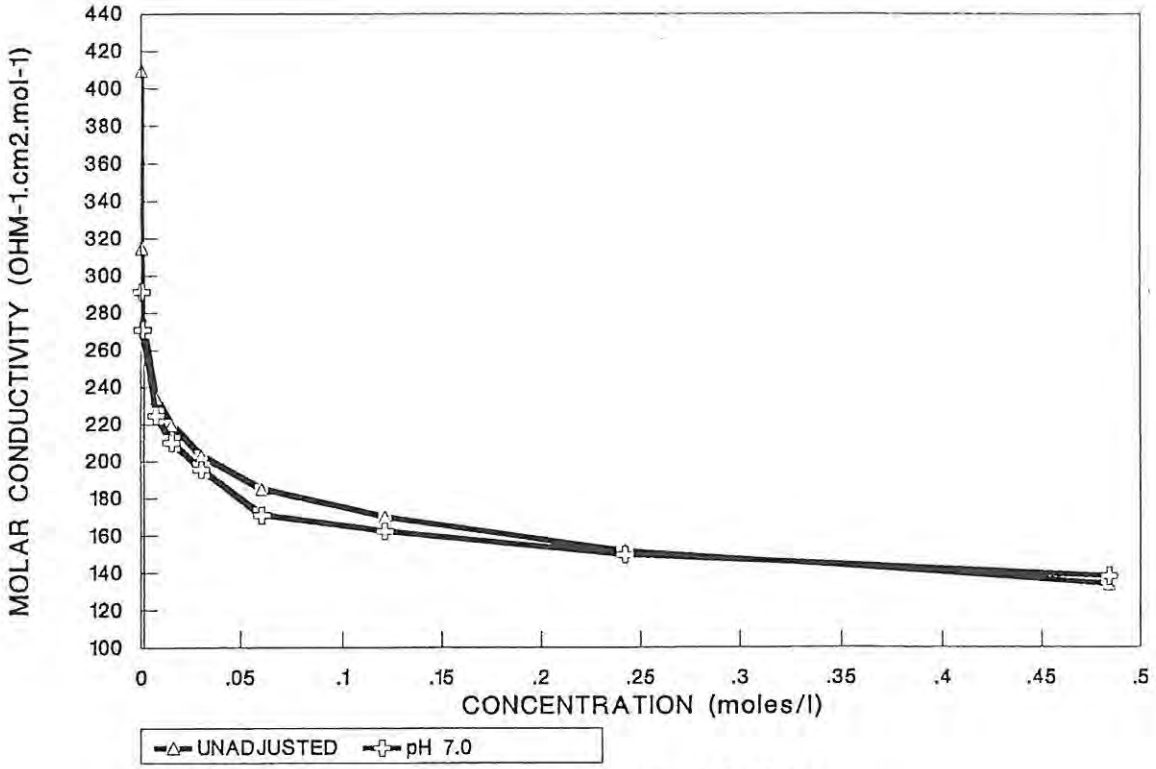

FIGURE 2.12 The effect of the (NH4)2SO4 concentration on the molar conductivity at pH 7.0 and in an unadjusted solution at 20 deg C.

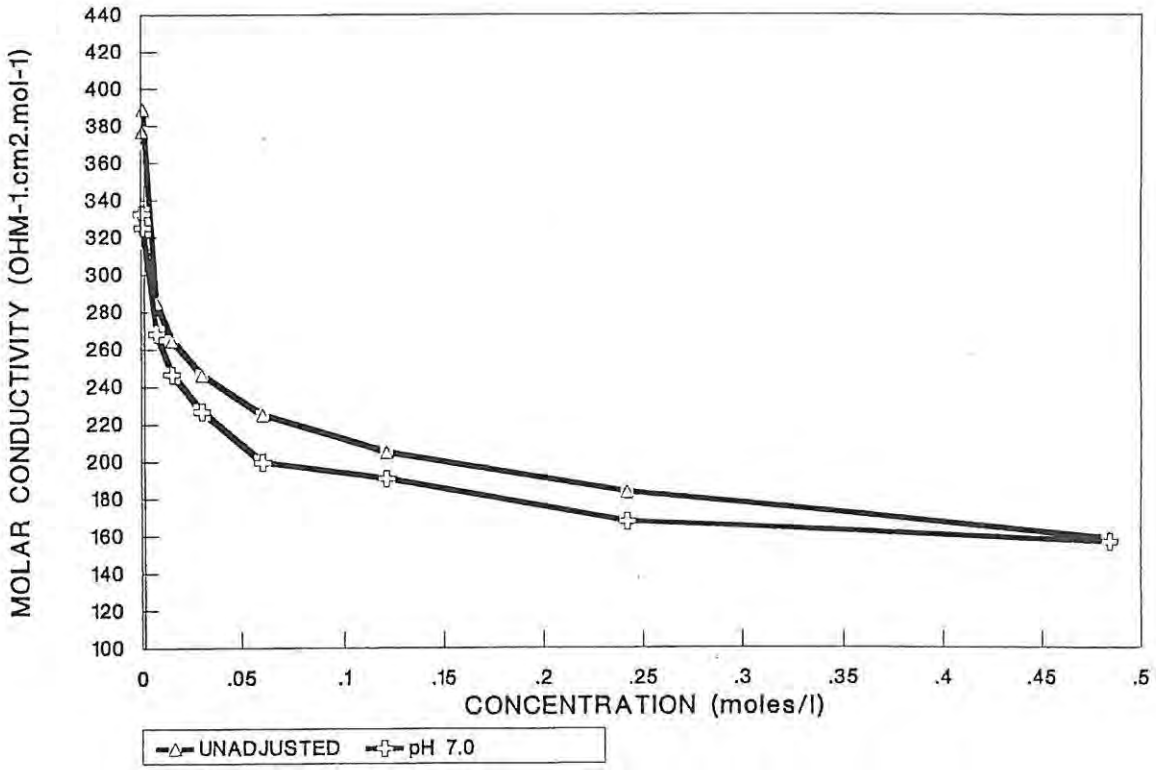

FIGURE 2.13 The effect of the (NH4)2SO4 concentration on the molar conductivity at pH 7.0 and in an unadjusted solution at 30 deg C.

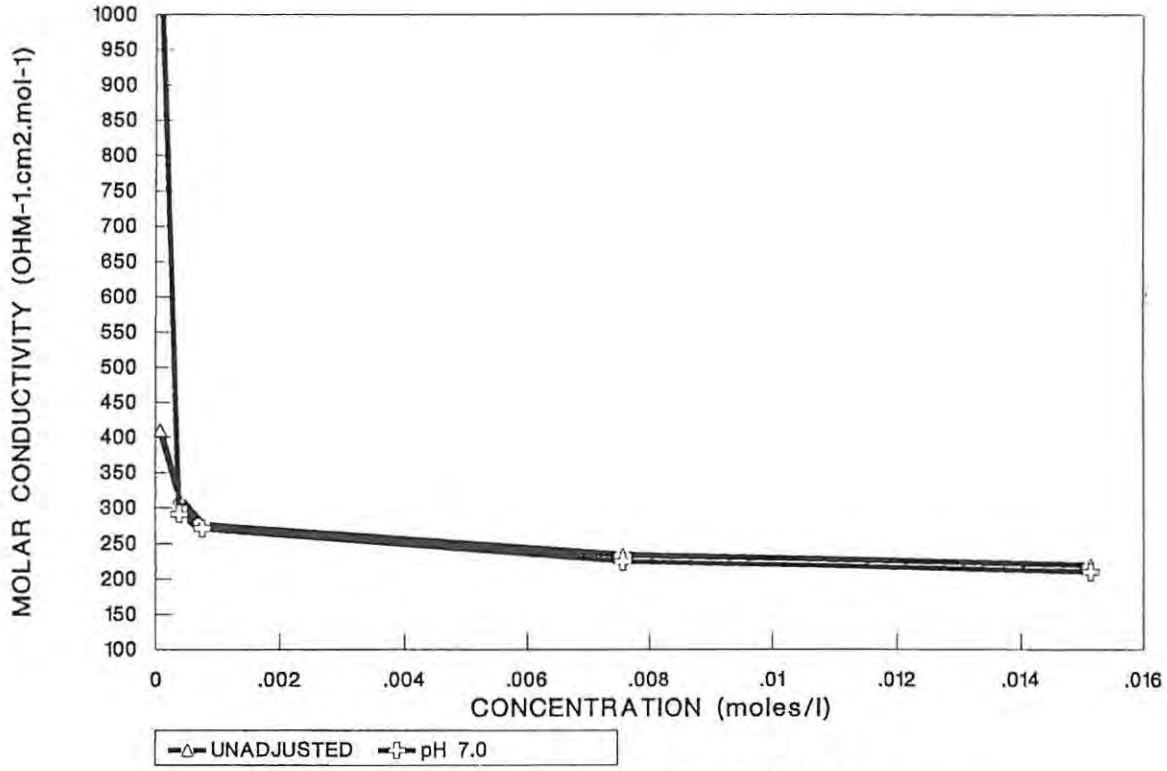

FIGURE 2.14 The effect of the (NH4)2SO4 concentration on the molar conductivity at pH 7.0 and in an unadjusted solution at 20 deg C.

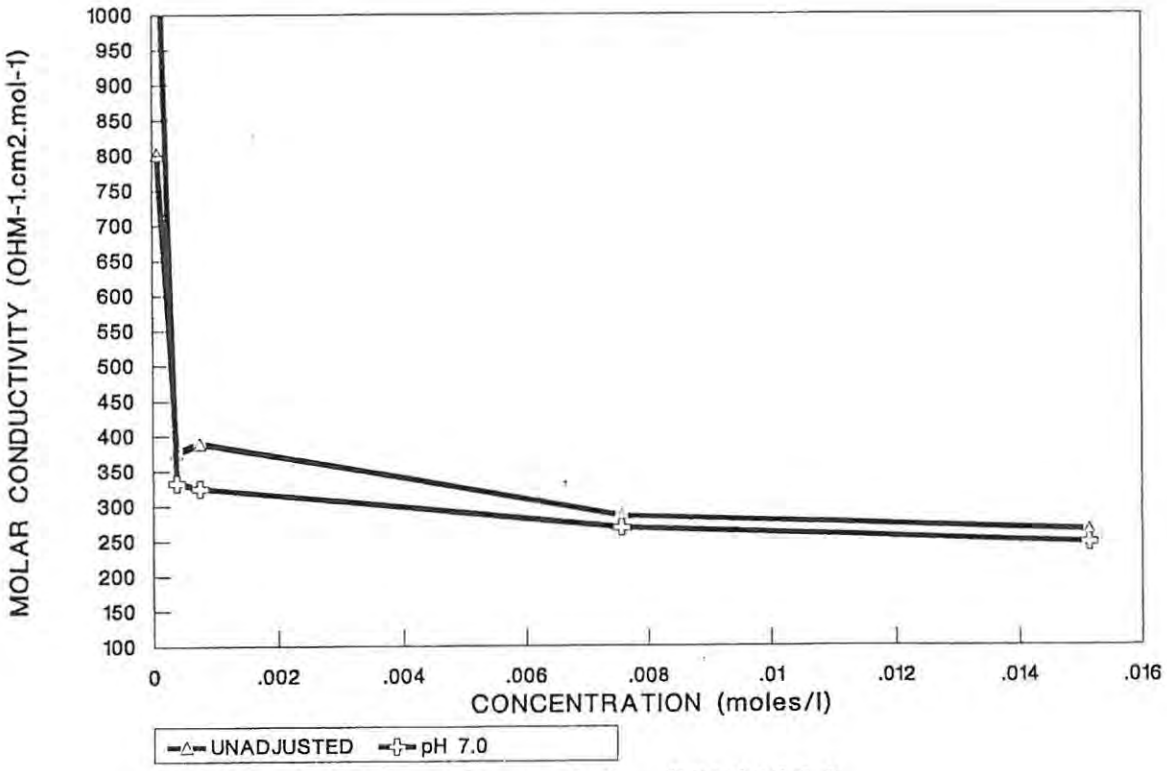

FIGURE 2.15 The effect of the (NH4)2SO4 concentration on the molar conductivity at pH 7.0 and in an unadjusted solution at 30 deg C.

As a result of being able to calculate the fraction of associated bivalent radical using equations 8 and 9, the ionic strength and the Ostwald constant, k', were calculated. Debye plots, as outlined by equation 11, were therefore generated out (Figures 2.16 to 2.19) for the various conditions. Regression analysis of the data of the linear part of the Debye plot yielded the following values for ΣB under the different conditions:

20°C; unadjusted pH	0,444
22,2°C; pH 7,0	0,416
30°C; unadjusted pH	0,361
28,8°C; pH 7,0	0,345

Data of Banks *et al*, 1931

18°C, unadjusted pH	0,408

At the lower concentrations in the solutions with unadjusted pH levels there is no longer linearity. This is possibly as a result of the bivalent ion no longer associating chiefly as $NH_4SO_4^-$, but associating also in part as HSO_4^- or being available as the free radical SO_4^{-}. This is evident in the plot which compares the change in H^+ concentration per change in $(NH_4)_2SO_4$ concentration plotted against the $(NH_4)_2SO_4$ concentration, with the fraction of bivalent ion associated as a result of increasing the $(NH_4)_2SO_4$ concentration (Figure 2.20).

It is clearly evident that the bulk of the change in H^+ ion concentration occurs as a result of the dissociation of the $(NH_4)_2SO_4$ at the lower concentrations of $(NH_4)_2SO_4$. The change in H^+ concentration per change in $(NH_4)_2SO_4$ concentration was calculated from:

$$\frac{\Delta[H^+]}{\Delta[(NH_4)_2SO_4]} = \Delta[H^+]_a \qquad 12.$$

where $\Delta[H^+]_a$ = change in $[H^+]$ with respect to the change in the $(NH_4)_2SO_4$ concentration.

24/...

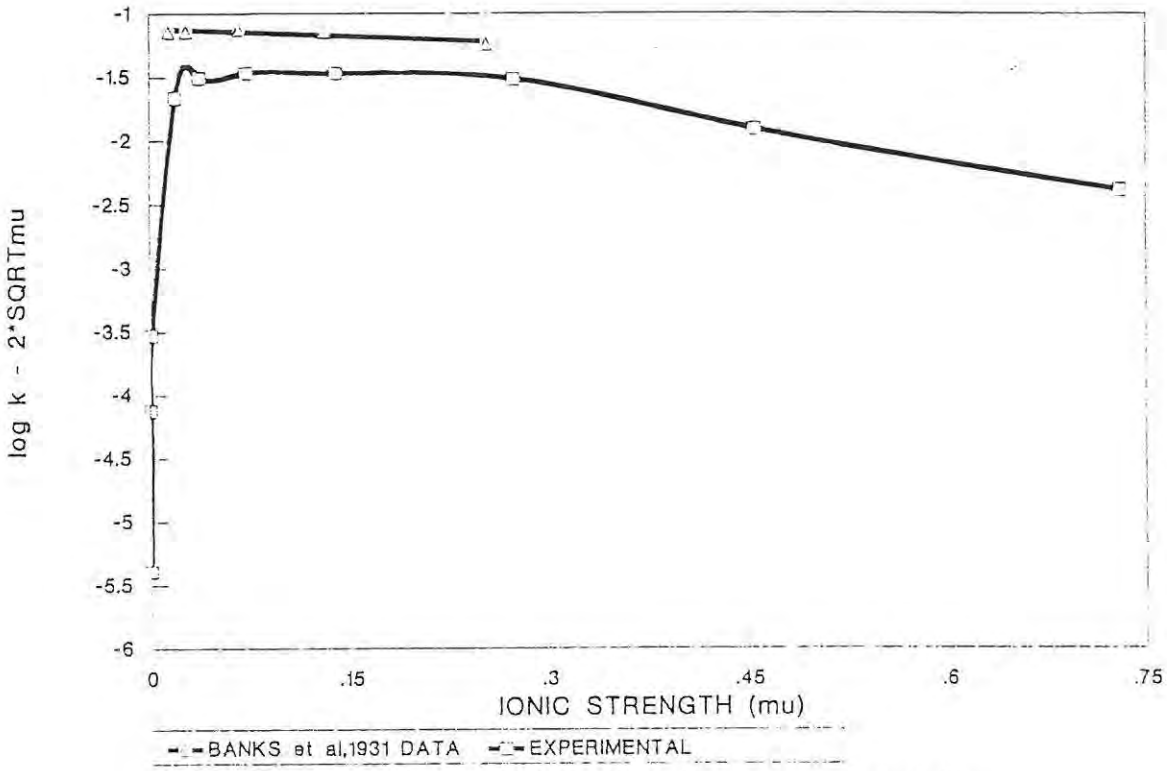

FIGURE 2.16 Debye-Hückel plot. Experimentai data at 20 deg C and unadjusted pH and the data of Banks et al 1931.

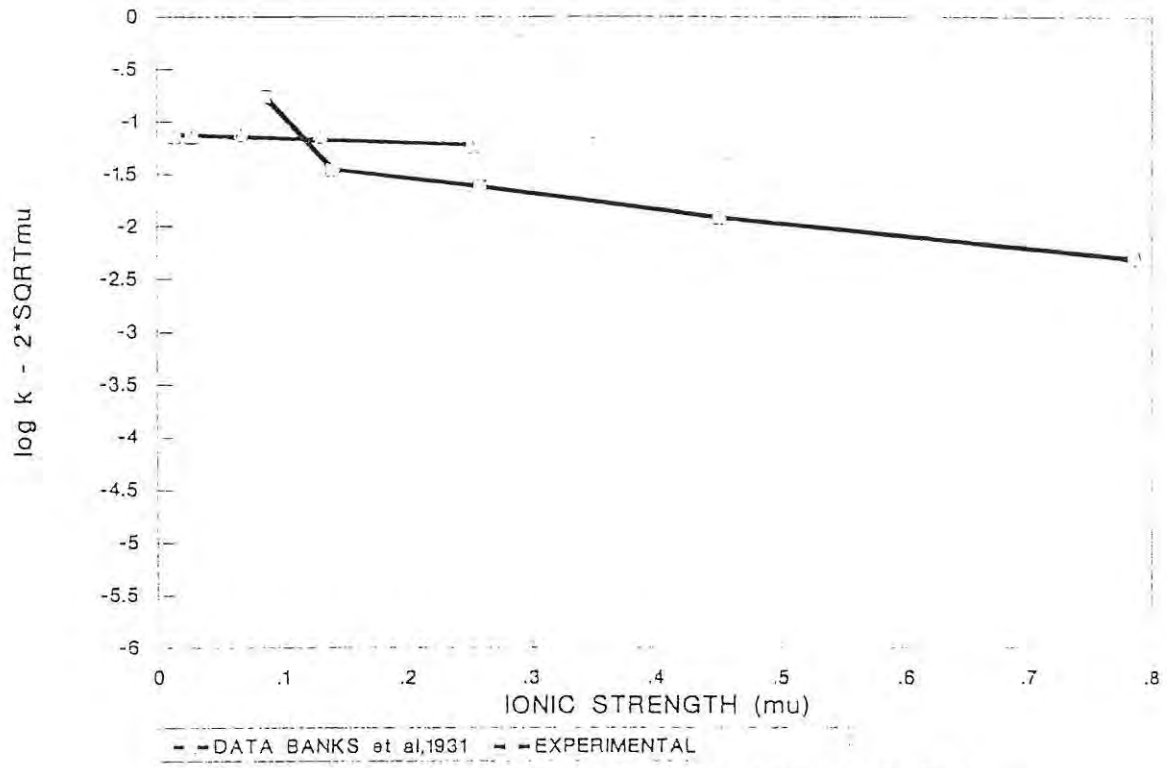

FIGURE 2.17 Debye-Hückel plot. Experimental data at 20 deg C and pH 7.0 and data of Banks et al 1931.

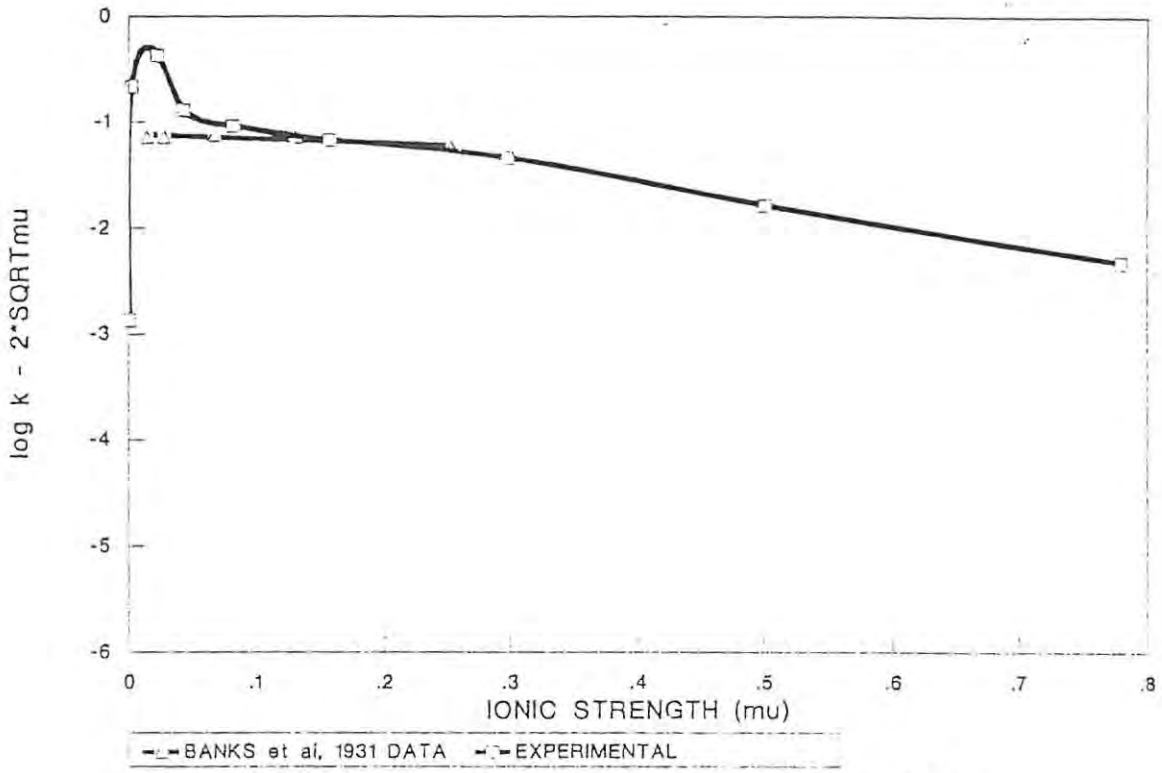

FIGURE 2.18 Debye-Hückel plot. Experimental data at 30 deg C and unadjusted pH and data of Banks et al 1931.

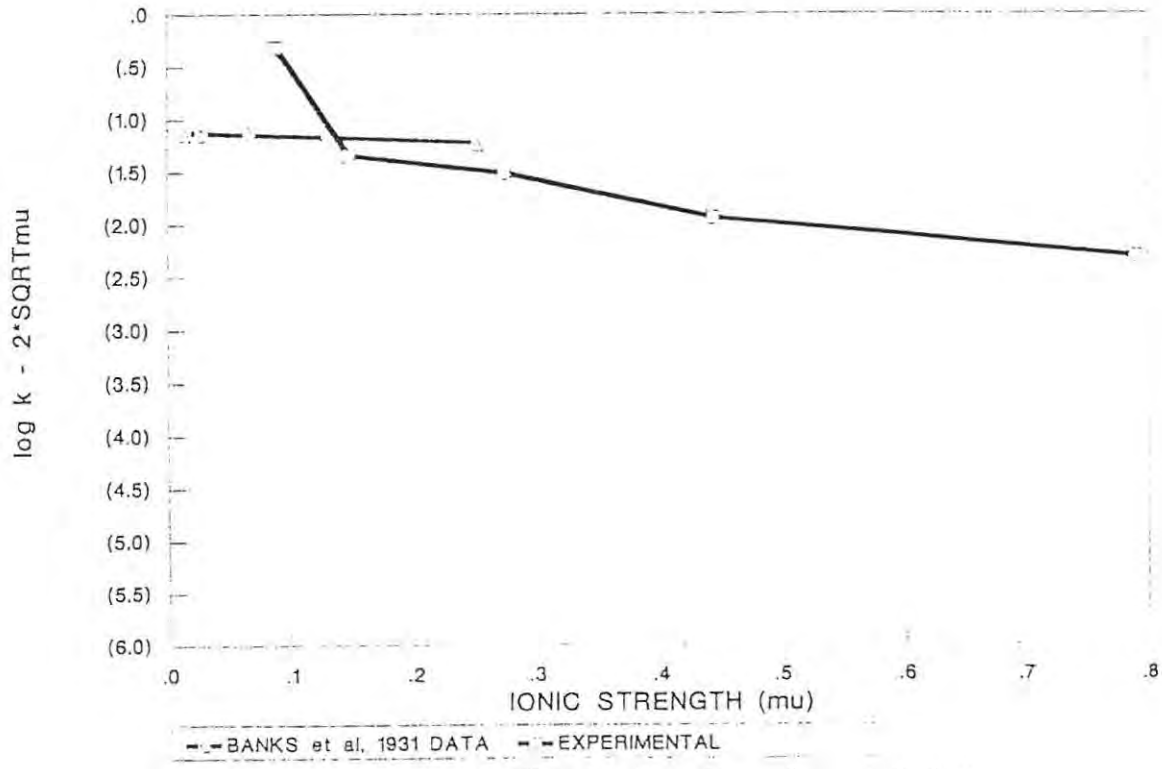

FIGURE 2.19 Debye-Hückel plot. Experimental data at 30 deg C and pH 7.0 and data of Banks et al 1931.

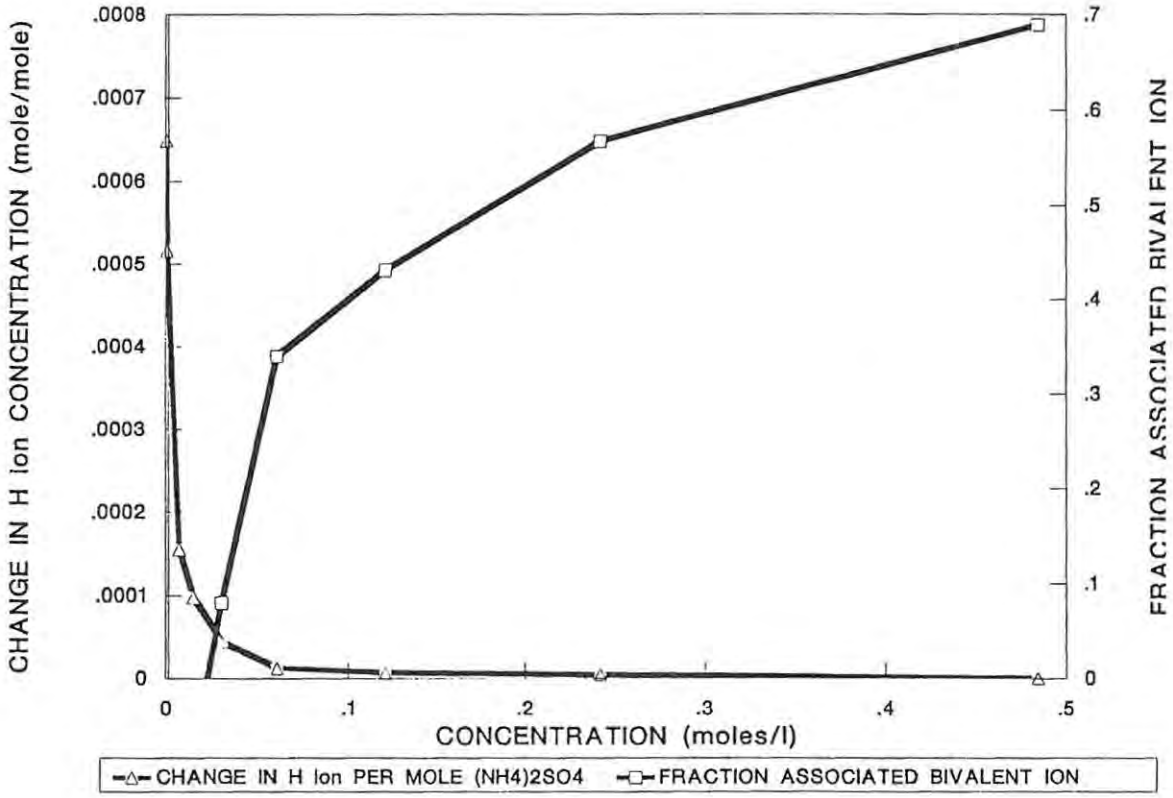

FIGURE 2.20 Effect of (NH4)2SO4 concentration on the H ion concentration at 22.2 deg C.

The ΔH^+ was determined from the change in pH as a result of the change in $(NH_4)_2SO_4$ concentration and is therefore the change in the free H^+ ion concentration. This is based on the assumption that if the NH_4^+ can yield a proton to an electrode for the electrode potential, it will also be able to yield a free mobile proton ion for the resultant increase in conductivity. The levels of molar conductivity obtained at the low concentrations are also far greater than those possible if the $(NH_4)_2SO_4$ were merely dissociating to $2NH_4^+ + SO_4^-$ since this could only give a total molar conductivity of 234,44 at 30°C and infinite dilution.

On calculating the effect of the $(NH_4)_2SO_4$ concentration on the concentration of NH_4^+ ions in solutions (equation 7), and the percentage of the NH_4^+ that is dissociated and free in solution, it is found that at the higher concentrations there is a gradual decrease in the percentage of NH_4^+ in solution, tapering off to approximately 65% (Figures 2.21 to 2.24). At the very low concentrations the increase in $(NH_4)_2SO_4$ concentration decreases the percentage of the ammonia which is free in solution as the NH_4^+ ion. This is possibly as a result of the NH_4^+ further dissociating. It is therefore proposed that the overall dissociation of $(NH_4)_2SO_4$ is as follows:

$$2NH_3 + 2H^+ + SO_4^- : NH_3 + NH_4^+ + HSO_4 : 2NH_4^+ + SO_4^- : NH_4^+ + NH_4SO_4 : (NH_4)_2SO_4$$

Increasing concentration

When comparing the Ostwald constant k' and the overall dissociation constant K, very similar values are found under the different conditions at the high concentrations of $(NH_4)_2SO_4$, i.e. the $NH_4^+ + NH_4SO_4 \rightleftarrows (NH_4)_2SO_4$ dissociation. At the lower concentrations a large variation in K which occurs is possibly as a result of the various intermediate species of the molecule which exist.

2.4.2 Dissociation of $(NH_4)_2HPO_4$

In contrast to the dissociation of $(NH_4)_2SO_4$ which results in a decrease in pH at the low concentrations, in the case of $(NH_4)_2HPO_4$ there is no significant change in pH over the entire range of concentrations (Figure 2.25). The contribution of the H^+ concentration to the total

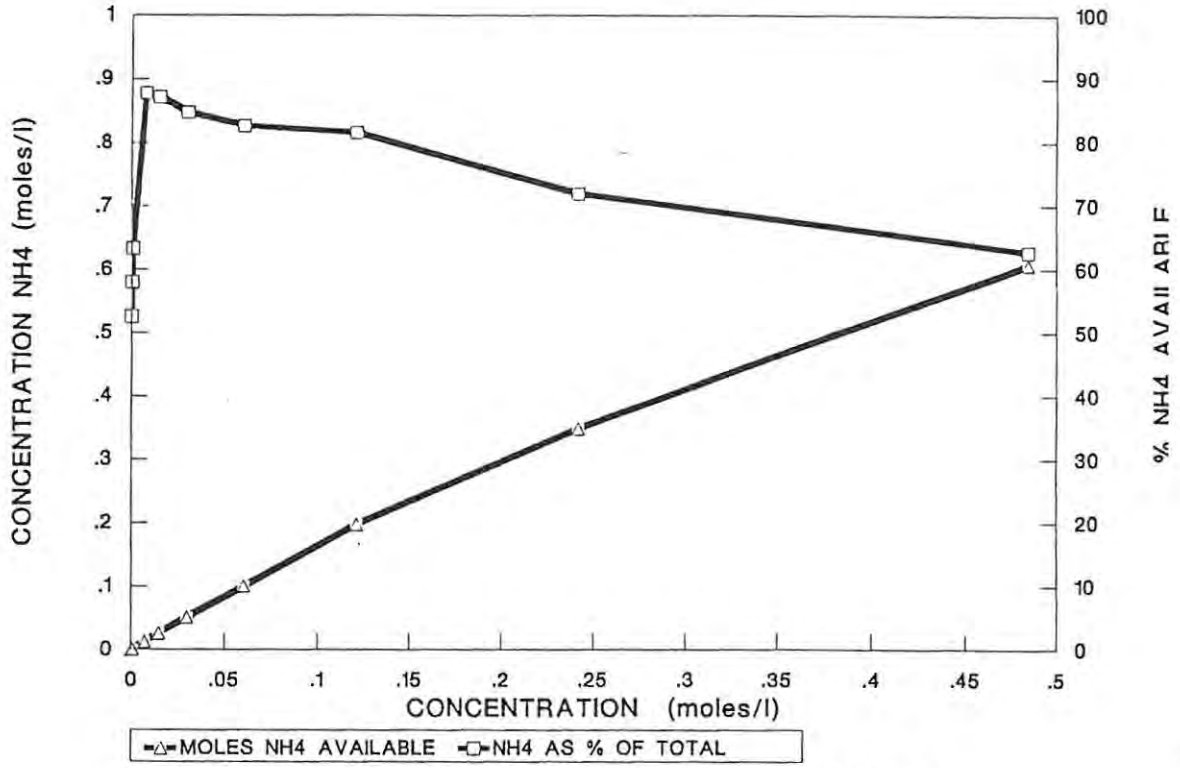

FIGURE 2.21 Effect of (NH4)2SO4 concentration on the free NH4 concentration and % of total NH4 as unassociated NH4 at 20 deg C and unadjusted pH.

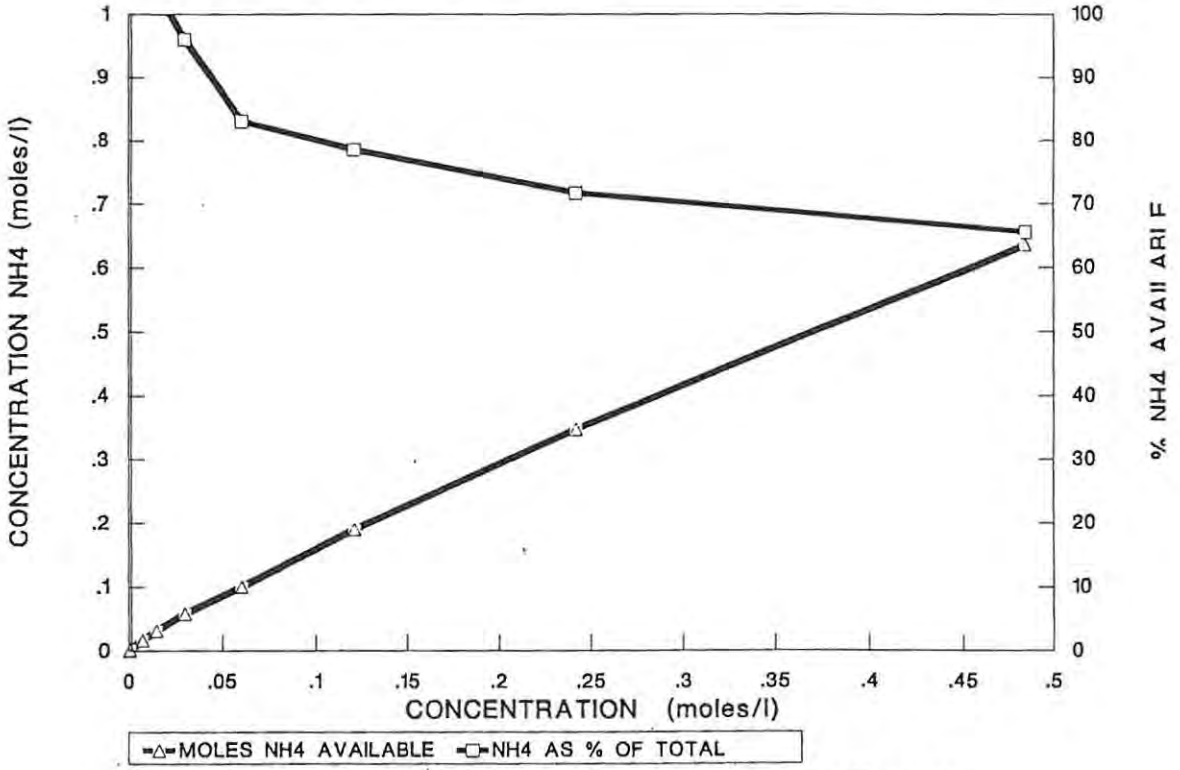

FIGURE 2.22 Effect of (NH4)2SO4 concentration on the free NH4 concentration and % of total NH4 as unassociated NH4 at 20 deg C and pH 7.0

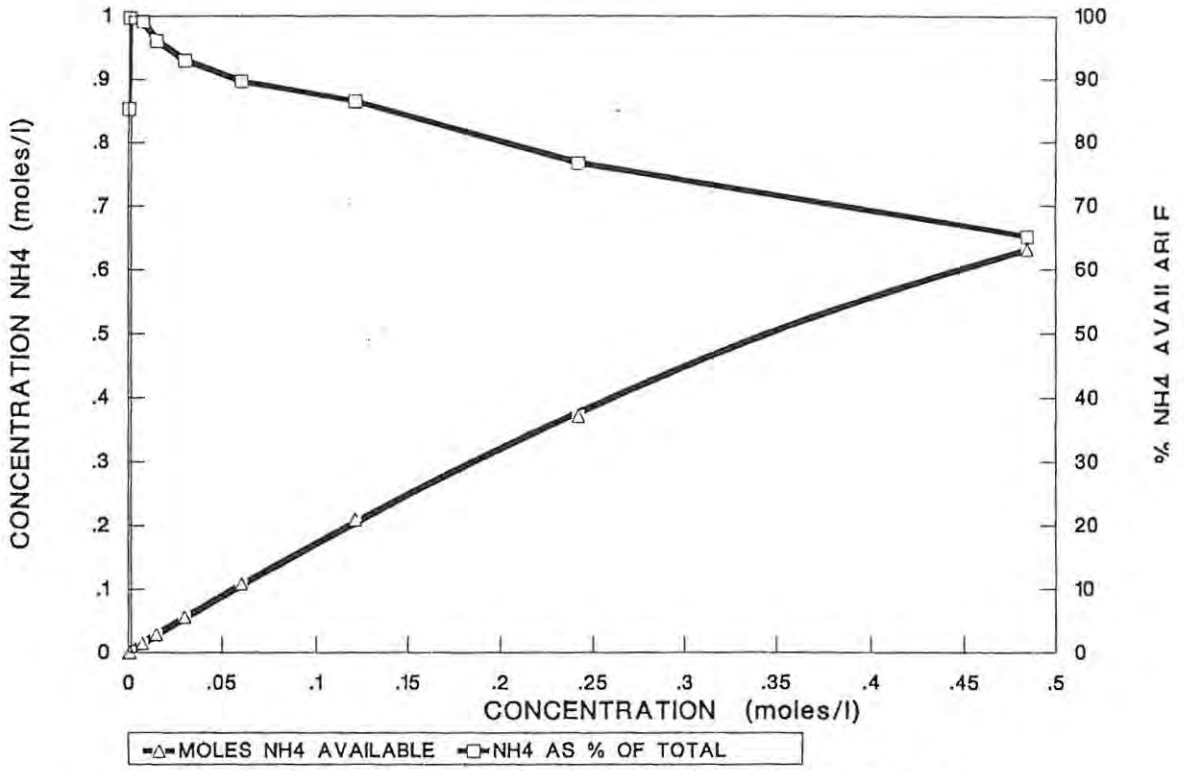

FIGURE 2.23 Effect of (NH4)2SO4 concentration on the free NH4 concentration and % of total NH4 as unassociated NH4 at 30 deg C and unadjusted pH.

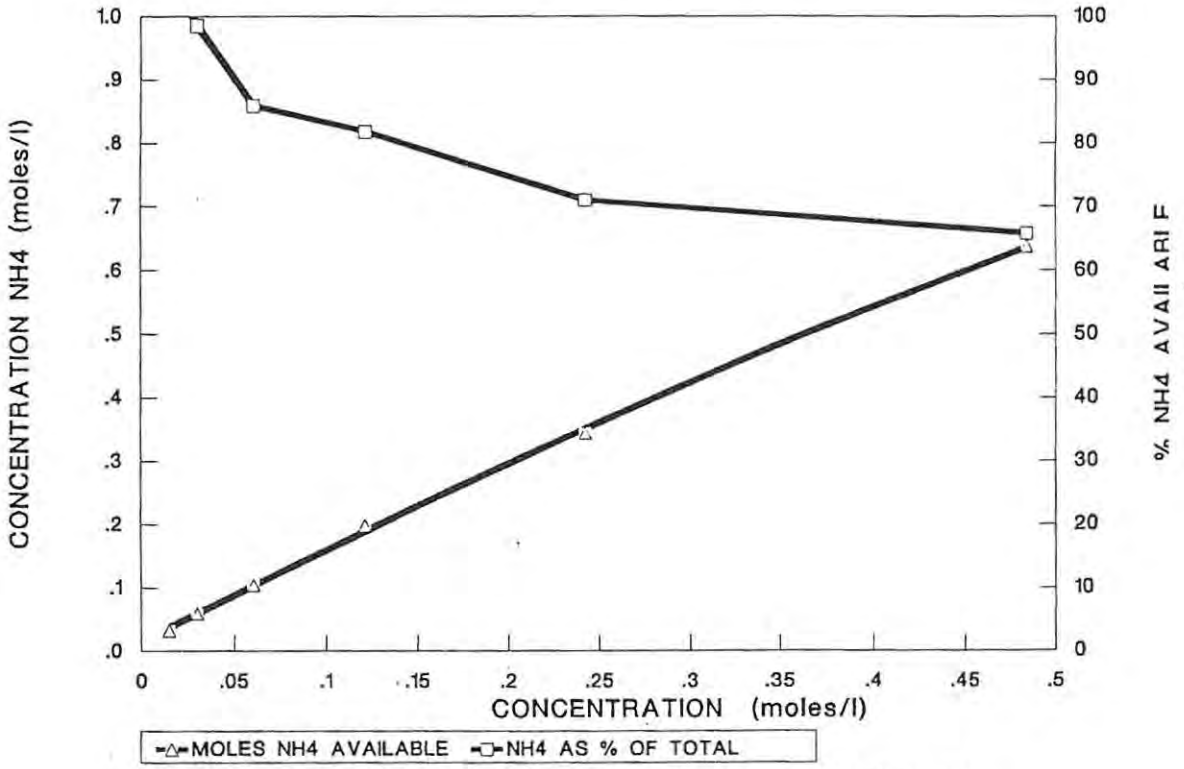

FIGURE 2.24 Effect of (NH4)2SO4 concentration on the free NH4 concentration and % of total NH4 as unassociated NH4 at 30 deg C and pH 7.0.

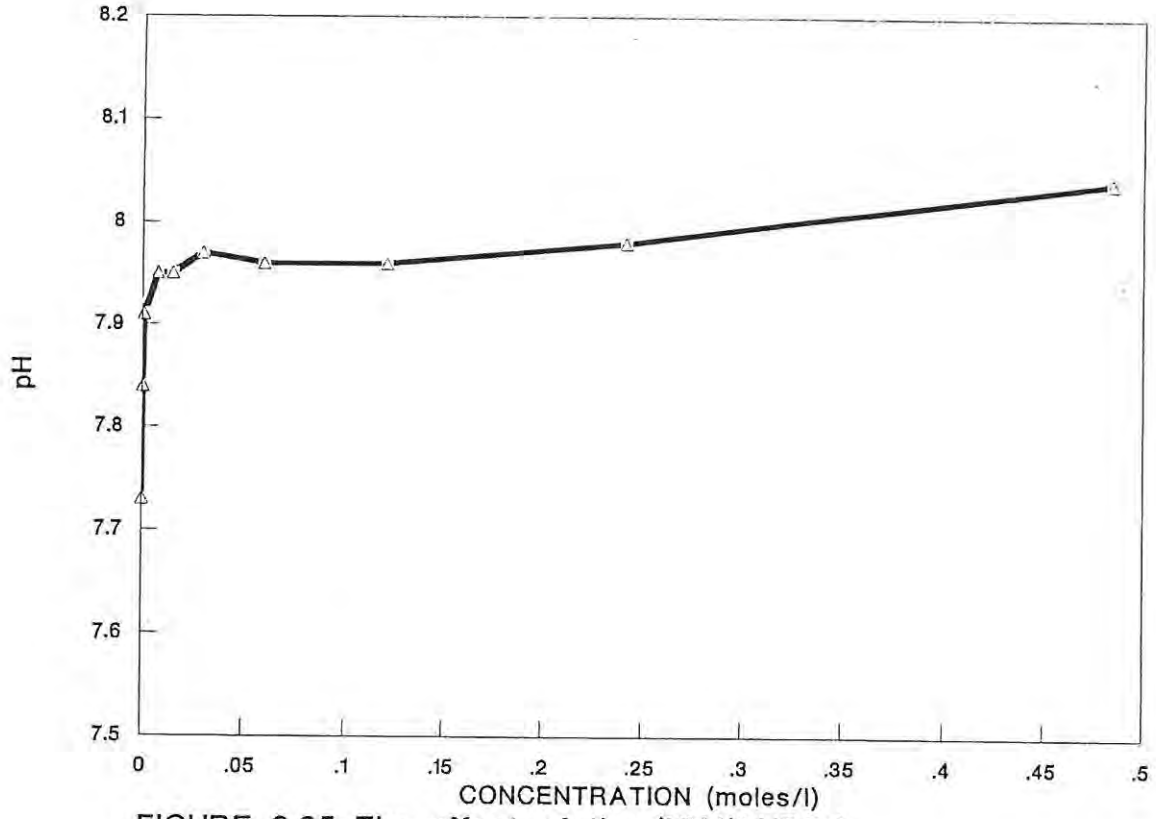

FIGURE 2.25 The effect of the (NH4)2HPO4 concentration on pH.

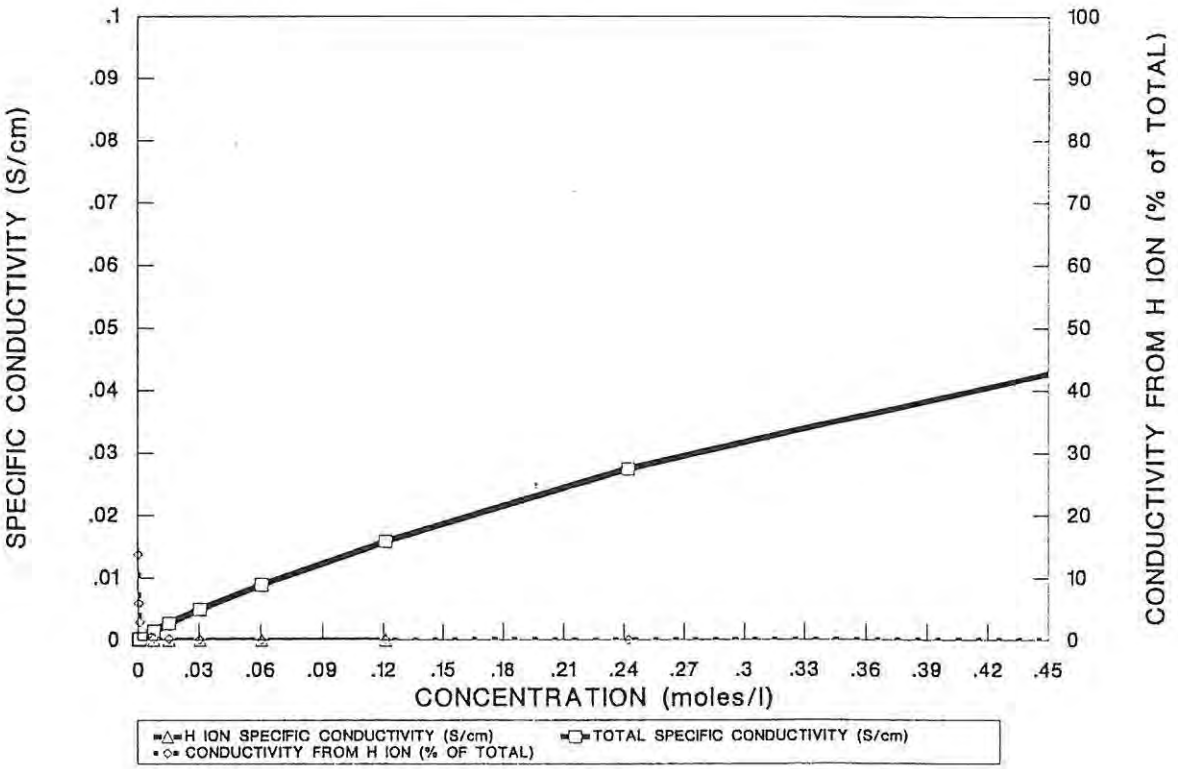

FIGURE 2.26 Effect of (NH4)2HPO4 concentration on the specific conductivity arising from the H ions and the "normal" dissociation at 30 deg C.

specific conductivity and as a percentage of the total conductivity is also insignificant above 5 mmoles/l (Figure 2.26). This is also evident when looking at the effect of the $(NH_4)_2HPO_4$ concentration on the molar conductivity (Figure 2.27). In the case of $(NH_4)_2SO_4$ the further dissociation of the molecule at the lower concentration results in an increase in the molar conductivity as a result of the higher mobility and equivalent conductivity of the H^+ ion. The limiting equivalent conductivity at infinite dilution is accounted for by the following dissociation in the case of $(NH_4)_2HPO_4$ at the higher concentrations:

$$2NH_4^+ + HPO_4^{-} \rightarrow (NH_4)_2HPO_4$$

However, it is proposed that at the lower concentrations further dissociation of the ammonium ions does indeed occur, with the further association of the resulting H^+ with the HPO_4^- ion. Therefore the overall dissociation is as follows:

$$2NH_3 + H_3PO_4 \rightarrow NH_3 + NH_4^+ + H_2PO_4 \rightarrow 2NH_4^+ + HPO_4^{-} \rightarrow (NH_4)_2HPO_4$$

If there is a further dissociation of the NH_4^+ to $NH_3 + H^+$ there should be a reduction in the pH as well as a concomitant increase in the molar conductivity as a result of the higher mobility and therefore equivalent conductivity of the H^+ ion. The limiting equivalent conductivity is therefore of the order of $270\Omega^{-1}.cm^2.mol^{-1}$ experimentally (Figure 2.27) and 270 as calculated from the values of Robinson and Stokes (1970) for 2 x NH_4^+ plus HPO_4^-.

As in the case of $(NH_4)_2SO_4$ the fraction of bivalent ion (HPO_4^-) that is associated increases with increasing concentration of $(NH_4)_2HPO_4$ (Figure 2.28). Greater linearity exists in the Debye-Hückel plot over the concentrations used when compared to $(NH_4)_2SO_4$, possibly as there are no free H^+ ions at the lower concentrations (Figure 2.29). Similar results to $(NH_4)_2SO_4$ are obtained for the effect of $(NH_4)_2HPO_4$ concentration on the concentration of free NH_4^+ that is dissociated and free in solution (Figure 2.30). As the concentration increases there is a gradual decrease in the percent NH_4^+ in solution, levelling off to approximately 40%.

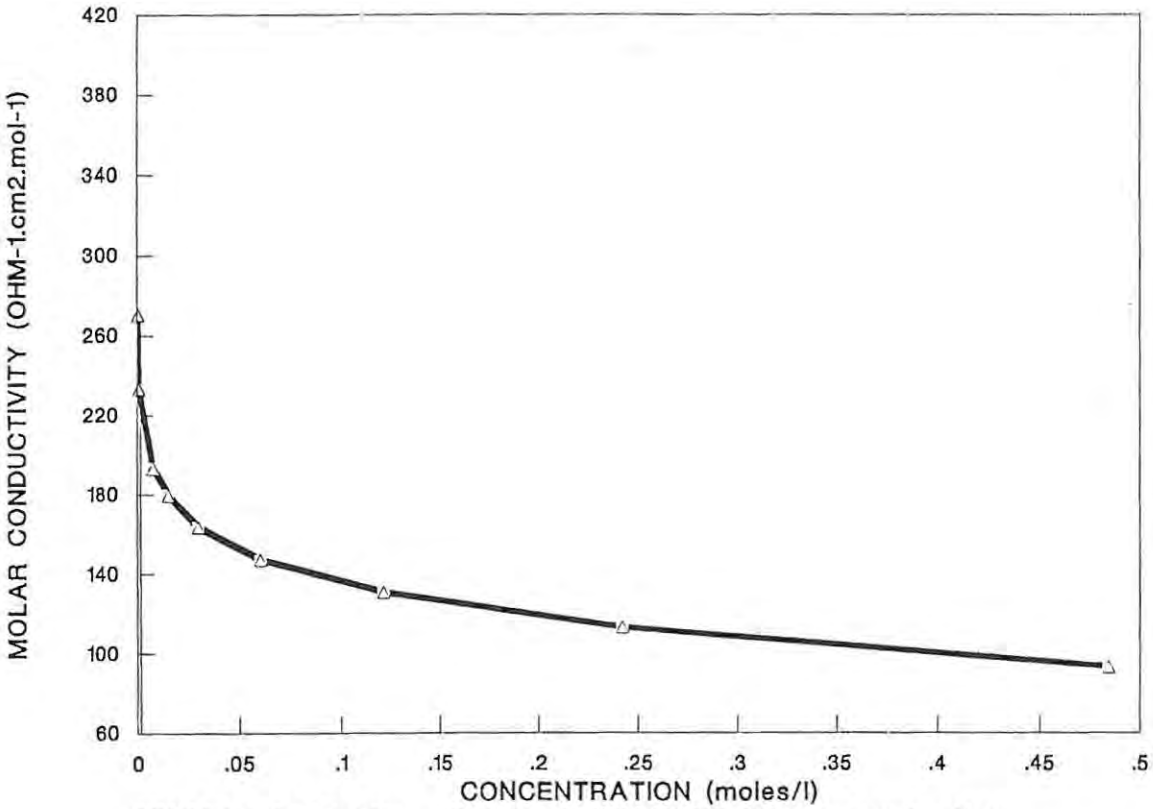

FIGURE 2.27 The effect of (NH4)2HPO4 concentration on the molar conductivity at 30 deg C.

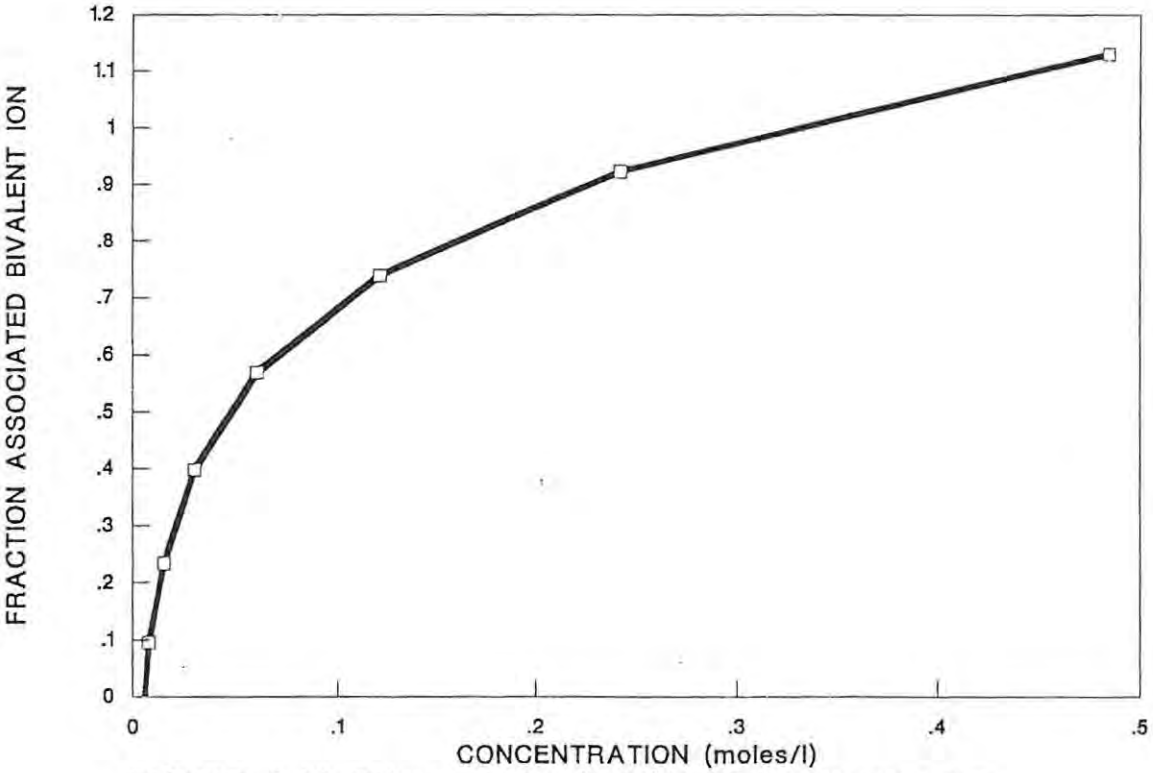

FIGURE 2.28 Effect of the (NH4)2HPO4 concentration on the fraction associated bivalent ion at 30 degC and unadjusted pH.

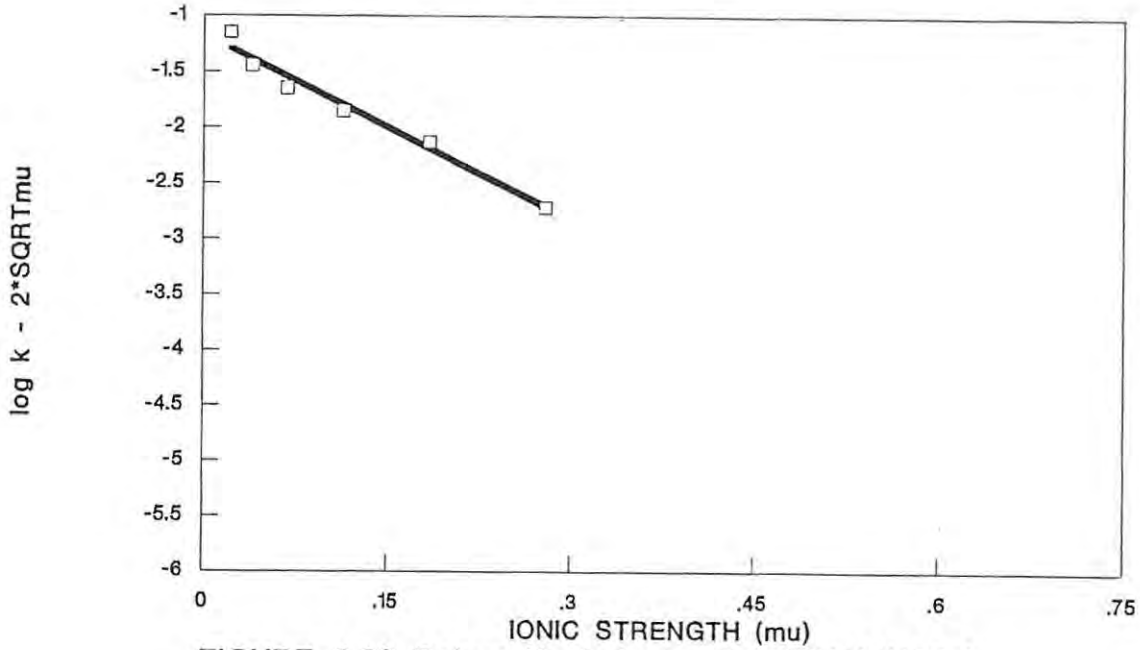

FIGURE 2.29 Debye-Huckel plot for (NH4)2HPO4.

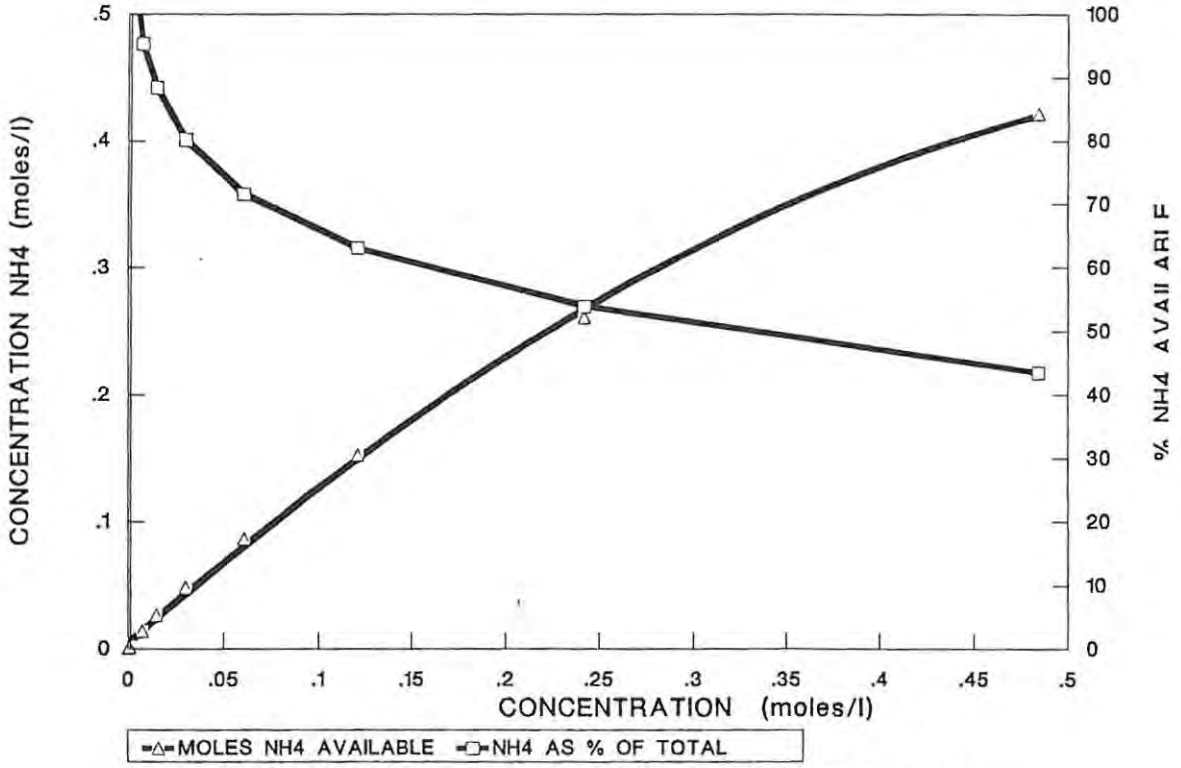

FIGURE 2.30 Effect of (NH4)2HPO4 concentration on the free NH4 concentration and % of total NH4 as unassociated NH4 at 30 deg C.

2.4.3 Effect of NH_4^+ on aspartokinase activity

Shaw *et al* (1983) showed that the activity of aspartokinase was activated by monovalent cations especially NH_4^+ and K^+. As this enzyme does not use NH_4^+ as a substrate, and as it is a key enzyme in the synthesis of lysine, it was decided to determine to what extent the activity of the enzyme is affected by the dissociation of the ammonium salt used.

Shaw *et al* (1983) calculated the aspartokinase K_m value for NH_4^+ to be 33mM at 1,6mM Mg^{2+} and 5mM ATP in *E. coli* B. As the levels of Mg^{2+} and ATP were not stoichiometric this value is possibly higher. On determining the K_m, for the total NH_4^+, of the aspartokinase of *Corynebacterium glutamicum*, the K_m value was found to be 16,24mM by a regression analysis on a Lineweaver-Burk plot (Figure 2.31B). For maximal activity a concentration of approximately 150mM was required (Figure 2.31A). From the Lineweaver-Burk plot the maximum activity was calculated to be 0,246 activity units.

The problem of the degree of dissociation of the ammonium salt in the enzyme assay was partially overcome by the preparation of the reagents, as the NH_4^+ source was NH_4Cl as a result of the reaction of the hydroxylamine hydrochloride with NH_4OH. The required NH_4^+ concentration was prepared by adding the required molar concentration of hydroxylamine hydrochloride and then adjusting the pH with NH_4OH. The extent of dissociation of NH_4Cl is far greater than that obtained with $(NH_4)_2SO_4$. The effect of the NH_4Cl concentration on the total specific conductivity and conductivity arising from the H^+ ions, or as a result of the further dissociation of the molecule at infinite dilution, is shown in Figures 2.32 and 2.33. The major effects of the conductivity arising from the H^+ ions is only evident at the very low concentrations, unlike $(NH_4)_2SO_4$. This is also evident from the effect of the NH_4Cl on the pH of the solution and the change in the H^+ concentration as a result of the change in the NH_4Cl concentration (Figures 2.34 and 2.35). The calculations for the dissociation of NH_4Cl were carried out as for classical univalent-univalent salts (Gladstone and Lewis, 1978). By calculating the fraction of NH_4Cl dissociated, it was possible to calculate the concentration of available NH_4^+ and the percentage of the total NH_4^+ available (Figures 2.36

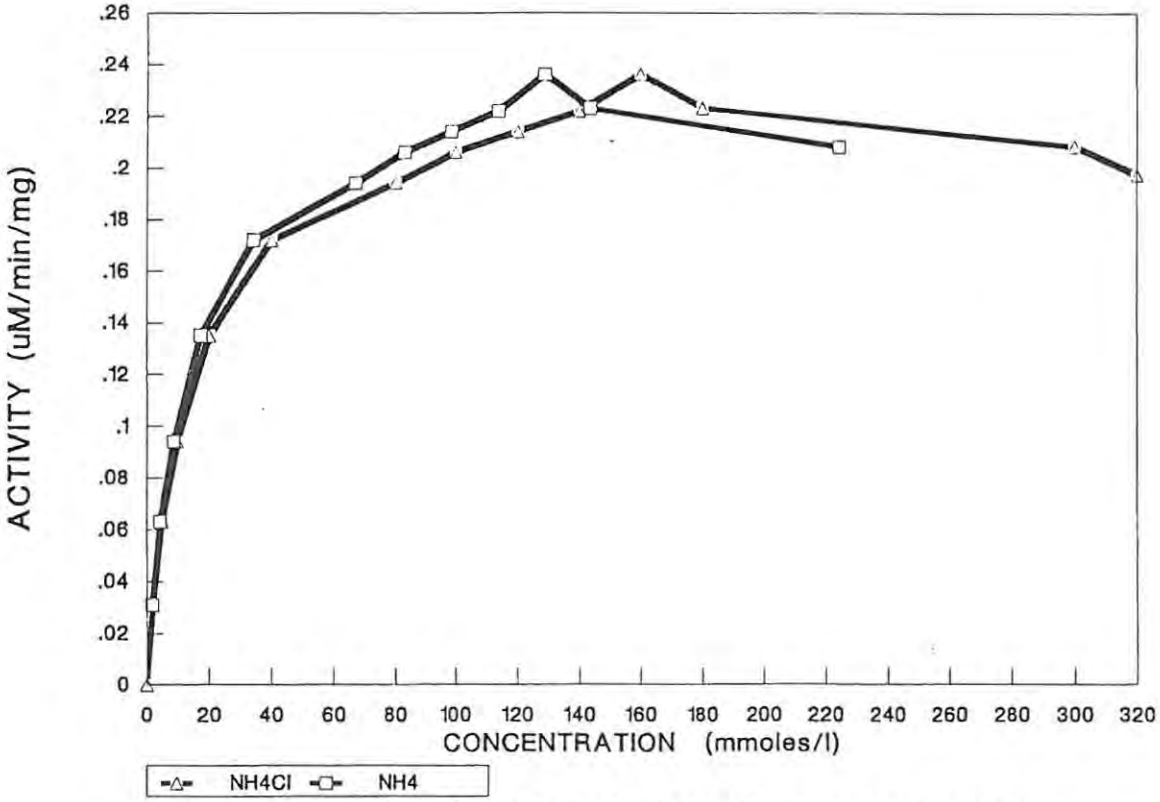

FIGURE 2.31A Effect of NH4Cl AND NH4 concentration on the aspartokinase activity.

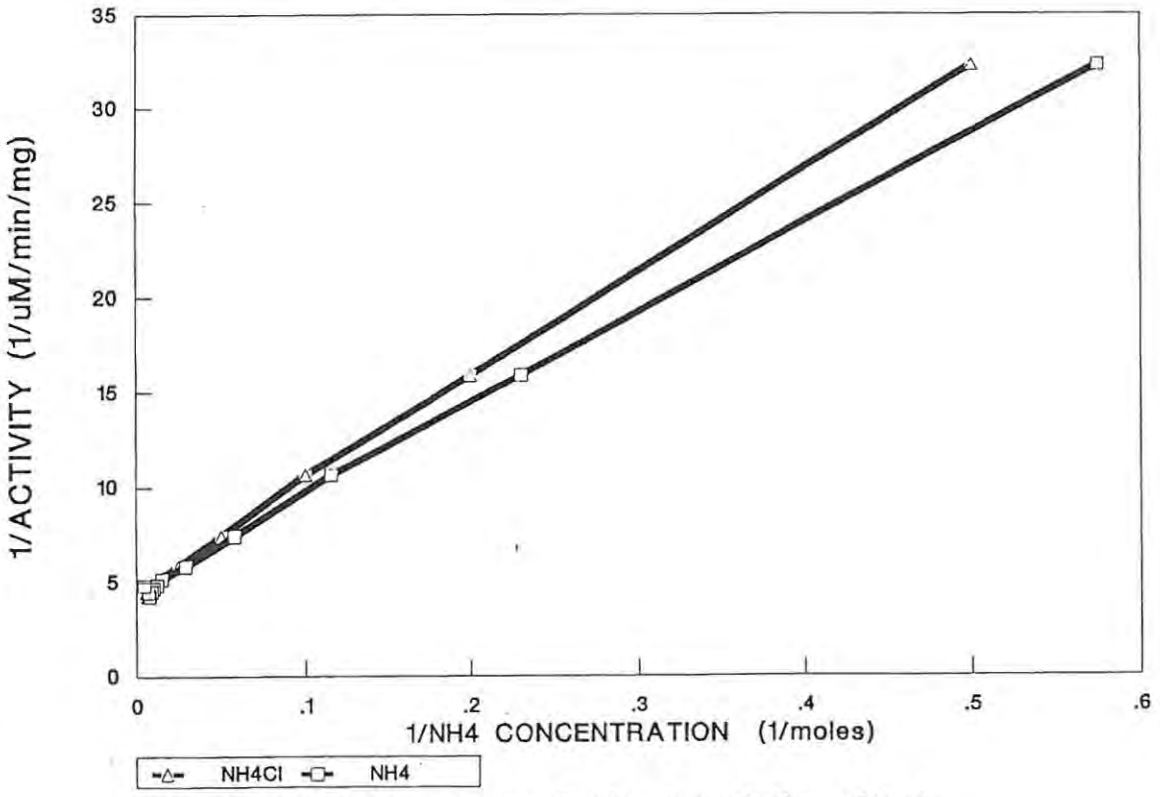

FIGURE 2.31B Lineweaver-Burk plot of the effect of NH4 on the aspartokinase activity.

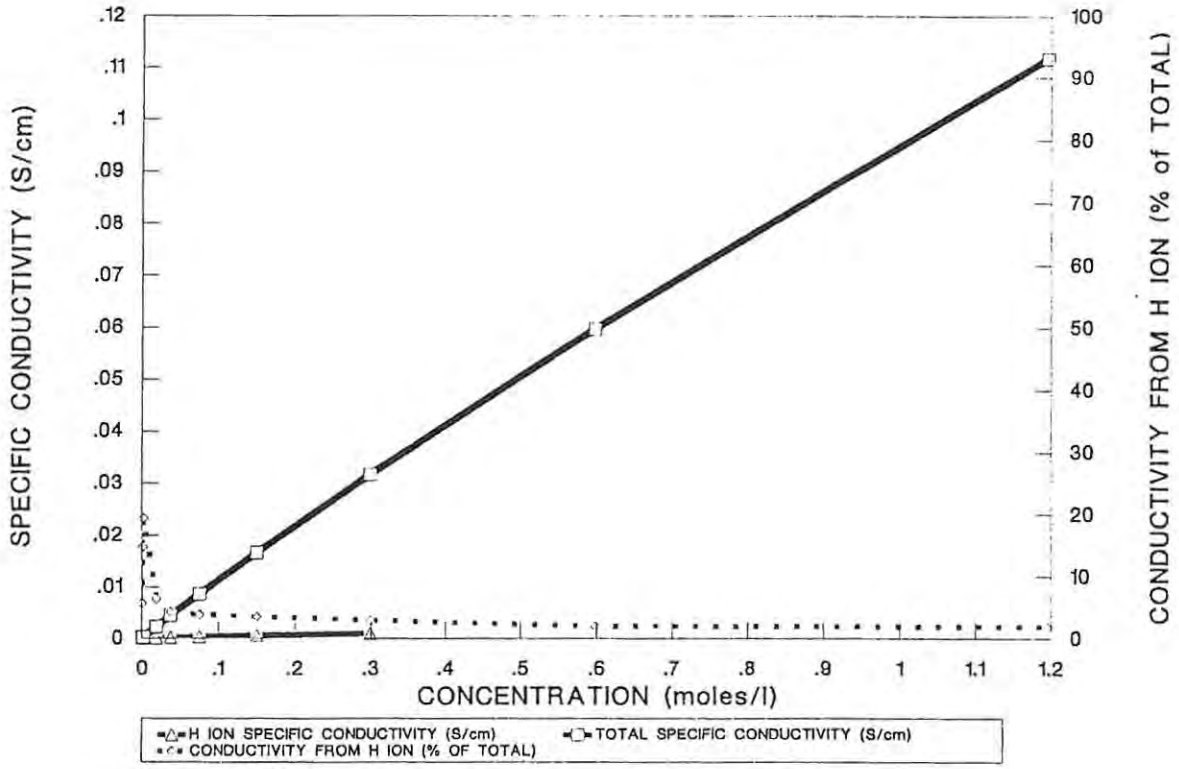

FIGURE 2.32 Effect of the NH4Cl concentration on the specific conductivity arising from the H Ions and the "normal" dissociation at 20 deg C.

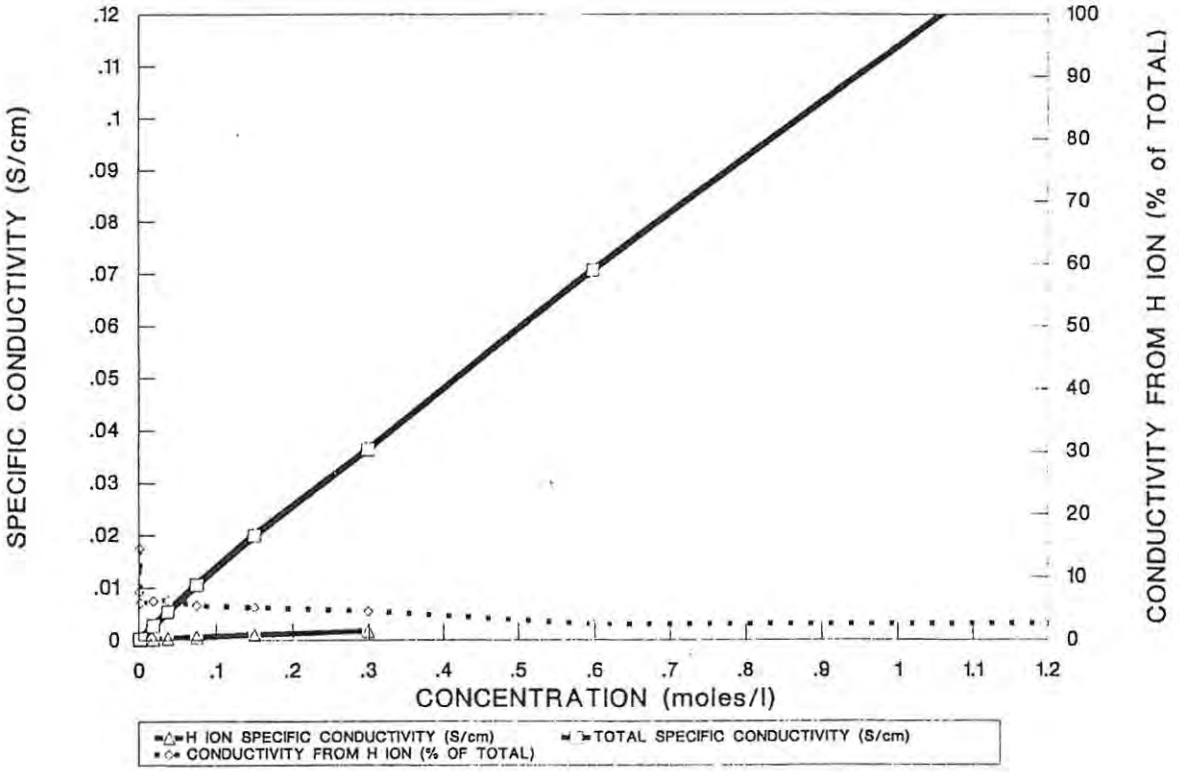

FIGURE 2.33 Effect of the NH4Cl concentration on the specific conductivity arising from the H Ions and the "normal" dissociation at 30 deg C.

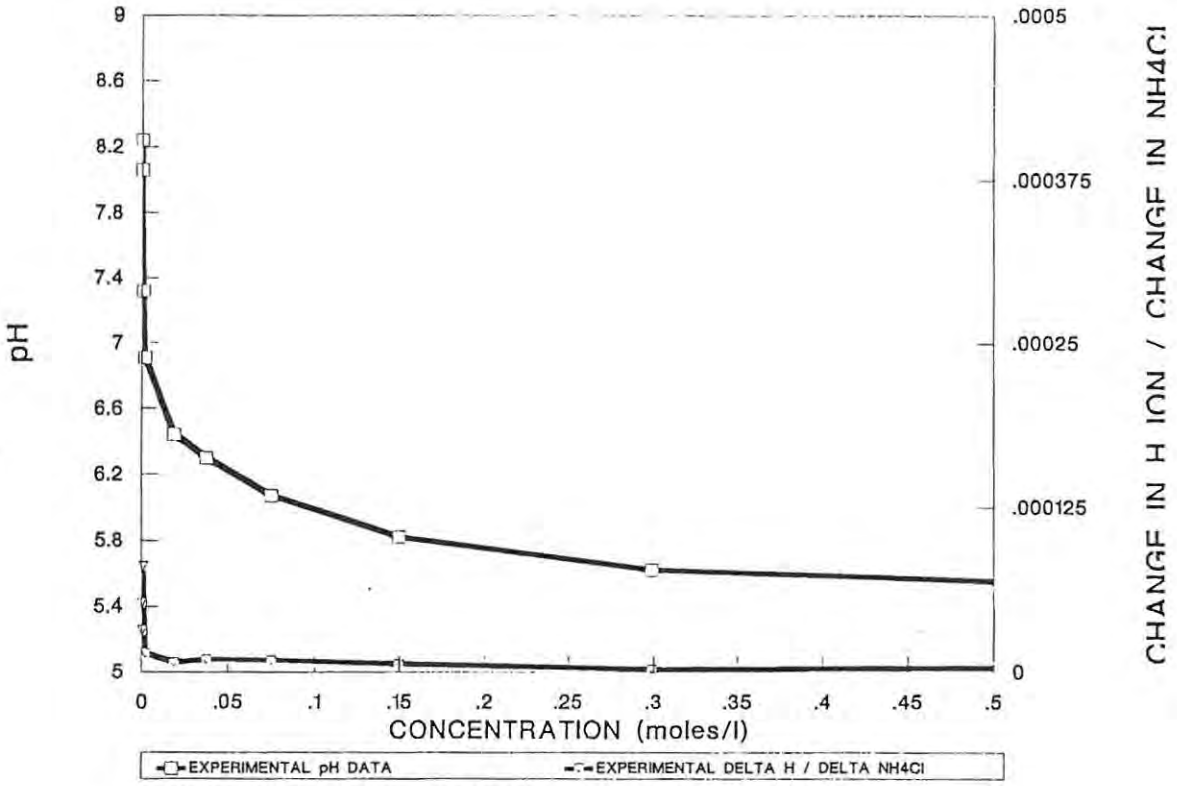

FIGURE 2.34 Effect of NH4CI concentration on the pH and the change in H ion concentration with a change in NH4CI concentration at 20 deg C.

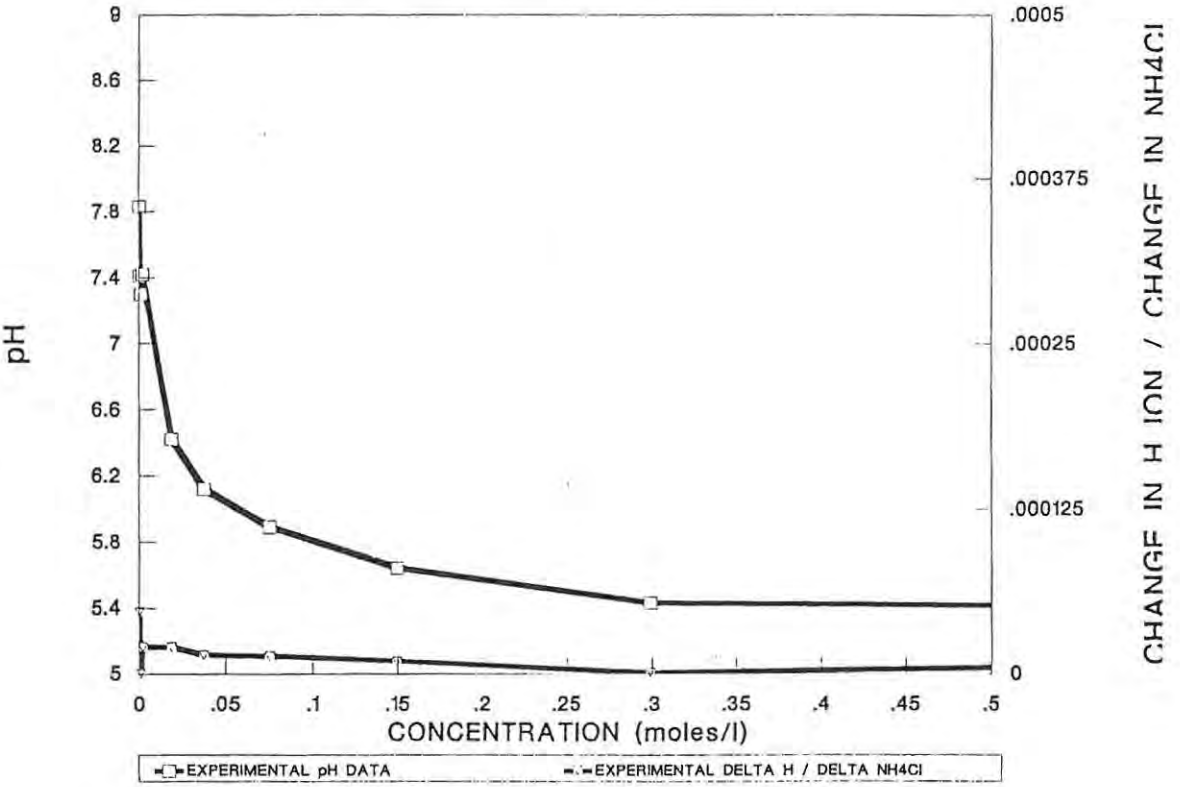

FIGURE 2.35 Effect of NH4CI concentration on the pH and the change in H ion concentration with a change in NH4CI concentration at 30 deg C.

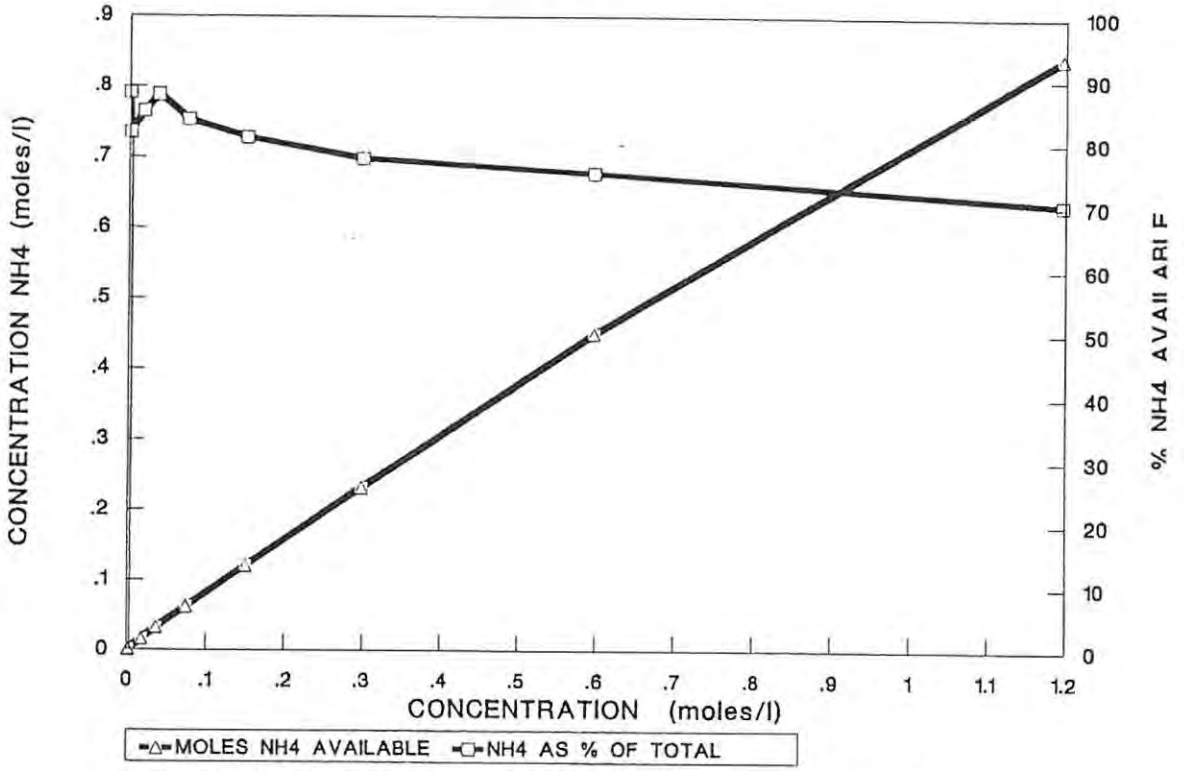

FIGURE 2.36 Effect of NH4Cl concentration on the free NH4 concentration and the % of total NH4 as unassociated NH4 at 20 deg C.

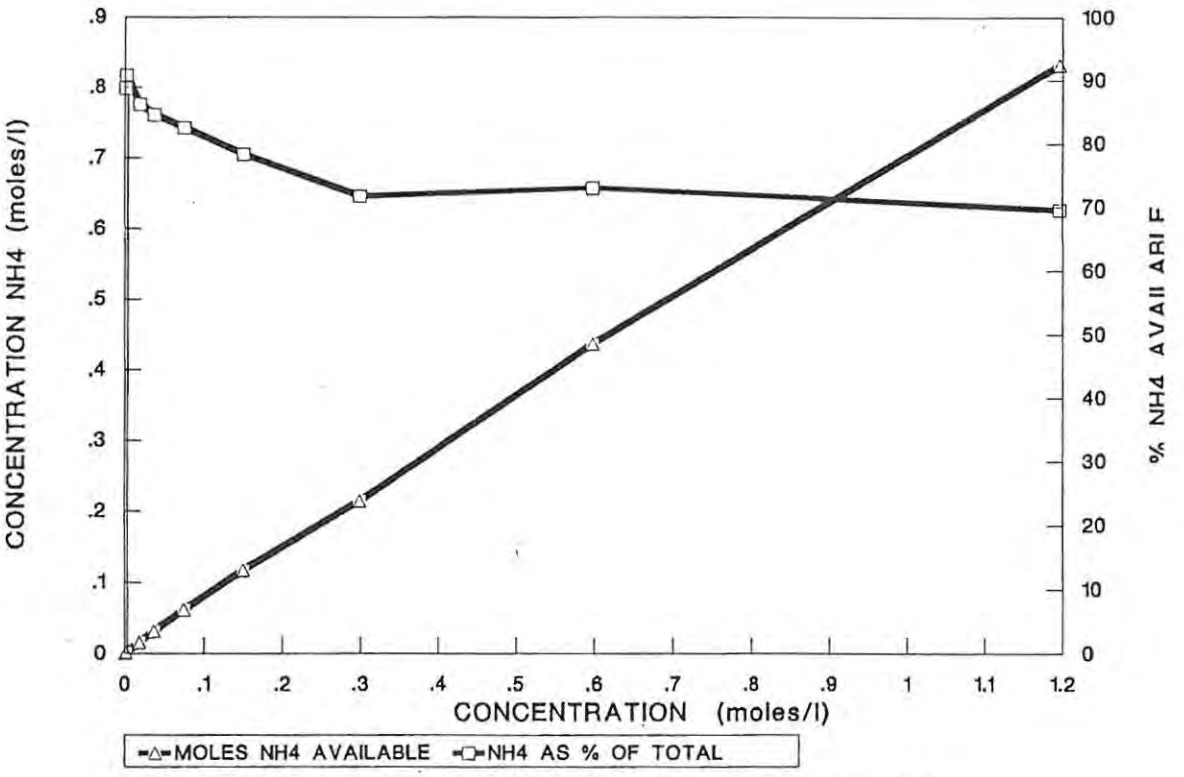

FIGURE 2.37 Effect of NH4Cl concentration on the free NH4 concentration and the % of total NH4 as unassociated NH4 at 30 deg C.

and 2.37). The fraction of the available NH_4^+ was determined from:

$$\alpha = {}^{\Lambda}/_{\Lambda_o} \qquad 13.$$

The value of Λ_o calculated from the limiting conductivities is 145,64 $\Omega^{-1}.cm^2.mol^{-1}$ at 20°C. By doing a regression analysis of a plot of the molar conductivity versus concentration, one finds a similar limiting equivalent conductivity to be approximately 151. This was done over the linear part of the curve and all of the concentrations other than the first two for both 20°C and 30°C (Figures 2.38 and 2.39).

The degree of dissociation of NH_4Cl at 30°C is approximately 90% at the lower concentrations, decreasing to 70% at the higher concentrations (Figure 2.37), thus making more NH_4^+ available to aspartokinase. This is however not the case for $(NH_4)_2SO_4$. At 30°C and pH 7,0, a 0,3 molar solution of $(NH_4)_2SO_4$ has approximately 350mM of NH_4^+ in solution. Ammonia is taken up in microorganisms by active transport. Therefore in a typical L-lysine fermentation broth containing 40g/l $(NH_4)_2SO_4$ (0,3M), 350mM of NH_4^+ are available for maximal activity. As all the $(NH_4)_2SO_4$ is put into the initial charge in fed-batch fermentations (Appendix I) as soon as the feeds are started, the $(NH_4)_2SO_4$ is diluted and therefore the rate of activity of aspartokinase is reduced. As the NH_4^+ is utilized for lysine synthesis the SO_4^- becomes the counter-ion for the resulting L-lysine formed and the free ammonium ion concentration decreases. The lysine is synthesized in the +1 form at pH 7,2.

It is therefore conceivable that the single most important cause of the reduction of the fermentation rate is the availability of NH_4^+ to aspartokinase and other enzymes such as glutamate dehydrogenase and glutamine synthetase. The glutamate dehydrogenase and glutamine synthetase are the key enzymes in the assimilation of NH_4^+.

2.4.4 Effect of $(NH_4)_2SO_4$ concentration on fed-batch fermentation

Two fed-batch fermentations were run using *Corynebacterium glutamicum* FP6 to produce L-lysine using culture media as outlined in Appendix I. The

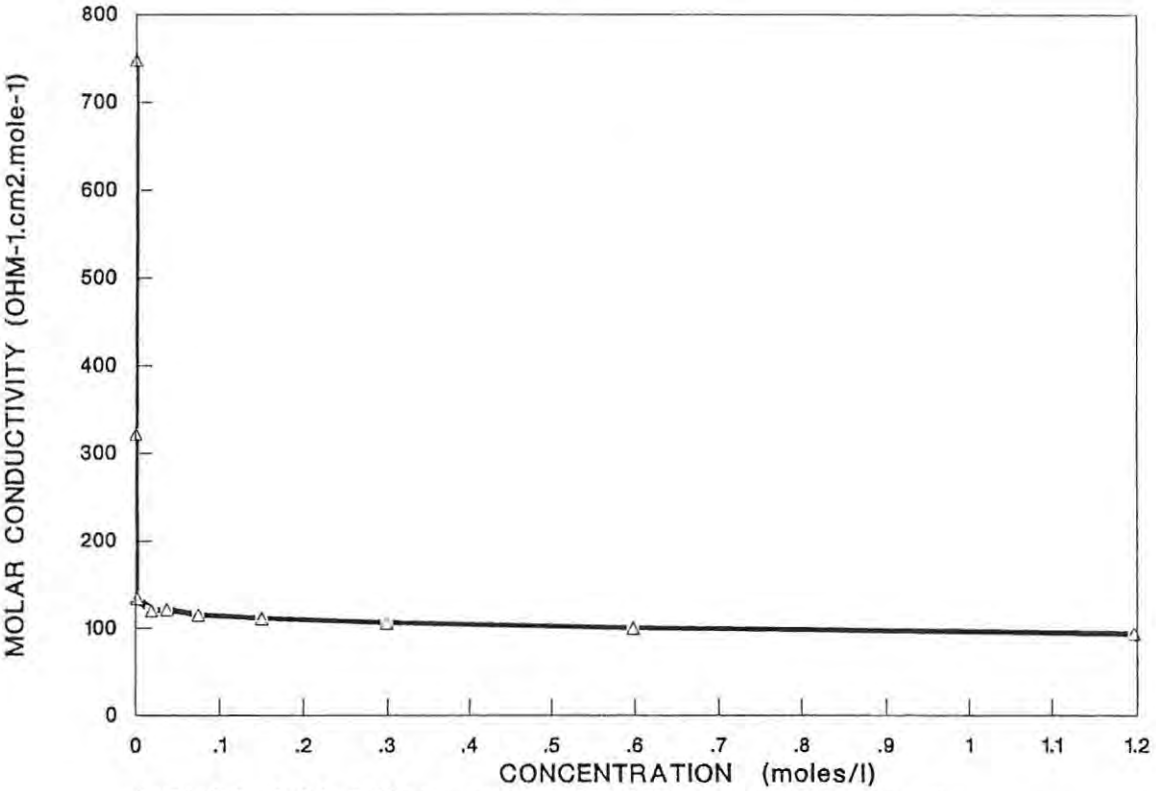

FIGURE 2.38 Effect of the NH4Cl concentration the molar conductivity at 20 deg C and unadjusted pH.

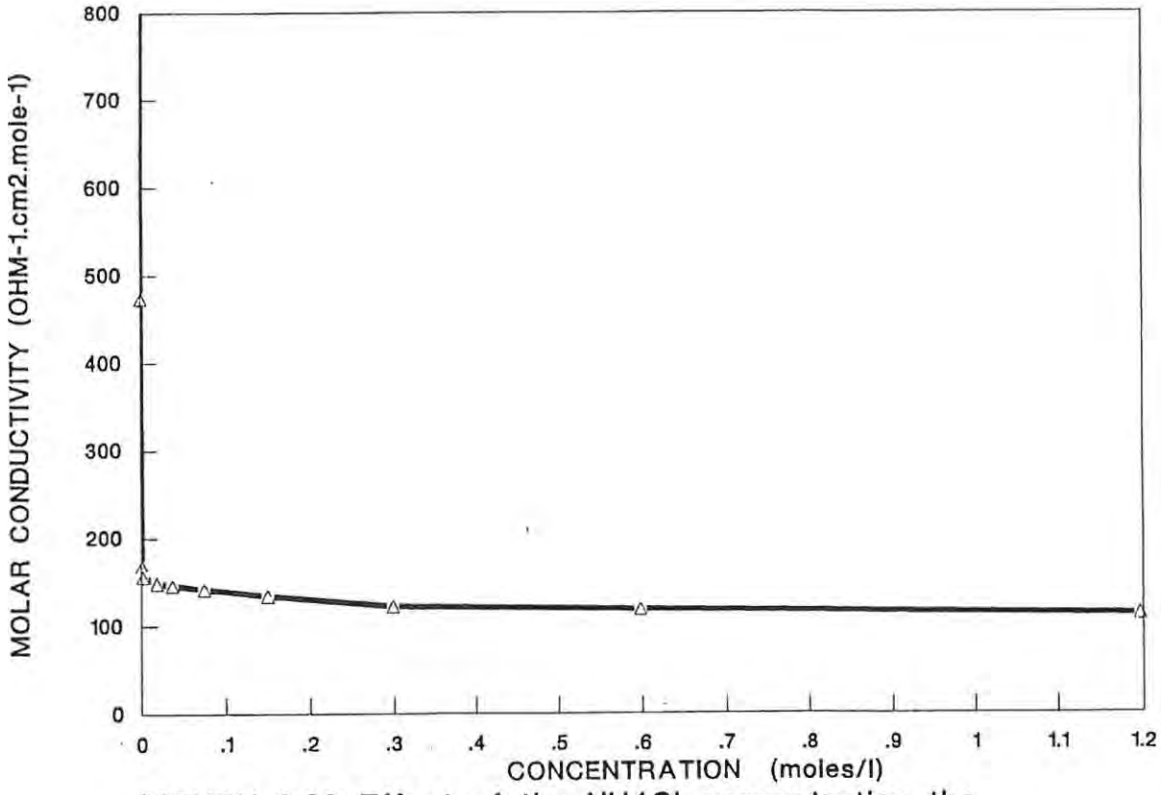

FIGURE 2.39 Effect of the NH4Cl concentration the molar conductivity at 30 deg C and unadjusted pH.

$(NH_4)_2SO_4$ concentration and the mode of addition of $(NH_4)_2SO_4$ in each was different. In the one fermentation 30g/l $(NH_4)_2SO_4$ (0,23M) was added, all of which was contained in the initial charge. In the second fermentation a total of 40g/l $(NH_4)_2SO_4$ (0,30M) was added. This concentration was added to both the initial charge and the second feed to ensure that the $(NH_4)_2SO_4$ concentration was maintained at approximately 40g/l throughout the fermentation.

The results of these fermentations are outlined in Figure 2.40 (30g/l fermentation) and Figure 2.41 (40g/l fermentation). On comparison of these data it is clearly evident that the overall rate of lysine synthesis in the 40g/l fermentation is a great deal higher than in the 30g/l fermentation: 1,0g/l/hr as compared to 0,69g/l/hr. The $(NH_4)_2SO_4$ concentration appears to affect the rate of fermentation but also the final yield which was found to be 0,325g/g in the case of the 40g/l fermentation and 0,290g/g in the case of the 30g/l fermentation. In the case of the 40g/l fermentation the maximum rate of lysine synthesis also attained a level of 1,60g/l/hr whereas in the case of the 30g/l fermentation this was only around the overall rate of lysine synthesis, namely 0,69g/l/hr. The maximum rate of lysine synthesis was calculated from the linear part of the synthesis curve.

Assuming that the dissociation of $(NH_4)_2SO_4$ in complex media is not that dissimilar to its dissociation in H_2O, at 40g/l $(NH_4)_2SO_4$ (0,303M) approximately 350mM of NH_4^+ would be available for aspartokinase activity, that is, maximal aspartokinase activity. At 30g/l $(NH_4)_2SO_4$ of the final fermentation volume, the initial charge has 54,54g/l of $(NH_4)_2SO_4$ and this is reduced to 30g/l by the feeds. At 30g/l approximately 300mM of NH_4^+ are available for aspartokinase activity. However as lysine synthesis proceeds and a greater proportion of the SO_4^- is associated with the lysine, less free NH_4^+ becomes available for maintaining maximal activity.

2.5 CONCLUSION

Using Debye-Hückel theory and conductivity analysis it is proposed that NH_4Cl, $(NH_4)_2SO_4$ and $(NH_4)_2HPO_4$ dissociate differently with decreasing

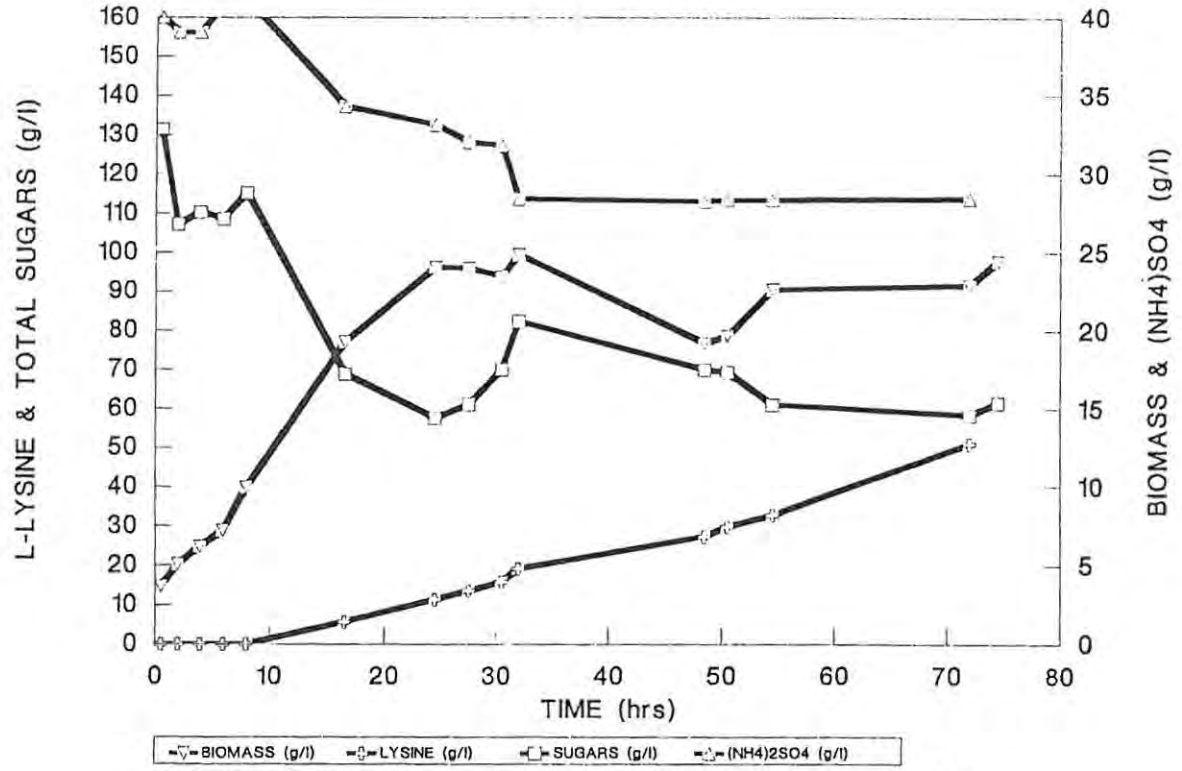

FIGURE 2.40 Effect of the (NH4)2SO4 concentration on the fermentation by C glutamicum. Initial (NH4)2SO4 concentration 40 g/l ending at 28.4 g/l.

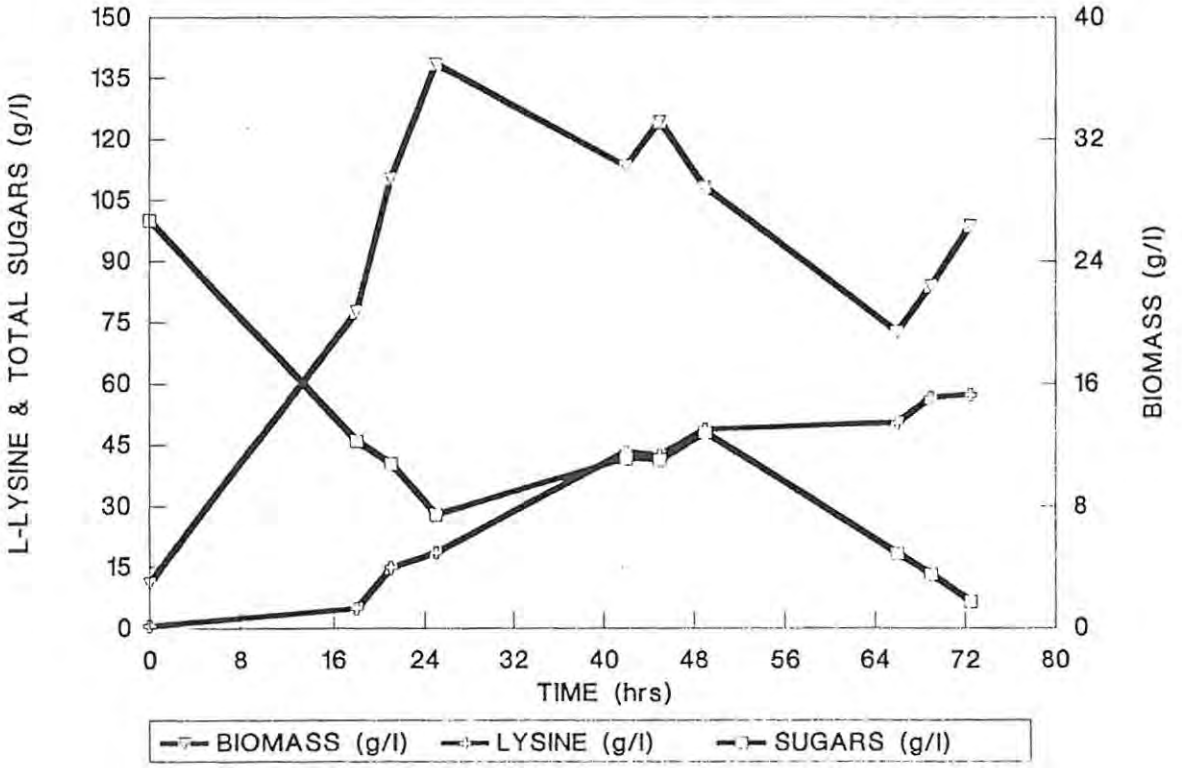

FIGURE 2.41 Effect of the (NH4)2SO4 concentration on the fermentation by C glutamicum. (NH4)2SO4 concentration maintained at 40 (g/l)

concentration. The following models are therefore proposed for their dissociation in solutions tending towards infinite dilution:

$$NH_3 + H^+ + Cl^-:NH_4^+ + Cl^-:NH_4Cl$$

Infinite dilution

$$2NH_3 + 2H^+ + SO_4^{--}:NH_3 + NH_4^+ + H^+ + SO_4^{--}:2NH_4^+ + SO_4^{--}:NH_4^+ + NH_4SO_4^-:(NH_4)_2SO_4$$

Infinite dilution

$$2NH_3 + H_3PO_4:NH_3 + NH_4^+ + H_2PO_4^-:2NH_4^+ + HPO_4^{--}$$

Infinite dilution

The major difference between the three compounds in solution is that $(NH_4)_2HPO_4$ does not affect the pH especially at the lower concentrations. The molar conductivity towards infinite dilution can be accounted for by the sum of limiting equivalent conductivities of the ions, $2NH_4^+$ and HPO_4^{--}. In the case of NH_4Cl and $(NH_4)_2SO_4$ there is a change in pH of the solution at lower concentrations, as a result of H^+ ions; however the effect only occurs at the extremely low concentrations in the case of NH_4Cl.

The dissociation of $(NH_4)_2SO_4$ affects not only enzymes such as aspartokinase where it plays no role as a substrate in the reaction, but also affects the overall physiology of the cell during lysine synthesis by *Corynebacterium glutamicum* FP6. As the organism utilizes the ammonia which is present in the culture media, the lysine which is concomitantly synthesized is liberated into the media. One mole of lysine is synthesized per 2 moles of ammonia (1 mole $(NH_4)_2SO_4$). As the fermentations are carried out at pH 7,2, at which pH the lysine is predominantly in the +1 form, 1 mole of lysine then associates with the SO_4^{--} creating a demand for an additional ion which is supplied as NH_4^+ via pH control, with NH_4OH. Since the counter-ion equivalents are utilized by the lysine synthesis there is therefore a reduction of the NH_4^+ concentration. Therefore the free NH_4^+ concentration available for use

44/...

either enzymatically or physiologically by the organism is also reduced. This will be elaborated on in Chapter 5.

CHAPTER 3

THE EFFECT OF THE FREE NH_4^+ AND ANIONIC COUNTER-ION CONCENTRATION ON LYSINE SYNTHESIS BY *CORYNEBACTERIUM GLUTAMICUM* FP6

3.1 SUMMARY

During the production of L-lysine by *Corynebacterium glutamicum* FP6, the lysine is produced in the +1 ionised form, which then associates with an available anionic counter-ion in solution. The quantity of lysine produced is dependent on the availability of the counter-ion in solution and the concentration of free NH_4^+. The concentration of free NH_4^+ changes as the ammonia is utilized for lysine synthesis and is displaced on the counter-ion by the lysine. It appears that as the concentration of free NH_4^+ drops below 150mM, both the rate of biomass synthesis and lysine synthesis decrease. The dissociation of the ammonium salt and the rate of utilization of the free ammonium ion are therefore of major importance in maintaining a maximum rate of lysine synthesis.

3.2 INTRODUCTION

L-lysine is an amphoteric molecule which may exist in the +2, +1, 0 or -1 ionic forms, depending on the pH of the solution. Lysine exists in the +1 ionic form at pH 7,2 which is the fermentation pH for *Corynebacterium glutamicum* to produce lysine (Lehninger, 1978). During fermentation, as the lysine is produced from the carbohydrate supplied, the ammonia required for lysine synthesis is supplied in the form of an ammonium salt (e.g. NH_4Cl, $(NH_4)_2HPO_4$ or $(NH_4)_2SO_4$), and supplemented with NH_4OH as a result of pH control. The lysine that is produced then associates with the anionic counter-ion which has been made available as a result of the NH_4^+ utilization. Unless additional NH_4^+ and counter-ion is added there is a depletion of the NH_4^+ concentration with the concomitant increase in lysine associated anionic counter-ion.

Depending on the type of ammonium salt being utilized there are a range of counter-ions available for the lysine to associate with in solution.

$$NH_4Cl \underset{k_1}{\overset{k_2}{\rightleftarrows}} NH_4^+ + Cl^-$$

$$(NH_4)_2HPO_4 \underset{k1}{\overset{k_2}{\rightleftarrows}} NH_4^+ + NH_4HPO_4^- \underset{k3}{\overset{k_4}{\rightleftarrows}} 2NH_4^+ + HPO_4^-$$

The lysine may therefore exist in solution, either singularly associated with the monovalent anionic form in conjunction with the ammonium ion, or associated in pairs with the divalent anion.

Several questions, relating to lysine synthesis and the free NH_4^+ concentration, are raised by these dissociation patterns:

1) What effect does the free ammonium ion concentration have on the rate of lysine synthesis?

2) Does the association of the lysine with the monovalent anionic species (in the case of $(NH_4)_2HPO_4$) drive the equilibrium towards the divalent anion, to allow the further association of another lysine molecule, and does the anion associated NH_4^+ become unavailable for lysine synthesis?

3) As the concentration of lysine increases does it cause the further association of the free NH_4^+ with the mono- or di-valent anions?

A series of experiments were therefore set up to determine the effect of the NH_4Cl or $(NH_4)_2HPO_4$ concentrations on the production of lysine by *C. glutamicum* FP6.

3.3 MATERIALS AND METHODS

3.3.1 Effect of NH_4Cl and $(NH_4)_2HPO_4$ on L-lysine fermentation

Fermentations were carried out to determine the effect of the ammonium salt and its concentration on the ability of *C. glutamicum* FP6 to produce

L-lysine by fed-batch fermentation. The ammonium salts used were NH_4Cl and $(NH_4)_2HPO_4$ at varying concentrations. The culture media used are as outlined in Appendices I and IV. All bacterial cultures were stored on LM agar and then used for inoculation of fermentation broth as outlined in Appendix IV. This broth was then used to inoculate the prefermentation stage of the fermentation (3 x 330ml) in 1 litre flasks. All shake-flask cultures were incubated at 30°C on a rotary shaker at 160rpm. In all fermentations, pH control was carried out by on-line addition of a 5,88 molar solution of NH_4OH. The following concentrations of ammonium salts were utilized:

AMMONIUM SALT	CONCENTRATION (g/l)
NH_4Cl	9,63
NH_4Cl	14,98
$(NH_4)_2HPO_4$	0
$(NH_4)_2HPO_4$	14,7
$(NH_4)_2HPO_4$	17,0
$(NH_4)_2HPO_4$	22,0
$(NH_4)_2HPO_4$	25,6
$(NH_4)_2HPO_4$	40,0

3.3.2 Analytical techniques

During the course of the fermentation, samples were aseptically withdrawn and the biomass, L-lysine, glucose, fructose and sucrose concentrations were determined as outlined in Chapter 2, section 2.3.4.1.

3.3.3 Dissociation of NH_4Cl and $(NH_4)_2HPO_4$

The dissociation of NH_4Cl and $(NH_4)_2HPO_4$ was calculated as outlined in Chapter 2. The following are definitions of terms utilized in the text:

Total NH_4^+ = total concentration of NH_4 added to the fermentation as the ammonium salt and as

NH_4OH for pH control

Residual NH_4^+ = total NH_4^+ minus the NH_4^+ that has been utilized for lysine synthesis

Free NH_4^+ = residual NH_4^+ calculated to a $(NH_4)_2HPO_4$ or NH_4Cl concentration and then converted to dissociated NH_4^+ using the dissociation theory as outlined in Chapter 2. This takes into account the NH_4^+ that has been utilized for lysine synthesis. It must be stressed that it has been assumed that the dissociation of these ammonium salts behaves similarly in culture media as in demineralised nanopure water.

3.4 RESULTS AND DISCUSSION

3.4.1 Effect of NH_4Cl concentration on L-lysine synthesis

Two fermentations were run using NH_4Cl as the source of counter-ion and NH_4^+ for lysine synthesis. The concentrations used were 9,45g/l and 14,91g/l (0,18M and 0,28M), expressed as a function of the final fermentation volume and not of the initial charge. The fermentation profiles in terms of biomass, lysine and sugars utilized are indicated in Figures 3.1 to 3.6. Also shown is the quantity of L-lysine produced as a function of the NH_4Cl added and as a function of the dissociated NH_4Cl, which is equivalent to the free NH_4^+ concentration. The maximum concentration of lysine produced per mole of NH_4Cl is of the order of 1,0 mole/mole NH_4Cl added and 1,1 mole/mole of dissociated NH_4Cl. Since the dissociation of NH_4Cl at concentrations ranging from 0,18M and 0,28M is of the order of 0,7 (Chapter 2), it would appear that lysine causes further dissociation of NH_4Cl. As the quantity of lysine produced can be greater than 1 mole lysine per mole of counter-ion, low levels of ammonium salts and other counter-ions possibly exist in the corn steep liquor (Figures 3.3 and 3.4).

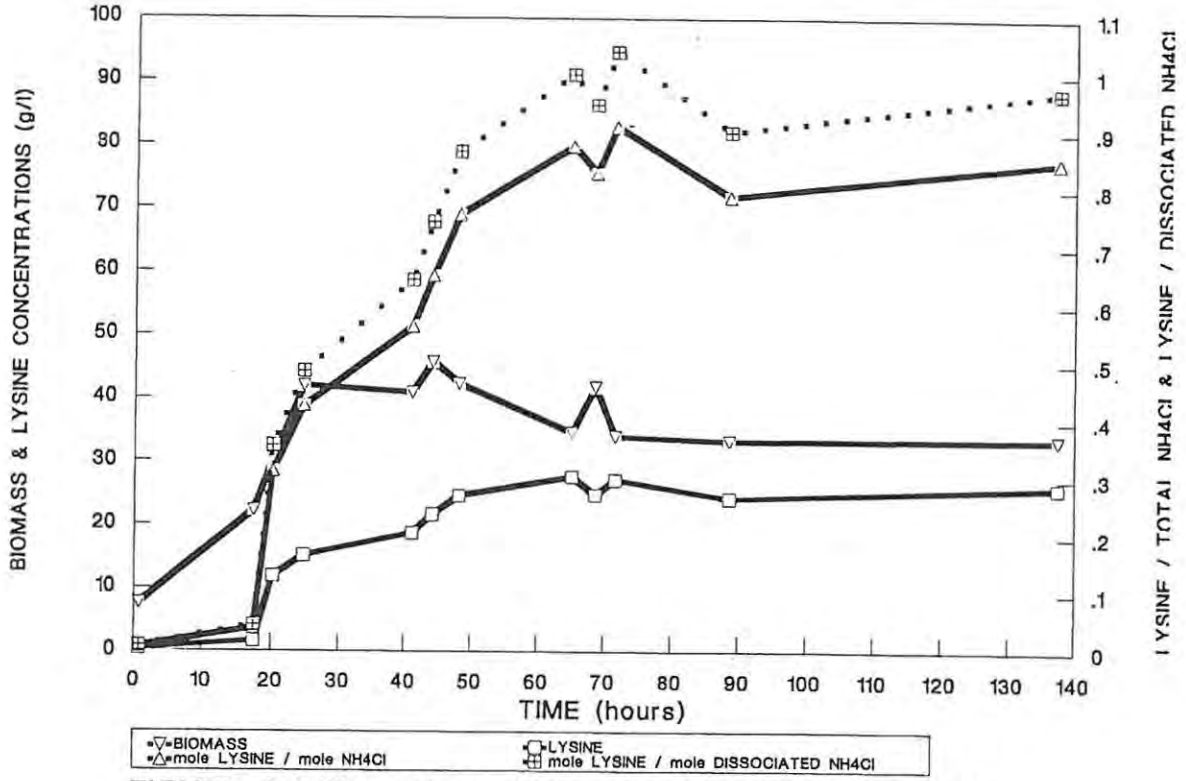

FIGURE 3.1 The effect of the NH4Cl concentration on the lysine and biomass production. Final NH4Cl concentration 9.45 g/l.

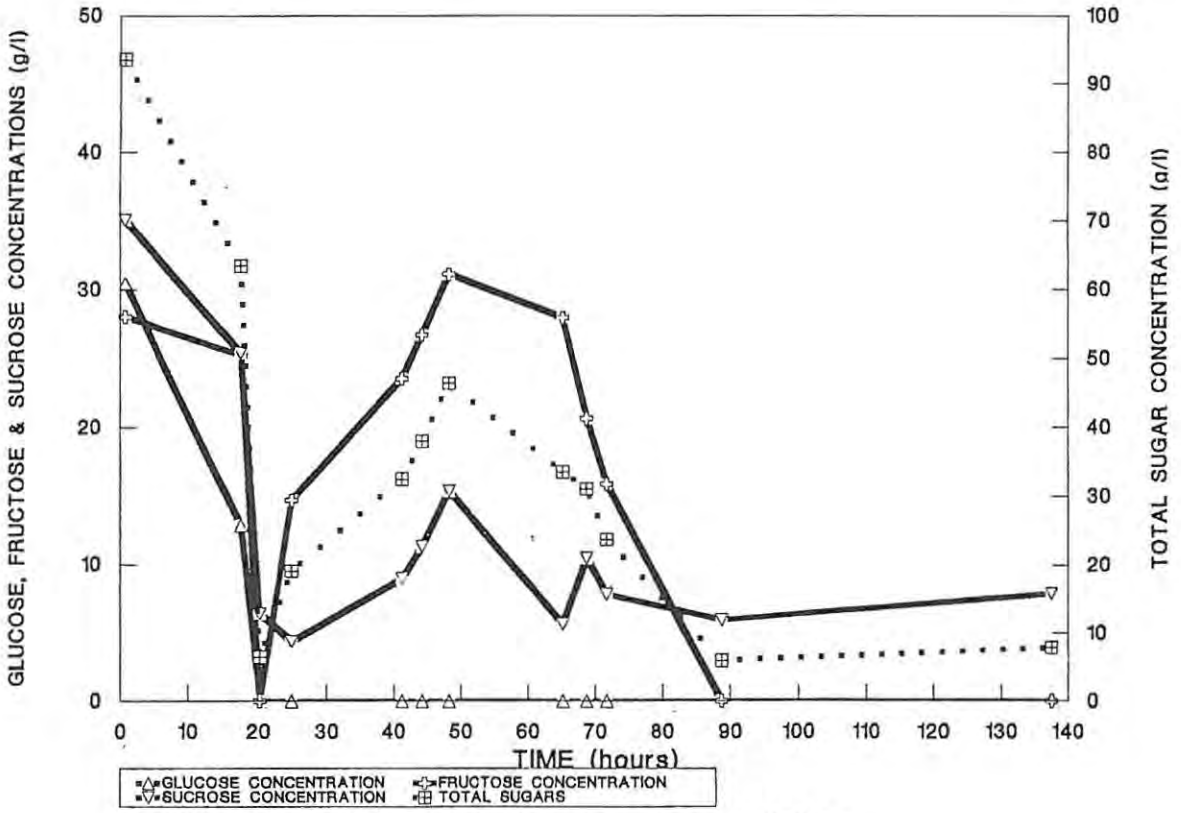

FIGURE 3.2 Sugar profiles during fermentation. Final NH4Cl concentration 9.45 g/l.

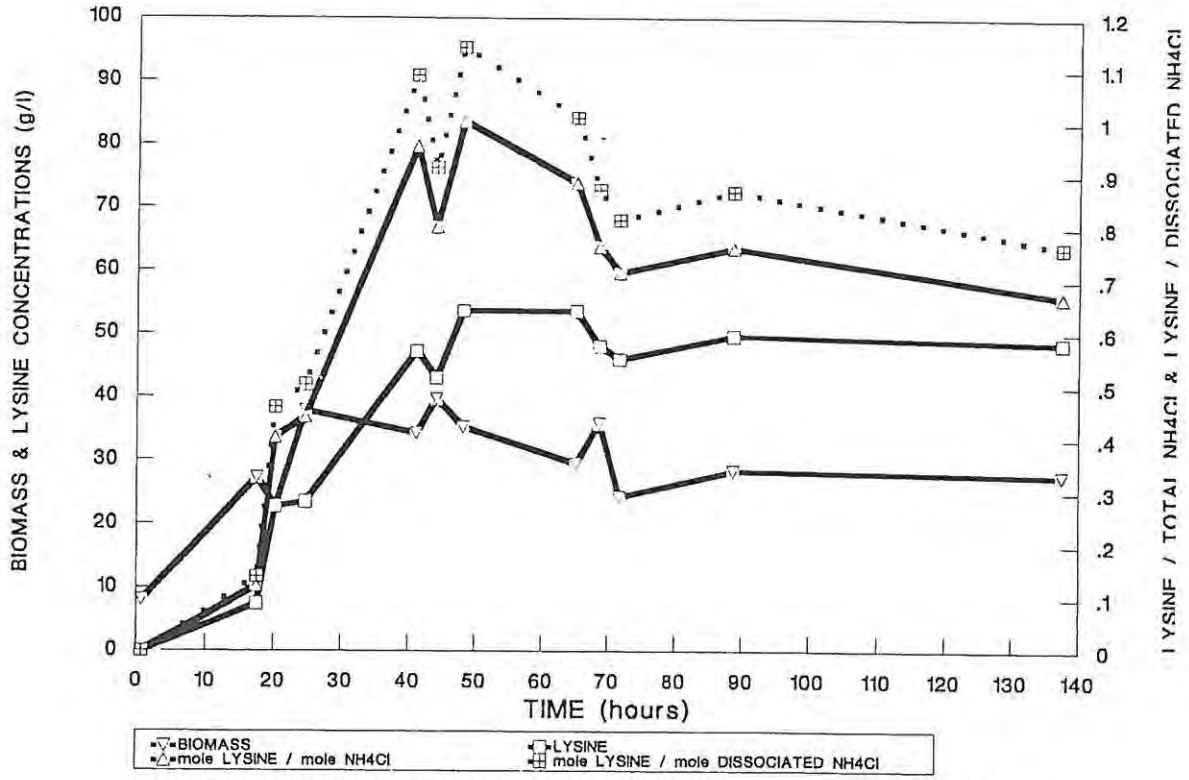

FIGURE 3.3 The effect of the NH4Cl concentration on the lysine and biomass production. Final NH4Cl concentration 14.91 g/l.

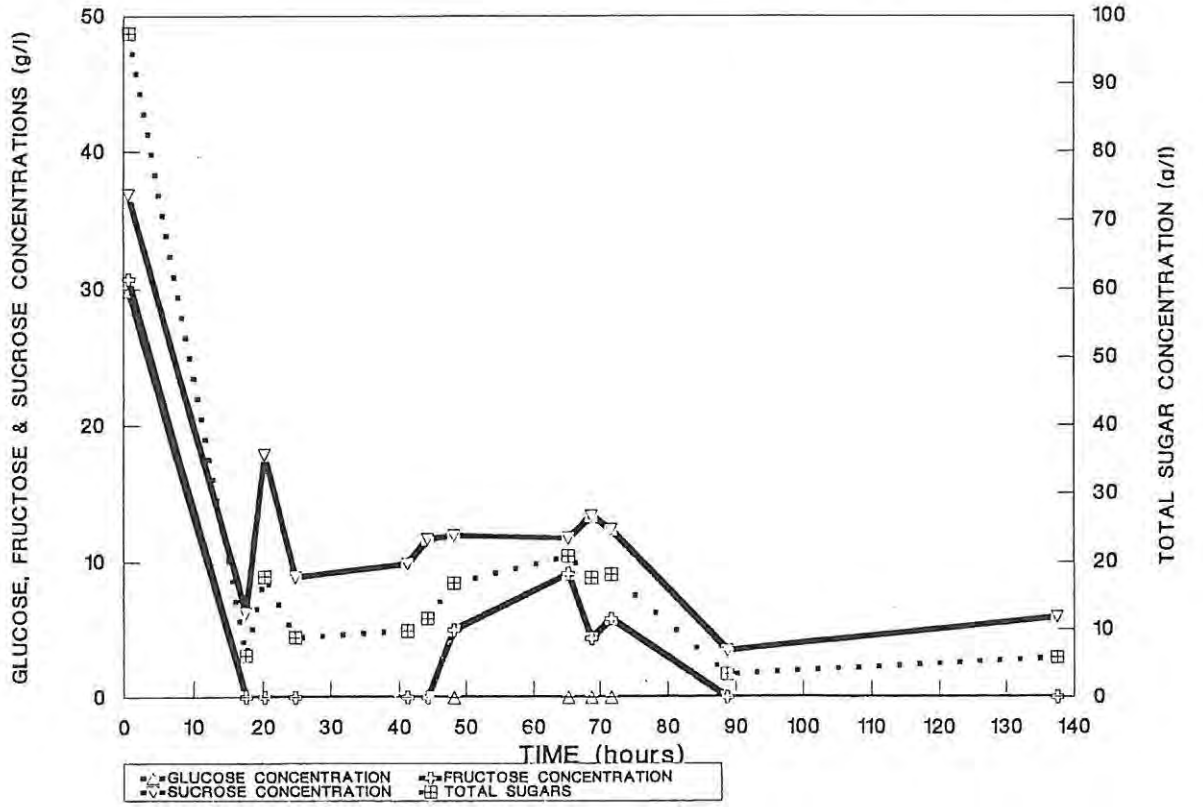

FIGURE 3.4 Sugar profiles during fermentation. Final NH4Cl concentration 14.91 g/l.

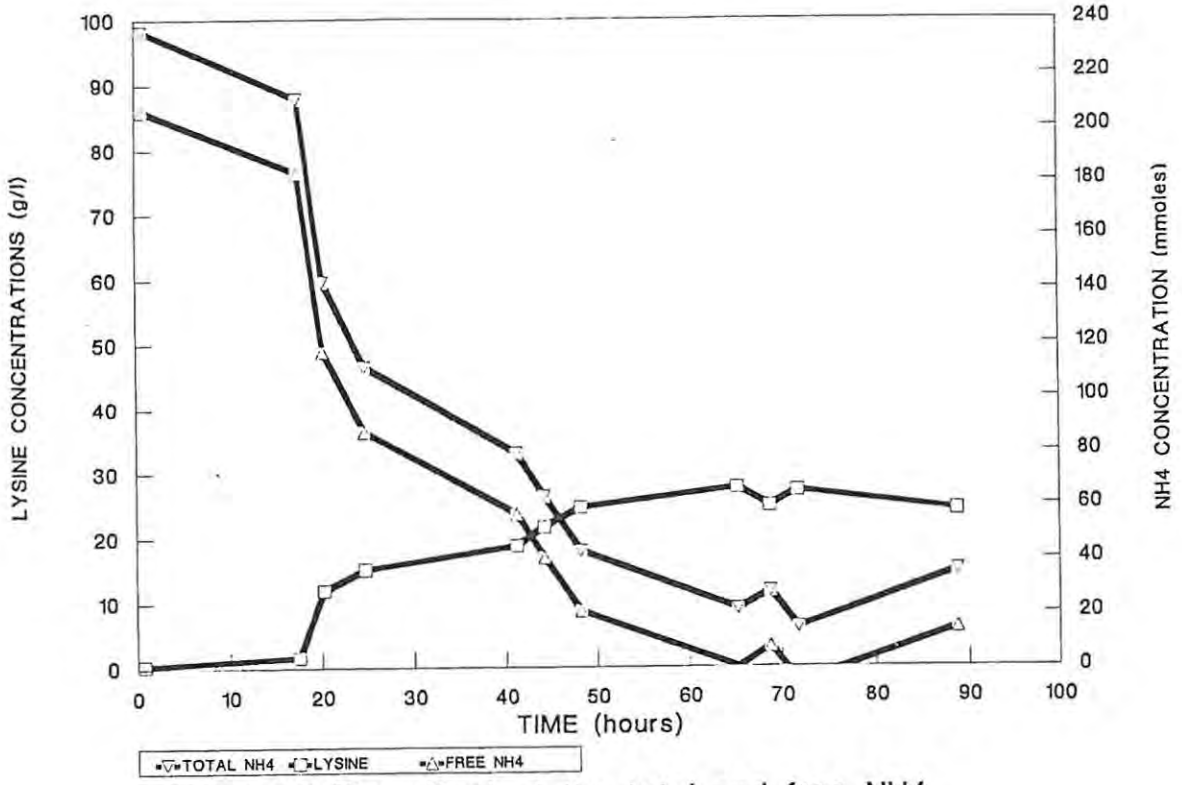

FIGURE 3.5 The effect of the total and free NH4 concentration on lysine synthesis. Final NH4Cl concentration 9.45 g/l.

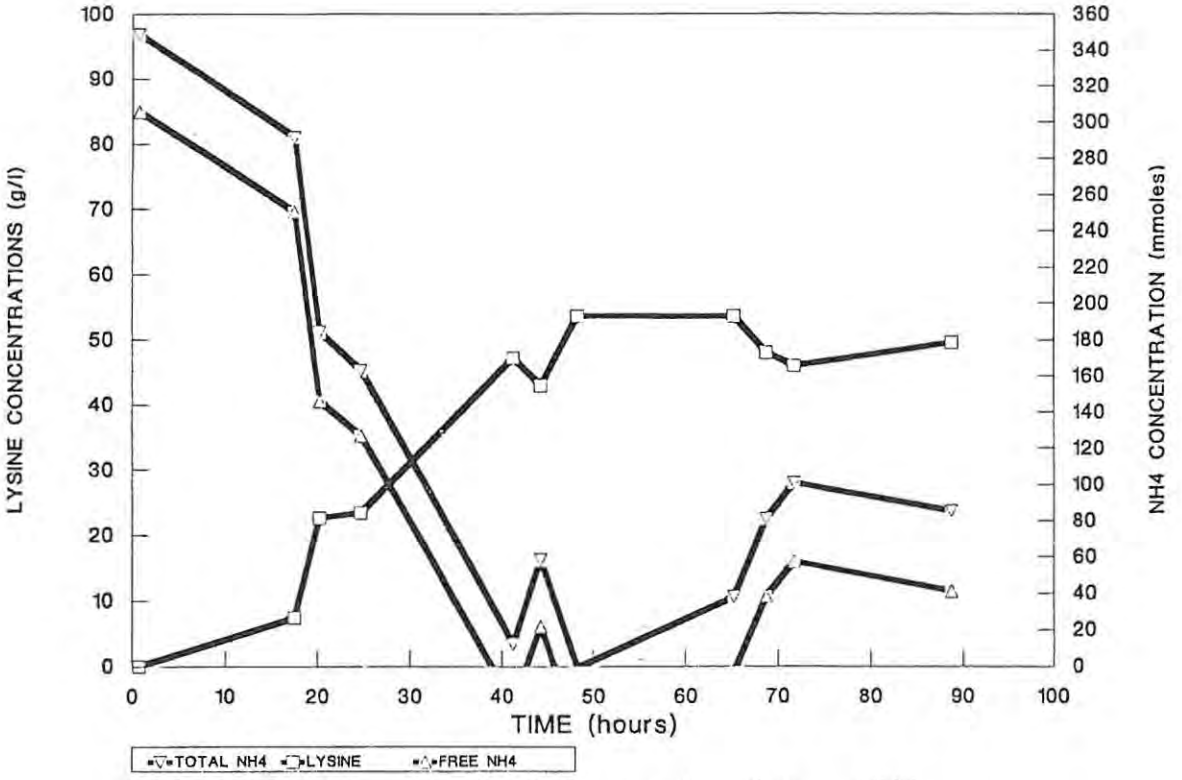

FIGURE 3.6 The effect of the total and free NH4 concentration on lysine synthesis. Final NH4Cl concentration 14.91 g/l.

The final titres of lysine, biomass and sugars achieved and the yield of lysine are outlined in Table 3.1.

TABLE 3.1 : Effect of the NH_4Cl concentration on the lysine fermentation

	NH_4Cl	
	9,63g/l	14,98g/l
Biomass concentration at 24 hours (g/l)	35,61	30,85
Biomass concentration at 48 hours (g/l)	36,74	28,93
Final lysine titre (g/l)	27,60	53,54
Final sugar titre (g/l)	33,52	20,82
Lysine yield (g/g)	0,17	0,30
Maximum rate lysine synthesis (g/l/h)	1,86	1,67
Overall rate lysine synthesis (g/l/h)	0,43	1,11

The biomass achieved in each fermentation is similar at 24 hours and 48 hours, within the experimental error of determining biomass in fermentation broth containing CSL. The lysine titre obtained appears to be dependent on the counter-ion concentration in the fermentation broth, i.e. the moles of lysine produced are dependent upon the counter-ion concentration, since in both cases the quantity of lysine produced is equivalent to the quantity of NH_4Cl added to the fermentation broth. The reason that the rate of lysine synthesis tails off after 60 hours in both cases appears to be the result of a reduction in the free ammonium ion concentration (Figures 3.5 and 3.6). During the synthesis of lysine from the carbohydrate and NH_4^+, the NH_4^+ arises from the NH_4Cl and additional NH_4^+ supplied as a result of the control of the pH of the fermentation. On export of the lysine from the cell, the lysine then associates with the Cl^- as it is in the +1 ionised form at pH 7,2. Therefore progressively less NH_4^+ becomes available to the organism for lysine synthesis and as a cofactor in enzyme catalysis. In both cases the reduction in the rate of lysine synthesis appears to manifest itself at approximately 150mM free

NH_4^+. As this concentration decreases, the rate of lysine synthesis becomes progressively less.

3.4.2 Effect of the $(NH_4)_2HPO_4$ concentration on lysine synthesis

The effect of the total ammonium phosphate concentration on the production of lysine was expressed graphically by plotting the lysine concentration relative to the total ammonium phosphate concentration (mmole/mmole) as a function of time (Figures 3.7 to 3.24). The effect of the free ammonia on lysine synthesis is indicated in Figures 3.8, 3.11, 3.14, 3.17, 3.20 and 3.23. The sugar utilization during fermentation is indicated in Figures 3.12, 3.15, 3.18, 3.21 and 3.24.

The quantity of lysine produced is stoichiometric at 2 moles of lysine per mole of HPO_4^- counter-ion in solution in the fermentations run at 17,0, 22,0 and 25,6g/l of ammonium phosphate. At 40g/l $(NH_4)_2HPO_4$ this stoichiometry is reduced to 1mole/mole, and it is unlikely that the $(NH_4)_2HPO_4$ will influence the lysine yield, as excess $(NH_4)_2HPO_4$ is present (Figure 3.24). It would thus appear that lysine drives the dissociation of $(NH_4)_2HPO_4$ towards $2NH_4^+$ and HPO_4^-.

At the lower phosphate concentrations (0 and 14,7g/l $(NH_4)_2HPO_4$) the concentration of lysine produced is less than stoichiometric to the counter-ion equivalents in solution. The rate of lysine synthesis appears to be coupled to the free ammonium ion concentration in solution. As the NH_4^+ concentration increases as a result of the $(NH_4)_2HPO_4$ in the sugar feed, there is a resumption in lysine synthesis (Figures 3.8 and 3.11).

At 22,0g/l and 25,6g/l $(NH_4)_2HPO_4$ there is a reduction in the free NH_4^+ concentration to below approximately 150mM only during the later stages of the fermentation, which affects the rate of lysine synthesis (Figures 3.17 and 3.20). This does not affect the maximum rate of lysine synthesis (Table 3.2), but reduces the overall rate of lysine synthesis, i.e. the rate of lysine synthesis as calculated from the start of lysine synthesis to when it ceases. The data indicated on the graph can however be misleading as no account is taken of the fact that the lysine

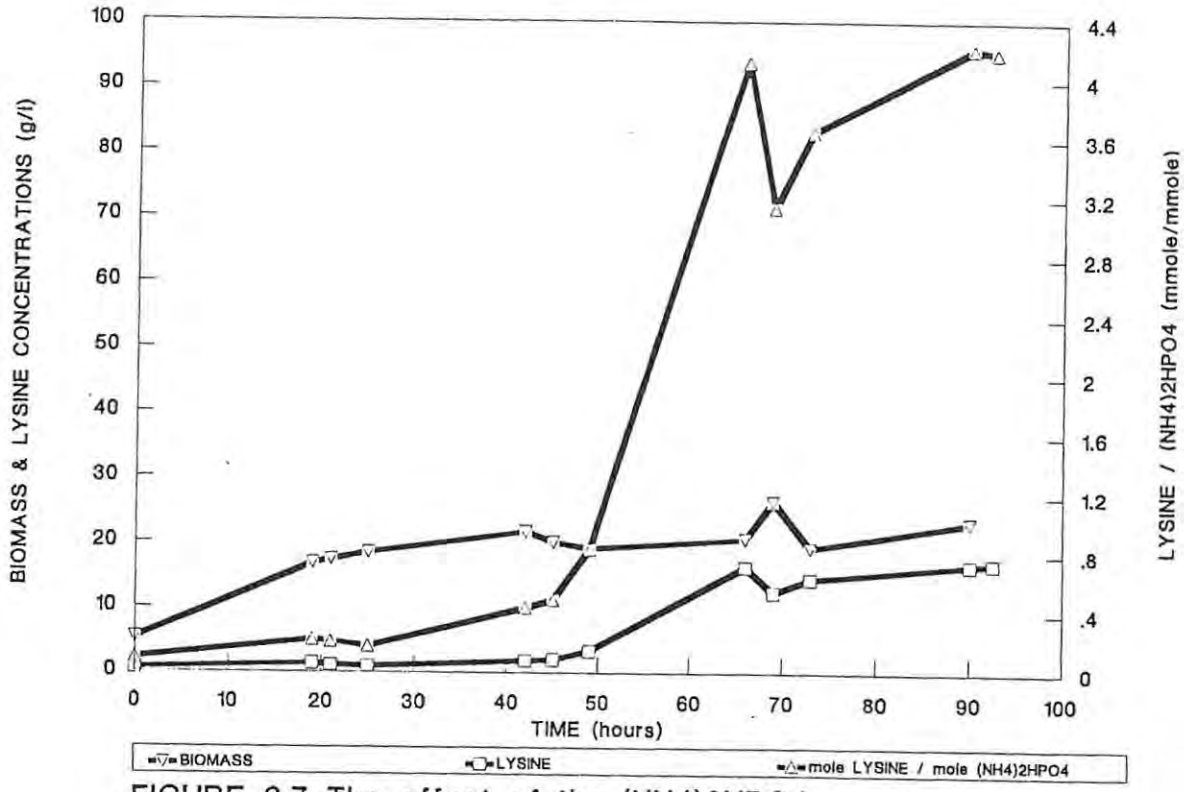

FIGURE 3.7 The effect of the (NH4)2HPO4 concentration on the lysine and biomass production. Final (NH4)2HPO4 concentration 0.0 g/l.

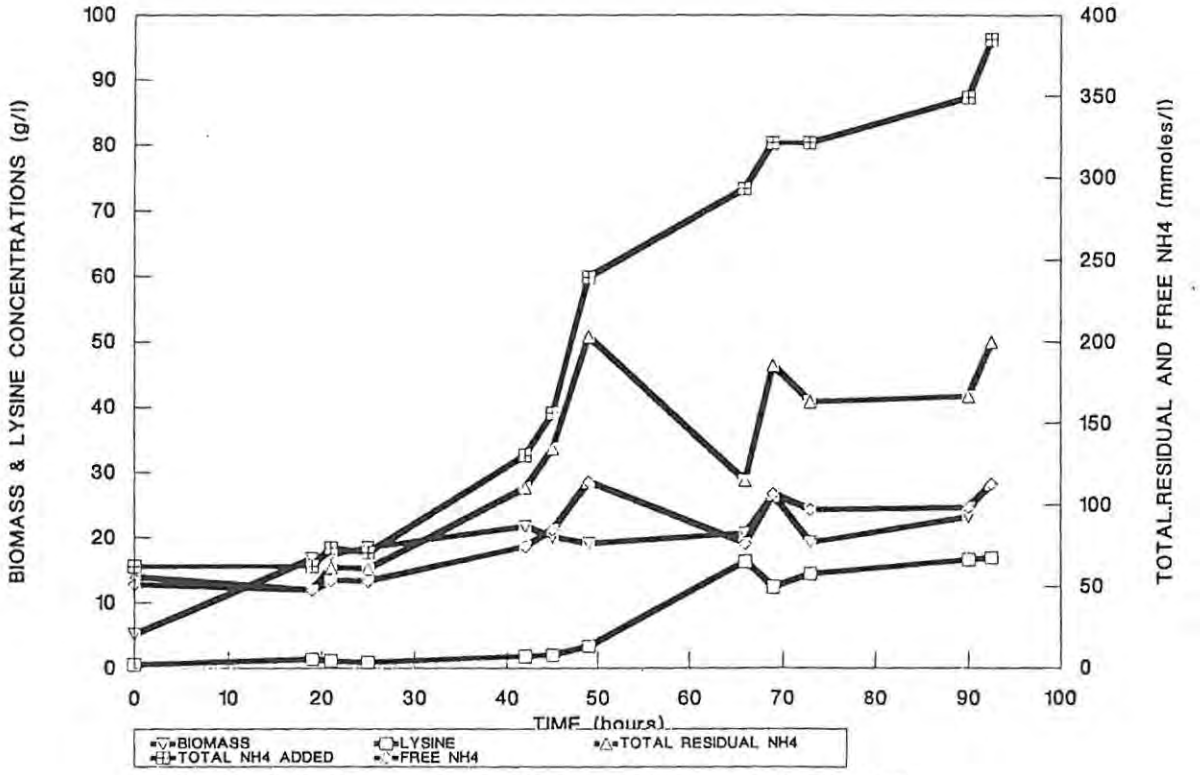

FIGURE 3.8 The effect of the total, residual and free NH4 concentrations on lysine and biomass production. Final (NH4)2HPO4 concentration 0.0 g/l.

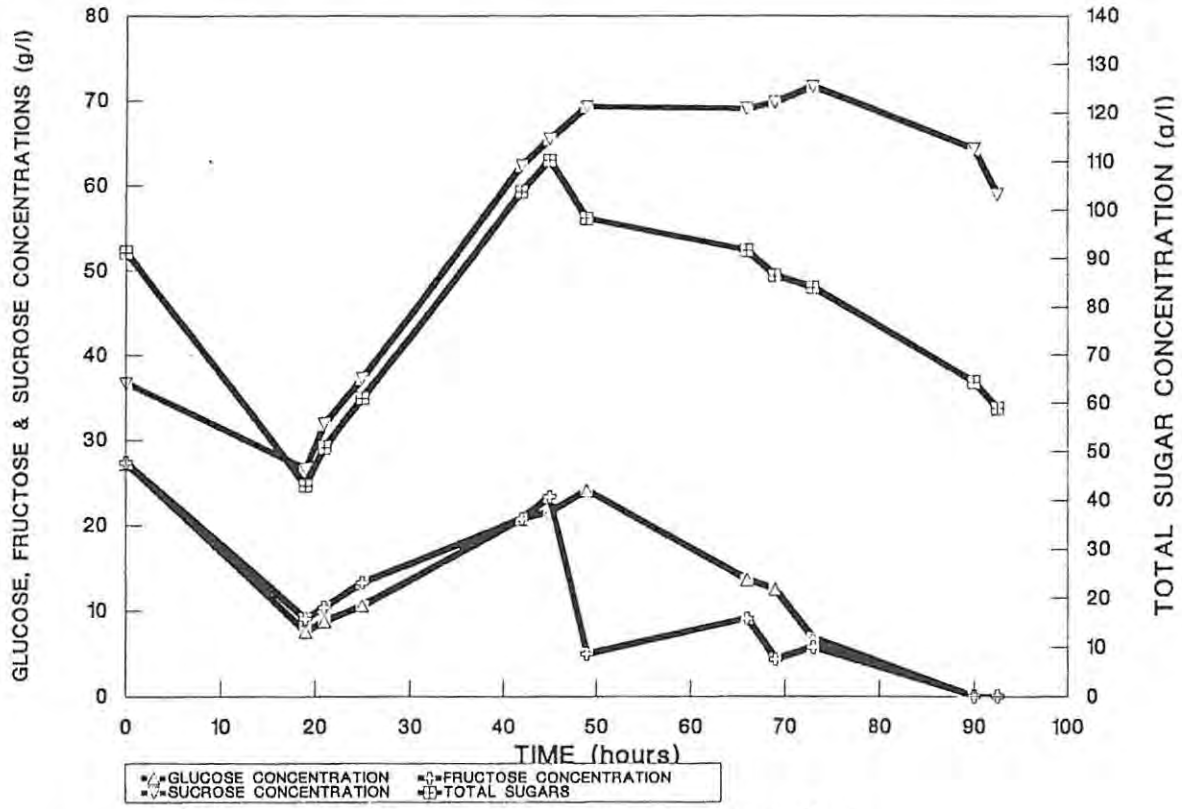

FIGURE 3.9 Sugar profiles during fermentation.
Final (NH4)2HPO4 concentration 0.0 g/l.

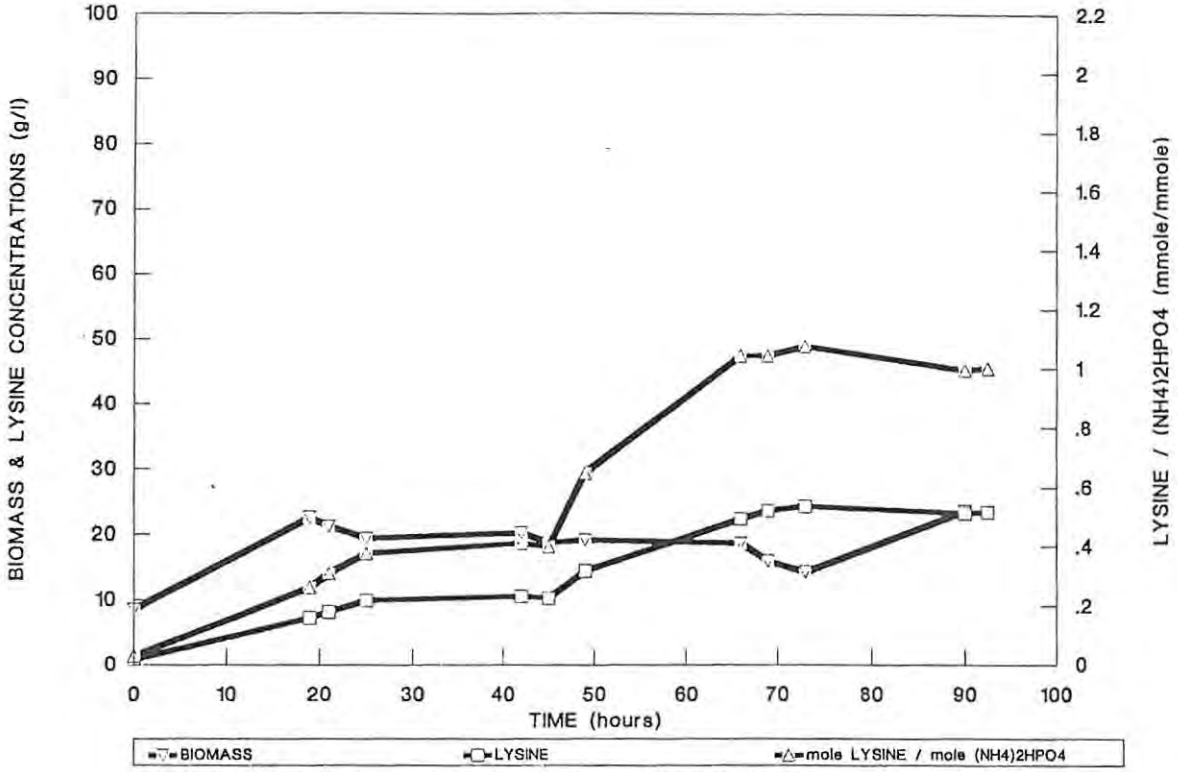

FIGURE 3.10 The effect of the (NH4)2HPO4 concentration on the lysine and biomass production. Final (NH4)2HPO4 concentration 14.7 g/l.

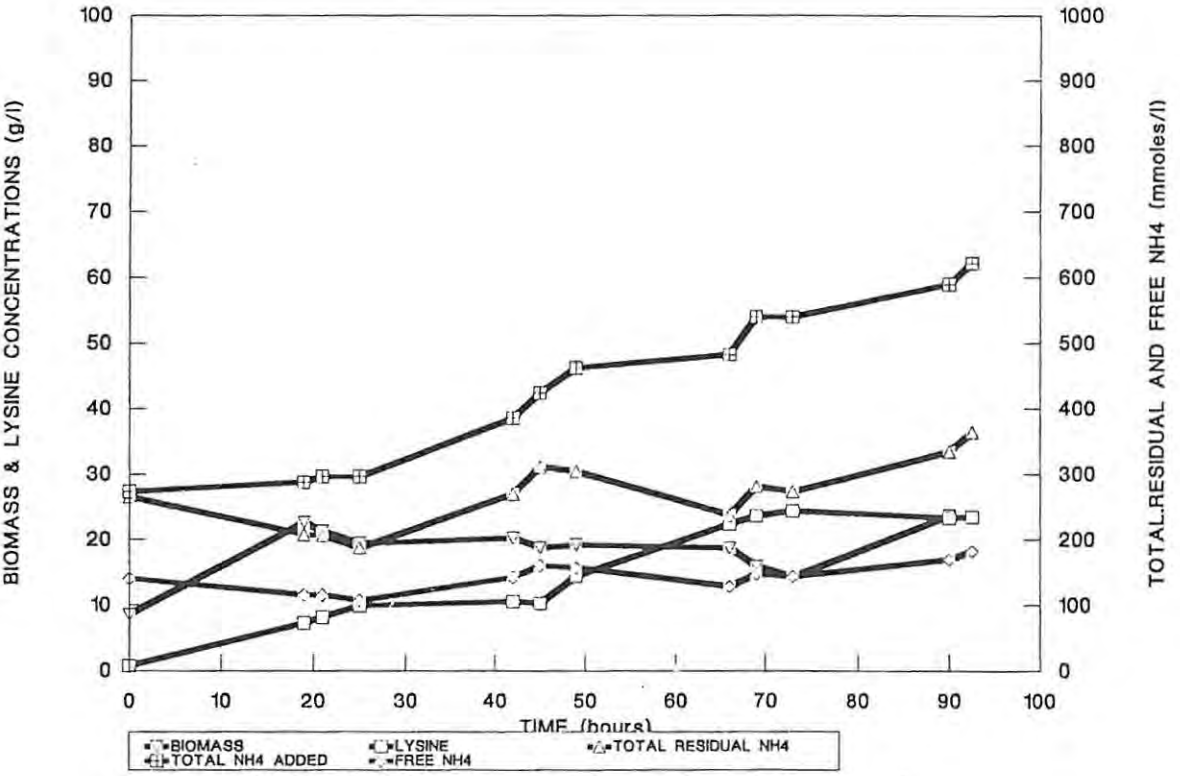

FIGURE 3.11 The effect of the total, residual and free NH4 concentrations on lysine and biomass production. Final (NH4)2HPO4 concentration 14.7g/l.

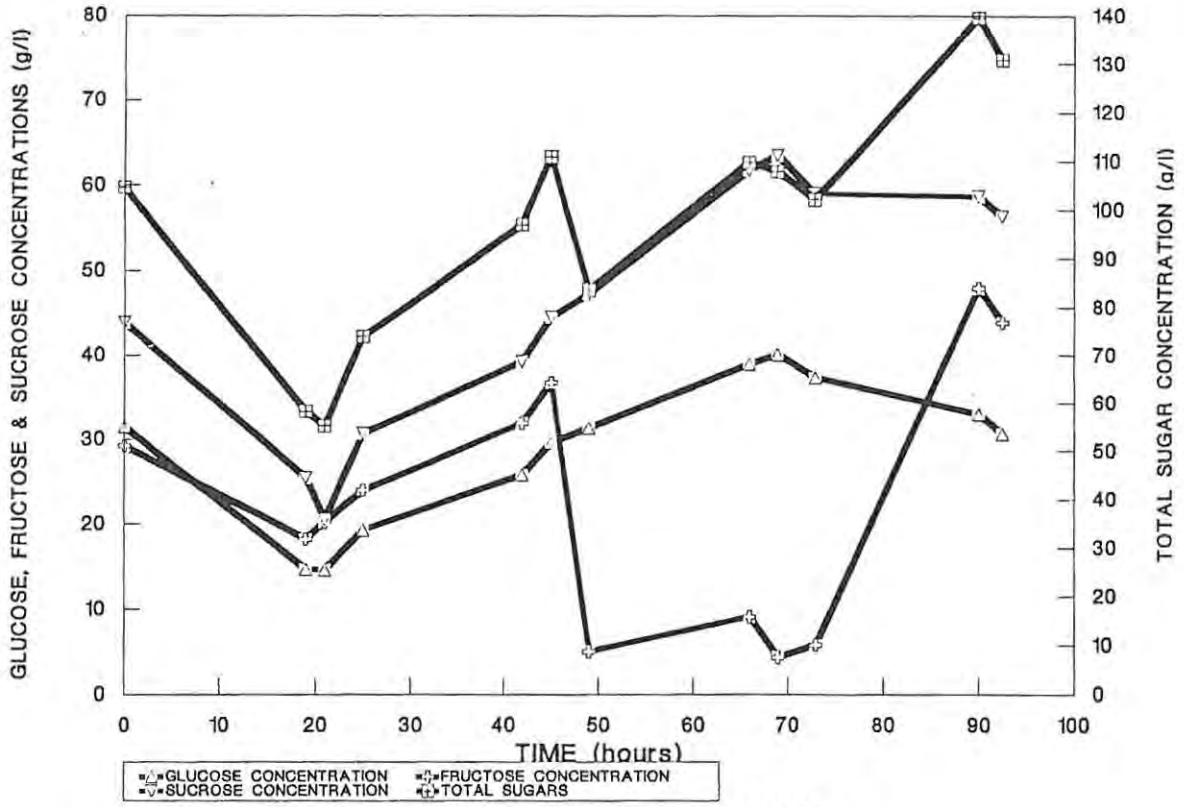

FIGURE 3.12 Sugar profiles during fermentation. Final (NH4)2HPO4 concentration 14.7 g/l.

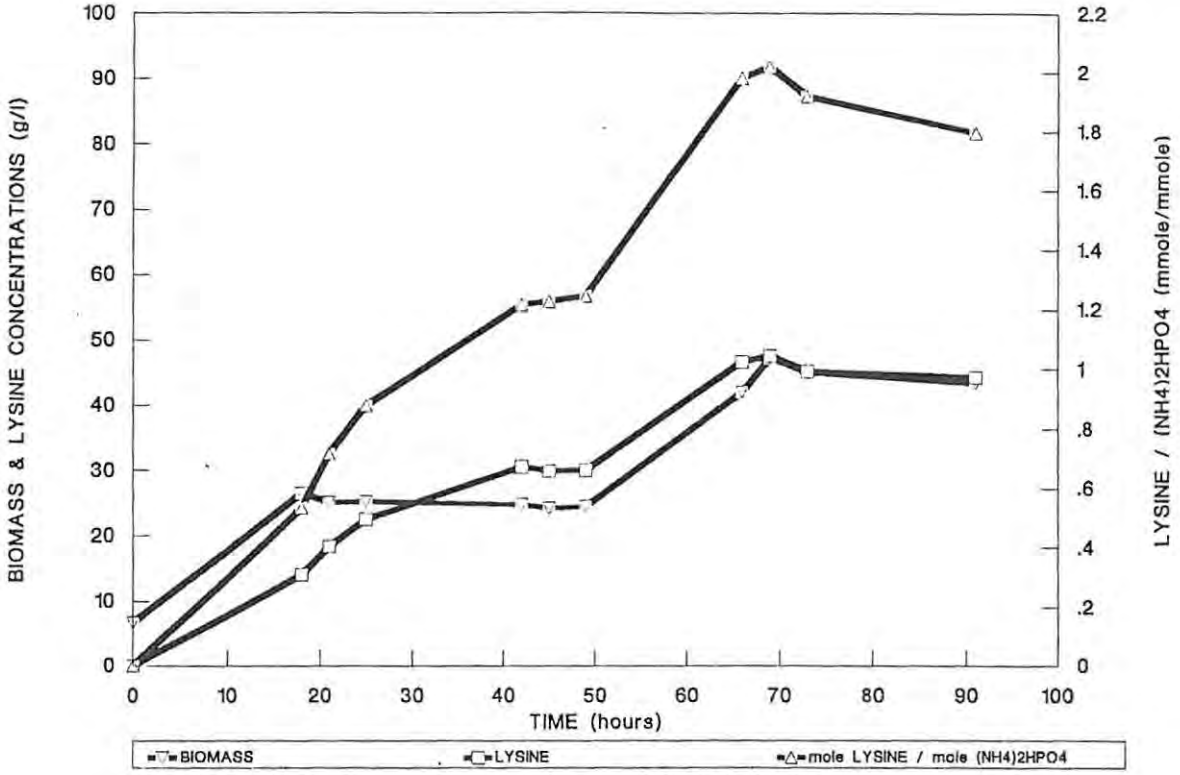

FIGURE 3.13 The effect of the (NH4)2HPO4 concentration on the lysine and biomass production. Final (NH4)2HPO4 concentration 17.0 g/l.

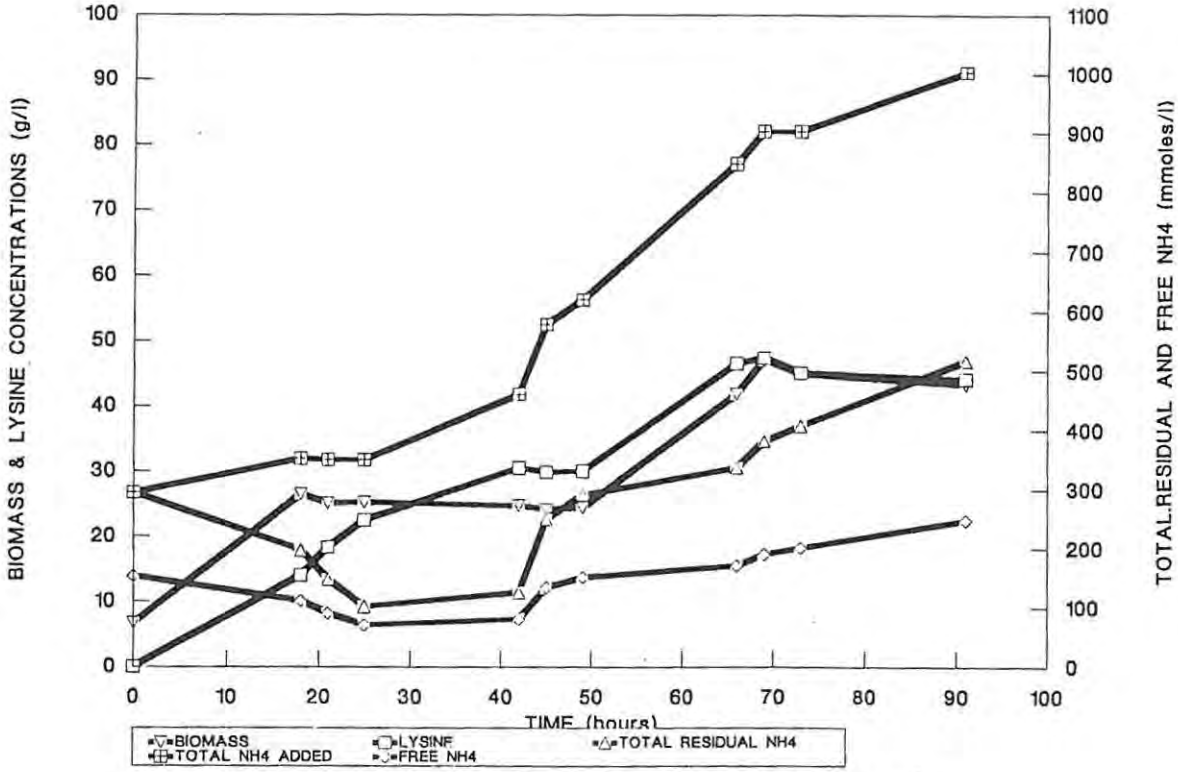

FIGURE 3.14 The effect of the total, residual and free NH4 concentrations on lysine and biomass production. Final (NH4)2HPO4 concentration 17.0 g/l.

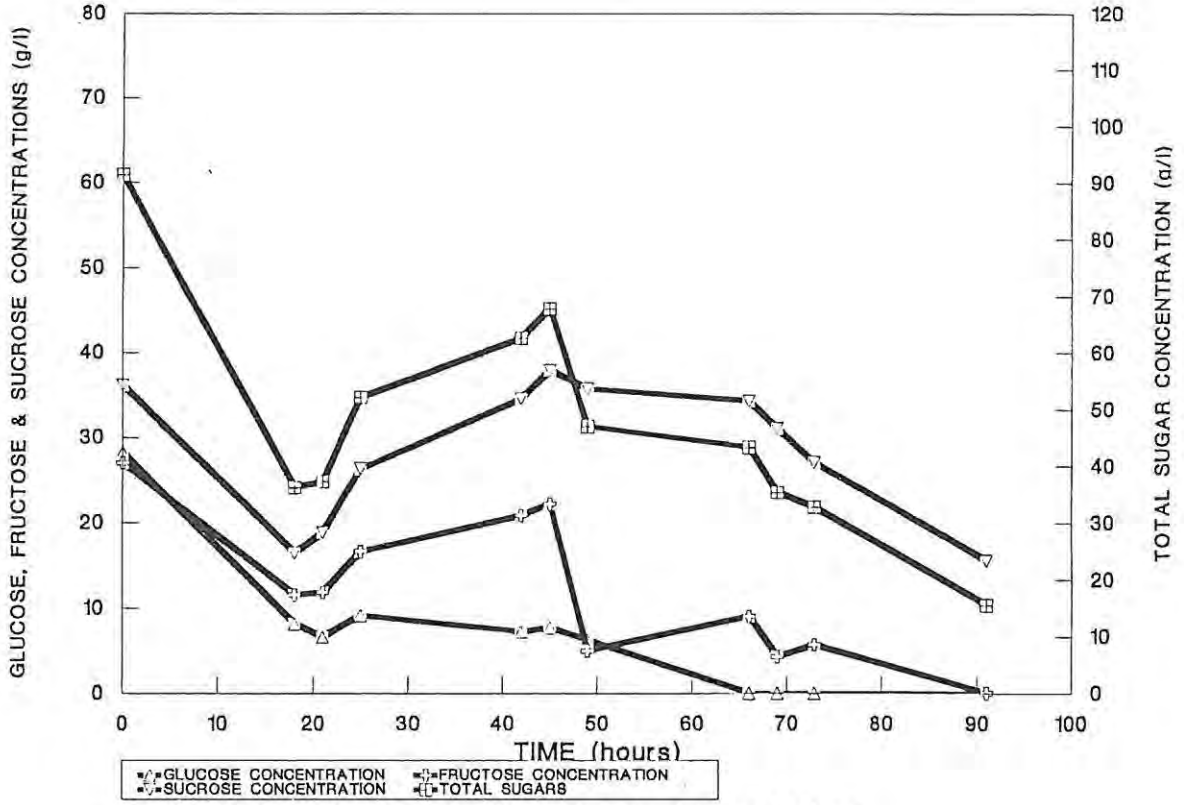

FIGURE 3.15 Sugar profiles during fermentation.
Final (NH4)2HPO4 concentration 17.0 g/l.

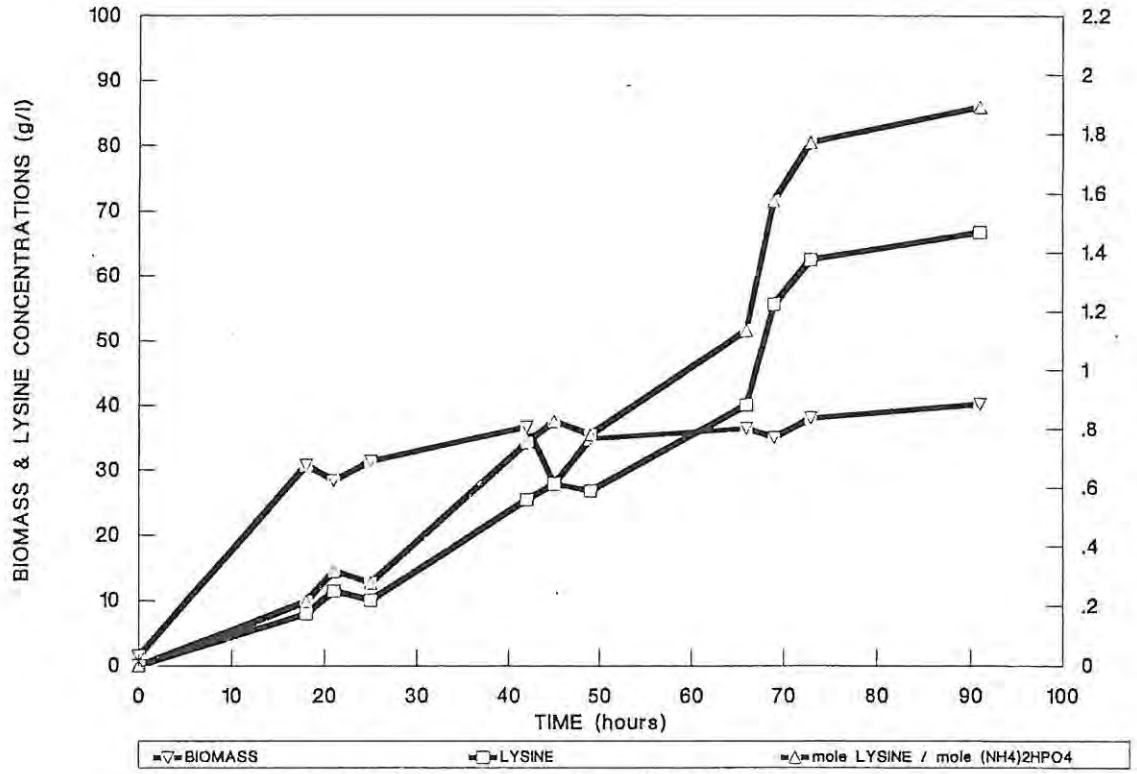

FIGURE 3.16 The effect of the (NH4)2HPO4 concentration on the lysine and biomass production. Final (NH4)2HPO4 concentration 22.0 g/l.

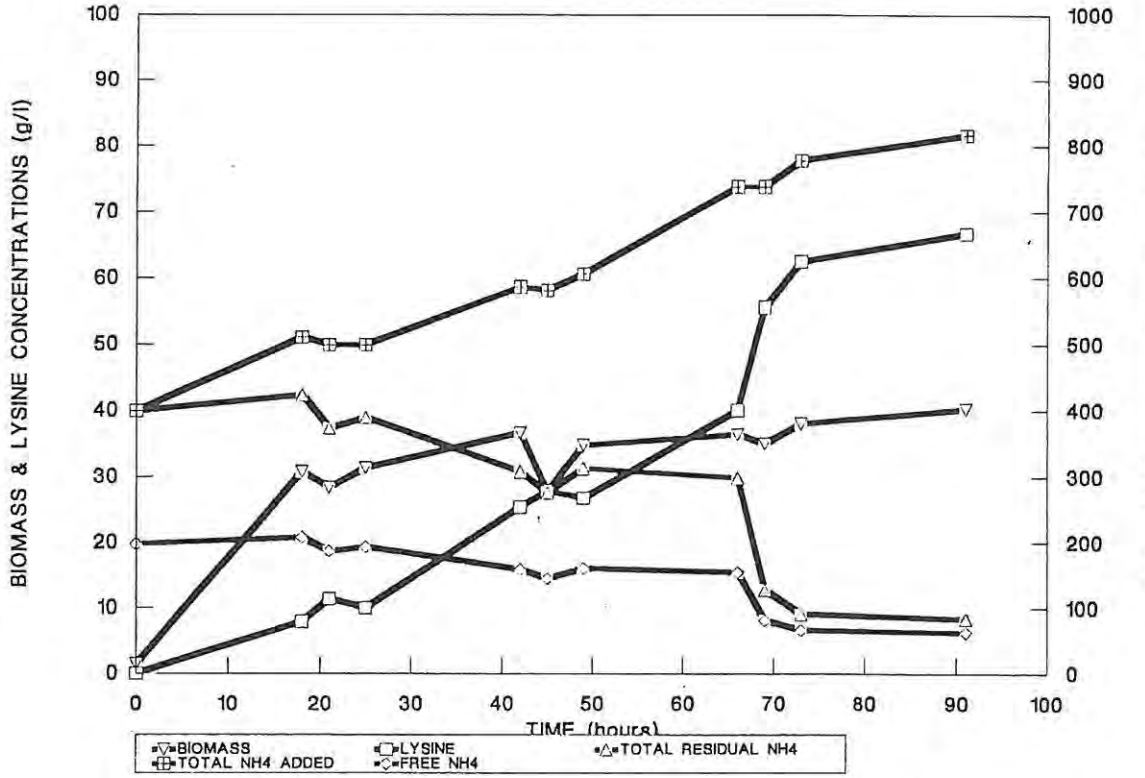

FIGURE 3.17 The effect of the total, residual and free NH4 concentrations on lysine and biomass production. Final (NH4)2HPO4 concentration 22.0 g/l.

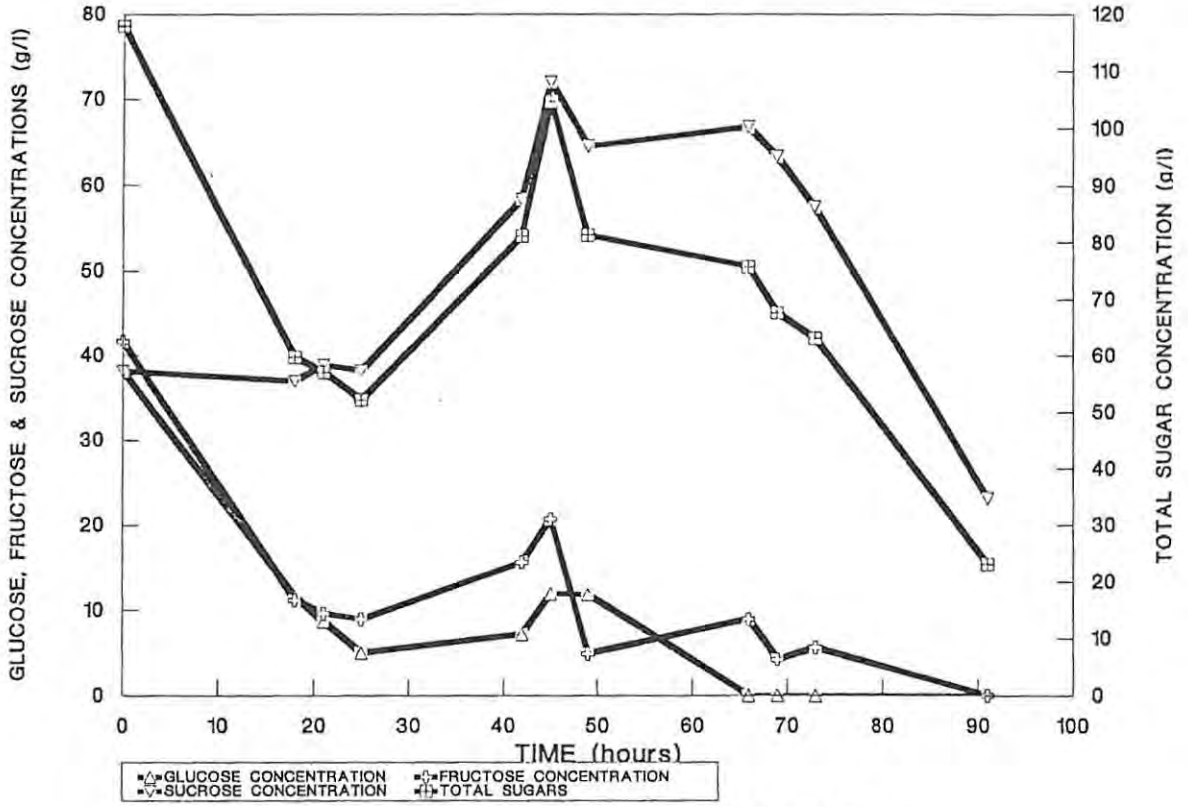

FIGURE 3.18 Sugar profiles during fermentation.
Final (NH4)2HPO4 concentration 22.0 g/l.

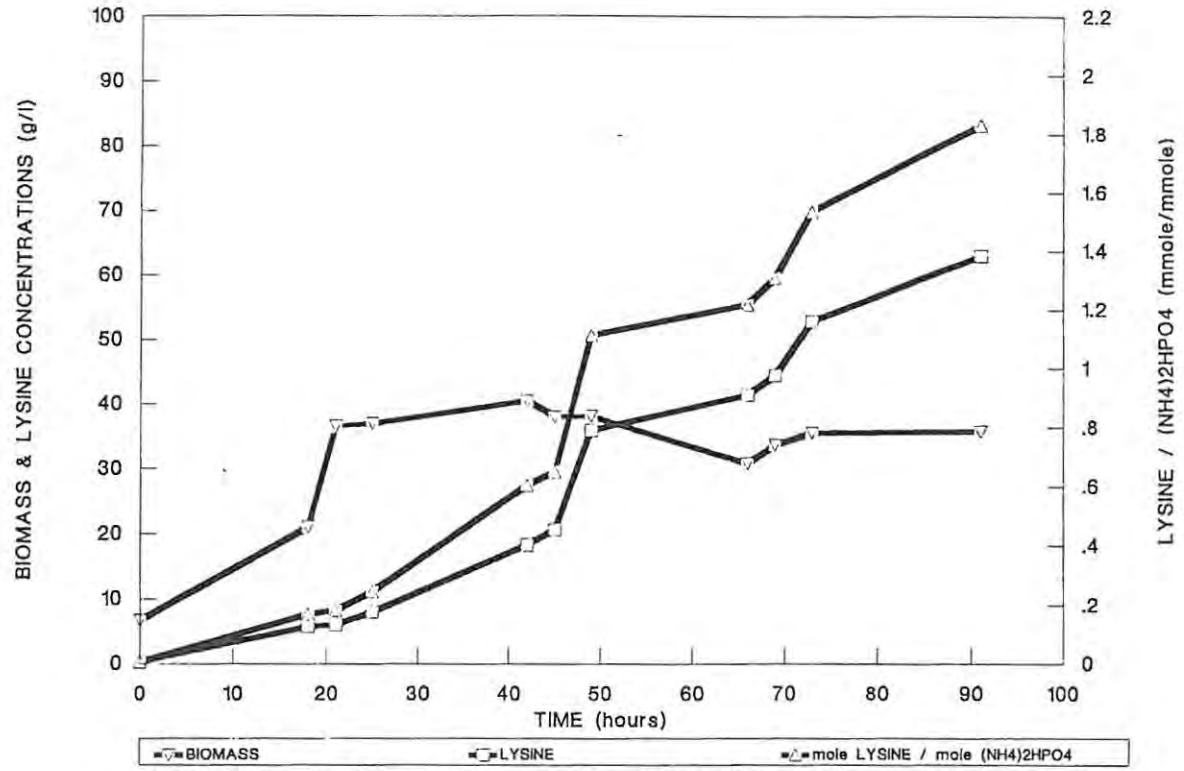

FIGURE 3.19 The effect of the (NH4)2HPO4 concentration on the lysine and biomass production. Final (NH4)2HPO4 concentration 25.6 g/l.

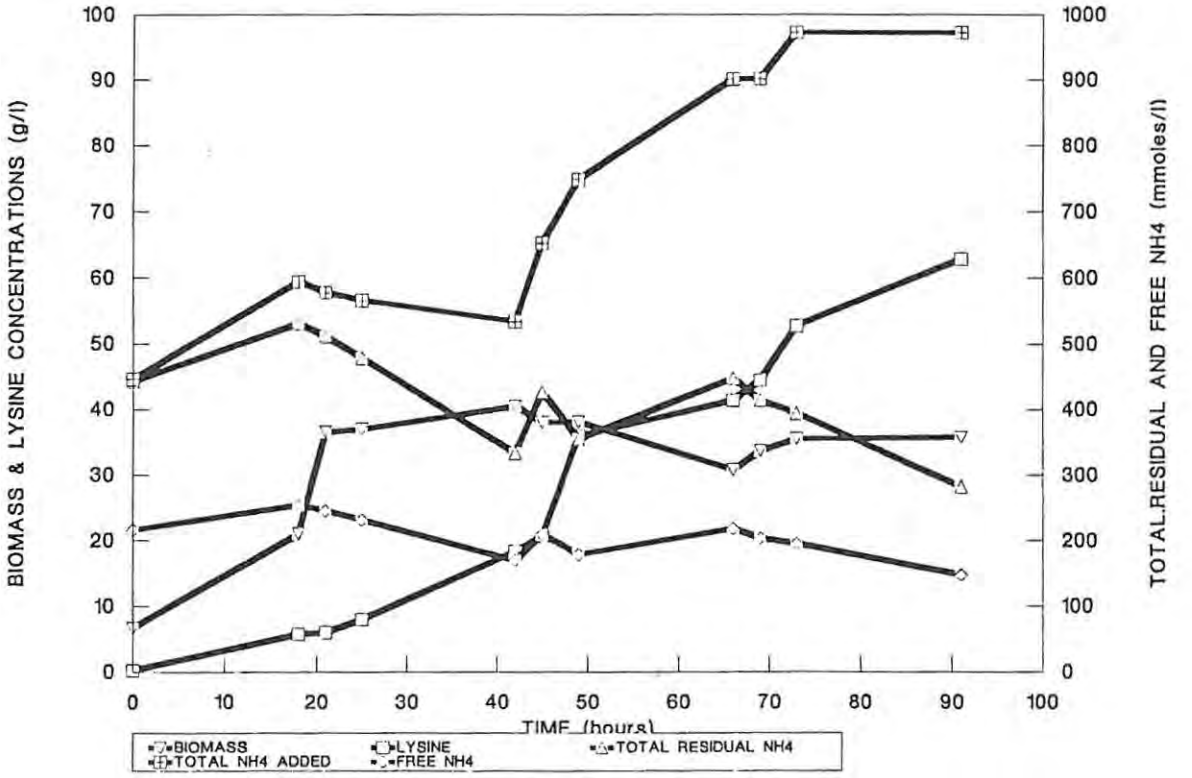

FIGURE 3.20 The effect of the total, residual and free NH4 concentrations on lysine and biomass production. Final (NH4)2HPO4 concentration 25.6g/l.

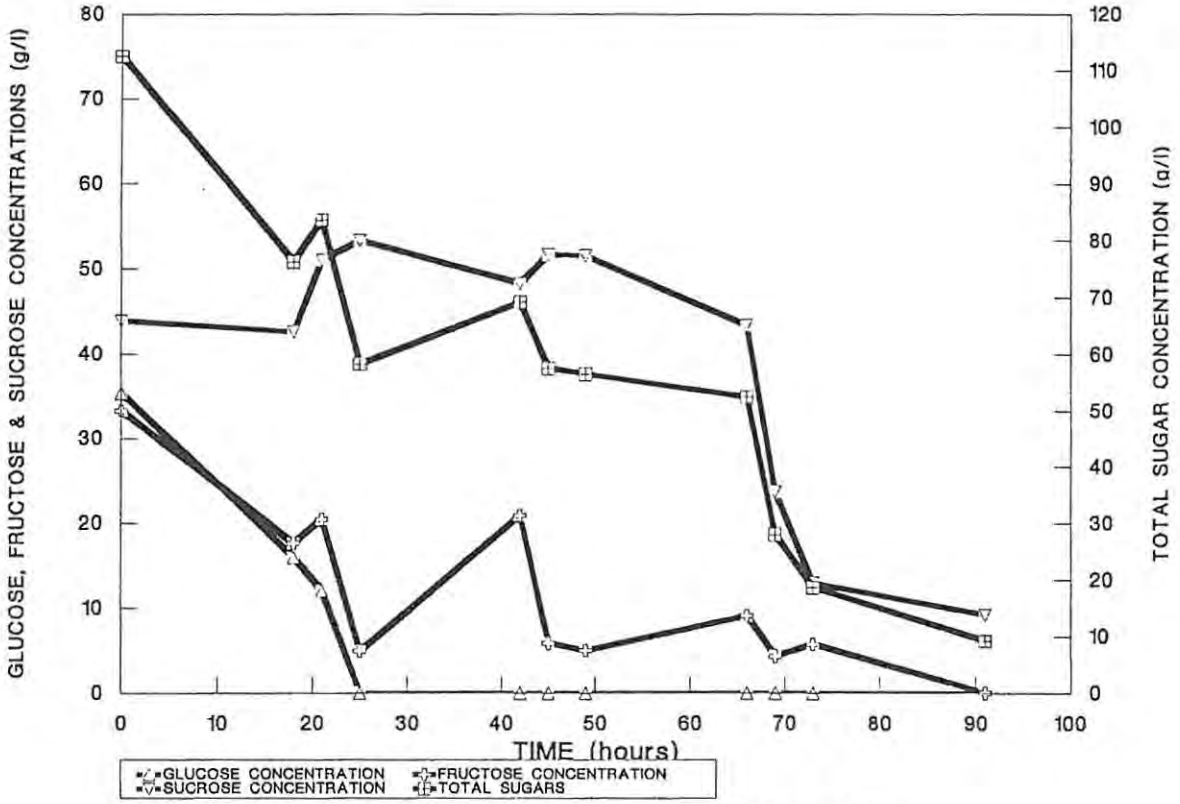

FIGURE 3.21 Sugar profiles during fermentation.
Final (NH4)2HPO4 concentration 25.6 g/l.

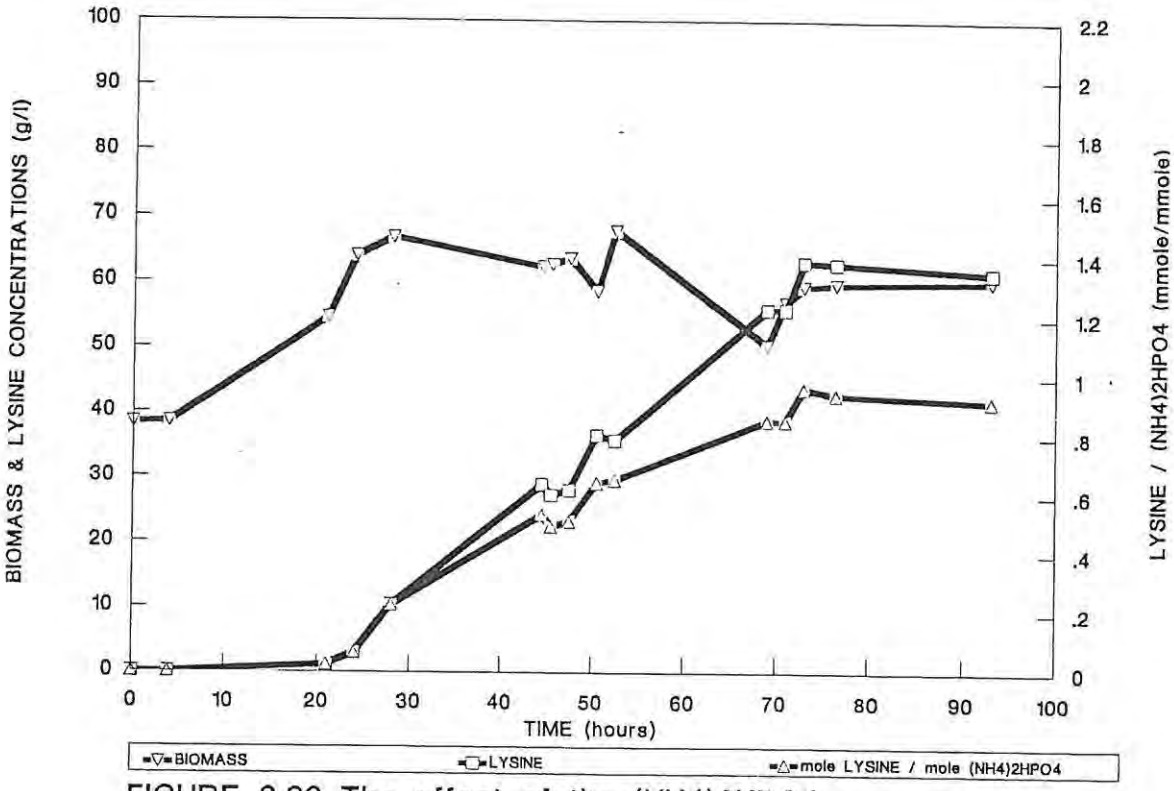

FIGURE 3.22 The effect of the (NH4)2HPO4 concentration on the lysine and biomass production. Final (NH4)2HPO4 concentration 40.0 g/l.

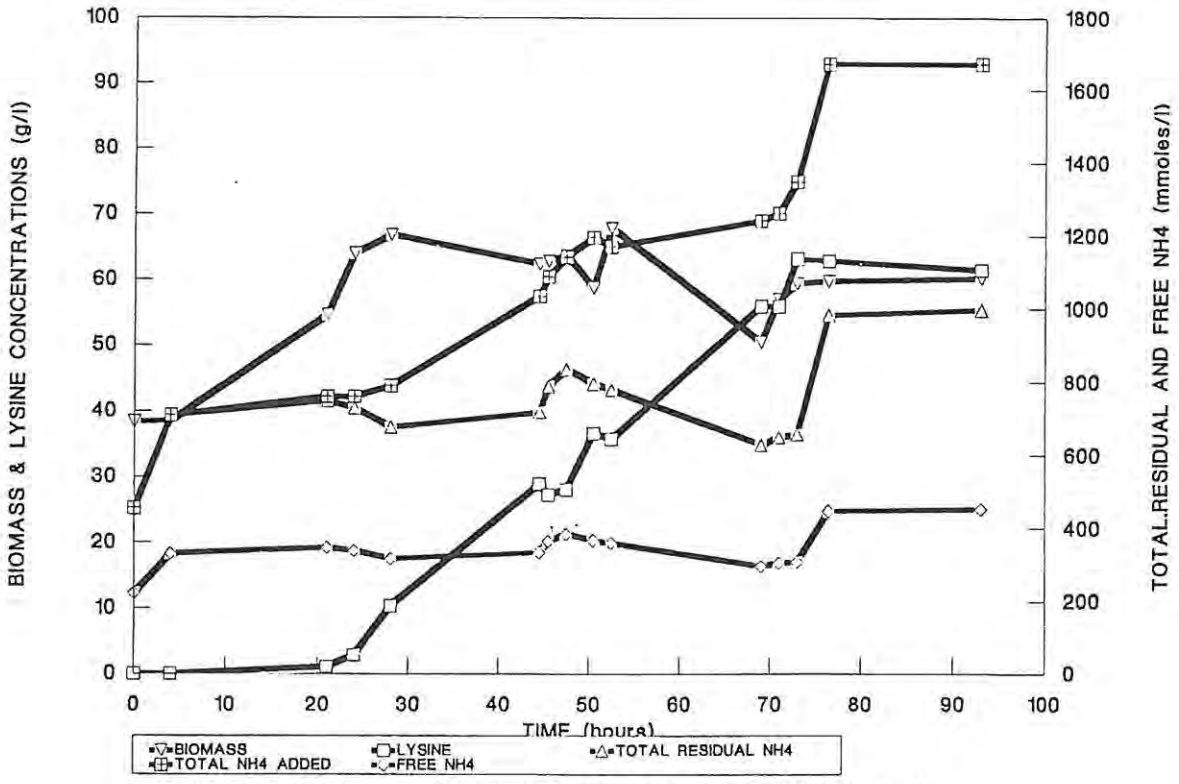

FIGURE 3.23 The effect of the total, residual and free NH4 concentrations on lysine and biomass production. Final (NH4)2HPO4 concentration 40.0g/l.

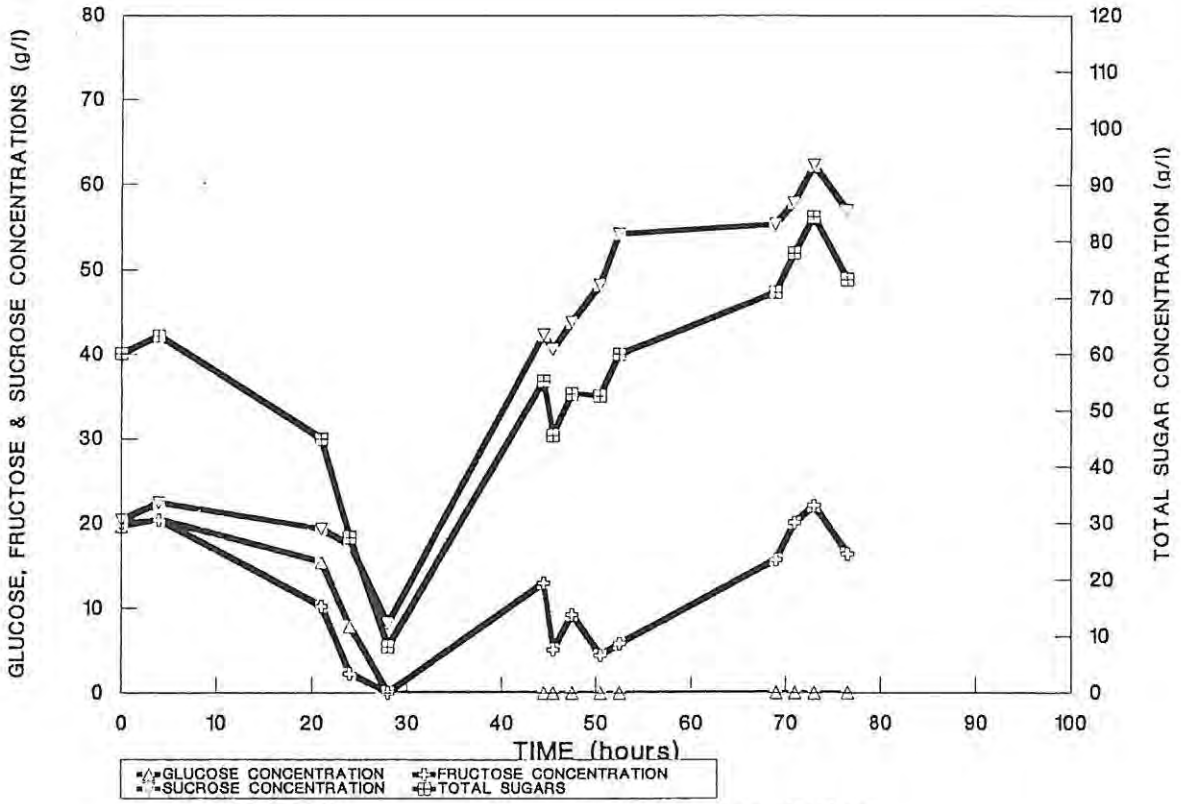

FIGURE 3.24 Sugar profiles during fermentation.
Final (NH4)2HPO4 concentration 40.0 g/l.

concentration is continuously being diluted as a result of the carbohydrate feed. At 40g/l $(NH_4)_2HPO_4$, where the free NH_4^+ concentration does not drop below 300mM, there is not a reduction in the rate of lysine synthesis (Figure 3.23), and the overall rate and the maximum rate of synthesis are equal (Table 3.2). The final titres of lysine attained at the higher phosphate concentrations are equal, however the rates of synthesis differ (Table 3.2).

At the lower phosphate concentrations there is an accumulation of residual sugar (Figures 3.9, 3.12, 3.15, 3.18, 3.21 and 3.24) as a result of the reduction in lysine synthesis. At 40g/l $(NH_4)_2HPO_4$ sugar accumulation also occurred as a result of the sugar concentration in the feed being higher. The total sugar concentration fed was 300g/l.

The $(NH_4)_2HPO_4$ concentration also appears to affect the biomass yield. However the maximum specific growth rate (hr^{-1}) remains unaffected at $0,22hr^{-1}$. The effect of the $(NH_4)_2HPO_4$ concentration on the final biomass titre is possibly also as a result of the free NH_4^+ concentration dropping below a critical level, thereby reducing the growth rates until the level has been restored by the $(NH_4)_2HPO_4$ in the feed, after which the growth rate increases again (Figure 3.10).

The biomass data as outlined in Figures 3.7, 3.10, 3.13, 3.16 and 3.19 does not take into account the dilution of the feed, so the increase in growth is actually more substantial. This increase in biomass appears not to be as a result of cell replication but rather as a result of the increase in cell mass. The free NH_4^+ concentration possibly affects the growth rate as a result of falling below 2 x K_m value for key enzymes required in amino acid synthesis, e.g. glutamate dehydrogenase, glutamine synthetase and aspartokinase. It has been shown that for maximum activity, aspartokinase requires 150mM of free NH_4^+ ions (Chapter 2).

3.5 CONCLUSION

Lysine and biomass synthesis are dependant on the concentration of free anionic counter-ions in solution, as a stoichiometry of ~1 is found with NH_4Cl (Cl^-) and lysine, while a stoichiometry of ~2 is found with

TABLE 3.2 : The biomass concentrations, lysine titre, lysine yield, lysine synthesis rate and specific growth rate in fermentations run at different $(NH_4)_2HPO_4$ concentrations

CSL CONC. (g/l)	TOTAL SUGAR CONC. (g/l)	$(NH_4)_2HPO_4$ CONC. (g/l)	BIOMASS CONC. @ 24 HOURS (g/l)	BIOMASS CONC. @ 48 HOURS (g/l)	LYSINE TITRE (g/l)	RESIDUAL SUGAR CONC. (g/l)	LYSINE YIELD (g/g)	LYSINE SYNTHESIS RATE		SPECIFIC GROWTH RATE
								MAXIMUM (g/l/h)	OVERALL (g/l/h)	(As per cell number) (h-1)
100	200	,0	13,70	14,66	16,86	58,89	,12	,37	,24	,229
100	200	14,7	11,53	11,58	24,32	130,85	,35	,21	,15	,159
100	200	17,0	19,23	18,83	47,47	15,58	,26	,59	,33	,223
100	200	22,0	30,47	34,42	66,71	23,09	,38	1,09	,86	,2
100	200	25,6	31,30	33,20	62,88	9,19	,33	,93	,83	,225
100	300	40,0	28,16	28,53	63,10	84,29	,29	1,15	1,14	,229

$(NH_4)_2HPO_4$ (PO_4^-) and lysine. Furthermore, the rate of synthesis of lysine and biomass appears to be dependent on the free NH_4^+ concentration as the maximum rates of lysine and biomass synthesis cannot be maintained at a free NH_4^+ concentration below 150mM.

The association of lysine with the free counter-ions also appears to drive the equilibria of the ammonium salts towards NH_4^+ and Cl^- in the case of NH_4Cl, and $2NH_4^+$ and HPO_4^- in the case of $(NH_4)_2HPO_4$, as suggested by the stoichiometry of ~1 for NH_4Cl and ~2 for $(NH_4)_2HPO_4$ with respect to lysine produced.

As there is an increase in the biomass concentration during lysine synthesis it is essential that this be taken into account when calculating the stoichiometry of carbon utilization during fermentation. As yet no suitable carbon balance exists for the lysine fermentation with the theoretical yield of lysine on glucose (expressed as mole/mole carbon) ranging from 0,66 to 0,75 (Stephanopoulos and Vallino, 1991). As the maximum lysine yield obtained during this series of experiments was of the order of 0,38, the carbon must be utilized for the synthesis of other compounds as well as for the generation of ATP by the oxidation of the glucose via the tricarboxylic acid cycle and the electron transport chain.

CHAPTER 4

CORYNEBACTERIUM GLUTAMICUM CARBON MASS BALANCE TO LYSINE, BIOMASS AND CO2: THE PROPOSED INFLUENCE OF CELL WALL SYNTHESIS

4.1 SUMMARY

Two distinct phases have been proposed for the growth of *Corynebacterium glutamicum* FP6 and the subsequent synthesis of lysine. They have been termed the replication phase and the maturation phase. During the maturation phase there is an increase in the biomass concentration, but not in the number of cells, due to the deposition of the polymer glycerol teichoic acid. Some of the polymer may be present as lysylglycerol-phosphate. The synthesis of the glycerol phosphate allows for the completion of the nucleotide balance required for lysine synthesis. The resultant theoretical maximum yield of lysine on glucose utilized is calculated to be 0,667g/g (mole/mole).

It appears that if an excess of glucose is supplied during the replication phase, deposition of the teichoic acid occurs prior to lysine synthesis thereby effectively reducing the lysine yield. The existence of futile cycles placing a demand on the energy requirements of the cell is a distinct possibility. These would also effectively reduce the lysine yield.

4.2 INTRODUCTION

It became evident that during the lysine synthesis phase of fermentations there was a continual increase in the biomass. Growth should have ceased due to the depletion of threonine, as protein synthesis could not continue as a result of the organism being a threonine auxotroph. Lysine synthesis cannot occur in the presence of threonine, as threonine and lysine both inhibit aspartokinase, preventing lysine synthesis (Tosaka and Takinami,1978, Tosaka *et al*, 1978). It was therefore decided to investigate which materials are synthesized by the cell and to what extent they contribute to the overall redox and energy balances during lysine synthesis.

It can be assumed that once lysine synthesis has been initiated, no protein or nucleic acid synthesis occurs as a result of the organism depleting the threonine in the culture media. Since the organism is an auxotrophic mutant for threonine and methionine it cannot synthesize

70/...

these amino acids. As the biomass appears to continue to increase once lysine synthesis starts, this increase in mass is possibly as a result of the deposition of non-proteinaceous material in the cell wall or as a result of deposition of a storage material.

The cell wall structure of Gram-positive bacteria consists of a region of peptidoglycan lying immediately external to the cytoplasmic membrane. It is 20-50nm or 20 to 40 molecular layers of peptidoglycan thick (Archibald *et al*, 1993). Covalently linked to the peptidoglycan are polysaccharides and the anionic polymers, teichoic and teichuronic acids. The relative amounts of each of the polymers present are influenced by physical conditions such as temperature and pH, chemical constituents, such as Mg^{++} and phosphate and cell age. A model of the cell wall and membrane of a Gram-positive bacteria, *Lactobacillus fermentii*, as depicted by van Driel *et al* (1971), is shown in Figure 4.1.

4.2.1 Peptidoglycans

Peptidoglycans are heteropolymers of distinctive composition and structure, and are synthesised uniquely by procaryotes. The monomeric constituents are two acetylated amino sugars, N-acetylglucosamine and N-acetylmuramic acid, and a small number of amino acids, some of which do not conventionally occur in proteins (Stanier *et al*, 1976). The amino sugars form glycan strands, composed of alternating residues of N-acetylglucosamine and N-acetylmuramic acid, β-1,4-linked, with the amino acids in a short peptide chain attached to the N-acetyl muramic acid (Figure 4.2A). The terminal carboxyl of the D-alanine on one subunit is cross-linked to the free amino group of a diamino acid (e.g. diaminopimelic acid) on the adjacent peptide subunit (Figure 4.2b). In the genus *Corynebacteria* the diamino acid in the peptide chain is meso-diaminopimelic acid (meso DAP) (Keddie and Cure, 1978). In other organisms other diamino acids may be used, e.g. lysine, ornithine, L-diaminopimelic acid and diaminobutyric acid. The meso DAP in the cell wall, along with the sugars arabinase and galactose, is regarded as one of the distinguishing features of 'legitimate' *Corynebacterium* spp (Keddie and Cure, 1978). This is in conflict with the work carried out by Yamada and Komagata (1970) who found that the strains of

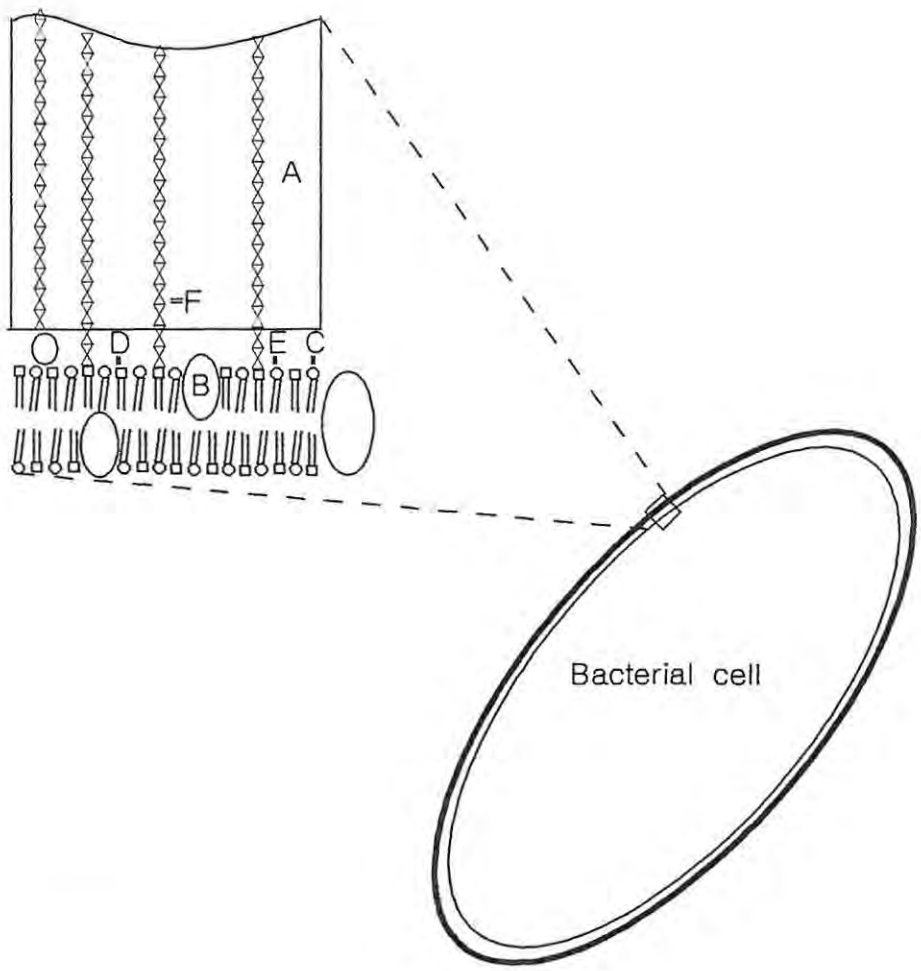

FIGURE 4.1 Model of Gram-positive cell wall. (A)=cell wall, (B)=protein, (C)=phospholipid, (D)=glycolipid, (E)=phosphatidyl glycolipid and (F)=lipoteichoic acid.
(van Driel et al, 1971)

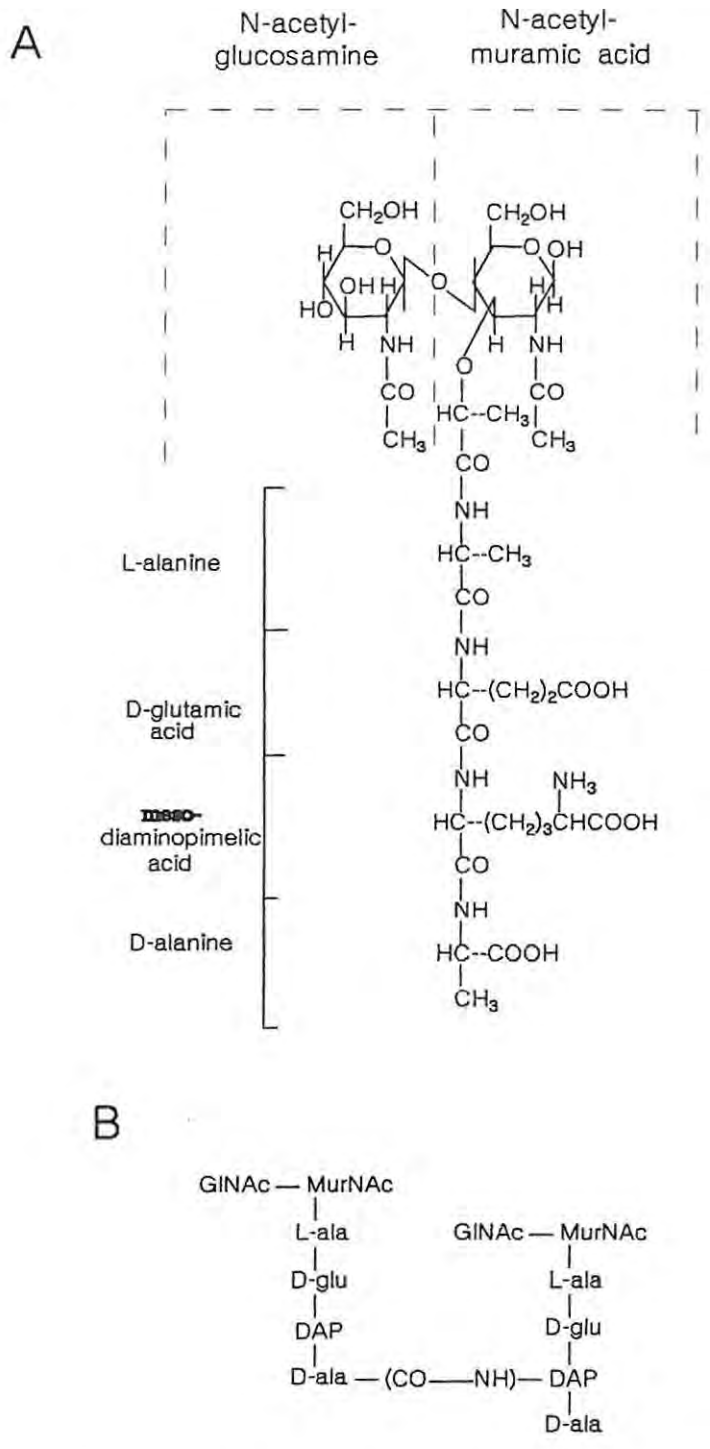

FIGURE 4.2 General structure of peptidoglycan. (A)= complete structure of a single subunit and (B)=cross-linking between the terminal carboxyl group of D-alanine on one subunit and the free amino group of the diamino acid on the adjacent subunit.

Corynebacteria which they examined contained either meso-DAP, L-DAP or lysine as the diamino acid. The amino acids which are found in the peptide of *Corynebacterium genitalium* are glutamate, alanine and diaminopimelic acid (Evangelista *et al* 1978). It is likely that some of the alanine is in the form of D-alanine and not L-alanine in this organism, as it is often found that the terminal alanine in the peptide is in the D-configuration.

In *Corynebacterium diphteriae* the peptide in the cell wall consists of both a tetrapeptide (L-Ala-D-Glu-meso-DAP-D-Ala) and a tripeptide (L-Ala-D-Glu-meso-DAP) subunits (Kato *et al*, 1968).

In most Gram-positive bacteria the peptidoglycan accounts for some 40 to 90% of the dry weight of the cell wall (Stanier *et al*, 1976).

One of the polymers which are covalently linked to the peptidoglycan is polysaccharide. The polysaccharide in *Corynebacteria* is usually made up of two or three of the following sugars: arabinose, ribose, galactose, glucose or mannose (Keddie and Cure, 1977). The presence of arabinase and galactose in the cell wall of the *Corynebacteriaceae* is used as one of the distinguishing features for taxonomic purposes (Schleifer and Kandler, 1972).

4.2.2 Polyolphosphate polymers (teichoic acids)

The peptidoglycan matrix of the cell wall is also covalently linked to polyolphosphate polymers known as teichoic acids. The teichoic acids are water-soluble polymers, containing ribitol or glycerol residues linked through phosphodiester linkages (Figure 4.3). The exact location in the cell wall is unknown, however covalent linkage to the peptidoglycan is possible. The glycerol based teichoic acids are also associated with the cell membrane and are known as lipoteichoic acid. They are covalently linked to the membrane glycolipid (Stanier *et al*, 1976). The glycerol teichoic acids are joined by 1,3- or 1,2-linkages and the ribitol joined by 1,5-linkages. Most teichoic acids contain large amounts of D-alanine, usually attached to positions 2 or 3 on the glycerol, or positions 3 or 4 on the ribitol (Figure 4.3). In addition to D-alanine, other

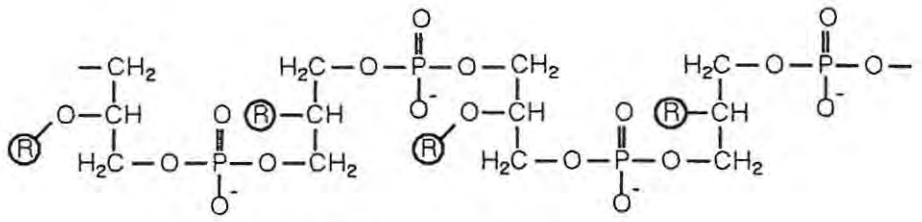

1,3 - Glycerol teichoic acid

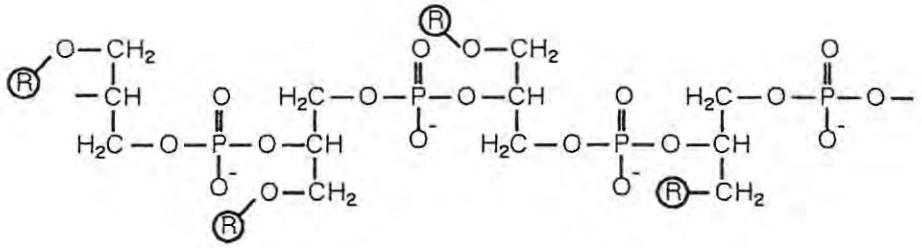

1,2 Glycerol teichoic acid

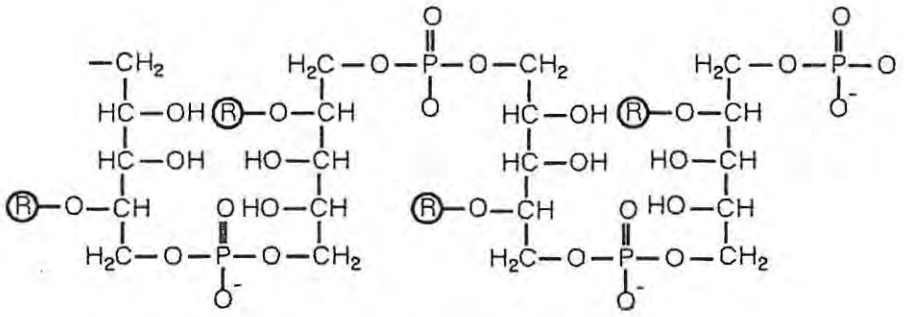

1,5-Ribitol teichoic acid

FIGURE 4.3 Glycerol and ribitol teichoic acids.
R= alanine, glucose, galactose,
N-acetylglucoseamine,
N-acetylgalactoseamine and succinate.

substituents that may be attached to the free hydroxyl group of glycerol and ribitol are glucose, galactose, N-acetylglucosamine, N-acetylgalactosamine or succinate. As the teichoic acids have a high density and regularly orientated charges they most certainly affect the passage of ions through the outer surface layers.

The teichoic acids are found in the cell walls of a large range of Gram-positive bacteria and may comprise 20-50% of the mass of the cell wall (Baddiley, 1968) and can account for 10% of the dry weight of the cell (Archibald *et al*, 1968).

The ribitol teichoic acid from *Bacillus subtilis* contains alanine and glucose residues at a molar ratio of 1:1 (phosphorus:glucose) and 1:0,46 (phosphorus:alanine) (Armstrong *et al*, 1960). The alanine residues in this teichoic acid are linked through their carboxyl groups to the hydroxyl groups of the polymer, and are in the D-configuration. The overall structure of the alanylglucosylribitol-5-phosphate for *Bacillus subtilis* is outlined in Figure 4.4. Under phosphate limited growth, *Bacillus subtilis* replaces the teichoic acid in the cell wall with another anionic polymer, teichuronic acid (Ellwood and Tempest, 1967). None of these units is joined via the glycosidic linkages having the β-configuration.

In *Lactobacillus arabinosus* the ratio of phosphorus:glucose:D-alanine was found to be 1:1,06:0,62 (Archibald *et al*, 1961). Here the glucose linkages are in the α-configuration in contrast to the β-linkage found in *Bacillus subtilis*. Where most of the ribitol was mono-glucosylribitol a small amount of di-glucosylribitol was also found. The chain length was found to be 8 to 12 units in length.

In *Staphylococcus aureus* the teichoic acid consists of ribitol, N-acetylglucosamine and alanine with the molar proportions of phosphorus:glucosamine:alanine being 1:0,57:0,75, i.e. some ribitol units do not have alanine or N-acetylglucosamine attached (Baddiley *et al*, 1962).

A new type of teichoic acid was isolated from the cell wall of

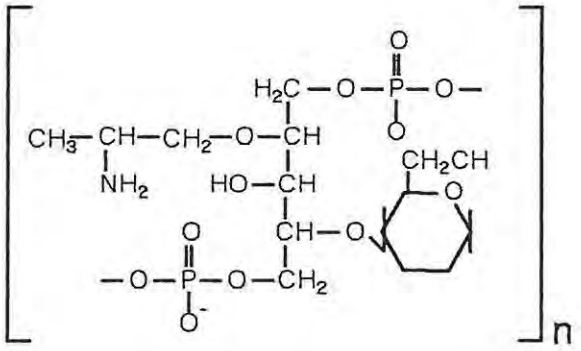

FIGURE 4.4 Alanylglucosylribitol-5-phosphate of **Bacillus subtillis.**

Staphylococcus lactis containing alanine:glucosamine:glycerol:phosphorus in molar proportions 1:1:1:8 (Archibald *et al*, 1965). On further structural elucidation, the teichoic acid was found to consist of glucosamine phosphate, glycerol phosphate, alanine and N-acetyl glucosamine phosphate. A similar structure was found in the glycerol teichoic acid of *Staphylococcus albus*, however here the amino sugar was found to be N-acetylgalactosamine (Ellwood *et al*, 1963).

The ribitol teichoic acid found in the walls of *Actinomyces streptomycini* contains glucosylribitol and glucoaminylribitol, but unlike that found in other bacteria contains no alanine, with succinate present as the monoester (Archibald *et al*, 1968). The ribitol teichoic acid of *Actinomyces violaceus* contains neither alanine nor succinic acid but acetate.

The glycerol teichoic acid from the walls of *Staphylococcus epidermis* make up 30% by mass of the cell wall containing phosphate, D-alanine and D-glucose in molar proportions of 1:0,25:0,50, with the glucose being in the β-configuration (Archibald *et al*, 1968).

4.2.3 Synthesis of Cell Wall Precursors

The synthesis of N-acetylglucosamine and N-acetylmuramic acid and their incorporation into the bacterial cell wall of *Escherichia coli* and *Bacillus subtilis* is outlined in Figure 4.5. The synthesis of the glutamate occurs via the glutamate synthase, glutamate dehydrogenase and glutamine synthetase enzymes as depicted below:

$$\text{Glutamine} + \alpha\text{-ketoglutarate} + \text{NADPH} \xrightarrow{\text{Glutamate synthase}} 2\ \text{glutamate} + \text{NADP}$$

$$\alpha\text{-ketoglutarate} + NH_4 + \text{NADPH} \xrightarrow{\text{Glutamate dehydrogenase}} \text{glutamate} + \text{NADP} + H_2O$$

$$\text{Glutamate} + NH_4 + \text{ATP} \xrightarrow{\text{Glutamine synthetase}} \text{glutamine} + \text{ADP} + Pi$$

Alanine is produced by the transamination of pyruvate from glutamate to α-ketoglutarate and alanine.

78/...

Glutamate + pyruvate ⇄ L-ketoglutarate + alanine

The meso-DAP and lysine are synthesized from aspartate via β-aspartyl-phosphate (Figure 1.1, Chapter 1).

The D-forms of these amino acids are produced by racemase enzymes.

The glycerol for the glycerol teichoic acid is synthesized via the Embden-Meyerhoff pathway where it is produced as glyceraldehyde-3-phosphate. The ribitol is possibly also produced via the HMP pathway from the ribulose-5-phosphate which is reduced to ribitol via a ribitol dehydrogenase (Hulley *et al*, 1963). It is not known whether in *Corynebacteria* this enzyme is $NADP^+$ or NAD^+ specific, as it is NAD^+ specific in *Aerobacter aerogenes* (Hulley *et al*, 1963).

4.2.4 Peptidoglycan and teichoic acid synthesis

A schematic representation of the synthesis of the peptidoglycan in *E. coli* and *B. subtilis* is as outlined in Figure 4.5 (Stanier *et al*, 1980 and Sonenshein *et al*, 1993).

The incorporation of teichoic acid into the cell wall of bacteria occurs via the precursors CDP-glycerol and CDP-ribitol (Shaw, 1962). Shaw proposed that the synthesis of these two compounds occurred by the following two mechanisms:

CTP + L-α-glycerol phosphate ⇄ CDP-glycerol + pyrophosphate

CTP + D-ribitol-5-phosphate ⇄ CDP-ribitol + pyrophosphate

with the reactions being catalysed by pyrophosphorylases.

Shaw (1962) was able to isolate and fractionate cytidine diphosphate glycerol pyrophosphorylase from *Lactobacillus arabinosus* and cytidine diphosphate ribitol pyrophosphorylase from *Staphylococcus aureus*. *Lactobacillus arabinosus* was found to contain both pyrophosphorylases. Both pyrophosphorylases were also found in *Bacillus subtilis*, *Propionibacterium shermanii* and *Staphylococcus aureus*.

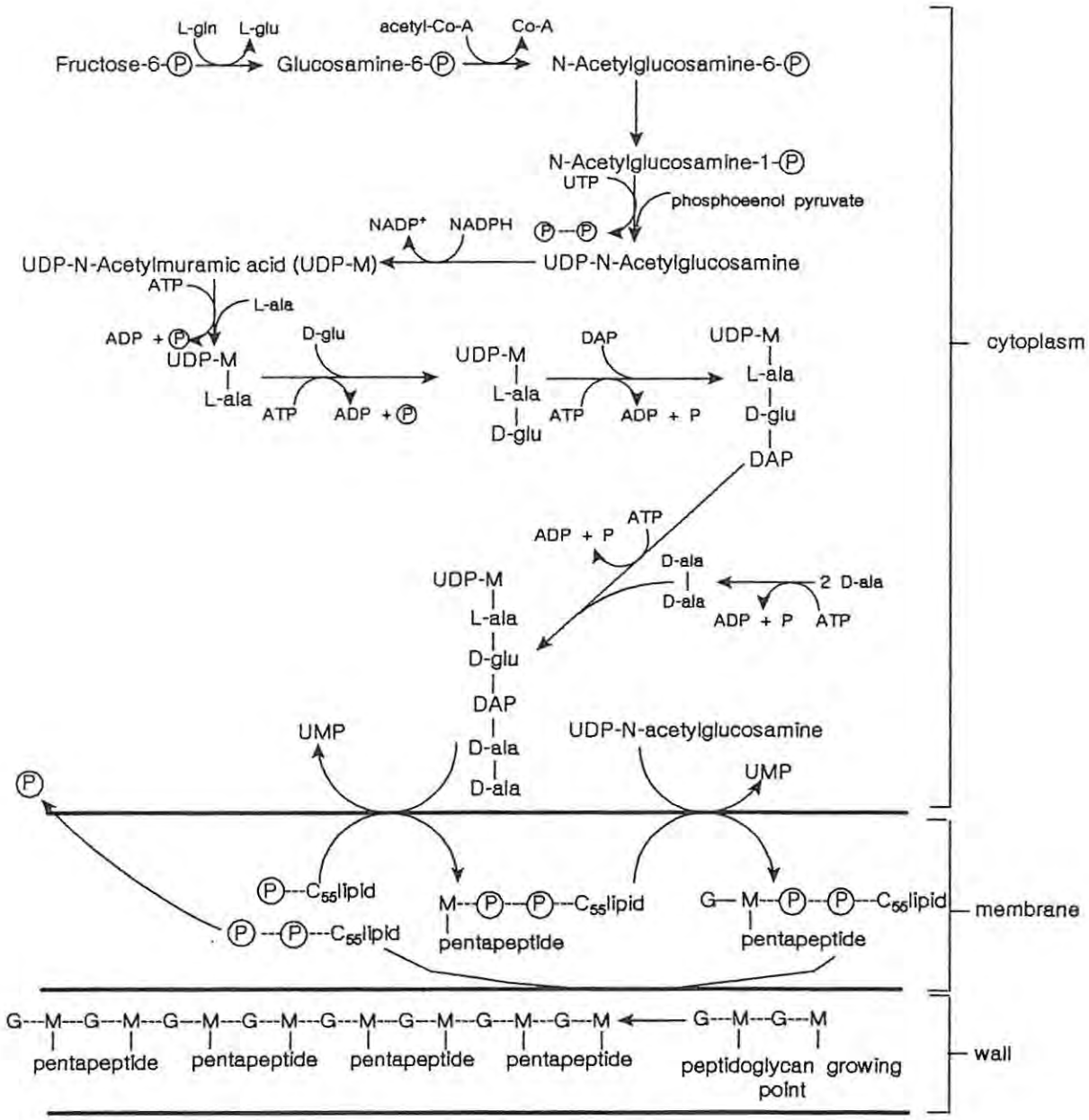

FIGURE 4.5 Biosynthesis of peptidoglycan in **B. subtilis** and **E. coli** (Sonenshein **et al**,1993, and Stanier **et al**,1980) Ala, alanine; DAP, diaminopimelic acid; Gln, glutamine; Glu, glutamic acid; G, N-acetylglucosamine; M, N-acetylmuramic acid and UMP, uridine monophosphate.

Berger and Glaser (1964) and Glaser (1964) described the *in vitro* synthesis of polyglycerophosphate and polyribitol phosphate from CDP-glycerol and CDP-ribitol, in *Lactobacillus plantarum*. They were able to show that penicillin and crystal violet inhibited the synthesis of ribitol teichoic acid. Novobiocin also irreversibly inhibited polyribitol synthesis, however it has also been shown to inhibit the accumulation of UDP-muramic acid peptides in *Staphylococcus aureus*. Both crystal violet and Novobiocin cause the accumulation of CDP-ribitol, CDP-glycerol, UDP-glucose and UDP-galactose by interfering with the *in vivo* synthesis of teichoic acid. Penicillin affects cell wall synthesis as UDP-muramic acid derivatives occur *in vivo*, in the presence of penicillin, but it has also been shown to cause the accumulation of CDP-ribitol in *S. aureus* (Sankkonen, 1961). Therefore the *in vivo* inhibition by crystal violet and Novobiocin is not definitive proof that these inhibitors directly affect teichoic acid synthesis *in vivo*.

The overall sequence for the synthesis of ribitol teichoic acid is therefore:

Ribulose-5-P + NADPH → ribitol-5-P + $NADP^+$

Ribitol-5-P + CTP → CDP-ribitol + PPi

n-CDP-ribitol + acceptor → CMP + ribitol-P_n-acceptor

$(Ribitol\text{-}P\text{-})_n$ + XDP-sugar → $[ribitol\text{-}P\text{-}]_n$ + XDP + sugar

It was originally believed that the teichoic acid is covalently linked to the peptidoglycan through multiple linkages to the D-alanine residues (Rogers and Garret, 1963), however this has been replaced by the view that one end of the polyribitolphosphate chain is attached to the peptidoglycan (Ghuysens and Strominger, 1963). In the absence of peptidoglycan synthesis, the synthesis of the polyribitol phosphate is limited by the availability of the acceptor and can only lengthen pre-existing chains. Roberts and Garret (1963) showed that easily extractable teichoic acid is formed in penicillin inhibited cells of *Staphylococcus aureus*.

An investigation was therefore undertaken to determine what materials could be synthesized by *Corynebacterium glutamicum* during lysine synthesis and to what extent they may contribute to the overall redox balance for lysine synthesis.

4.3 MATERIALS AND METHODS

4.3.1 Organism

The organism used throughout all fermentations was *Corynebacterium glutamicum* FP6.

4.3.2 Media and culture conditions

A range of fed-batch fermentations were carried out at different yeast extract concentrations, namely 25g/l, 35g/l, 45g/l and 55g/l. The remaining ingredients in the initial charge and sugar feed to the fermentation are outlined in Appendix V. The inoculum preparation was carried out as outlined in Chapter 2 (section 2.3.4).

The fermentations were inoculated using the following inoculation train:

LM Slant	(culture time 48 hours)
↓	
4 x 25ml	(culture time 24 hours)
↓	
4 x 225ml TNIY broth	(culture time 16-18 hours)

The LM and TNIY media are as outlined in Appendix I. The 4 x 250ml TNIY cultures were then pooled and used to inoculate the fed-batch fermentations. The final fermentation volume was 10 litres. During the first 20-30 hours of fermentation the glucose was fed at a rate ranging from 2 to 4,5g/l/h, after which the rate was increased to 10 to 11g/l/h. The feed rate was calculated per litre of initial charge.

The fermentations were run in Chemap LA 3000 fermenters at 30°C, pH 7,2, agitation rate 1 100rpm and an air flow rate of 1v/v/min (per final

fermentation volume). The pH was controlled using a 10M NH_4OH solution. When required, 2M H_2SO_4 was also used to control pH.

Where fermentation off-gas CO_2 concentrations were required to enable mass balance calculations to be carried out, the fermentation was run in a 1 800 litre pilot plant which has on-line O_2 and CO_2 monitoring using Braun gas analysers. The fermentation media used is outlined in Appendix VI. The culture conditions used were identical to above, however the agitation rate and aeration rates used were 180rpm and 0,5v/v/m (per final fermentation volume).

The inoculum train used for the 1 800 litre pilot plant was:

LM Slant	(culture time 48 hours)
↓	
4 x 250ml LM Broth	(culture time 24 hours)
↓	
19 litres TNIY broth	(culture time 16-18 hours)
↓	
Prefermenter 180 litres TNIY broth	(culture time 8-10 hours)

The 180 litre prefermenter was used to inoculate the 1 800 litre (final volume) fermentation stage.

4.3.3 Analyses

Seventy ml samples were aseptically drawn at regular time intervals during the fermentations and the following analyses were carried out:

4.3.3.1 Cell counts

Bacterial cell counts were carried out by doing decimal dilutions of the cultures and then plating onto LM agar (Appendix I) and by counting using a haemocytometer. The plate counts were carried out to ensure that all fermentations were monoseptic.

4.3.3.2 Biomass

The biomass during the course of the fermentation was determined gravimetrically on duplicate 10ml samples by centrifugation and drying of the pellet at 105°C to constant mass.

4.3.3.3 L-lysine

The L-lysine concentration in the culture media after removal of the biomass by centrifugation was determined by HPLC as outlined in Chapter 2 (section 1.3.4.1.2).

4.3.3.4 Glucose

The residual glucose concentration in the culture media after removal of the biomass by centrifugation was determined by HPLC as outlined in Chapter 2 (section 1.3.4.1.3).

4.3.3.5 Scanning electron microscopy

The broth was harvested from the fermentations and washed once with 0,1M phosphate buffer. A 1:10 dilution of the cells was then filtered onto 0,2 micron filters. The filters were placed into 2,5 % m/m glutaraldehyde in 0,1m phosphate buffer for 16 hours, after which the glutaraldehyde solution was replaced with a fresh solution of the same concentration for 2 hours. The cells were dehydrated using an ethanol series. The concentrations used were 20, 40, 60, 80, 100 and 100 percent. The ethanol was then substituted with amylacetate by increasing the concentration relative to that of the ethanol. The concentrations used were 30, 60, 80, 100 and 100 percent by volume. The cells were then critical point dried from liquid CO_2 using a Polaron E3000 critical point dryer and were sputter coated with gold using a Polaron E5100 sputter coater. The scanning electron microscopy was then performed using a Jeol JSM 840 scanning electron microscope.

4.3.3.6 Transmission electron microscopy

The cells which were harvested as in section 4.3.3.4 were centrifuged at 1 000 x g and washed in 2,5% m/m glutaraldehyde in 0,1M phosphate buffer. The cells were then fixed in 1% m/m osmium tetroxide after which they were washed twice in phosphate buffer by centrifugation at 10 000 x g. The cells were then dehydrated in ethanol series using the same concentrations as above (10 minutes at each concentration). A transition to epoxy resin via propylene oxide was carried out at the following ethanol/propylene oxide concentrations; 75:25, 50:50 and 25:75. The cells were kept at each concentration for 15 minutes. Infiltration of the cells with resin using increasing concentrations of epoxy resin in propylene oxide was then performed. The relative concentrations used were 25:75, 50: 50, 75:25 and 100 for 4 hours at each stage. Finally the cells were embedded in pure Araldite CY212/Taab 812 epoxy resin mixture polymerised at 60°C for 36 hours. Ultrathin sections (60nm) were cut on an RMC MT-7 ultramicrotome. The sections were mounted on 300 mesh copper grids and stained with 5% m/m aqueous uranyl acetate and Reynolds citrate (Cross, 1993). The sections were viewed using a Jeol JEM 100CXII transmission electron microscope.

4.3.4 Isolation and extraction of cell wall components

4.3.4.1 Isolation of soluble biomass fraction

A 100ml sample of fermentation broth was taken and washed three times with 50ml of 2,0g/l cetyltrimethylammonium bromide (CTAB) with sonication of the cell suspension for 10 minutes in a sonic water bath after resuspending the cells each time. At each step the cells were centrifuged at 8 000 x g for 10 minutes. The pooled volumes of supernatant were then treated with 3 volumes of acetone and 3 volumes of ethanol at 4°C for 72 hours. The resulting precipitate was then sequentially washed with 20ml volumes of acetone, ethanol and ether to remove the remaining lipids. The biomass concentration in the fermentation sample, the residual biomass concentration from the extracted sample and the mass of precipitate were determined

gravimetrically after drying to constant mass at 60°C in a vacuum oven at -200kpa.

4.3.4.2 Isolation and characterization of teichoic acid

The teichoic acid was isolated from the cell mass by a method adapted from Armstrong *et al* (1960). A 400ml sample of a 72 hour old fermentation broth was centrifuged at 8 000 x g and then washed once with an equivalent volume of cold (4°C) distilled water. The cells were then successively resuspended in 2 x 100ml 0,2% m/v CTAB. At each stage the cells were sonicated in a sonic water bath for 15 minutes before centrifugation at 8 000 x g. The pooled 200ml CTAB solution was treated with 800ml of 99,9% ethanol at 4°C for 24 hours. The resulting precipitate was collected by centrifugation at 8 000 x g and washed with 100ml cold ethanol and the precipitate was then dried under vacuum (-200kpa) at 30°C. The carbon, hydrogen and nitrogen concentrations in the precipitate were determined using a Leco CHN-932 analyser. The total phosphorus was determined by digestion using a sulphuric acid and nitric acid (5N) solution and then by analysis using Ionic Coupled Plasma Photometry. A 15g/l sample was also hydrolysed for 2 hours using 0,1M NaOH. This was then analysed for glycerol, L-lysine and phosphate. The glycerol concentration was determined by HPLC as outlined in Chapter 2 (section 2.3.5.3). The lysine was determined by the previously described technique (Chapter 2, section 2.3.5.2). The sample was also analysed by Fast Atomic Bombardment (FAB) mass spectroscopy to determine the molecular mass. A Finnegan Mat TSQ700 mass spectrometer with an Ion Tech B15 power supply was used.

The cell mass which was obtained after the second CTAB wash was successively washed with 2 x 150ml 99,9% cold ethanol and then dried at 30°C under vacuum (-200kpa). This material was used for hydrolysis at a concentration of 2% m/v in either 0,05M NaOH or 0,1M NaOH over 24 hours at 60°C. A time profile was then set up of the glycerol, L-lysine and phosphate concentrations.

For analysis of the NaOH hydrolysed CTAB extract and cell material other standards were included such as D-ribulose, D-ribitol, D-glucose,

D-fructose, n-acetylglucosamine, glucosamine and lactic acid. For amino acid analysis the standard also included all 20 commonly found amino acids.

The biomass obtained from various fermentations (fermentations D, H and I, Chapter 5, section 5.4.2) were harvested and washed twice with 4°C de-ionised water, by centrifugation. The wash water was also used for hydrolysis and analysis. These samples were then used for hydrolysis with H_2O_2 (5% m/v) and 6N HCl to determine the glycerol-3-phosphate, glycerol and amino acid contents.

4.4 RESULTS AND DISCUSSION

4.4.1 The possible existence of two distinct phases of the cell cycle

In a typical base case fed-batch fermentation, the first 24 hours is the growth phase during which exponential growth occurs and manifests itself by both an increase in cell numbers, as obtained by haemocytometer count, and by an increase in the biomass (Figure 4.6).

The biomass concentration continues to increase after the increase in cell numbers ceases. If the total number of cells in the reactor is plotted relative to the total biomass in the reactor a similar result is found, i.e. after the 24 hour growth phase the cell number remains relatively constant initially until the dilution of the reactor by the feed reduces the cell numbers, and there is a continuous increase in the biomass concentration (Figure 4.7).

The increase in the mass of the biomass after cell growth is possibly due to the deposition of cell material. Examination of the structure of the cells over the time course of a fermentation by transmission electron microscopy showed a distinct morphological change in the cell wall (Figure 4.8A). The morphological change in the cells from the growth phase to the lysine synthesis phase is also evident from the scanning electron micrographs (Figure 4.8B). During the fermentation to produce L-lysine on this media, replication of the cells ceases when the threonine is depleted. Due to the auxotrophic requirements of the

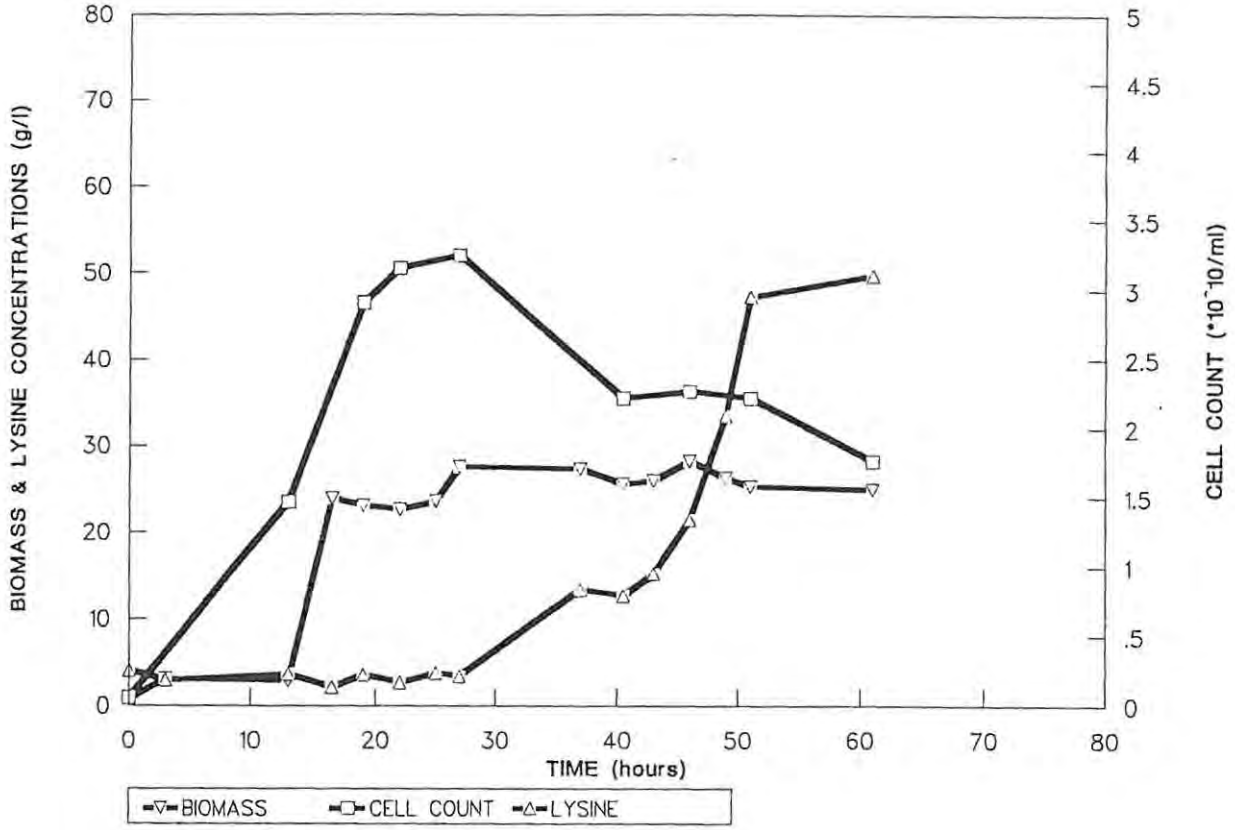

FIGURE 4.6 Change in the biomass, lysine and cell count during fermentation.

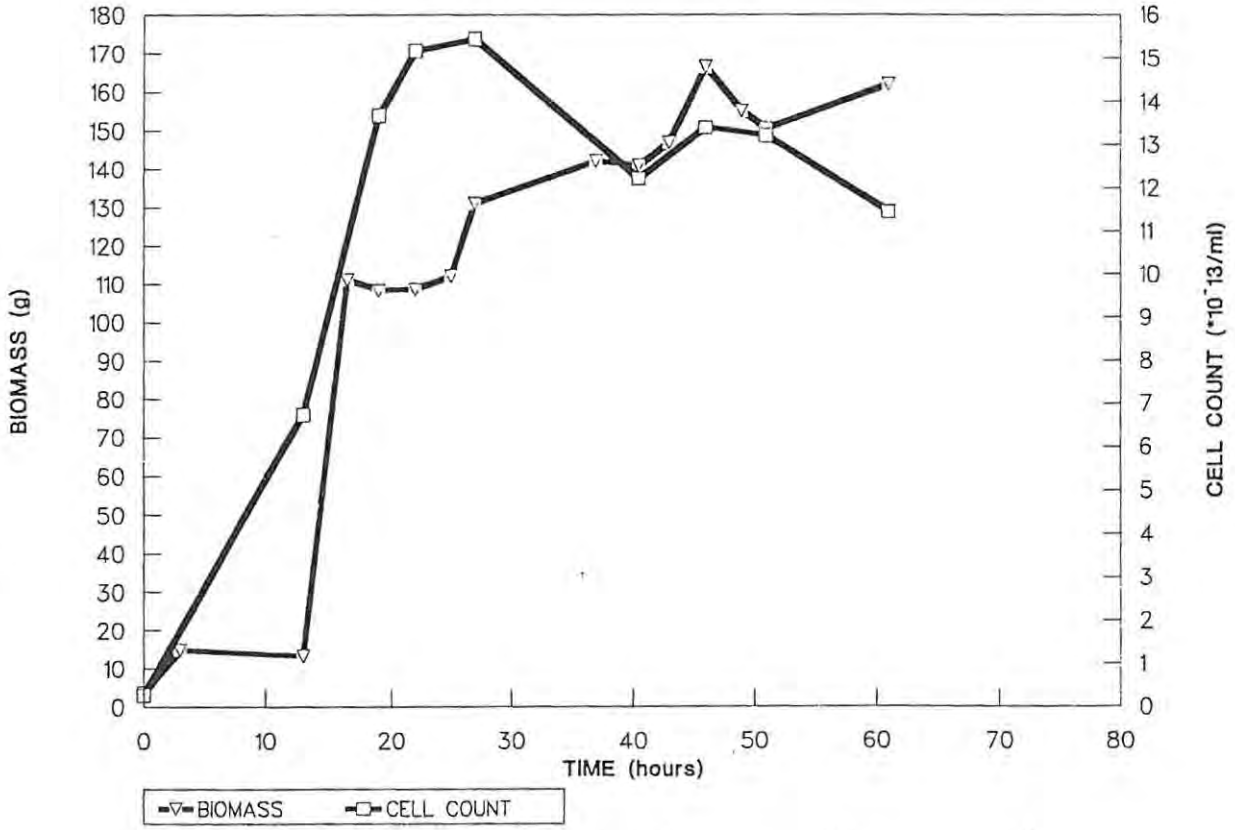

FIGURE 4.7 Change in the total reactor biomass and cell count during fermentation.

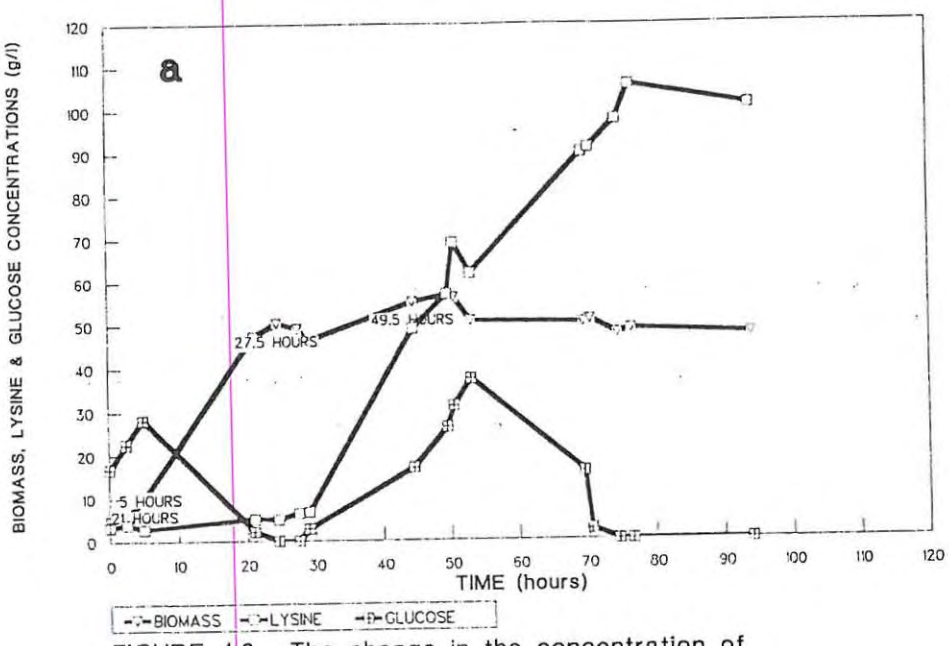

FIGURE 4.8 The change in the concentration of biomass, lysine and glucose during fermentation. The sample times for the TEM are also shown.

FIGURE 4.8A The change in the cell wall morphology of **Corynebacterium glutamicum** during fermentation. as shown by transmission electron microscopy. (magnification 89600).

a= fermentation profile indicating TEM sample times

Sample times for the TEM:

b= 2.1 hours

c= 5.0 hours

d= 27,5 hours

e= 49,5 hours

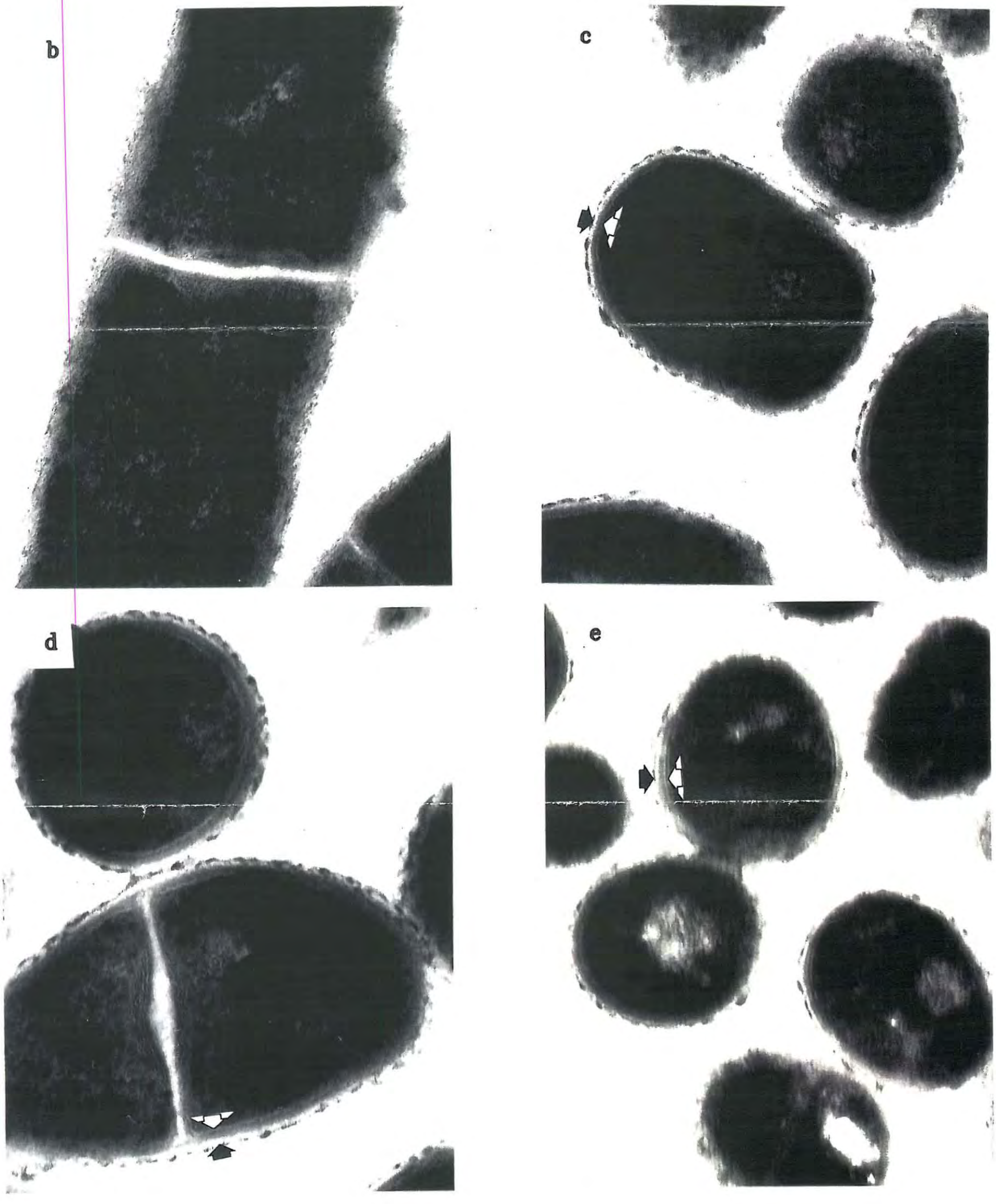

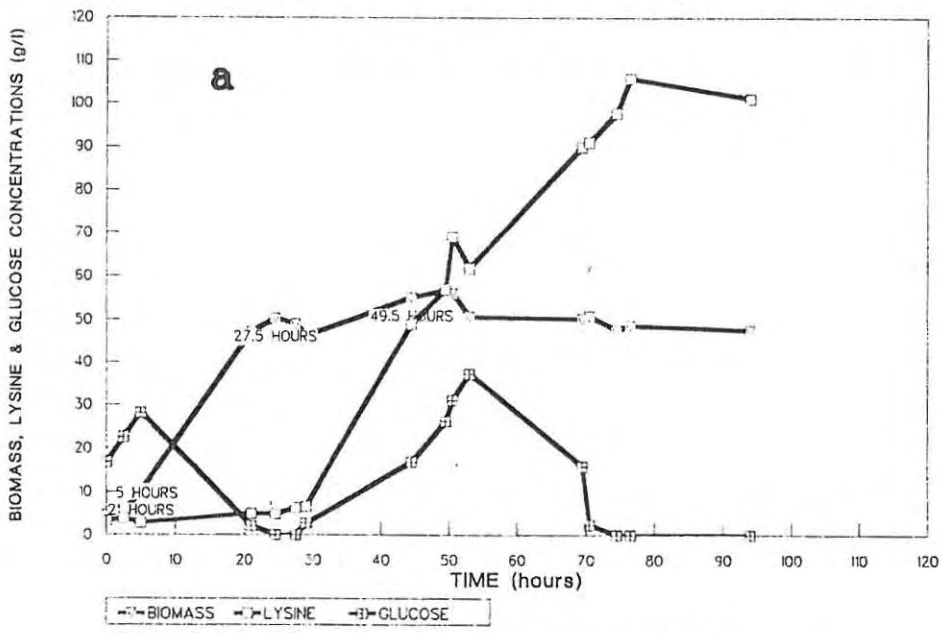

FIGURE 4.8 The change in the concentration of biomass, lysine and glucose during fermentation. The sample times for the SEM are also shown.

FIGURE 4.8 B The change in the cell wall morphology of **Corynebacterium glutamicum** during fermentation. as shown by scanning electron microscopy

a= fermentation profile indicating SEM sample times

Sample times for the SEM:

b= 2.1 hours

c = 5.0 hours

d = 27,5 hours

e = 49,5 hours

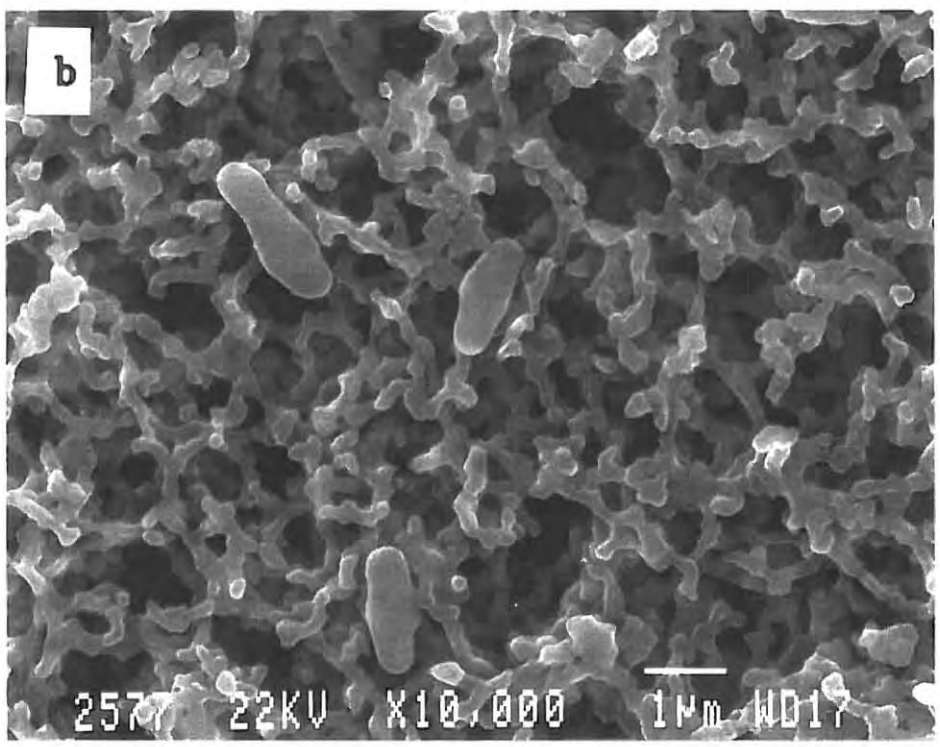

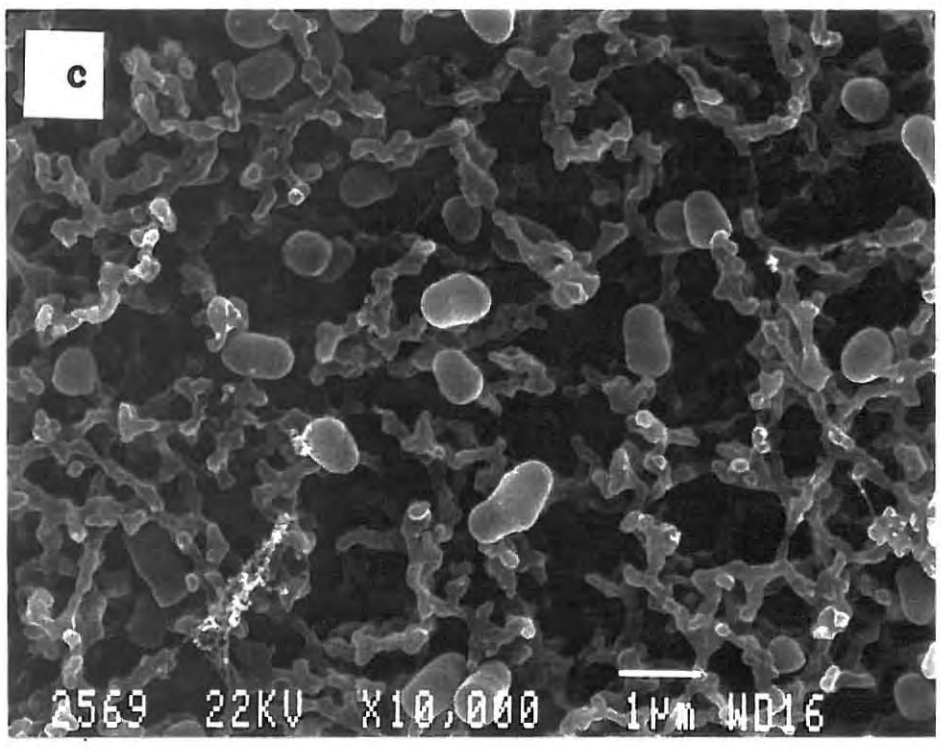

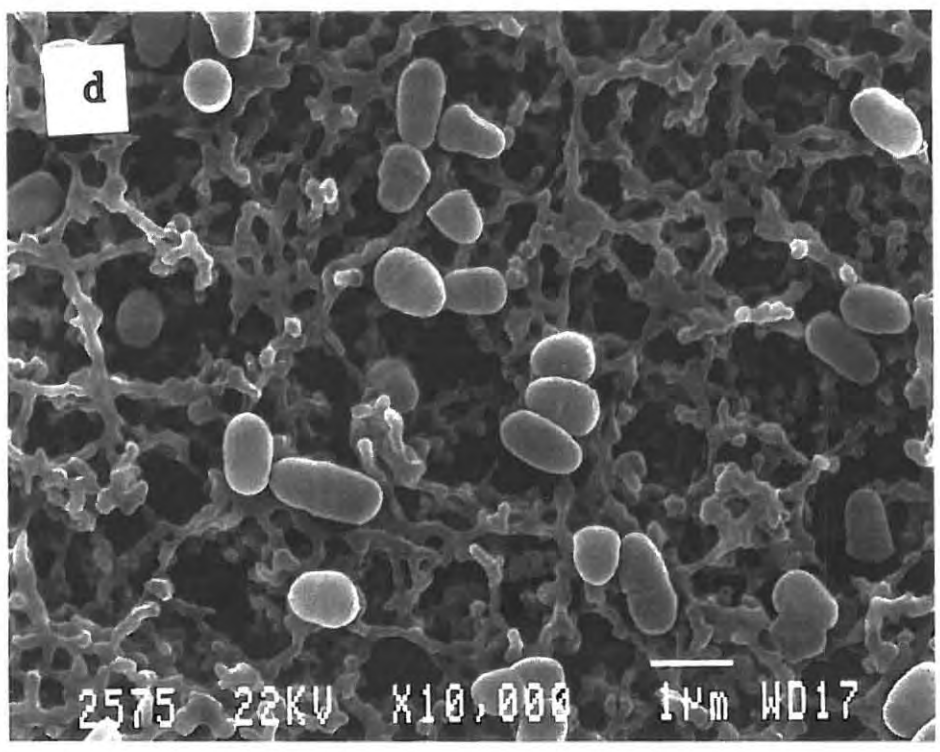

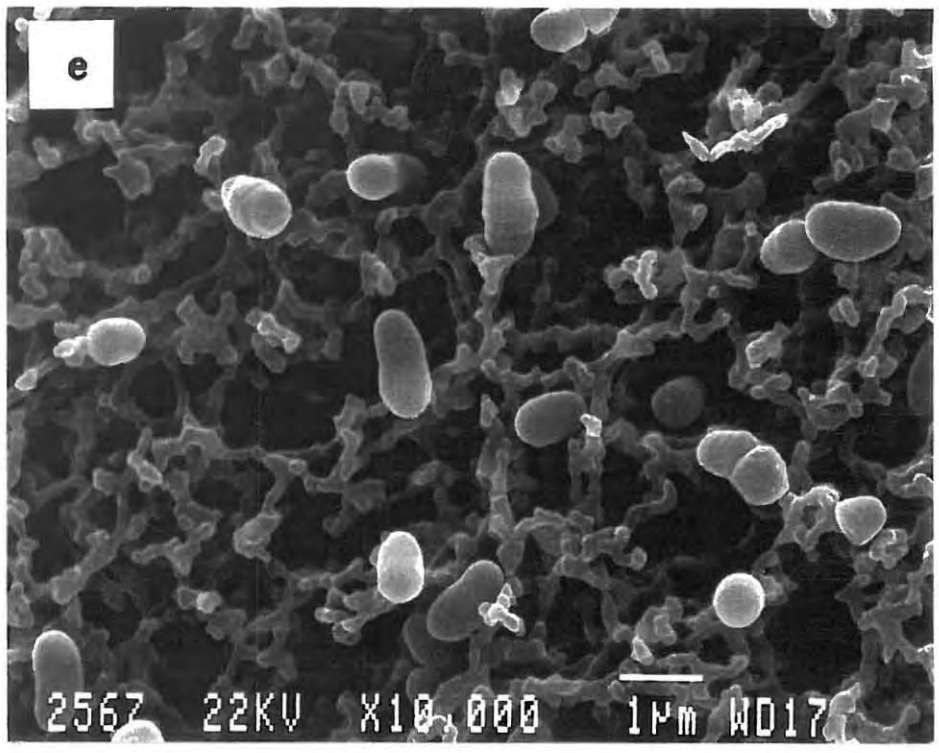

organism, protein and nucleic acid synthesis will therefore cease at this point. The organism will be capable of synthesizing only a small range of molecules. These will be in the form of storage materials, e.g. teichoic or teichuronic acids or poly-β-hydroxybutyric acid. Coello *et al* (1993) found that during phosphate limited continuous culture of *Corynebacterium glutamicum* ATCC 21513, morphological changes in the organism occurred. No polyhydroxybutyric acid was produced. They also found that the organism was capable of depositing polyphosphates and speculated on the possibility of the deposition of teichoic acid polymers, but these were not analysed for. As shown using transmission electron microscopy, a thickening of the cell wall was evident during lysine synthesis (Figure 4.8A). It is therefore reasonable to assume that the deposition of cell material occurs in the cell wall and is possibly either glycerol or ribitol teichoic acid, as the peptidoglycan forms the outer surface of the cell wall to maintain the cell's structural integrity. The synthesis of this teichoic acid is possibly also linked to the synthesis of lysine, and lysine synthesis may cease when teichoic acid synthesis ceases.

Two distinct phases therefore occur during the process to synthesize lysine. During the first phase typical microbial growth occurs which manifests itself as an increase in cell numbers. During the second phase "growth" continues to occur, as can be seen by the increase in the biomass concentration. However when compared with the haemocytometer count (cell count) this increase in biomass is as a result of an increase in physical mass of each cell. A distinct cycle therefore appears to occur; during the first phase with growth occurring by replication which continues until threonine limitation occurs (Chapter 5, section 5.4.4) and replication ceases. During the second phase of the cycle "growth" occurs, in the true sense of the word, by the increase in cell mass. It is therefore proposed that these two phases of the cell cycle are termed the replicative phase and the maturation phase.

4.4.2 Effect of the yeast extract concentration and the initial sugar feed rate on cell replication, maturation and lysine synthesis

4.4.2.1 Fermentation conditions

A range of base case fermentations were run using different concentrations of yeast extract and a range of glucose feed rates during the replicative phase of the fermentation. These are outlined in Table 4.1. The glucose feed rates used are given as a range and the individual fermentation feed rates are shown in the figures as results.

TABLE 4.1 : Base case fermentation conditions to determine the effect of the yeast extract concentration and the glucose feed rate during the replication stage, on the fermentation.

[a]YEAST EXTRACT CONCENTRATION (g/l)	[b]GLUCOSE FEED RATE (g/l/h)	NUMBERS OF FERMENTATIONS
25	~ 2,7	3
35	~ 2,7	3
45	2,1 - 2,9	10
55	2,3 - 4,5	14

(a) Concentration expressed per final fermentation volume as g/l

(b) Feed rate expressed as per initial fermentation volume as g/l/h

4.4.2.2 Data analysis

The concentrations in all samples were corrected for volume errors which were the results of sampling and evaporation from the fermenters. As sample volumes of approximately 70ml were taken, large volume errors in excess of 15% were therefore overcome. This ensured that mass balance calculations were carried out on the corrected volume of the fermentations.

The biomass yield during the replication phase on the glucose utilized during the replication phase was calculated from:

$$Y_{(xr/sr)} = \frac{V_{tr} \times X_r}{\{(VF_{to} - VF_{tr})S_f\} - (V_{tr} - S_r)}$$

where $Y_{(xr/sr)}$ = biomass yield on glucose during replication (g/g)

X_r = biomass concentration at the end of replication phase (g/l)

V_{tr} = fermenter volume at the end of replication phase (l)

VF_{to} = feed volume at the start of fermentation (l)

VF_{tr} = feed volume at the end of the replication phase (l)

S_f = glucose concentration in the feed (g/l)

S_r = residual glucose concentration in the fermenter (g/l)

The lysine "yield" with respect to the glucose utilized in the replication phase, as calculated from the lysine titre at the end of fermentation (end of maturation phase) relative to the glucose utilized during the replication phase was obtained from:

$$"Y"_{(p/sr)} = \frac{V_{tm} \quad P_{tm}}{\{(VF_{to} - VF_{tr})S_f\} - (V_{tr} - S_r)}$$

Where $"Y"_{(p/sr)}$ = fermentation lysine yield on glucose used during replication (g/g)

V_{tm} = fermentation volume at the end of the maturation phase (l)

P_{tm} = lysine concentration at the end of maturation phase (g/l)

The overall lysine yield on the fermentation was obtained from:

$$Y_{p/s} = \frac{V_{tm} - P_{tm}}{\{(VF_{to} - VF_{tm})S_f\} - (V_{tm} - S_m)}$$

where VF_{tm} = feed volume at the end of the maturation phase (l)

S_m = residual glucose concentration in the fermentation at the end of the maturation phase (g/l)

4.4.2.3 <u>The effect of the glucose feed rate on fermentation</u>

Using the data from the 45g/l yeast extract and 55g/l yeast extract experiments it was found that in both cases the biomass yield on the glucose utilized during the replication phase ($Y_{xr/sr}$) decreased with the increasing glucose feed rate (Figures 4.9A and 4.9B). The data was expressed both on a volumetric basis (g/l/h) and as a utilization rate (g/g/h). As all the glucose had been utilized by the end of the growth phase, the volumetric feed rate is actually also a volumetric glucose utilization rate. There was also a decrease in the biomass titre (Figures 4.10A and 4.10B). The lysine "yield" as calculated from the lysine titre at the end of fermentation relative to the glucose utilized during the replication phase ($Y_{p/sr}$) also decreased with increasing initial glucose feed rate and utilization rate (Figure 4.11A and 4.11B). The effect of the initial glucose feed rate and specific utilization rate on the lysine yield on glucose utilized during the maturation phase (lysine synthesis phase) at 45 and 55g/l yeast extract is shown in Figures 4.12A and 4.12B. At 45g/l yeast extract the lysine yield lies between 0,26 and 0,34g/g and at 55g/l yeast extract the lysine yield lies between 0,34 and 0,37. In both cases there appeared to be a decrease in the final lysine titre obtained with increasing initial glucose feed rate and glucose utilization rate (Figures 4.13A and 4.13B). In the fermentations using 55g/l yeast extract there appeared to be a transition at an initial glucose feed rate of 3,3g/l/h or a specific utilization rate of 0,4g/g/h at which point there is marked effect on both the lysine yield and final lysine titre. The effect was less marked in the case of the 45g/l yeast extract fermentations as it is believed that the range of initial glucose feeds used here lie over the transition point. This would account for the increased scatter in the data. However the overall effect is still evident.

At both yeast extract concentrations an increase in the initial glucose utilization rates appears to cause an increase in the biomass titre

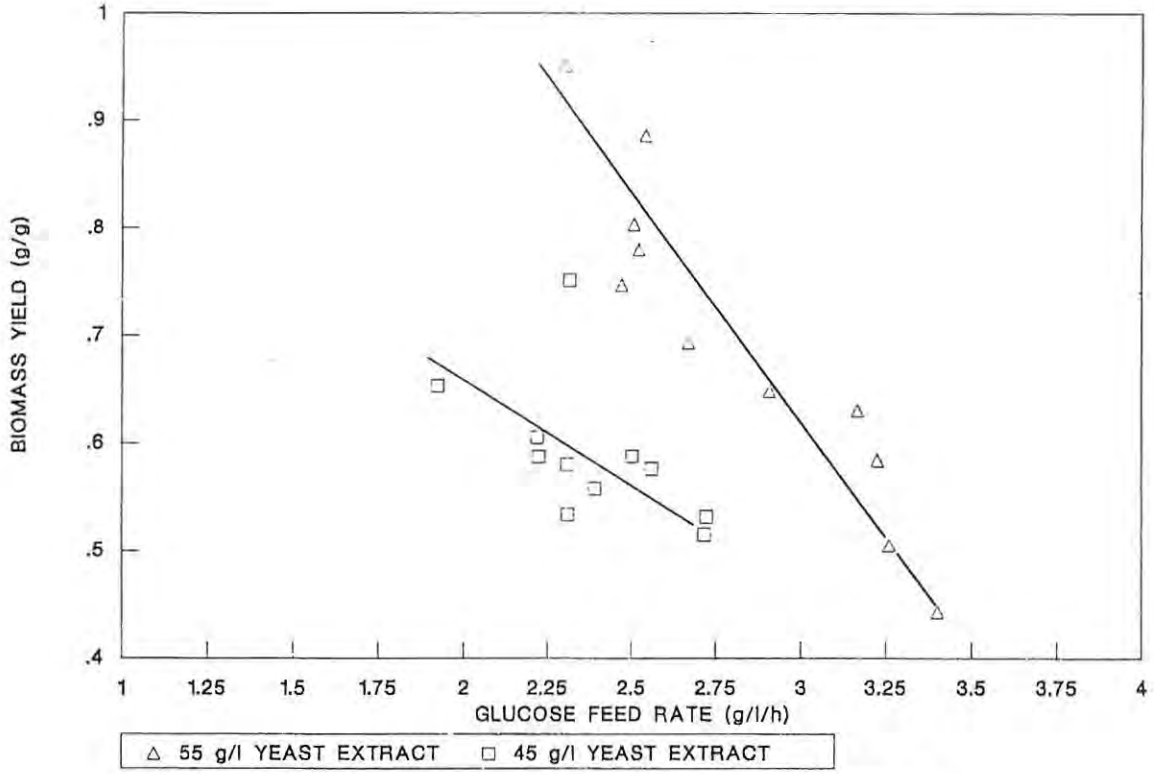

FIGURE 4.9A The effect of the glucose feed rate during the replication phase on the biomass yield at the end of the replication phase.

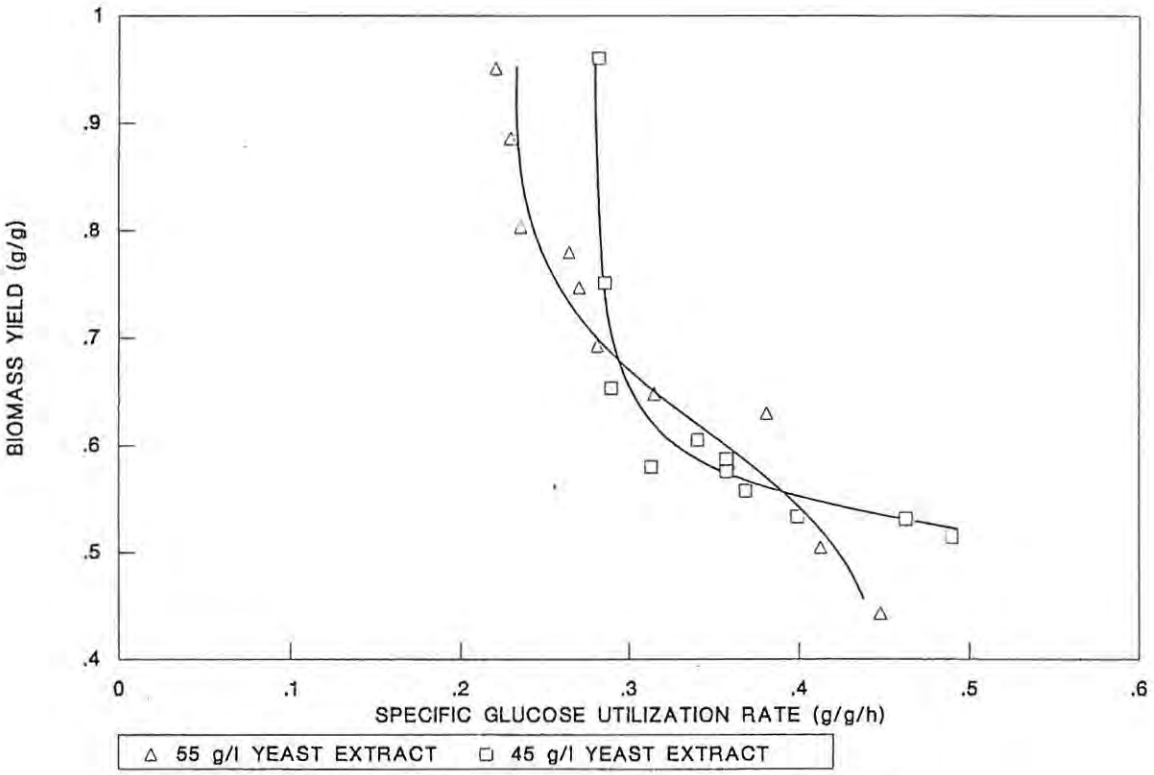

FIGURE 4.9B The effect of the glucose utilization rate during the replication phase on the biomass yield at the end of the replication phase.

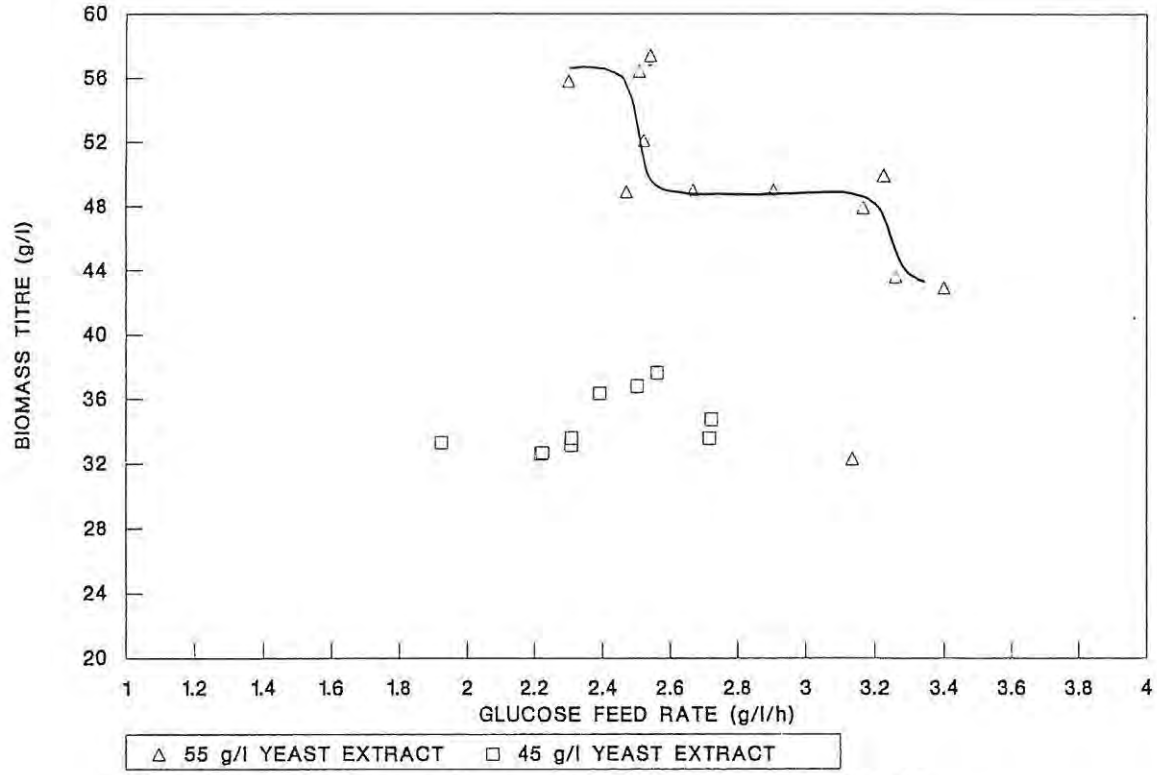

FIGURE 4.10A The effect of the glucose feed rate during the replication phase on the biomass titre at the end of the replication phase.

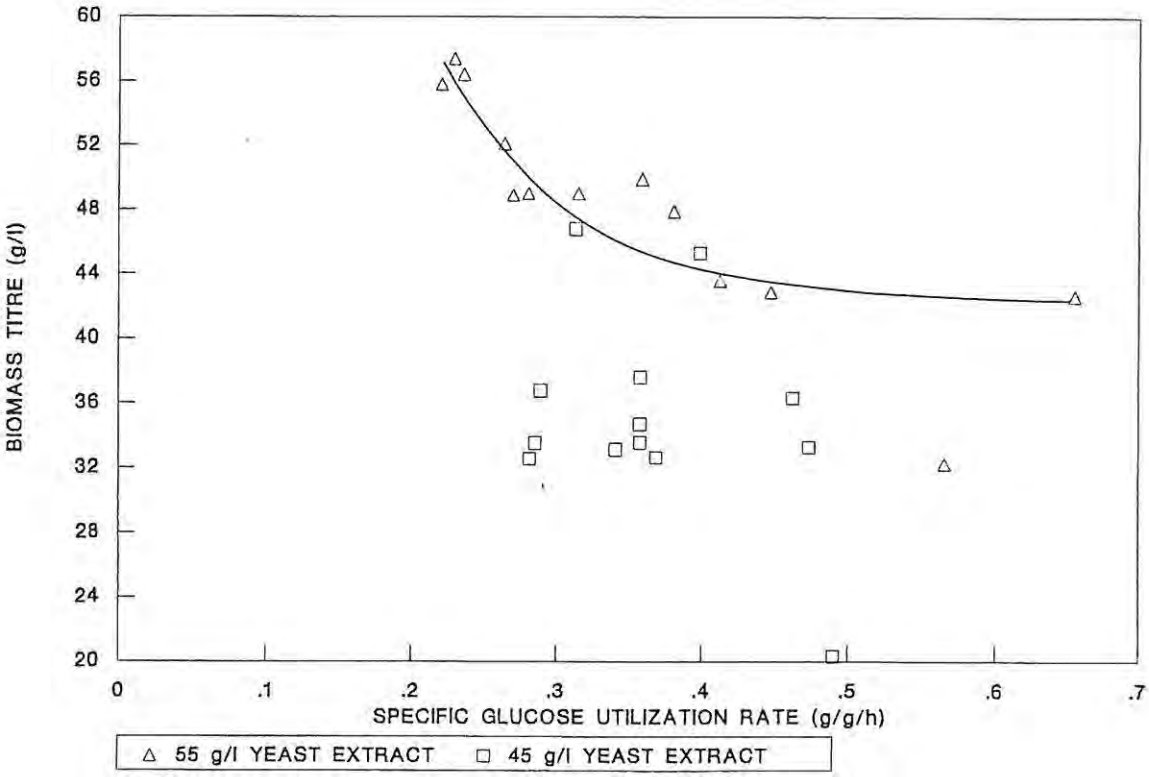

FIGURE 4.10B The effect of the glucose utilization rate during the replication phase on the biomass titre at the end of the replication phase.

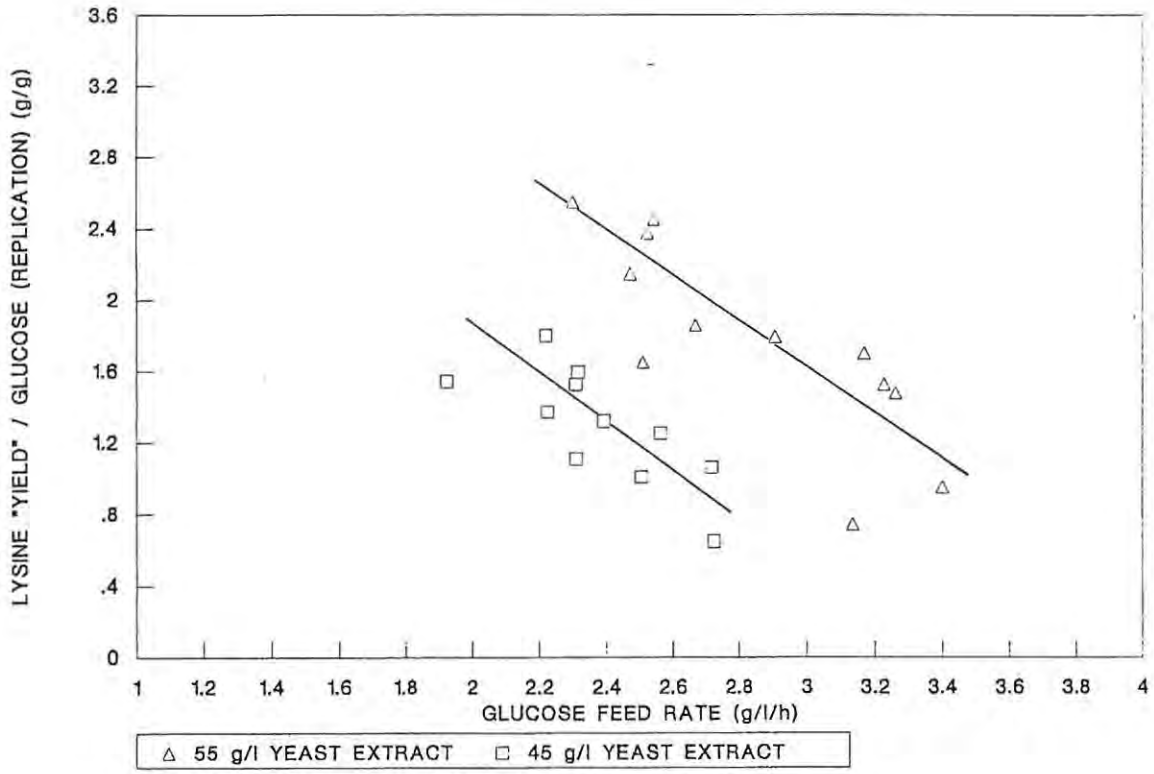

FIGURE 4.11A The effect of the initial glucose feed rate on the lysine "yield" i.e. the lysine per glucose used during the replication phase.

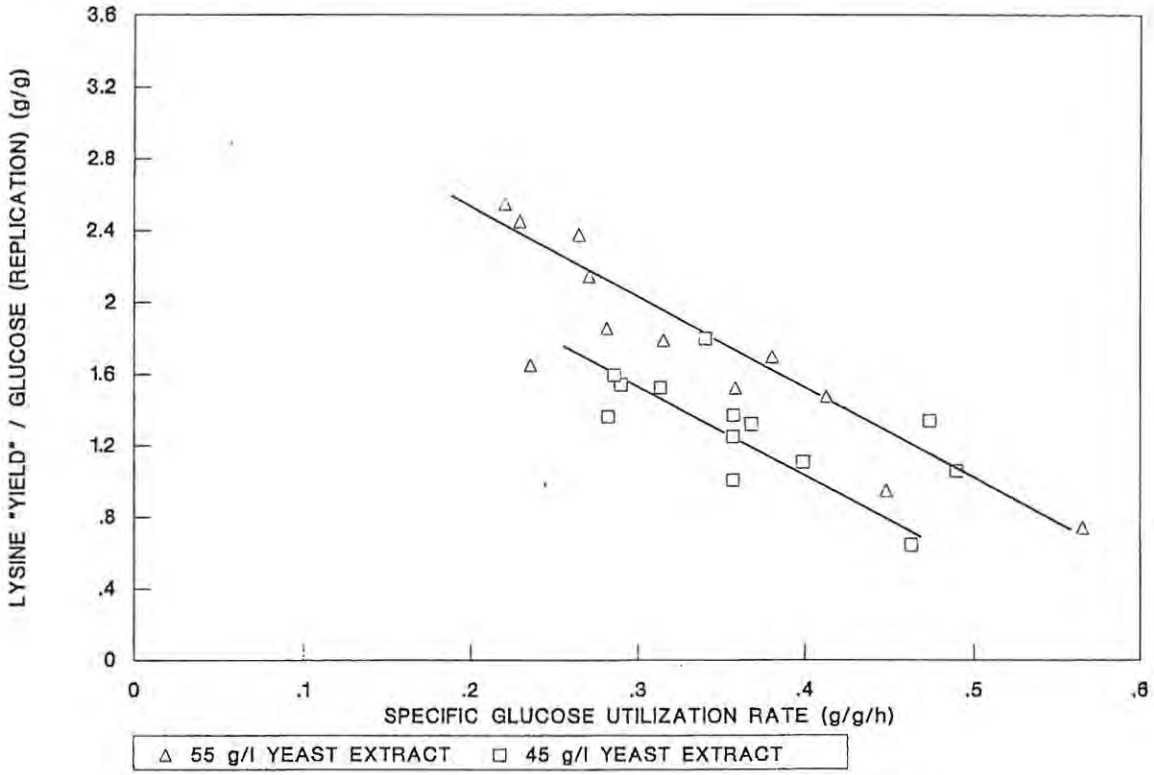

FIGURE 4.11B The effect of the specific glucose utilization rate on the lysine "yield" i.e. the lysine per glucose used during replication.

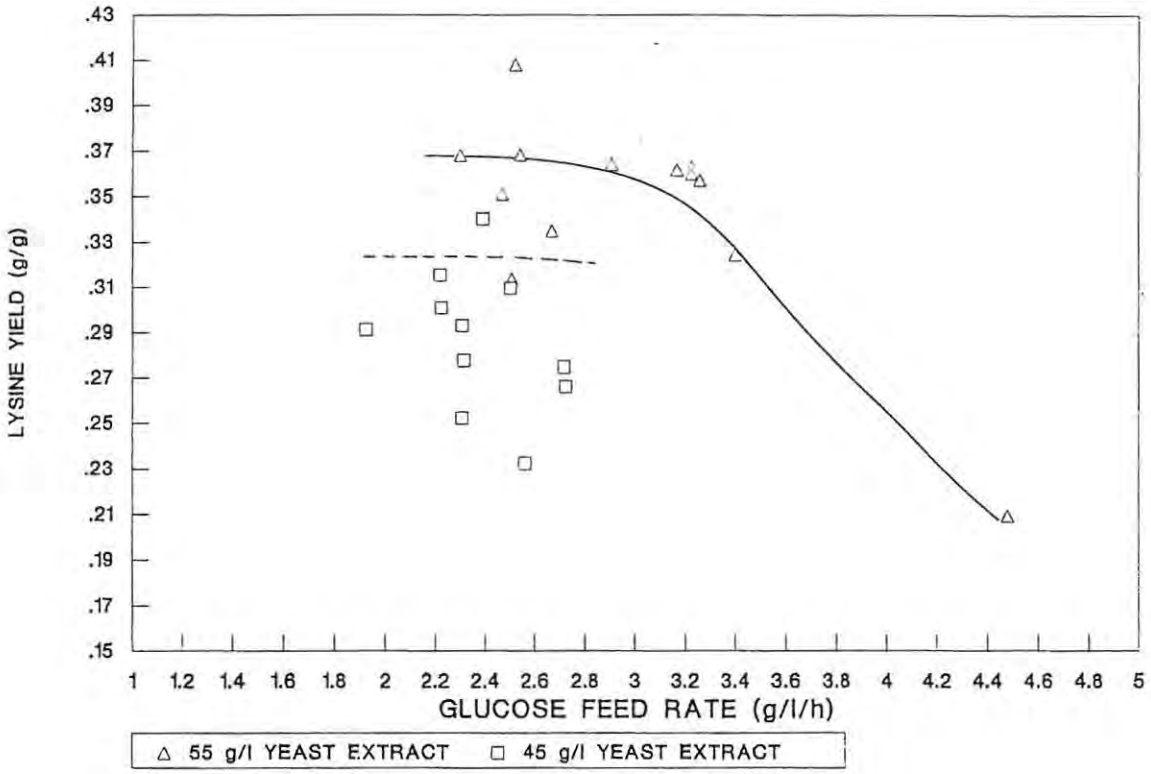

Figure 4.12A The effect of the initial glucose feed rate on the lysine yield during the maturation phase.

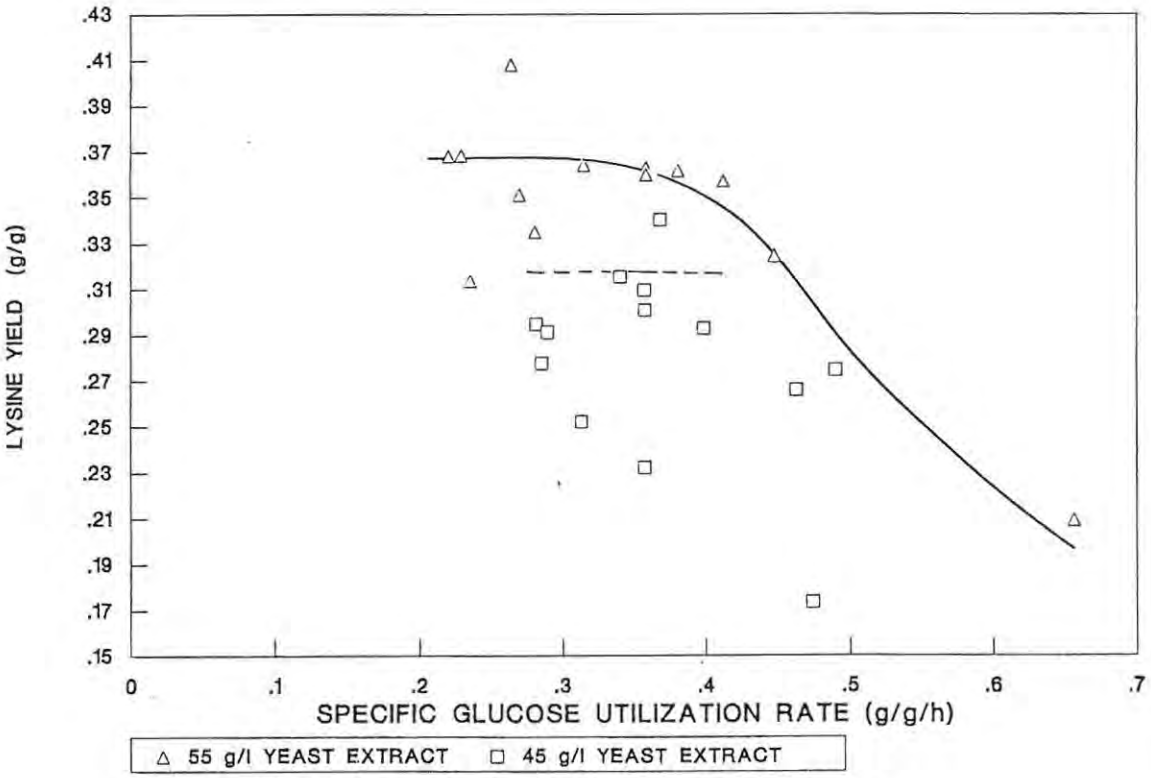

Figure 4.12B The effect of the specific glucose utilization rate on the lysine yield during the maturation phase.

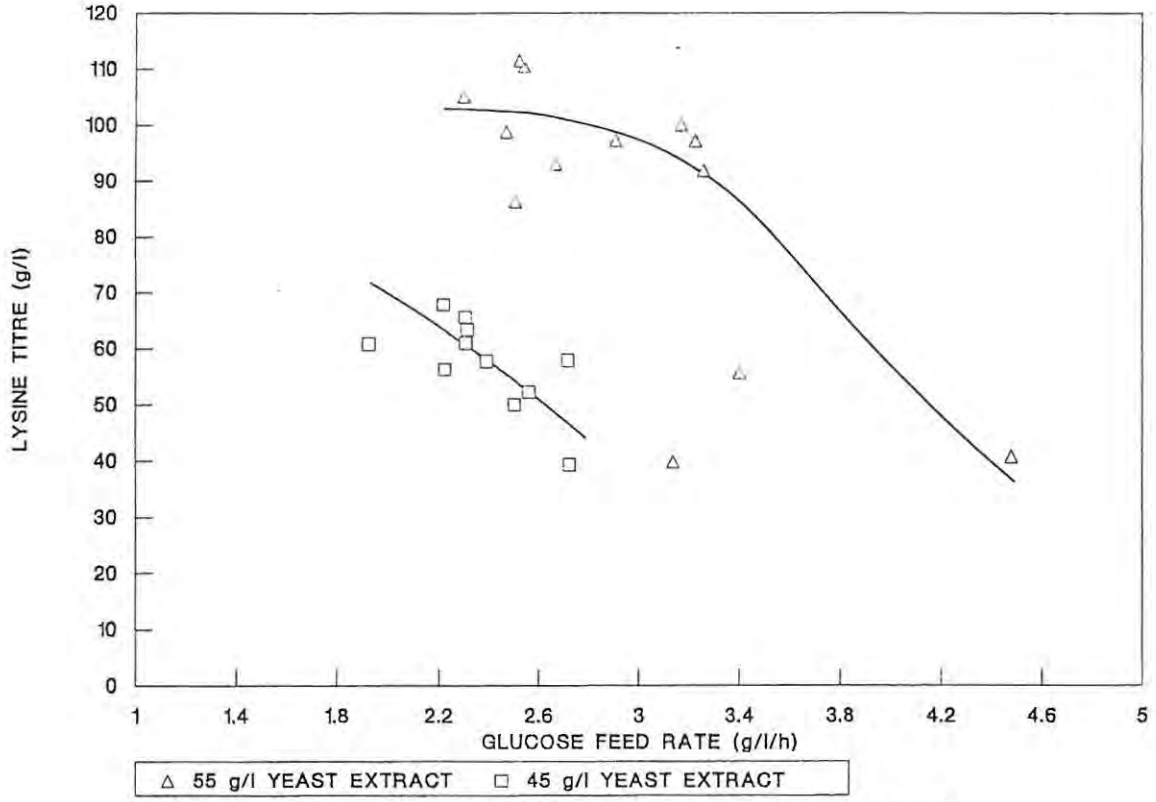

FIGURE 4.13A The effect of the initial glucose feed rate on the lysine titre.

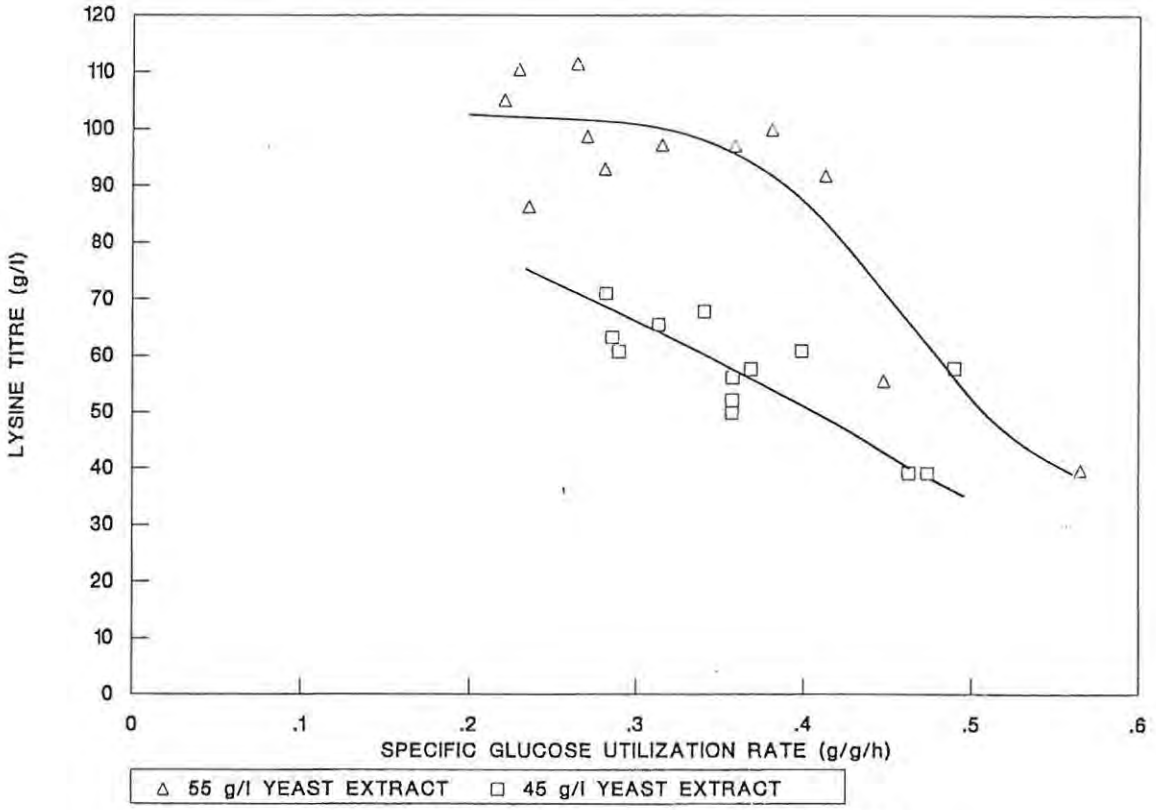

FIGURE 4.13B The effect of the specific glucose utilization rate on the lysine titre.

obtained during the maturation phase (Figure 4.14B). The same effect is not as clearly evident when this data is expressed relative to the feed rate (Figure 4.14A).

The transition effect is greater when looking at the effect of the initial glucose feed rate on the biomass yield per glucose utilized during the maturation stage (Figure 4.15A), at the different yeast extract concentrations. At 55g/l yeast extract there is a sharp transition which occurs at a feed rate of 3,15g/l/h. This transition occurs at approximately 2,5g/l/h in the case of the 45g/l yeast extract fermentations. As the yeast extract contains 3,4% m/m threonine and the biomass yield is dictated by the threonine concentration as a result of the organism's auxotrophic requirement for threonine, the threonine to glucose requirement can be calculated by these transition points. The end of the replication phase is taken to be 23 hours and 27 hours respectively for the 45g/l and 55g/l yeast extract fermentations (or 1,53g/l and 1,87g/l threonine).

At a replication phase of 27 hours and a glucose feed rate of 3,15g/l/h the organism's threonine to glucose requirement is 22mg threonine/g glucose for 55g/l yeast extract. At a replication phase of 24 hours and a glucose feed rate of 2,5g/l/h the organism's threonine to glucose requirement is 25,5mg threonine/g glucose at 45g/l yeast extract.

Expressing the quantity of "biomass" produced during the maturation phase per mass of lysine produced and plotting this against the specific glucose utilization rate, this is found to be constant at approximately 0,30g "biomass" per gram of lysine up to a specific glucose utilization rate of 0,4g/g/hr (Figure 4.16). Above this the biomass increases with a concomitant reduction in lysine titre (Figure 4.15A and 4.15B).

Plotting the lysine yield on biomass (specific lysine yield) and the lysine titre versus the yeast extract concentration used for fermentation the resultant interactions are not linear (Figure 4.17). Linearity is to be expected, as a specific mass of biomass should only be capable of producing a constant mass of lysine under constant conditions. This is possibly due to the fact that in the

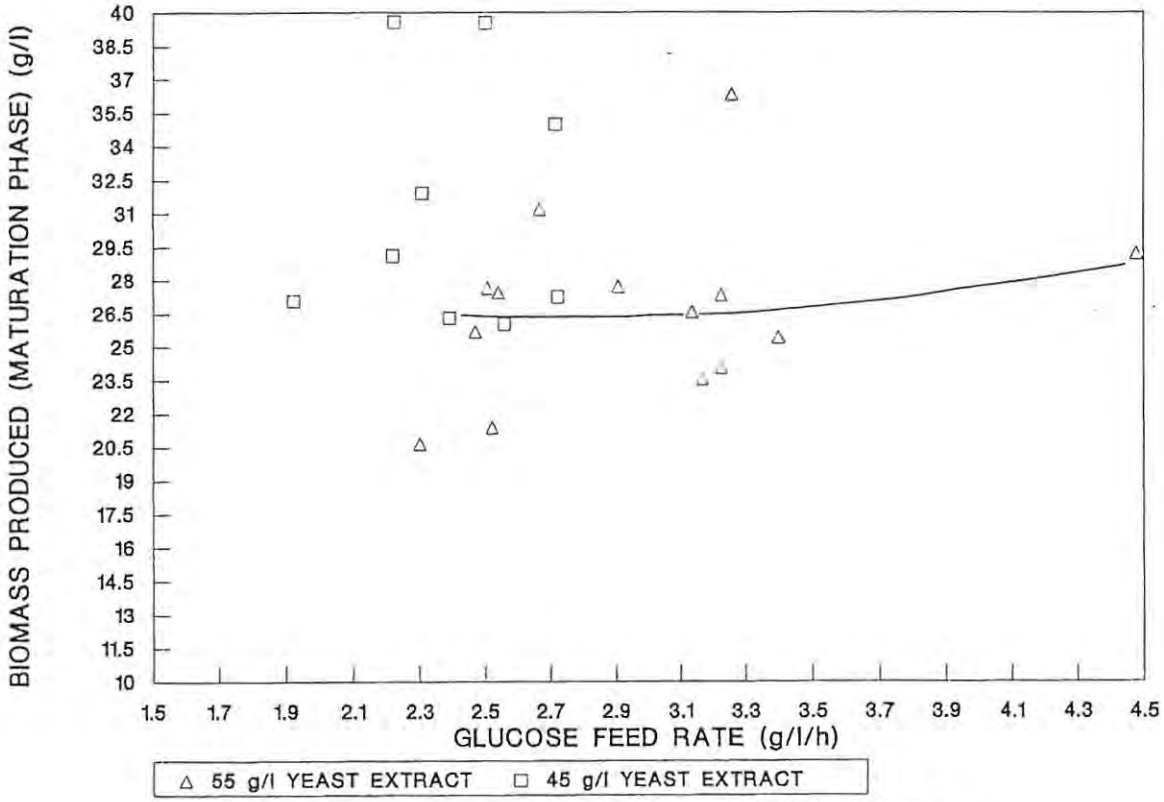

FIGURE 4.14A The effect of the glucose feed rate on the biomass titre during the maturation phase.

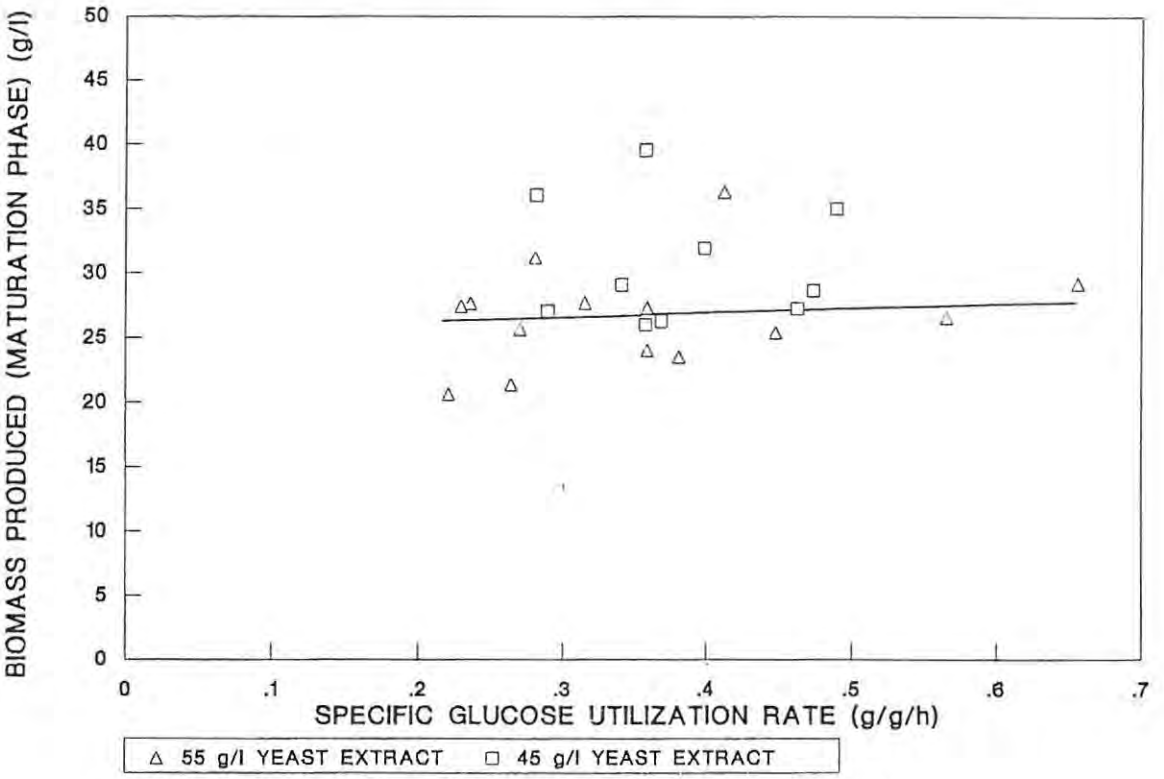

FIGURE 4.14B The effect of the specific glucose utilization rate on the biomass titre during the maturation phase.

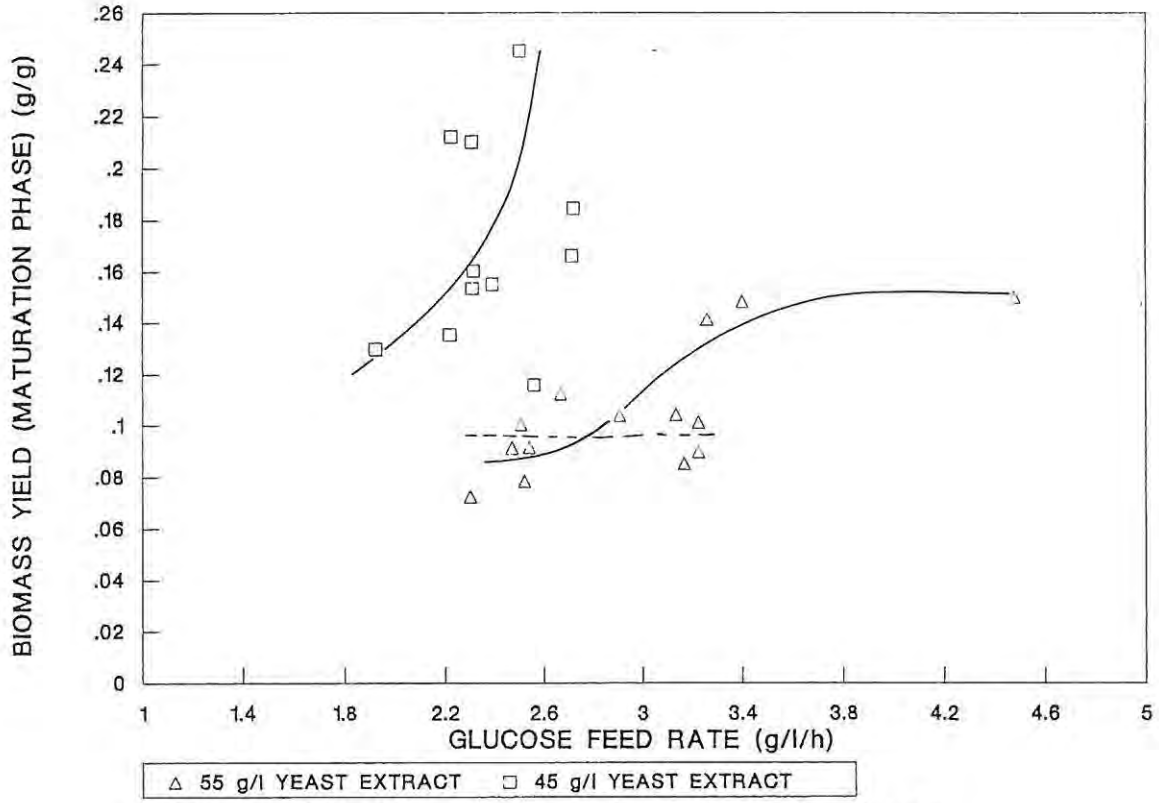

FIGURE 4.15A The effect of the glucose feed rate on the biomass yield during the maturation phase.

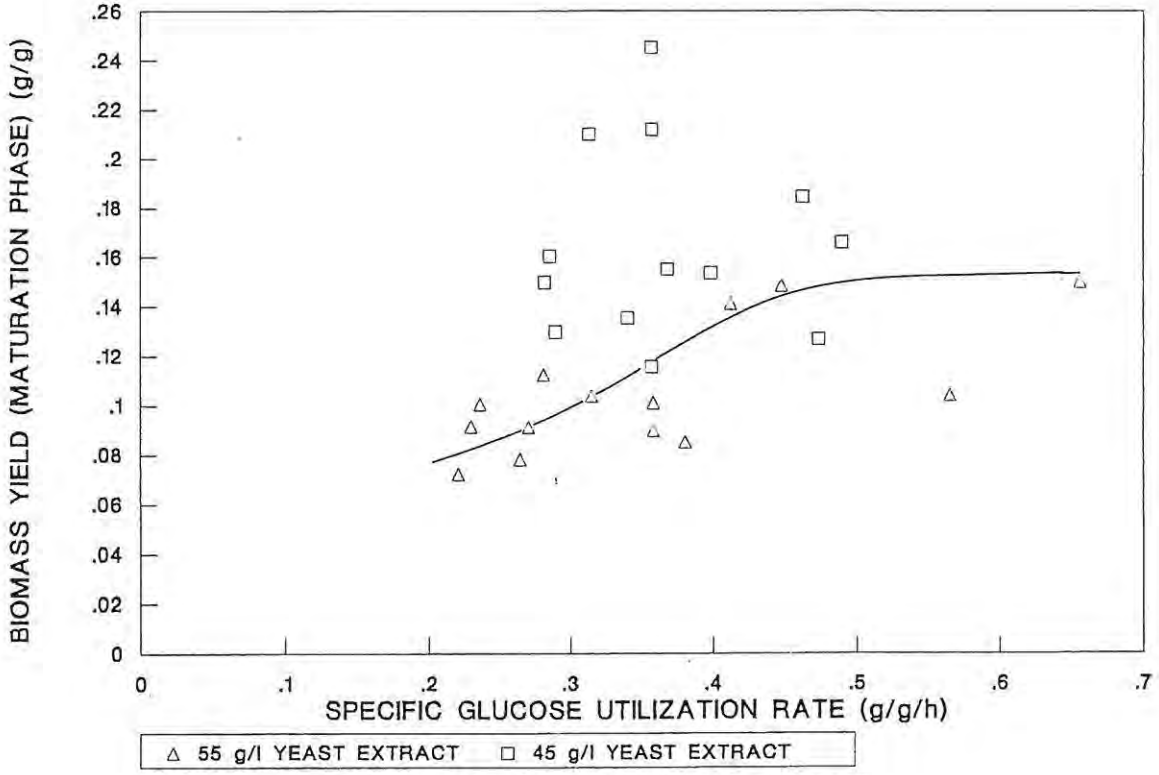

FIGURE 4.15B The effect of the initial glucose utilization rate on the biomass yield during the maturation phase.

102/...

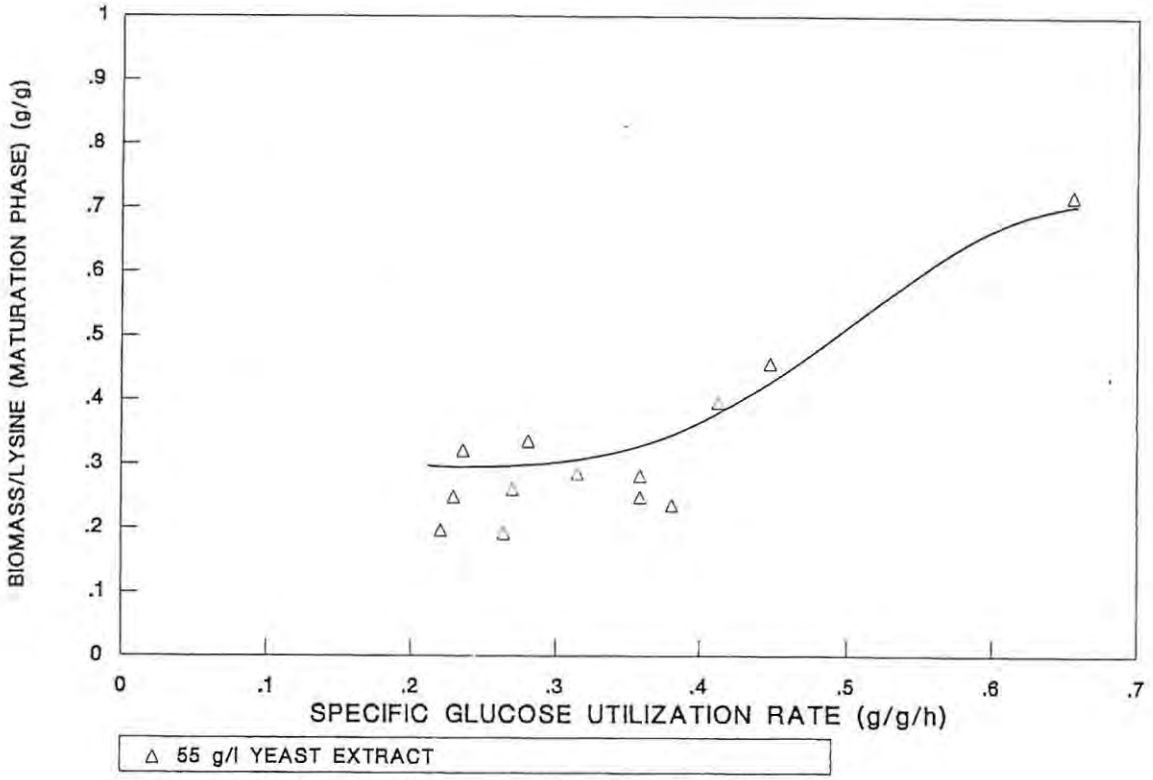

Figure 4.16 The effect of the specific glucose utilization rate on the "biomass" produced per mass of lysine during the maturation phase.

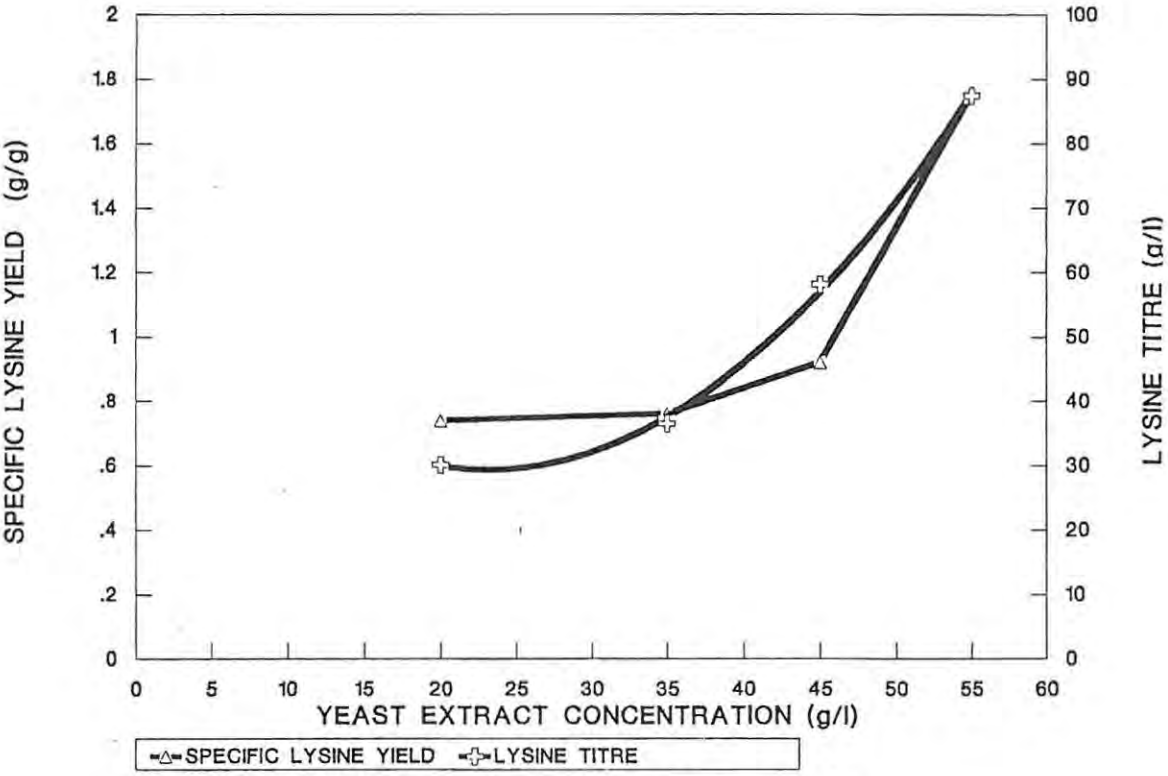

FIGURE 4.17 The effect of the yeast extract concentration on the specific lysine yield and the lysine titre.

fermentations at the lower yeast extract concentrations the initial feed rate was not optimum thereby allowing completion of the cell cycle during the growth phase when threonine was present and therefore inhibiting lysine synthesis. It is proposed that if the cells enter the maturation phase, this phase has to be completed before replication can be re-initiated. If for any reason a proportion of the cells enter the maturation phase during the "replication" phase, they will complete part of their cell cycle during this phase without the concomitant production of lysine.

The sharp transition which occurs at the respective glucose feed rates is the maximum level that the glucose feed rate should be allowed to attain before it adversely affects the lysine yield. However there does appear to be a trend in which the lysine titre decreases over the entire range of feed rates utilized, with increasing feed rate. At the lower feed rates the fermentations are in glucose limitation as the residual glucose concentration is below 200mg/l and the growth is linear (results not shown). The organisms would therefore be catabolite depressed with respect to glucose.

4.4.3 The identification of the storage material produced during the maturation phase

4.4.3.1 Soluble fraction of biomass

The soluble biomass fractions at the end of the replication phase and at the end of the maturation phase (as determined in section 4.3.4.1) are shown in Table 4.2.

TABLE 4.2 : The biomass and soluble biomass fractions at the end of the replication phase and the end of the maturation phase

	BIOMASS (g/l)	TOTAL MASS (g)	SOLUBLE FRACTION (g/l)	SOLUBLE FRACTION (g)
Replication Phase	35,96	183,40	19,04	97,11
Maturation Phase	49,66	407,21	31,73	260,19
FINAL FERMENTATION VOLUME 9,0 LITRES				

As shown in Table 4.2 the major proportion of the soluble biomass fraction is produced during the maturation phase concomitant with lysine production. This fermentation produced 69,34g/l of lysine or a total of 3,8 moles in 9 litres. If all the soluble fraction is taken to be glycerol teichoic acid (see below), with the molecular weight of the monomer being 158,5, this indicates that 3,56 moles of lysine are produced per mole of glycerol teichoic acid. This is also equivalent to 0,28 moles glycerol teichoic acid/mole lysine. This however does not take the insoluble fraction of teichoic acid into account or the possibility of other materials being synthesized.

If it is assumed that all the biomass produced during the maturation phase is glycerol teichoic acid with a repeating unit molecular mass of 158,5, and a structure as outlined in Figure 4.3, and this is expressed as a function of the lysine produced relative to the biomass produced and then plotted against the glucose utilization rate during the replication stage, it was found that for a major proportion of the feed rates the resulting teichoic acid is produced at a yield of approximately 0,36 moles glycerol teichoic acid per mole of L-lysine synthesized (Figure 4.16). This is however dependent on the point at which the end of the replication phase is taken.

4.4.3.2 Characterization of the soluble fraction of biomass

The relative carbon, hydrogen and nitrogen concentrations of the ethanol precipitate arising from the CTAB extract are as outlined in Table 4.3.

TABLE 4.3 : Carbon, hydrogen and nitrogen content of the ethanol precipitate of the CTAB extract. Also shown are the theoretical concentrations for glycerol teichoic acid and ribitol teichoic acid and their alanyl and lysyl derivatives.

	CARBON	HYDROGEN	NITROGEN	OXYGEN	PHOSPHORUS
Glycerol teichoic acid	23,48	4,22		52,12	20,18
Ribitol teichoic acid	27,17	4,56		54,30	14,01
Alanyl glycerol phosphate	31,86	5,79	6,19	42,44	13,70
Alanyl ribitol phosphate	33,34	6,64	4,86	44,40	10,74
Lysylglycerol phosphate	38,30	6,79	9,92	34,01	10,97
Lysylribitol phosphate	38,26	7,59	8,11	37,07	8,97
[a]Lysine glycerol phosphate	35,94	7,17	9,33	37,24	10,30
[a]Lysine ribitol phosphate	36,01	6,84	7,62	41,27	8,41
Sample	38,55	6,46	7,03	(35,76)	12,20

[a] This molecule assumes that the lysine forms a salt on the unoccupied oxygen of the phosphate group.

( ) Calculated by difference.

From this data (Table 4.3) the CTAB extracted material can be any of the lysine glycerophosphate compounds, either linked as an ester at the C-2 or C-3 position or forming a salt on the oxygen of the phosphorus.

The infrared spectra of the material indicated an organophosphorus compound (Figure 4.18) with bands at the following wavenumbers:

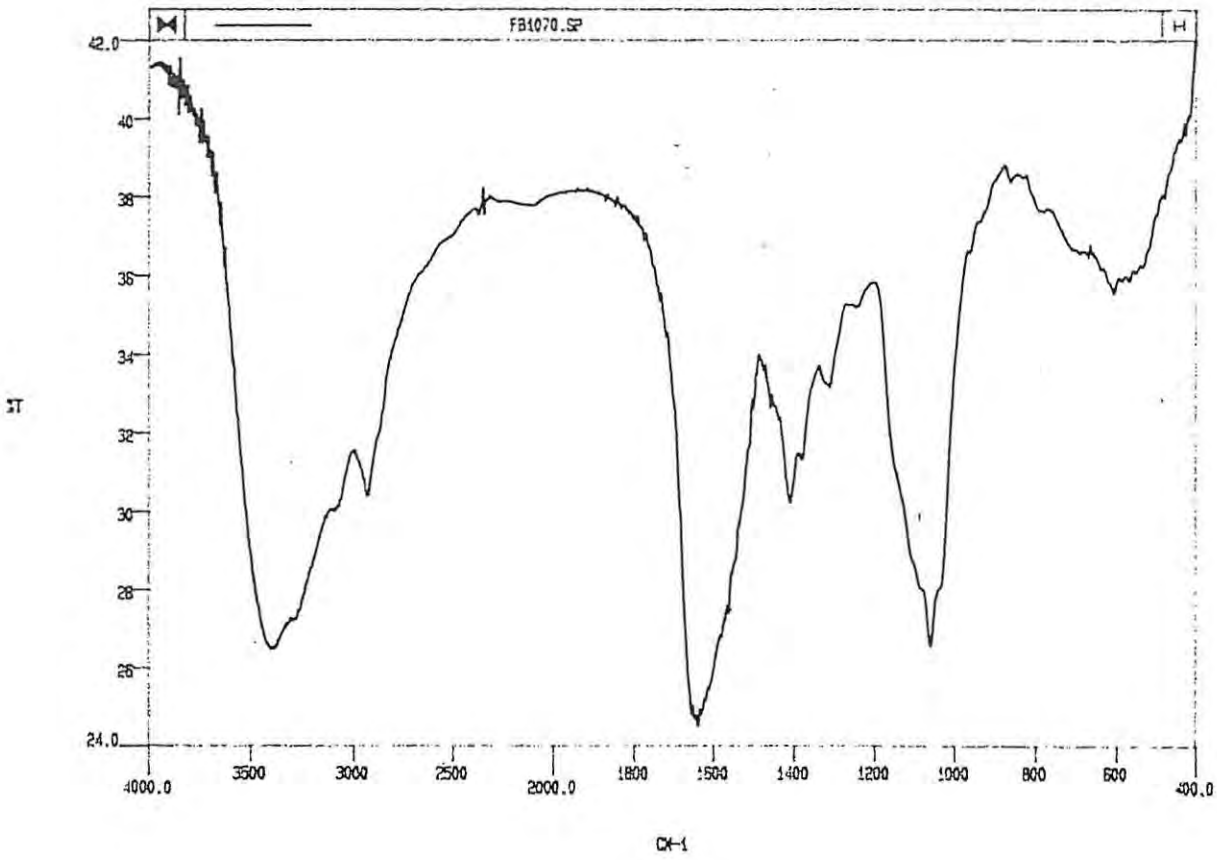

FIGURE 4.18 Infrared spectrum of the CTAB extract.

$3400cm^{-1}$	-OH
$2900cm^{-1}$	-CH
$1450cm^{-1}$	CHOH
$1200cm^{-1}$	P=O
$1050-990cm^{-1}$	P-O-L (aliphatic)
600	OH (out of plane)

The FAB mass spectroscopy gave a parent ion of a molecular mass of 284,1, therefore indicating the presence of lysoglycerol phosphate which has a molecular mass of 302,25 (Figure 4.19). This is based on the assumption that the lysylglycerolphosphate will lose one H_2O molecule during analysis. It has been found that if a strong acid is present H_2O may be lost during FAB analysis (Vekey and Zerilli, 1991). It is believed that this did occur in this case reducing the molecular weight of the parent ion from 302,25 to 284,1. It appears that a proportion of the lysylglycerolphosphate is either not in the form of a polymer and is therefore easily extractable using CTAB or the ethanol precipitation in the extraction process allows the acidic nature of the polymer to hydrolyse itself. Glycerol phosphate cannot be concentrated above 40% m/m as it hydrolyses itself (Merck Index, 1978).

After hydrolysis of the material using 0,05M NaOH for 16 hours at 65°C it was in fact found to contain lysine, glycerol and orthophosphate in equimolar concentrations (Figure 4.20). It was also found that 19,4% of the unwashed mass of biomass was extracted by the two cell washes using 0,2% m/v CTAB yielding glycerol teichoic acid, and recovered by ethanol precipitation. However the CTAB removed a total of 54% m/m of the cell dry mass. It is possible that the ethanol precipitation is not entirely effective in precipitating all the teichoic acid and other extracted materials. In *Bacillus subtilis* the chain length of the teichoic acid was found to range between 5 and 20 monomeric units (Archibald *et al* 1993). The lower molecular weight units may not have been effectively precipitated.

Hydrolysis of the residual cell mass (Figure 4.21) at 0,05M and 0,1M NaOH at 100°C yielded additional lysine, glycerol and phosphate at equimolar concentrations. The hydrolysis profile does not conclusively prove that

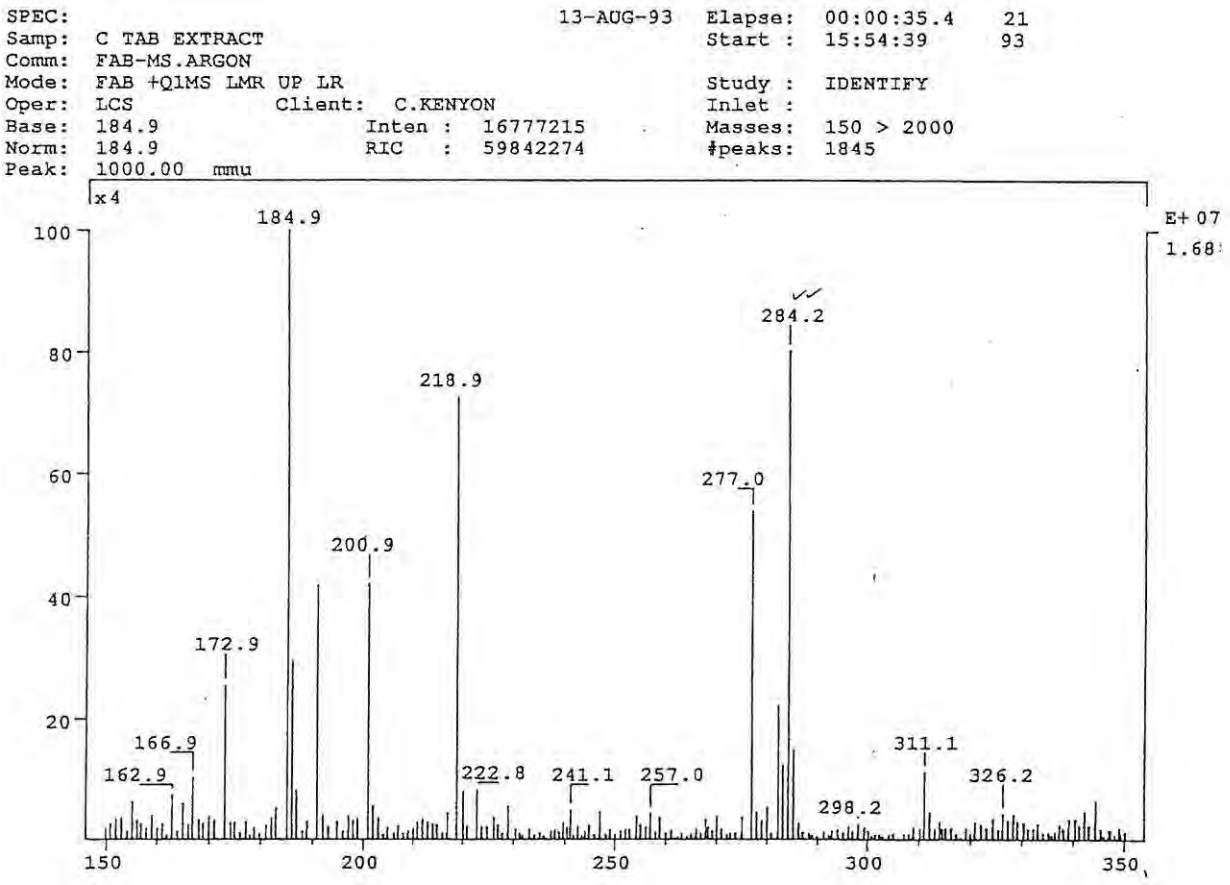

FIGURE 4.19 FAB mass spectrum of the CTAB extract.

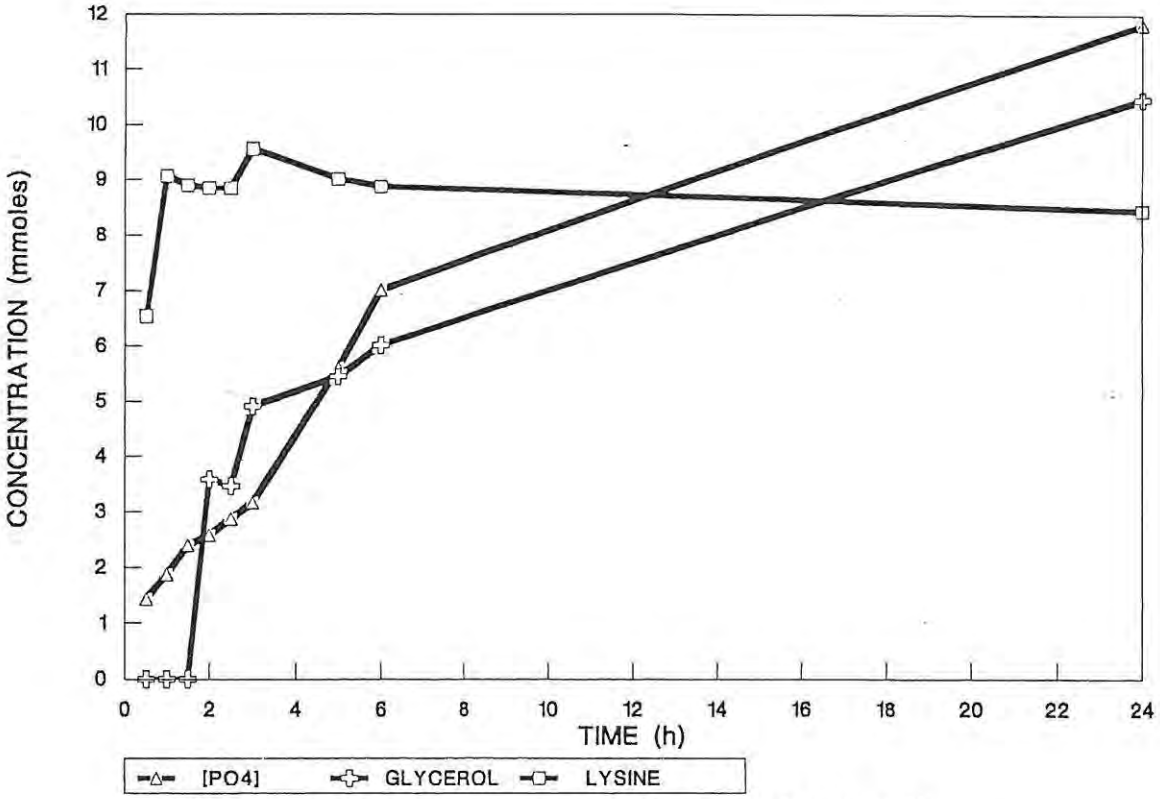

FIGURE 4.20 Hydrolysis of the CTAB extract with 0.05M NaOH at 65 deg C.

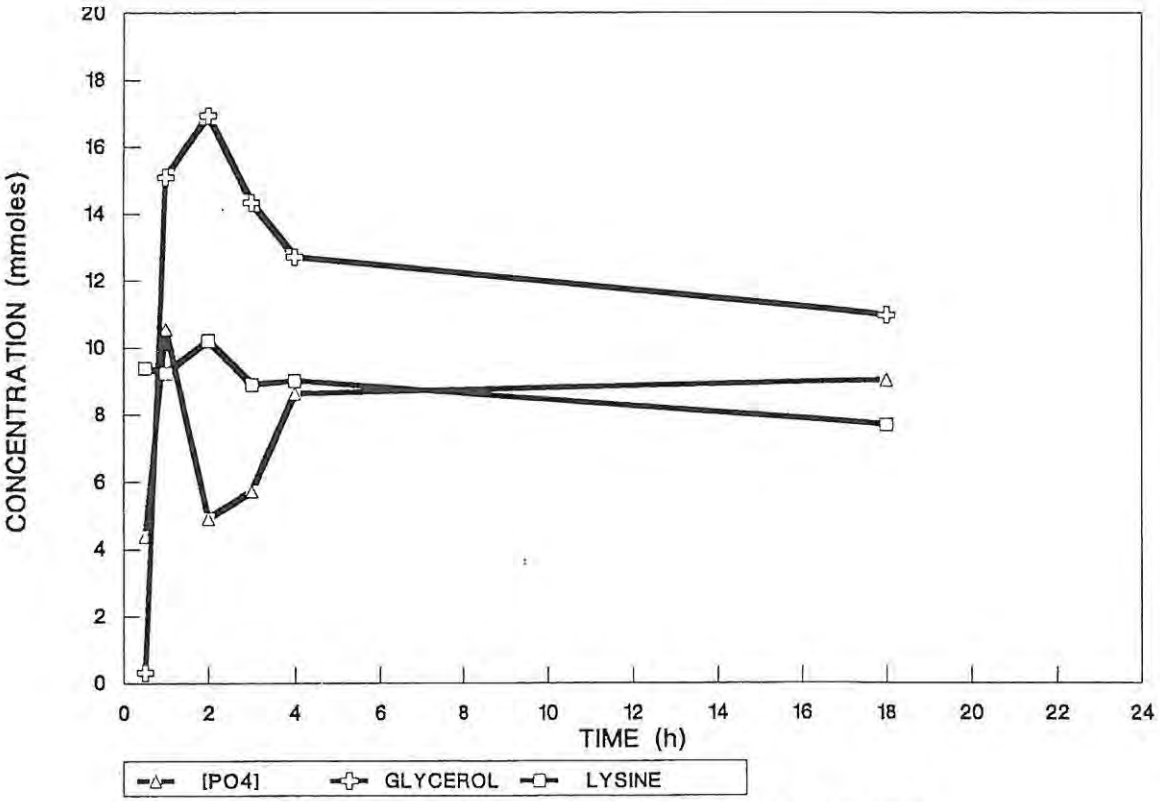

FIGURE 4.21 Hydrolysis of the residual cell mass with 0.05M NaOH at 100 deg C.

the lysine is covalently bonded by an ester linkage either at the C-1 or C-2 position, depending on whether the polymer is present as 1,2- or 1,3-glycerol phosphate. It is feasible that the lysine is present as a salt with the oxygen of the phosphate group. The other alternative is that the rate of hydrolysis of the lysine from the polymer is greater than the glycerol-phosphate backbone. The FAB mass spectroscopy indicated that at least some of the material is present as lysylglycerolphosphate.

The quantitative hydrolysis of CTAB extracted material and biomass, to give glycerol and phosphate, was not entirely resolved. The complete hydrolysis of glycerol-3-phosphate to glycerol and phosphate appears to be almost impossible, with maximum efficiencies of 2 percent being claimed to be the maximum in the literature (Dawson *et al*, 1969). The conditions of hydrolysis used were 10N HCl at 100°C for 3 hours. The use of H_2O_2 to oxidize the teichoic to glycerol-3-phosphate was used. On subsequent hydrolysis with 6N HCl efficiencies ranging between 2 and 10 percent were obtained (Table 4.4). All samples were analysed for the presence of polyols and amino acids.

TABLE 4.4 : The glycerol, glycerol-3-phosphate (G-3-P), and amino acid content of various CTAB extracts and biomass. All results are expressed as % m/m of the material.

	[a]G-3-P	[b]Glycerol	[c]Alanine	[d]Proline	[e]Lysine
CTAB extract	18,12 10,49	1,18 1,52	1,31 0,00	4,37 4,30	7,26 0,00
Biomass	12,11 12,20	5,40 6,50	5,14 4,15	6,98 8,08	3,46 3,59

[a] A 0,1% m/v solution of the sample was treated with 5% H_2O_2 for 30 minutes, after which NaOH was added to a concentration of 0,3N and allowed to react for 24 hours.

[b] A 0,1% m/m solution of the sample was treated with 6N HCl for 24 hours. It was then neutralised, centrifuged and then suitably diluted for analysis.

[cde] A 0,2% m/m sample was treated as for ([b]).

The high levels of glycerol-3-phosphate and proline in the CTAB extracts were expected as the CTAB preferentially extracts acidic and negatively charged species. The high levels of glycerol-3-phosphate in the cells are an indication of the levels that may be attained. Due to the inefficiency of the hydrolysis these levels may in fact be higher. All the above samples, on being suspended in water, indicated the presence of between 5 and 7% m/m glycerol-3-phosphate. This is either an artifact of the analysis, or a proportion of the material is soluble or solubilised in the cell wall due to the highly acidic nature of glycerol-3-phosphate. This is possible if its counter-ion is removed during the washing process.

On washing the cell mass with distilled water and then titrating the supernatant with increasing concentrations of NaOH and precipitating with ethanol, it was found that there was a concomitant increase in the ethanol precipitable material (Figure 4.22). On hydrolysis of the material obtained at a concentration of 0,4M NaOH, using increasing concentrations of NaOH at 65°C for 16 hours, a titration profile was obtained as outlined in Figure 4.23. During the first addition of NaOH prior to high temperature hydrolysis it is believed that the first 0,025M NaOH is used in reacting at position 1 (Figure 4.23) on the polymer. The increase in precipitable material between 0,025M and 0,125M NaOH is as a result of the titration of the amino groups on the lysine residue (positions 2 and 3, Figure 4.23) and the hydrolyses of the polymer at position 5. The increase in the soluble lysine concentration during hydrolysis is as a result of the hydrolyses of the lysine at position 4. The final material which precipitated therefore is disodium glycerol phosphate. It could not have been proline, as proline is soluble in ethanol. On hydrolysis using 8N NaOH at 100°C for 16 hours, the material was quantitatively found to contain glycerol, phosphate, proline and lysine. However if a conservative 10% hydrolysis efficiency is assumed,

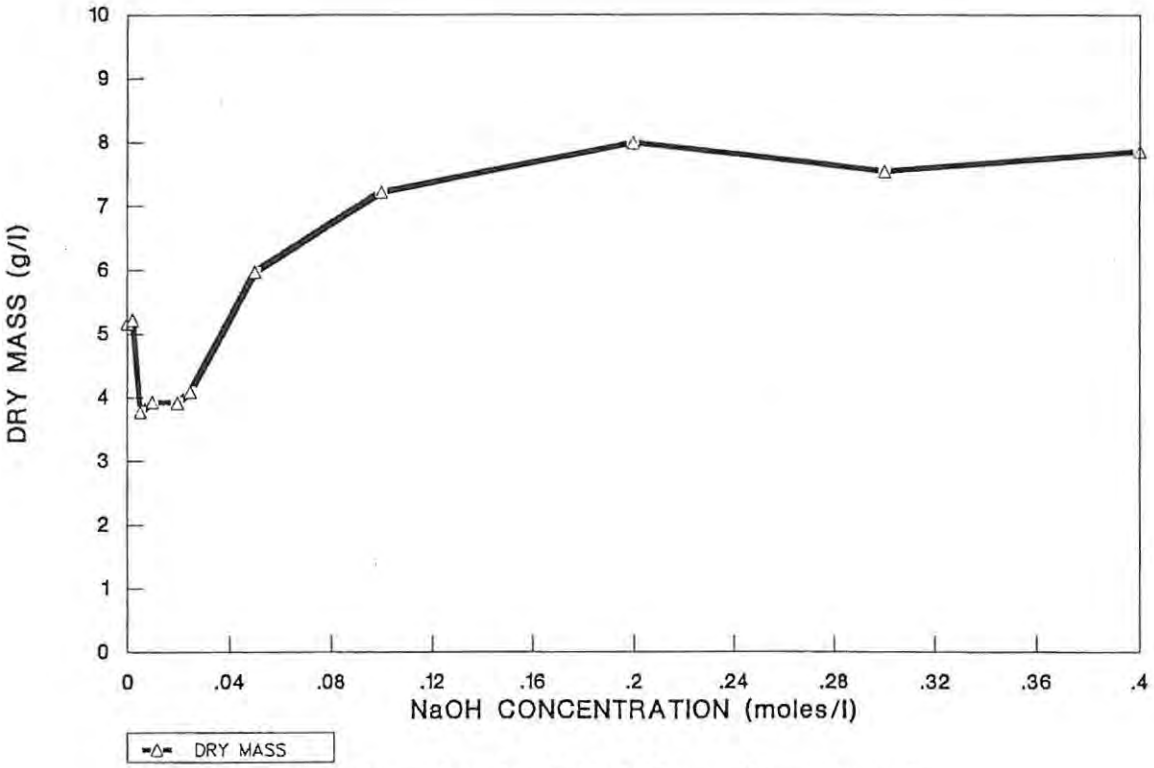

FIGURE 4.22 The effect of NaOH on the ethanol precipitable material from water washed cells. Expressed as g/l of the fermentation broth.

113/...

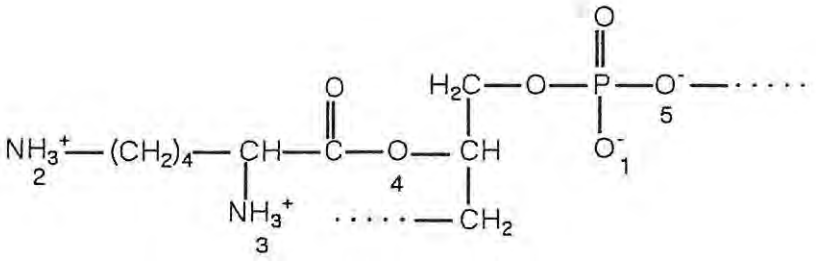

FIGURE 4.23 The structure of lysylglycerolphosphate.

the material was predominantly glycerol phosphate.

Assuming that only lysine, CO_2 and glycerol teichoic acid are synthesized during the maturation phase of growth, as outlined in Figure 4.24, a redox and energy balance may be carried out on this process (Figure 4.24). The pathway is drawn on the basis that 3 moles of glucose enter glycolysis to produce 2 moles of L-lysine, 0,5moles of glycerol teichoic acid and 3 moles of CO_2. The overall redox balance is zero. The ATP balance is -2. This may be accounted for by the electrons of the $FADH_2$, arising from the oxidation of succinate to fumarate, entering oxidative phosphorylation and producing 2 moles of ATP. The only remaining compound not accounted for is the GTP produced by succinyl-CoA synthetase. This would however be consumed by the phosphorylases which catalyse the polymerization of glycerol-3-phosphate to teichoic acid.

4.4.3.3 <u>Theoretical lysine yield taking cell wall synthesis into account</u>

An overall mass balance was carried out on a 1 800 litre fermentation to reduce the errors caused by sampling when running a 10 litre laboratory fermentation.

The theoretical biomass yield during the lysine synthesis phase (maturation phase) was calculated on the basis that 0,5 mole of glycerol teichoic acid is synthesized per mole of lysine produced. The theoretical lysine yield is taken to be 2,0 moles lysine per 3,0 moles (i.e. 0,67) (Figure 4.24) glucose metabolised during the lysine synthesis phase, with one mole of glucose being utilized for teichoic acid synthesis and maintaining the redox balance within the cells, i.e. 0,5 moles glucose being used for the synthesis of glycerol-3-phosphate and 0,5 moles glucose entering the TCA cycle to generate reduced NADPH. It is assumed that there is no increase in the cell number during this stage and all the increase in biomass concentration can be attributed to an increase in cell mass (i.e. heavier cells) as a result of the deposition of the glycerol teichoic acid in the cell wall.

The theoretical molecular balance during the lysine synthesis stage therefore is given by the equation:

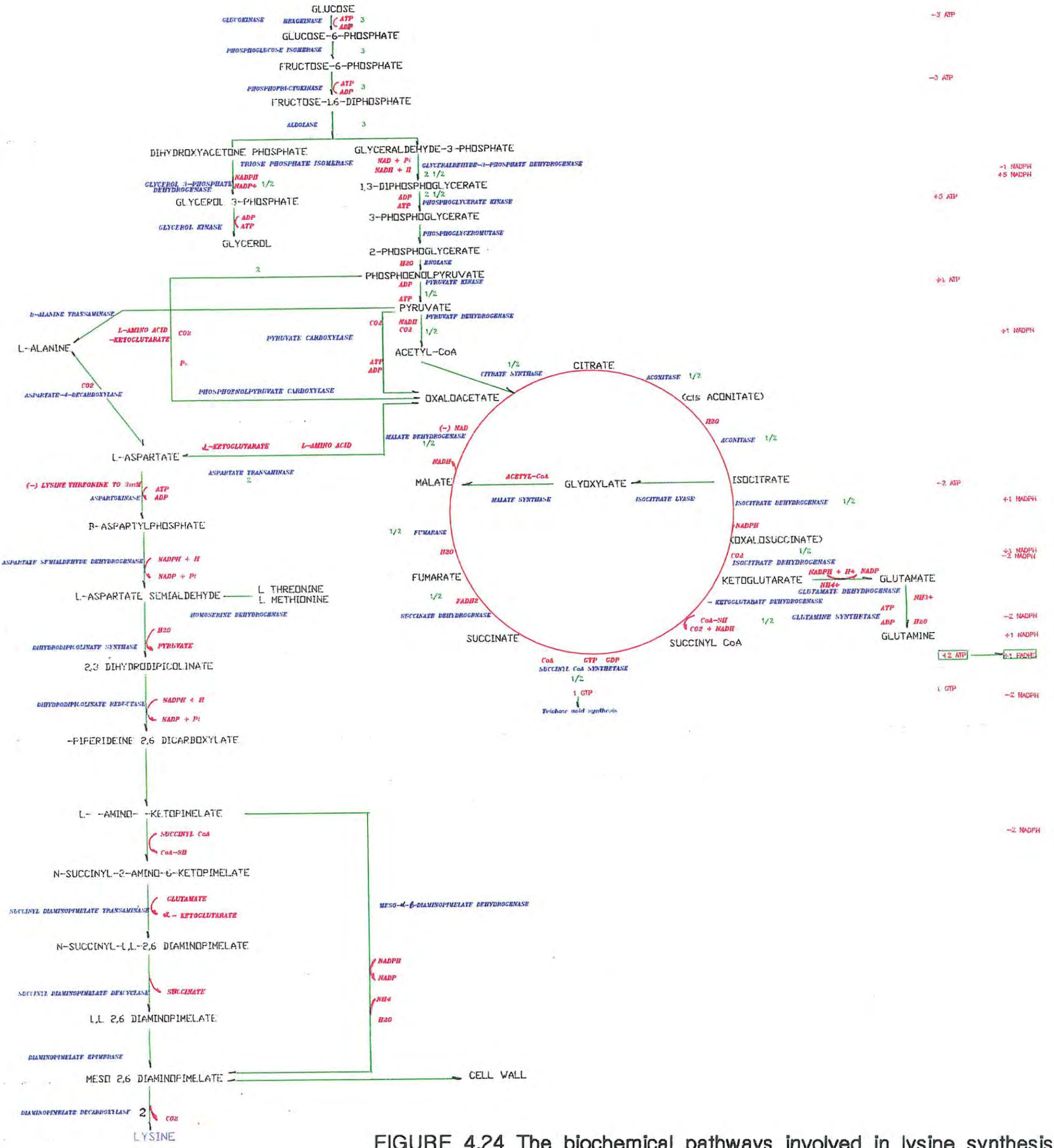

FIGURE 4.24 The biochemical pathways involved in lysine synthesis. Included is the proposed nucleotide balance, assuming that the process starts with 3 moles of glucose resulting in the synthesis of 2 moles of lysine.

$$3C_6H_{12}O_6 + HPO_4^- + 2NH_4^+ + 2NH_3 + O_2 \longrightarrow$$

$$2C_6H_{15}O_2N_2^+ + 3CO_2 + 1[C_3H_7O_5P]_n + 9H_2O$$

The fermentation profile in terms of biomass, L-lysine and glucose is as outlined in Figure 4.25. As previously stated, during the maturation phase there is a continuous increase in the biomass, even though the fermentation is being diluted as a result of the glucose feed.

During the replication phase the respiratory quotient (mole CO_2/mole O_2) is reduced from 1,2 to 0,9, however it gradually returns to a level of 1,2 with a concomitant change in the lysine yield to a maximum level of 0,34 (Figure 4.26). The lysine yield expressed here is the cumulative lysine yield. The CO_2 produced per mole of lysine synthesised during the lysine synthesis phase plateaus at approximately 7,5 moles/mole (Figure 4.27). This is a great deal higher than the 1,5 moles/mole as outlined by the theoretical balance. Futile cycles possibly exist where energy is consumed, thereby increasing the quantity of carbon entering the TCA cycle and oxidative phosphorylation.

By plotting the biomass produced during this maturation phase, calculated as moles glycerol teichoic acid per mole of L-lysine synthesized, it was found that the level increases to approximately 0,34 moles biomass (as glycerol teichoic acid) per mole of lysine produced (Figure 4.28). As the organism no longer requires RNA during lysine synthesis and RNA may make up as much as 30% of the cell mass during active growth, the difference in this yield to that of the theoretical yield of teichoic acid may be accounted for by the reduction in RNA.

4.5 CONCLUSION

Two distinct phases appear to occur during the fermentation of glucose to lysine by *Corynebacterium glutamicum* FP6. During the first stage, or replication phase, no lysine is synthesised and active cell growth by replication occurs. At the end of the replication phase the threonine in the culture media is depleted and cell multiplication ceases. During the

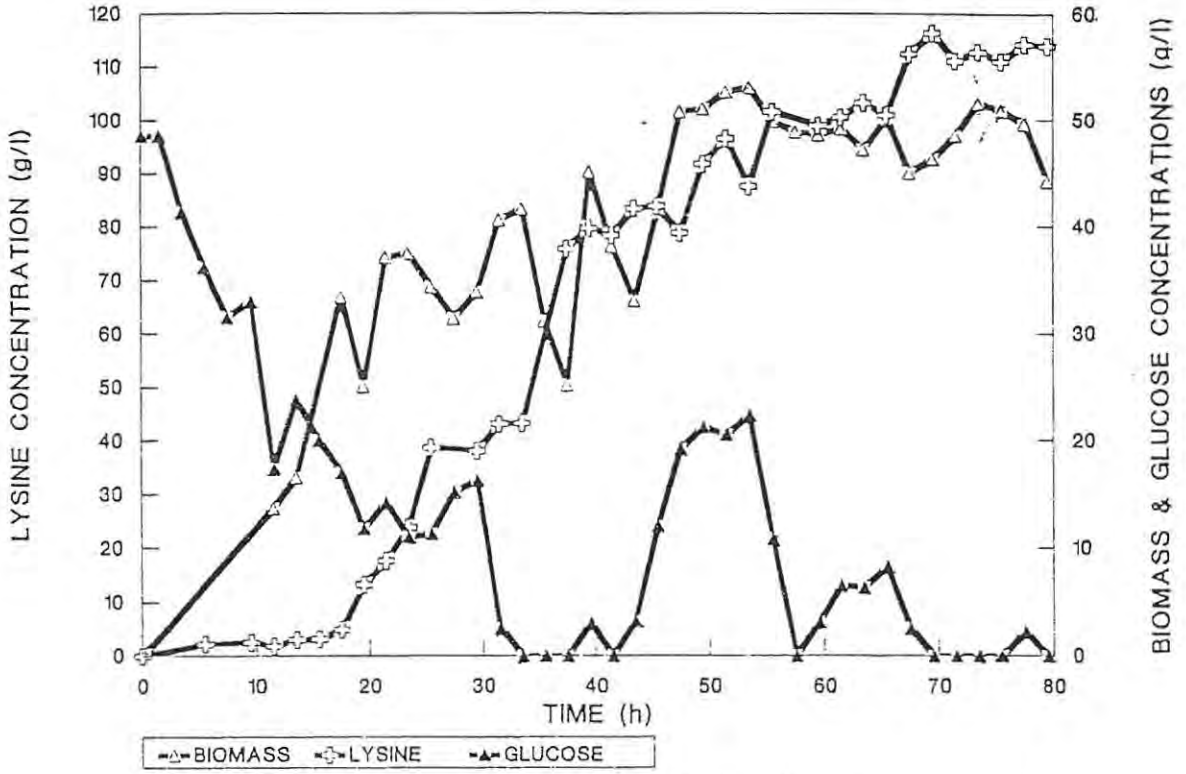

FIGURE 4.25 Fermentation profile indicating the change in the biomass, lysine and glucose concentrations with time.

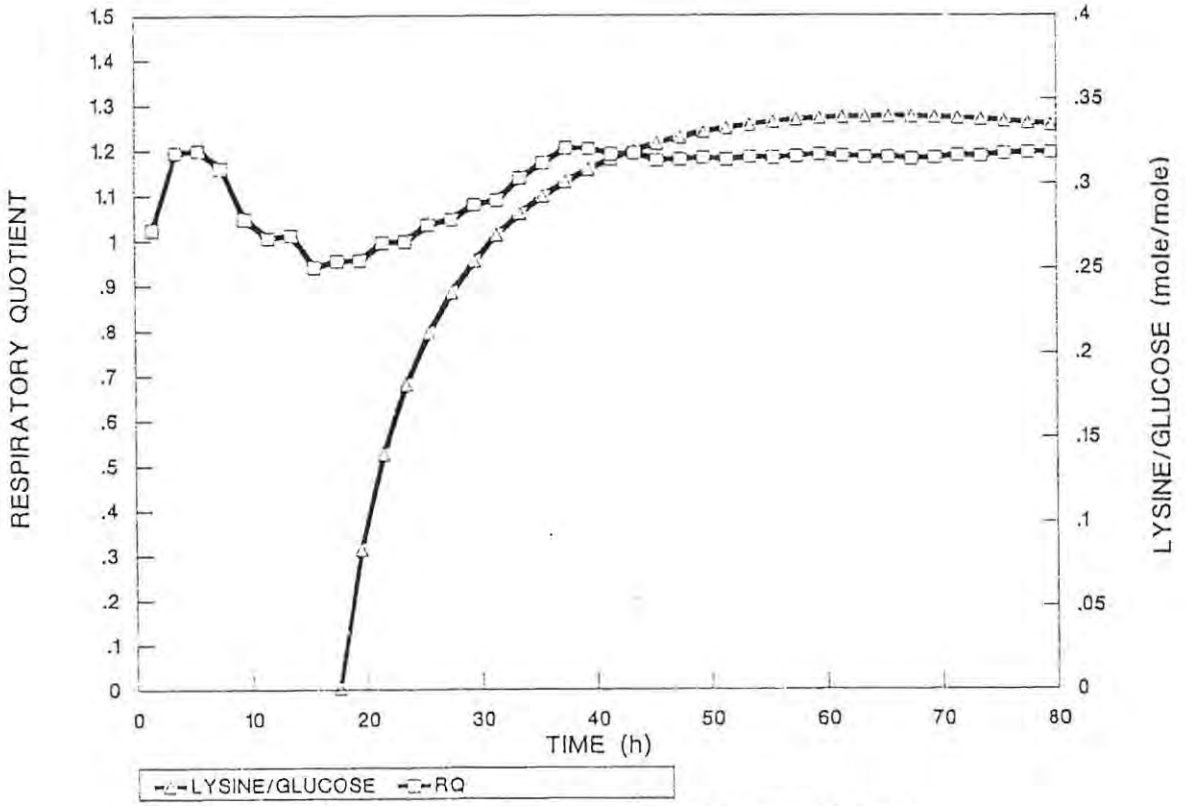

FIGURE 4.26 The change in respiratory quotient and lysine yield during fermentation.

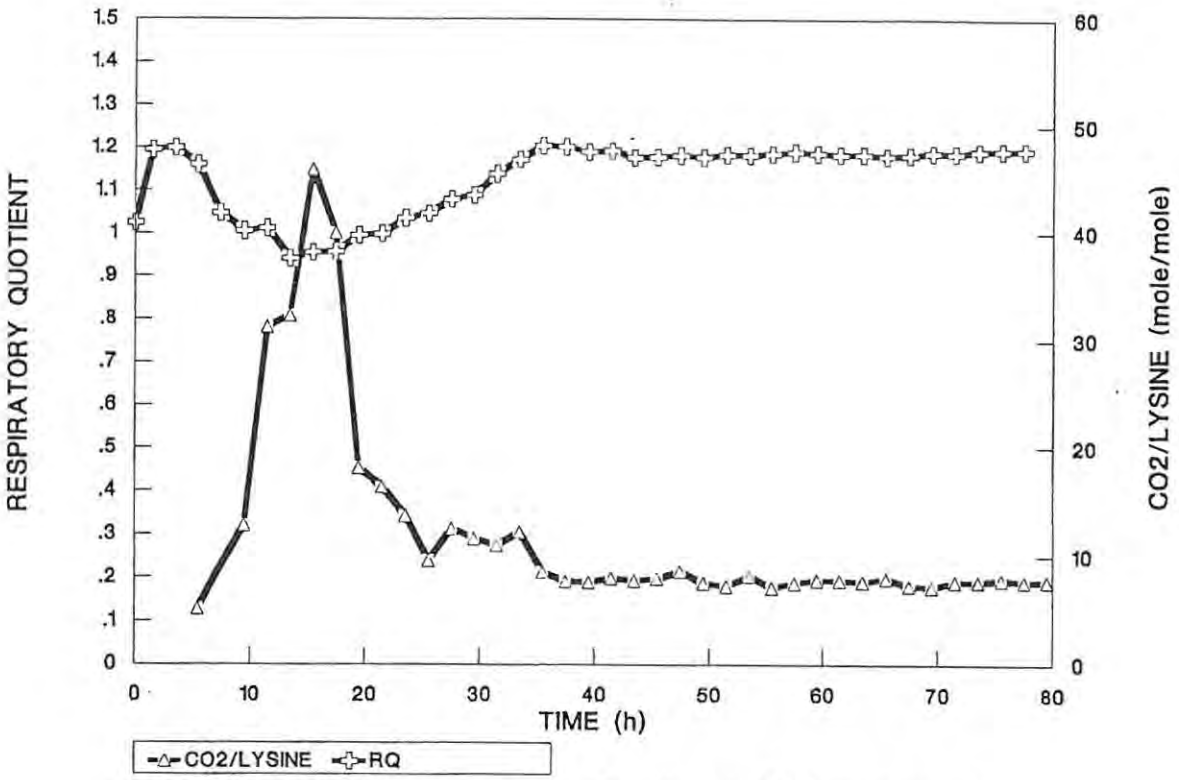

FIGURE 4.27 The change in the moles CO2 produced per mole lysine during the course of the fermentation.

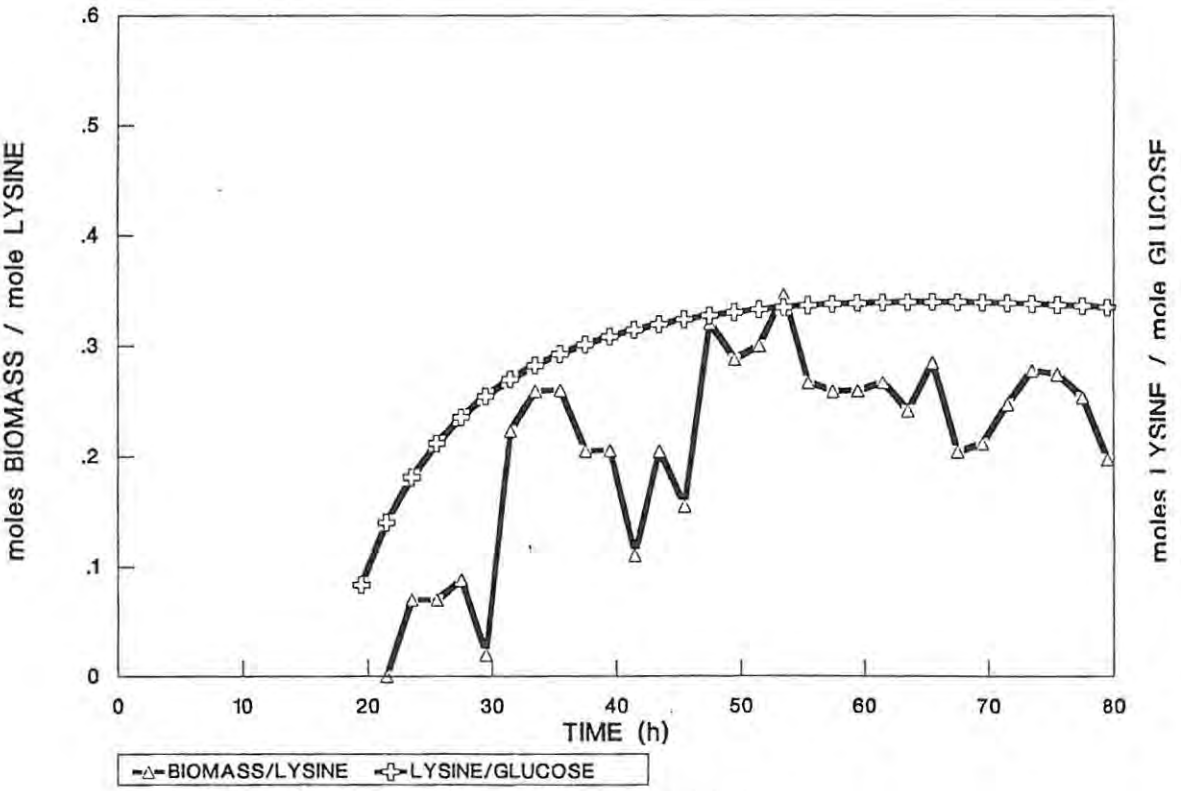

FIGURE 4.28 The change in biomass (as telchoic acid) per mole of lysine produced and the lysine yield on glucose during fermentation.

second stage, or maturation phase, the biomass concentration increases, but this is only as a result of an increase in the physical mass of the cells and not an increase in cell numbers. It appears that the major molecule which is produced causing this increase in cell mass is glycerol teichoic acid, with a proportion of it existing as lysylglycerolphosphate. The production of this material completes the nucleotide balance within the cell (making it zero) thereby allowing a theoretical lysine yield on glucose utilized to be calculated. The theoretical maximum lysine yield on glucose is 0,67 mole/mole or g/g. This yield does not take the glucose required during the replication phase into account. Due to the highly acidic nature of the glycerol-3-phosphate, the lysine probably acts as the counter-ion to this molecule intracellularly.

The manner in which the fermentation is run also affects the lysine yield. If a high glucose feed rate is used during the replication phase, before threonine depletion, it appears that part of the glycerol teichoic acid is laid down during growth, without the concomitant synthesis of lysine. During the replication phase the threonine and low levels of lysine cause concerted feedback inhibition of lysine synthesis. Once this teichoic acid is laid down, completing the nucleotide balance by some means other than lysine synthesis, the cell has basically completed part of its cycle without having to "waste" energy producing lysine. There is thus an optimum sugar utilization rate during the replication phase which gives a maximum lysine yield during the maturation phase. Excess glucose enables the cells to complete the cell cycle prior to lysine synthesis.

The maximum lysine yield obtained during this series of experiments was of the order of 0,37. This is 55% of the theoretical maximum yield of 0,67. There are possibly "futile" cycles which exist in ammonia transport and assimilation causing the inefficient utilization of ATP and therefore a reduction in lysine yield. The fact that the cell appears to be capable of completing its cell cycle prior to lysine synthesis would indicate that lysine synthesis itself may be a "futile cycle" enabling the cell to complete cell wall synthesis and the nucleotide balance during a phase of "growth" out of the normal replicative phase.

Producing the theoretical maximum yield is therefore only a matter of exploiting the futile cycles which exist.

CHAPTER 5

AMMONIA ASSIMILATION, AMMONIA TRANSPORT, AMINO ACID METABOLISM AND FUTILE CYCLES

5.1 SUMMARY

Corynebacterium glutamicum assimilates NH_4^+ via two routes for the synthesis of lysine. It is able to utilize the low affinity glutamate dehydrogenase or the high affinity glutamine synthetase. The affinity constants of these enzymes for ammonia indicate that glutamate dehydrogenase is only capable of assimilating NH_4^+ and glutamine synthetase NH_3 on the basis of the concentration of NH_4^+ and NH_3 at the K_m values for each enzyme and the extent of dissociation of NH_4^+ at that concentration. When the organism is utilizing the glutamate dehydrogenase system it appears that a futile cycle exists around the transport of NH_4^+ as a result of the dissociation of the NH_4^+ to NH_3 and H^+. The NH_3 then diffuses out of the cell. As the transport of NH_4^+ into the cell requires energy this is a drain on the energy requirements of the cell during lysine synthesis, thereby reducing the yield of lysine on glucose. Typical yields obtained throughout lysine synthesis during this type of fermentation are 0,4g/g. It is however possible to run fermentations where the yields of lysine on glucose of approximately 0,66g/g are attainable for periods during lysine synthesis. These fermentations are run under ammonia limitation to ensure that the high affinity glutamine synthetase mechanism of ammonia assimilation is being utilized.

5.2 INTRODUCTION

As yields of only 55% of the theoretical lysine yield have been attained, it is postulated that this is due to the presence of a futile cycle(s). The possibility that one futile cycle exists around the transport and assimilation of ammonia was therefore investigated.

The assimilation of NH_4^+ by bacteria occurs via glutamate dehydrogenase (L-glutamate:$NADP^+$ oxidoreductase (deaminating), EC.1.4.1.3) or via the ATP-dependent glutamine synthetase (L-glutamate:ammonia ligase (ADP forming), EC.6.3.1.2) and glutamate synthase (L-glutamine:2-oxoglutarate amino transferase (NADPH-oxidising), EC.2.6.1.53) pathways, (Tyler, 1978) as outlined in equations 1 to 4.

$$(NH_4^+)\ \text{extracellular} \xrightarrow{NH_4^+\ \text{carrier}} (NH_4^+)\ \text{intracellular} \qquad 1.$$

$$NH_4^+ + \text{glutamate} + ATP \xrightarrow{\text{Glutamine synthetase}} \text{Glutamine} + ADP + P_i \qquad 2.$$

$$\text{Glutamine} + \alpha\text{-ketoglutarate} + NAD(P)H \xrightarrow{\text{Glutamate synthase}} 2\ \text{Glutamate} + NAD(P) \qquad 3.$$

$$\alpha\text{-ketoglutarate} + NH_4^+ + NAD(P)H \xrightarrow{\text{Glutamate dehydrogenase}} \text{Glutamate} + NAD(P) \qquad 4.$$

The levels of these enzymes in bacteria are dependent on the intracellular concentration of NH_4^+ (Brown, *et al* 1973). In *Pseudomonas aeruginosa* grown in nitrate or limiting ammonia, the glutamine synthetase (GS) and glutamine synthase (GOGAT) levels are high, and no glutamate dehydrogenase was detected in these cultures (Brown *et al*, 1973). At high levels of NH_4^+ no glutamine synthetase activity was detected and the glutamine synthase activity was reduced. The NADP linked glutamate dehydrogenase was derepressed in the presence of high ammonia concentrations. The response in *Klebsiella aerogenes* was similar, with the repression of the glutamine synthetase by high concentrations of ammonia (Brown, 1973). The glutamate dehydrogenase in *Klebsiella aerogenes* is NADP linked.

5.2.1 Glutamine synthetase (GS)

Glutamine synthetase catalyses the ATP-dependent production of glutamine from ammonia and glutamate (Tyler, 1978). The *Escherichia coli* enzyme has a molecular weight of 600 000 and consists of a dodecamer of identical subunits arranged in two hexagonal units layered 4,5nm apart. In addition, the divalent cations Mg^{2+} or Mn^{2+} are required for stability.

Each catalytic site is shared between two adjacent subunits on the hexagon (Figure 5.1) where a specific tyrosyl residue (Tyr-397) on each subunit can be adenylated from ATP by an adenyl transferase enzyme (ATase) (Ottaway, 1988). Blocking the tyrosyl residue inhibits the active site and therefore the enzyme activity. Each subunit is capable of independent catalysis, therefore the fraction of full catalytic potential that is available is related approximately linearly to the average number of adenylated subunits per GS molecule. If all subunits are adenylated the GS is inactive (Tyler, 1978). The adenylated form is

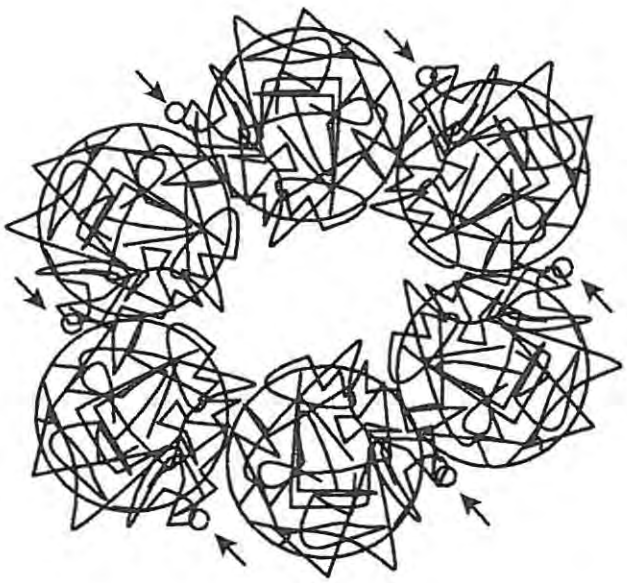

FIGURE 5.1 Plan view of the hexagonal arrangement of the subunits of a glutamine synthetase molecule from **Salmonella typhimurium** Also shown are the catalytic sites. (Ottaway, 1988)

more sensitive than the unmodified form to feedback inhibition by products of glutamine metabolism. A diagram of the functioning of glutamine synthetase in *E. coli* is shown in Figure 5.2.

The ATase has a molecular weight of 130 000 daltons. There are two factors which determine whether adenylation or deadenylation predominates, namely the levels of several metabolites and the interaction of ATase with a small regulatory protein, P_{II}. The levels of α-ketoglutarate and glutamine have an antagonistic effect on ATase activity. When the relative concentration of α-ketoglutarate is high, the deadenylation activity of ATase is increased, and when the glutamine concentration is high, the adenylation reaction is favoured. In addition, ATP stimulates the ATase to adenylate. P_{II} is a tetramer with a molecular weight of approximately 11 000. It exists in two states: P_{II} (P_{IIA}) which is an unmodified form that stimulates adenylation of GS by ATase and an uridylylated P_{II} (P_{IID}) which enhances the deadenylation of GS. The modified form (P_{IID}) is produced by the covalent attachment of a UMP residue on P_{II} by the action of a uridylyltransferase (UTase). The activity of this enzyme is also modulated by the relative concentrations of α-ketoglutarate and glutamine. The uridyl residue may be removed by uridylyl-removing enzyme (UR) which is the same protein as UTase. The degree of adenylation of GS is affected by the relative levels of α-ketoglutarate and glutamine *in vivo* (Senior, 1979) and *in vitro* (Segal *et al*, 1975).

The GS in *Klebsiella aerogenes* is functionally similar to that of *E. coli* with some minor differences in pH optima, divalent cation dependence and an isoactivity point of pH 7,55 relative to 7,15 in *E. coli* (Blender *et al*, 1977). As with *E. coli* it is also repressed by high levels of ammonia and glutamine in the media.

In all enteric bacteria grown in the presence of high levels of ammonia the GS is highly adenylated with a concomitant loss in biosynthetic activity (Tyler, 1978). The absolute levels of GS in these cells is also inversely related to the availability of nitrogen in glucose minimal media. Cells grown in glucose minimal media containing very low levels of ammonia have high levels of deadenylated GS. Cells grown in nutrient

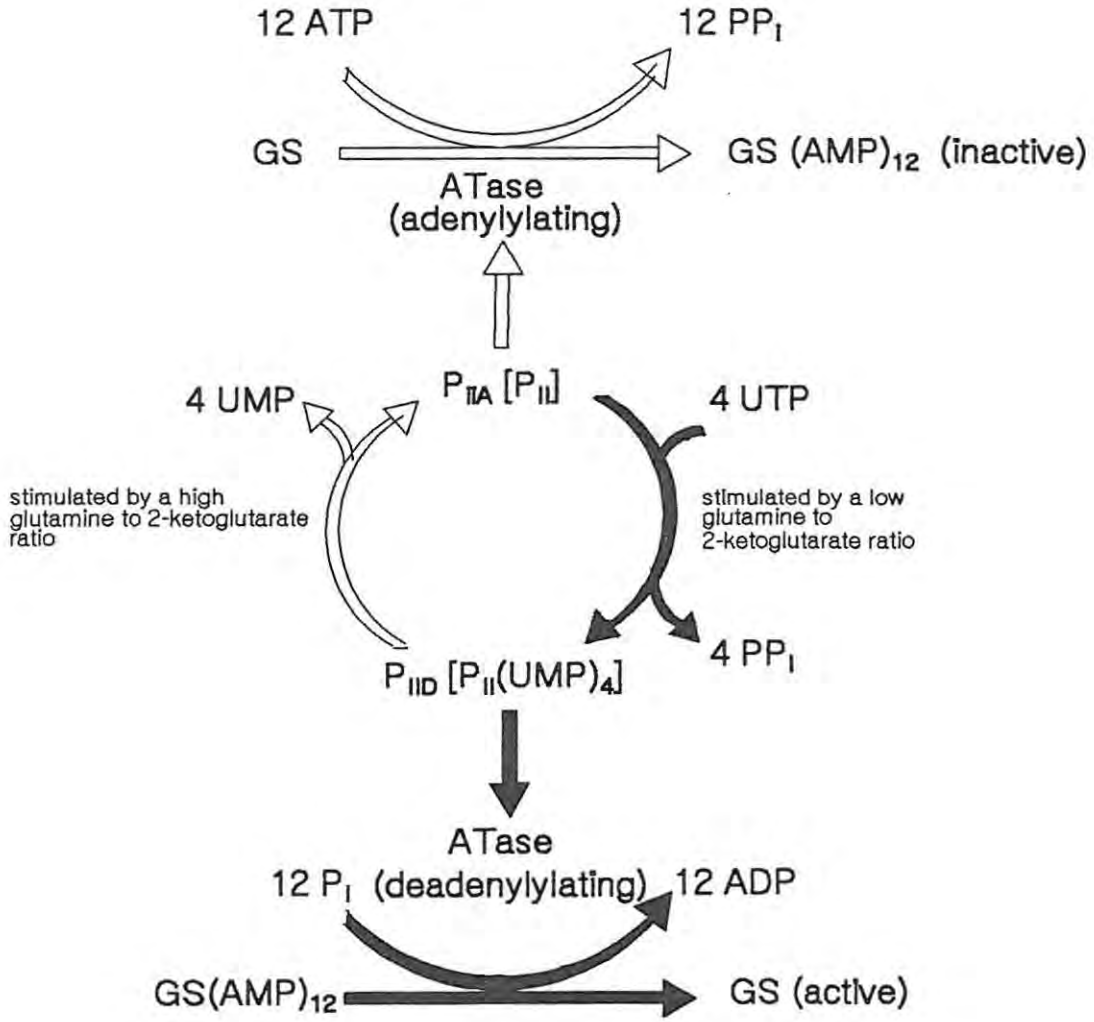

FIGURE 5.2 Covalent modification of glutamine synthetase
UR/UTase, uridylyl-removing enzyme/uridylyltransferase
ATase, adenyl transferase
P_{II}, regulatory protein
(Magasanik and Neidhardt, 1987).

broth contain low levels of highly adenylated GS.

The enzymatic activity of the glutamine synthetase proteins from *Bacillus subtilis* (Deuel and Stadtman, 1970; Fisher and Sonenshein, 1984) and *Clostridium acetobutylicum* (Usdin *et al*, 1986) are not regulated by adenylation. In addition, the cloned glutamine synthetase of *Azosprillum brazilense* (Bazouklian and Elmerich, 1986) and *Thiobacillus ferrooxidans* (Barros *et al*, 1986) are all capable of regulation by adenylation when cloned into *Escherichia coli*. Fisher and Wray (1989) found that the glutamine synthetase of *Streptomyces coelicolor* is also subject to post-translational covalent modification by adenylation which is regulated by the availability of ammonium.

5.2.2 Glutamate synthase enzyme

Glutamate synthase (GOGAT) has been purified in *E. coli* and *K. aerogenes* and in both cases the enzyme consists of a dimer of two unequal subunits. The smaller subunits have molecular weights of 53 000 daltons in both organisms and the larger subunit from *K. aerogenes* has a molecular weight of 175 000 daltons while in *E. coli* it has a molecular weight of 135 000 daltons (Tyler, 1978). Intracellularly the enzyme in *Escherichia coli* may have a molecular weight of 800 000 indicating an association of 4 dimers.

Very little is known about the regulation of glutamate synthase other than the primary form of regulation is repression by glutamate and activation by glutamate deprivation (Reitzer and Magasanik, 1987). In *Escherichia coli, Salmonella typhimurium* and *Klebsiella aerogenes* glutamate synthase is repressed when the sole source of nitrogen is degraded to, or provides glutamate (Reitzer and Magasanik, 1987). These nitrogen sources are glutamate, arginine, glutamine, histidine and proline (Lehninger, 1977). When ammonia is added to these media the glutamine synthase is not repressed (Bender, *et al*, 1976 and Brenchley *et al*, 1975). The ammonia causes repression of the nitrogen regulation systems (Ntr systems) that degrade these nitrogen sources, and the major source of nitrogen for glutamate is then ammonia. Aspartate which is readily transaminated to glutamate rapidly enters *Salmonella typhimurium*

in the presence of ammonia, because aspartate represses glutamate synthase even in the presence of ammonia (Brenchley *et al*, 1975). No data exists which is inconsistent with the hypothesis that glutamate represses glutamate synthase, however the lack of repression may occur by some glutamate producing nitrogen sources in ammonia containing media as a result of failure to form enzymes responsible for their degradation.

In enteric bacteria the preferred nitrogen source is ammonia, however when this becomes restricted the bacteria responds by greatly increasing the expression of a number of operons (Magasanik, 1982). These nitrogen regulated operons (Ntr) encode products that facilitate the assimilation of low concentrations of ammonia by means of glutamine synthetase-glutamate synthase pathways and then the utilization of alternative nitrogen sources.

5.2.3 Amino acid utilization

During the aerobic growth of a heterotrophic microorganism the amino acids in the culture media will be utilized for protein synthesis, but a proportion of them will undergo oxidative degradation by re-entering the TCA cycle. The point of entry of the various amino acid carbon skeletons into the TCA cycle is outlined in Figure 5.3. The entry points are via acetoacetyl-CoA, acetyl-CoA, α-ketoglutarate, succinyl-CoA, fumarate and oxaloacetate. Some amino acids are capable of entering at two points. Threonine is cleaved to give glycine and acetyl-CoA. The glycine enters the TCA cycle via pyruvate and acetyl CoA. Threonine may in addition enter through succinyl-CoA. Alanine enters the TCA cycle via acetyl-CoA, however this is via a transamination reaction which also produces glutamate. Phenylalanine is fragmented to produce acetoacetyl-CoA as well as fumarate, therefore entering at both points. Leucine and tryptophan are fragmented to produce both acetoacetyl-CoA and acetyl-CoA. Cysteine enters the TCA cycle at acetyl-CoA, however glutamate is also a by-product of this conversion.

The by-products of the conversion of the amino acids to allow the carbon skeletons to enter the TCA cycle are outlined in Table 5.1. These are the by-products of consequence to the assimilation of NH_4^+ and

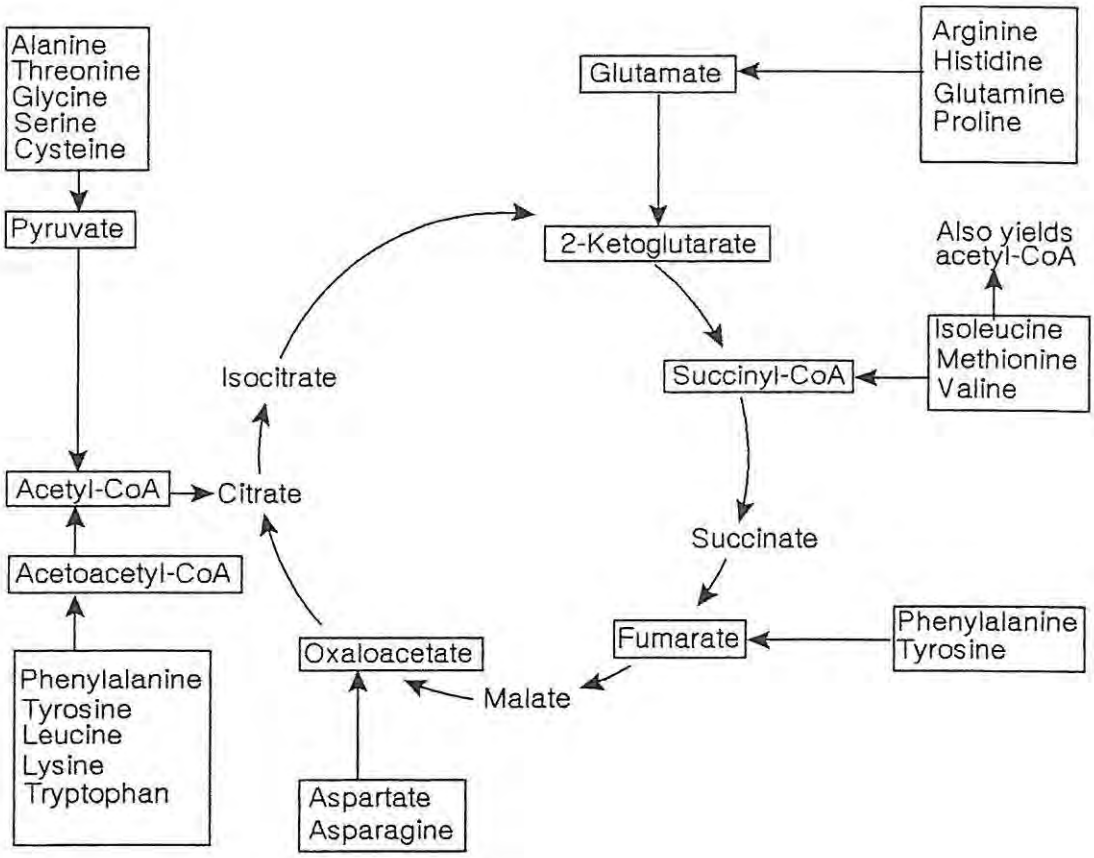

Figure 5.3 Pathways by which the carbon skeletons of amino acids enter into the tricarboxylic acid cycle. Leucine tryptophan and isoleucine undergo fragmentation in such a way that the products enter the cycle by two different routes (Lehninger, 1978).

129/...

glutamate/glutamine metabolism.

TABLE 5.1 : Pathway of entry of carbon skeletons of amino acids in TCA cycle

AMINO ACID	ENTRY POINT ON TCA CYCLE	BY-PRODUCTS OF CONVERSION
Alanine	acetyl-CoA	glutamate
Cysteine	acetyl-CoA	glutamate
Threonine	acetyl-CoA/succinyl-CoA	NH_4^+
Glycine	acetyl-CoA	NH_4^+
Serine	acetyl-CoA	NH_4^+
Arginine	α-ketoglutarate	glutamate
Histidine	α-ketoglutarate	glutamate
Glutamine	α-ketoglutarate	glutamate
Glutamate	α-ketoglutarate	-
Ornithine	α-ketoglutarate	glutamate
Proline	α-ketoglutarate	glutamate
Phenylalanine	acetoacetyl-CoA	glutamate
Tyrosine	acetoacetyl-CoA/fumarate	glutamate
Leucine	acetoacetyl-CoA/acetyl-CoA	glutamate
Lysine	acetoacetyl-CoA	glutamate
Tryptophan	acetoacetyl-CoA/acetyl-CoA	NH_4^+
Isoleucine	succinyl-CoA/acetyl-CoA	glutamate
Valine	succinyl-CoA	glutamate
Methionine	succinyl-CoA	NH_4^+/glutamate
Aspartate	oxaloacetate/fumarate	NH_4^+/glutamate
Asparagine	oxaloacetate	NH_4^+

5.2.4 Genetic regulation of glutamine synthetase, nitrogen regulation and the gln ALG operon

The gln ALG operon encodes for 3 gene products (Table 5.2), with the mutants in these gene products giving varying phenotypes (Magasanik, 1982). Also indicated in Table 5.2 is the location of these genes on the *E. coli* chromosome. A total of 7 gene products are responsible for the synthesis and regulation of glutamine synthetase (Table 5.2). The target of regulation of GS has been shown to affect catalytic activity, transcription or both (Reitzer and Magasanik, 1987). The phenotypes are defined in the footnote of Table 5.2.

TABLE 5.2 : The gln genes (Reitzer and Magasanik, 1987)

GENE	C.L.	PEPTIDE SIZE	GENE PRODUCT	PHENOTYPES OF MUTANTS	REGULATION OF GS
glnA	86	55 000	GS	Gln^-, Ntr^-, Gln^-, NtrC	-
gln L (ntrB)	86	36 000	NR_{II}	GlnC, NtrC, GlnR, Ntr^-, Gln^+/C, Ntr^+	T
gln G (ntrC)	86	50 000	NR_I	GlnR, Ntr^-, Gln^-, Ntr^-	T
rpoN (glnF, ntrA)	68	75 000	σ^{60}	Gln^-, Ntr^-	T
glnB	55	11 000	P_{II}	GlnC, Ntr, Gln^-, Ntr^-	CA,T
glnD	4	?	UTase/UR	Gln^-, Ntr^+	CA,T
glnE	?	?	Atase	Gln^+, Ntr^-	CA

Footnote:

gln	glutamine synthetase
Gln^+	normal regulation
Gln^-	no enzymatic activity
GlnC	high concentration of GS even in cells grown on a poor source of carbon with ammonia and glutamine
GlnR	intermediate concentration of GS irrespective of the concentration of the media
Ntr	refers to enzymes and permeases under nitrogen control, e.g. histidase
Ntr^+	increased concentration of GS
Ntr^-	no increased concentration of GS in cells on glucose with a poor source of nitrogen
NtrC	high concentration of GS on cells grown on glucose with an excess of ammonia and glutamine
GS	glutamine synthetase; UTase/UR, uridylyltransferase/uridyl-removing enzyme; ATase; adenyltransferase
CA	catalytic activity
T	transcription
C.L.	chromosomal location (minutes)

The functional properties of the genes involved in glutamine synthetase are as follows (Magasanik, 1982, Reitzer and Magasanik, 1987 and Magasanik and Neidhardt, 1987).

glnA The *glnA* gene is the structural gene for glutamine synthetase. *gln*$^-$ mutants have no enzymatically active glutamine synthetase and therefore require glutamine for growth (i.e. phenotype is *gln*$^-$). Using mutants with altered gene products, e.g. heat labile enzyme or enzymatically inactive glutamine synthetase antigen it has been shown that the concentration of antigen produced in these cells corresponds to that of the wild type if grown under ammonia deficient conditions and even when the mutants were grown in excess ammonia. This indicates that a functional glutamine synthetase is required for the repression of the *glnA* expression in response to ammonia. Some *gln*$^-$ mutants have a *NtrC* phenotype.

The *glnA* gene is located at 86 minutes in the chromosomes of *Escherichia coli*, *Klebsiella aerogenes*, *Klebsiella pneumoniae* and *Salmonella typhimurium*.

rpoN (glnF) The gene product of *rpoN* is σ^{60}, one of the subunits required for binding of the core RNA polymerase. It is essential for the activation of transcription of the genes, enabling the utilization of the amino acids arginine, histidine and proline, during nitrogen limited growth. Another mutation causing the requirement for glutamine in *Escherichia coli* occurs at 68 minutes on the chromosome. In all cases there is an inability to produce glutamine synthetase to a level higher than that produced in wild type cells grown on a poor carbon source with an excess of glutamine or ammonia, i.e. the condition resulting in the complete repression of glutamine synthetase. This concentration of enzyme is insufficient for growth in medium not supplemented with glutamine. Mutations in *rpoN* also cause the loss of the cell's ability to produce histidase and other similar enzymes

in response to ammonia deprivation (Gaillardin and Magasanik, 1978). The gene product of *rpoN* is σ^{60} one of the subunits required for binding of the core RNA polymerase. These mutations therefore also have a Ntr$^-$ phenotype.

glnG (NtrC) A mutation closely linked to *glnA* will suppress the Gln$^-$ phenotype resulting from rpoN mutations. These mutations result in the GlnR phenotype and the Ntr$^-$ phenotype in the presence or absence of a functional *rpoN* gene. The structural product of glnG is NR_I. NR_I is a dimer of identical subunits with a molecular weight of 110 000. NR_I in its phosphorylated form activates the initiation of transcription of *glnA* at the σ^{60}-dependent promoter glnAp 2.

glnD Mutants in *glnD* have an impaired ability to grow in the absence of glutamine (Gln$^-$). These mutations confer the inability to produce UTase, the enzyme required for the conversion of P_{II} to $P_{II}UMP$, and the glutamine synthetase is highly adenylated. These mutants also lack the ability to convert P_{IIUMP} to P_{II}, indicating that both activities are associated with the same protein. The mutants have an Ntr$^-$ phenotype. The Gln$^-$ phenotype of *glnD* mutants is not solely due to the overadenylation of the glutamine synthetase, but also to a lower level of glutamine synthetase as a result of the adenylated glutamine synthetase interacting with NR_{II} preventing the transcription of *glnA*.

glnB The *glnB* gene is the structural gene for P_{II}, a component of the adenylation system of glutamine synthetase. Some mutants in this gene have a similar phenotype to *glnD* mutants, i.e. Gln$^-$, Ntr$^-$ and overadenylated glutamine synthetase. P_{II} is a 11 000 dalton peptide. The effect of the loss of UTase/UR activity can be suppressed by the loss of P_{II}, therefore double mutants in *glnD* as well as *glnB* no longer require glutamine for growth and have the same level of glutamine synthetase, irrespective of the presence of ammonia in the growth media. The lack of P_{II} allows NR_I to exist in the

the active phosphorylated form even when the intracellular glutamine concentration is high.

P_{II} appears to antagonise the synthesis of glutamine synthetase and the activation of the synthesis of nitrogen controlled enzymes such as histidase accounting for the Gln^-, Ntr^- phenotypes of mutants in *glnD* and *glnB* which cannot convert P_{II} to $P_{II}UMP$. The *glnB* mutants lacking the ability to produce P_{II} have the GlnC phenotype, however these mutants display essentially normal regulation of nitrogen controlled enzymes, i.e. GlnC, Ntr^+ phenotype. The lack of P_{II} does not abolish the cell's ability to adenylate and deadenylate the glutamine synthetase in response to changes in the growth medium, however these processes proceed at a slower rate.

glnE The *glnE* gene is the structural gene for adenylyltransferase and a mutation in this gene has a Gln^+, Ntr^- phenotype. The effect of P_{II} on the synthesis of glutamine synthetase is independent of the ATase activity, but its effect on the adenylation of glutamine synthetase is exerted through ATase.

glnL (NtrB) The glnL gene encodes for NR_{II} which is a 68 000 dalton peptide. NR_{II} catalyses the conversion of NR_I to NR_I-phosphate, which then activates the initiation of transcription of *glnA*. This occurs in the absence of P_{II}. The regulation of glutamine synthetase in mutants in the *glnL* gene is almost normal. They have more glutamine synthetase than wild type cells when grown on glucose in the presence of ammonia and glutamine. The regulation of enzymes under nitrogen control appears to be normal, i.e. Gln^+/C, Ntr^+ phenotype. Mutations in glnL can suppress the Gln^- phenotype resulting from mutations in *glnB* and *glnD*. The inability of *glnB* and *glnD* mutants to activate the synthesis of glutamine synthetase results from the presence of P_{II}, which in these mutants cannot be converted to $P_{II}UMP$. A *glnL* mutation in these mutants enables the cell to produce glutamine synthetase, in spite of the presence of P_{II}, indicating that

the glnL gene product is inhibitory to P_{II}.

In *Bacillus subtilis* the *glnA* gene occurs on a dicistronic operon where it is the second gene (Schreier *et al*, 1989 and Straunch *et al*,1989). The promoter-proximal gene codes for a small protein, GlnR. Mutations in GlnR cause transcription from the *glnRA* promoter to be constitutive with respect to the nitrogen source (Schreier *et al*, 1989; Fisher and Sonenshein, 1991). The GlnR protein specifically inhibits transcription of the *glnRA* operon *in vitro*, binding with a high affinity to a sequence located between positions -60 and -20 of the *glnRA* promoter region (Fisher and Sonenshein, 1991). Mutations in the *glnA* gene also cause constitutive transcription with respect to the nitrogen source even when the glutamine is provided at high concentrations and enters the cells efficiently (Dean *et al*, 1977; Fisher and Sonenshein, 1984). When *Bacillus subtilis* genes are cloned into *Escherichia coli* both the *glnR* and *glnA* genes are required for nitrogen source-dependent regulation. Therefore the Gln R protein, although able to bind to the promoter and repress transcription, cannot itself respond to the available nitrogen source.

5.2.5 Transcription of glnALG operon

The glutamine synthetase operon or glnALG operon in *E. coli* consists of the glnA, glnL and glnG genes occupying approximately 4 500 base pairs in a contiguous region on the chromosome. This is sufficient for the 3 structural genes producing polypeptide products having molecular weights of 55 000, 36 000 and 50 000 daltons respectively (Magasanik, 1982).

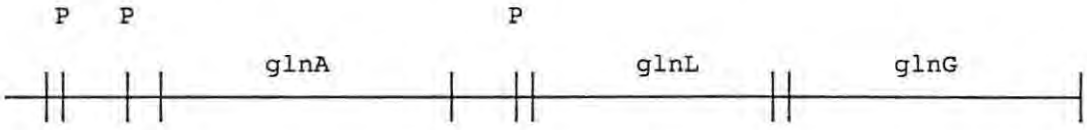

Figure 5.4 : The glnALC operon

The operon has three promoters: *glnAp1* with a transcriptional start site

located 187 base pairs upstream from the translational start site of *glnA*; *glnAp2* with a transcriptional start site 73 base pairs upstream from the translational start site of *glnA* and *glnLp* with a transcriptional start site located 256 base pairs downstream from the translational termination site of *glnA* and 33 base pairs upstream from the translational start site in *glnL* (Reitzer and Magasanik, 1987) (Figure 5.4). Having 3 promoters enables the cell to maintain a low level of glutamine synthetase and NR_I (the glnG gene product) during growth in the presence of excess nitrogen and to rapidly increase the level of glutamine synthetase and NR_I when nitrogen deprivation occurs. The *glnAp1* and *glnLp* promoters require core polymerase and σ^{70} for transcription. The *glnAp1* and *glnLp* promoters have nucleotide sequences characteristic of the majority of promoters in enteric bacteria in the regions of 10 and 35 base pairs from their respective transcriptional start sites. The initiation of transcription from these promoters is negatively regulated by NR_I and NR_I-phosphate, as a result of NR_I being able to bind a specific sequence of nucleotides which overlap the transcriptional start site of *glnLp*, the -35RNA polymerase contact site and the transcriptional start site of *glnAp1*. The initiation of transcription at *glnAp1* is stimulated by catabolite-activating protein (CAP) and cyclic AMP (cAMP). The characteristic binding site for CAP-cAMP is located between 65 and 81 base pairs upstream from the transcriptional start site of *glnAp1*.

The *Ap2* promoter has been located between base pair 27 and base pair 11 relative to the start of transcription. The sequence is similar to that found in other nitrogen-regulated promoters from which transcription requires σ^{60}, the *rpoN* gene product. Mutants in *rpoN* are unable to initiate transcription at *glnAp2*, under nitrogen limitation. In glucose containing media, as a result of reduced activation of transcription of *glnAp1* by CAP-cAMP and repression at *glnAp1* by NR_I, these mutants require glutamine for growth. If the glucose is substituted with a poor carbon source such as succinate, this glutamine requirement is suppressed. A mutation in *glnG* resulting in the loss of NR_I also suppresses the requirement for glutamine in these mutants.

The initiation of transcription at *glnAp2* requires NR_I, however *glnG*

mutants do not require glutamine, as glutamine synthetase is produced as a result of transcription via *glnAp1*. The level of glutamine synthetase is however low, as the mutants are unable to increase it in response to nitrogen deprivation. The ability of a variety of amino acids to be utilized in glucose containing media depends on the presence of NR_I and σ^{60}. If these two proteins are absent these amino acids are not utilized, indicating that the proteins are essential for the activation of transcription of the corresponding genes in response to nitrogen limitation. These compounds can also be used as the sole source of nitrogen in media containing a poor carbon source, therefore a separate system is responsible for the activation of these genes in response to carbon starvation (Reitzer and Magasanik, 1987).

For the efficient activation of transcription of *glnAp2* the *glnL* gene product NR_{II} is required. It catalyses the phosphorylation of NR_I by ATP to NR_I-phosphate. The NR_I-phosphate is then responsible for the activation of transcription.

The *glnRA* operon of *Bacillus subtilis* contains a sequence located between promoters -60 and -20 of the *glnRA* promoter region to which the Gln R protein binds (Fisher and Sonenshein, 1991). The region contains a large inverted repeat sequence (centered at position -50) and a series of short directly repeated sequences. Deletions and point mutations that affect the dyad symmetry sequence cause constitutive expression of the operon. The Gln R protein is therefore a repressor of the *gln RA* operon (Fisher and Sonenshein, 1991). It appears that glutamine synthetase monitors the availability of the critical nitrogen source in *Bacillus* and signals Gln R by interaction or modification. Evidence exists that glutamine synthetase plays a major role in the regulation of other genes. Mutations in *glnA* that cause constitutive transcription of the *gln* operon (with respect to nitrogen source) also cause constitutive expression of genes normally activated by nitrogen limitation. These genes include urease and asparagenase (Atkinson and Fisher, 1991). Gln R appears to be the regulator of the *glnRA* operon but glutamine synthetase transmits the information on nitrogen availability to multiple regulatory proteins.

5.2.6 Regulation of the transport of amino acids and ammonia

5.2.6.1 Amino Acid Transport

Fumanage *et al* (1978) showed that mutants of *Salmonella typhimurium* with increased levels of glutamine synthetase also had increased rates of uptake of the amino acids glutamine, arginine, aspartate, and lysine, but not proline. The opposite was also found to be true in strains with reduced glutamine synthetase activity. In addition, Kutsu *et al* (1979) demonstrated nitrogen control over the synthesis of four amino acid transport systems by periplasmic binding protein components. These systems function in the transport of histidine, glutamine, lysine-arginine-ornithine (LAO) and glutamate-aspartate. Again mutant strains with elevated levels of glutamine synthetase activity were isolated and the data suggests the presence of elevated levels of several transport systems, namely the high affinity histidine transport system, together with those of glutamine, arginine and glutamate. The by-product of the conversion of all these amino acids on entry to the TCA cycle is glutamate.

Kutsu *et al* (1979) believe that the regulation of the synthesis of these transport proteins arises in the "*glnR*" gene product. The "*glnR*" region of the gene or nitrogen regulatory locus was defined as being composed of the *ntrB* and *ntrC* cistrons (MacFarland *et al*, 1981). These are now taken to be the *glnG* and *glnL* genes (Magasanik, 1982). The transport of these amino acids is under the same genetic control as the structural genes for their utilization, e.g. histidase. Kutsu *et al* (1979) showed evidence that the membrane bound components are similarly regulated. Not only did they find increased levels of the histidine binding protein, a product of the *hisJ* gene, but also the cytoplasmic membrane protein, the product of the *hisP* gene. The HisP protein makes up part of the membrane bound histidine transport complex consisting of HisQ, HisM and HisP (Ames, 1990). Energy is consumed in the form of ATP during the transport of histidine.

A Na^+ cotransport type system, as occurs with proline permease in *Escherichia coli* and *Salmonella typhimurium*, also exists for the

transport of other amino acids (Maloy, 1990).

5.2.6.2 Ammonia Transport

Brill (1975) suggested that many free living nitrogen fixing bacteria are able to scavenge traces of ammonia from the immediate environment before the nitrogenase complex is repressed. Henderson (1971) indicated that NH_4^+ at physiological pH exists as the ammonium ion which is impermeable to biomembranes, suggesting the requirement for a specific NH_4^+ transport system(s).

Stevenson and Silver (1977) provided evidence for possibly two energy dependent ammonia uptake systems existing in *Escherichia coli*. The number of documented ammonia transport systems in microorganisms has increased (Kleiner, 1985). In all cases these were investigated by measuring the uptake of the ammonium analogue methylammonium ($CH_3NH_3^+$). Jayakumar *et al* (1985) demonstrated that the $CH_3NH_3^+$ transport occurs via $K^+/CH_3NH_3^+$ exchange. The accumulation of $CH_3NH_3^+$ required both ATP and a proton-motive force. The antiport reaction is coupled to K^+ efflux and driven by the K^+ electrochemical gradient. As a membrane potential is proposed as the driving force for NH_4^+ transport, this implicates NH_4^+ as the transported species and not NH_3.

Kleiner (1981) was able to show that in *Azotobacter vinelandii*, *Klebsiella pneumoniae*, *Clostridium pasteurianum* and *Rhodospirillum rubrum* a 100 to 200-fold NH_4^+ concentration gradient can be maintained across the membrane, indicating an energy linked system. In both *Escherichia coli* (Stevenson and Silver, 1977) and *Nostoc muscorum* (Kashyap and Johar, 1984) it appears that two NH_4^+ transport systems exist, i.e. a high affinity system and a low affinity system. As these uptake systems are inducible, mutants are selectable and an alteration in the kinetic constants of transport in the low and high affinity systems of the mutants occurs, therefore transportation across the membrane must occur via a specific carrier(s).

Castorph and Kleiner (1984) were able to select for NH_4^+ negative mutants (Amt^-) of *Klebsiella pneumoniae*. The strain is unable to accumulate NH_4^+ intracellularly. When grown on nitrogen sources other than NH_4^+, e.g.

amino acids, the mutant constantly loses NH_3 by diffusion, with a concomitant reduction in growth. The regulation of the enzymes involved in ammonia assimilation namely glutamine synthetase, glutamate synthase and glutamate dehydrogenase was qualitatively the same in both the wild type and mutant strains, however the degree of adenylation of the glutamine synthetase in mutant strains was always less than in the wild type strain. This indicates a higher affinity of the glutamine synthetase for the NH_3. The lack of growth on amino acids by the mutant strain is a result of the loss of NH_3 through the dissociation of $NH_4^+ \rightarrow NH_3 + H^+$ which arises when NH_4^+ is produced as a result of the intracellular metabolism of the amino acid. In the wild type the escaping NH_3 is constantly reabsorbed after protonation to NH_4^+. Castorph and Kleiner (1984) therefore proposed that a futile cycle exists, with the continual loss of NH_3 and reabsorption of NH_4^+ creating the cyclic retention of NH_4^+. The NH_4^+ carriers in many strains are repressed by their own substrate (Kleiner, 1985), but unlike other systems which are repressed by their cognate solute, there is no change from the low affinity system to the high affinity system. The high affinity transport system for leucine, isoleucine and valine (LIV-I) is repressed by leucine, but this repression is accompanied by derepression of the low-affinity transport system (LIV-II). This allows the organism to maintain a relatively constant amino acid pool. As no change occurs in the affinity of the NH_4^+ transport system, this suggests that at high external NH_4^+ concentrations diffusion of NH_3 through the membrane is fast enough to support the cell's demand for nitrogen. In the same way a high internal and low external NH_3 concentration will result in the net outward diffusion of NH_3. This occurs when the organism degrades organic nitrogenous compounds with the formation of intracellular NH_4^+. Since the excreted NH_3 is retrieved after protonation there is no net excretion of NH_3. As there is a change in the membrane potential as a result of the electrogenic transport of NH_4^+ this has to be balanced by an energy-dependent export of protons (Figure 5.5) (Kleiner, 1985). Thus a futile cycle of NH_3 excretion/NH_4^+ absorption occurs. This draws severely on the energy metabolism of the organism. Kleiner (1985) calculated the energy requirements for the cyclic retention of NH_4^+ by *Klebsiella pneumoniae* under specific culture conditions and found NH_3 assimilation to be 6 times slower than NH_3 diffusion, which means that each NH_3 molecule

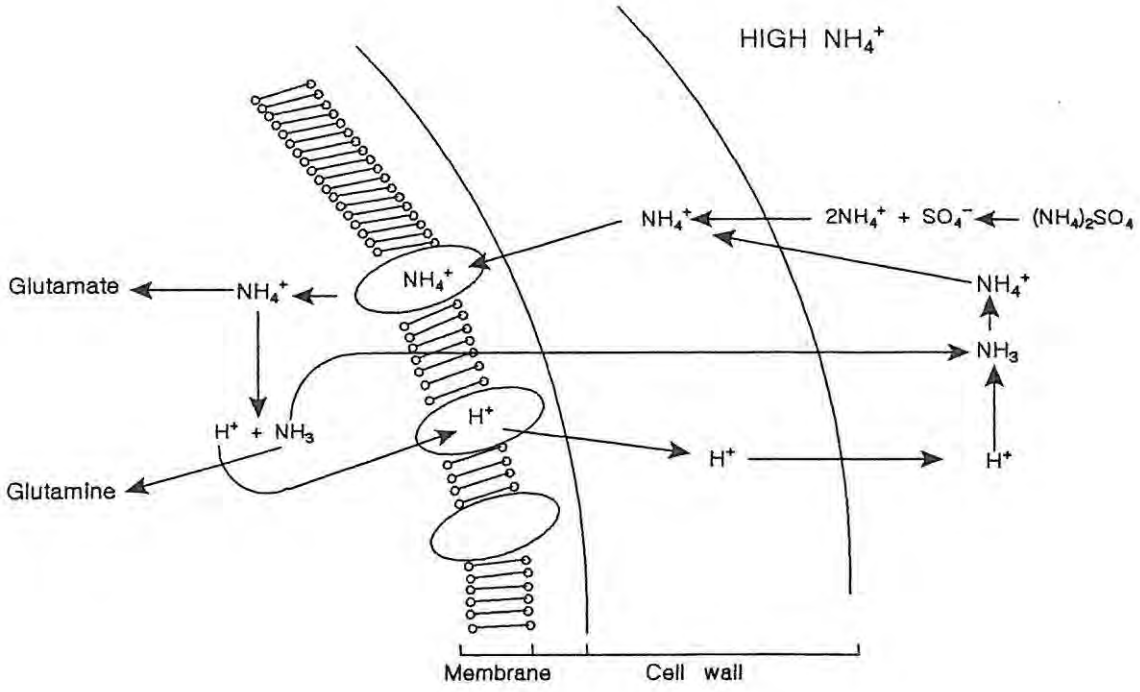

Figure 5.5 Cyclic NH_3/NH_4^+ retention, (Kleiner, 1985).

passes through the futile cycle 6 times before it is assimilated by the glutamine synthetase. This is however dependent on the organism, surface area of the organism, extracellular and intracellular NH_4^+ concentrations and the permeability of the organism to NH_3. The rate of assimilation of the NH_4^+ by the organism, and thus the activity of the glutamine synthetase in the cell is also however of importance.

Jayakumar *et al* (1986) using strains of *Escherichia coli* with specific mutations in the *glnALG* operon were able to show that certain glutamine synthetase deficient mutants ($GlnA^-$) lost ammonium transport (Amt) as a result of the polar effects on the *glnL* and *glnG* loci, which are responsible for nitrogen regulation. The Amt was demonstrated when cells were cultured with glutamate or glutamine as the nitrogen source, and 95% repression of the activity occurred by growth of the wild-type cells on media containing ammonia. $GlnA^-$ mutants with polar mutations on the glnL and glnG genes, and therefore having the Reg^- phenotype, (i.e. they fail to turn on nitrogen-regulated operons such as histidase), expressed less than 10% of the Amt activity observed for the parental strain. The *glnL* and *glnG* gene products activate the transcription of *glnA*, the glutamine synthetase structural protein. GlnG mutants having a $GlnA^+$ and Reg^- phenotype also had low levels of Amt. However, $GlnA^-RegC$ (i.e. a phenotype constitutive for histidase) contained over 70% of the parental Amt activity. The *glnG* gene product is therefore necessary for the expression of Amt and has similar control over nitrogen regulated systems. The product of *glnL* which activates the *glnG* gene product appears to be bifunctional. The constitutive expression of Amt in some GlnL mutants indicates the role of the *glnL* gene product in the repression of Amt by ammonia. The loss of Amt in other GlnL mutants suggests the role of the *glnL* product in the activation of expression of the Amt. Nitrogen regulation was lost in these mutants as the histidase activity was also reduced in these strains.

Jayakumar *et al* (1986) postulated that in organisms capable of fixing nitrogen, e.g. *Azotobacter vinelandii*, the regulation of Amt occurs primarily by feedback inhibition via glutamine, as the recovery of Amt in ammonia grown cells was not affected by chloramphenicol and therefore did not require protein synthesis. In a non nitrogen fixing organism, such

as *Escherichia coli*, recovery of the Amt in ammonia grown cells was affected by chloramphenicol and control therefore occurs at the level of gene expression.

An investigation was therefore undertaken to determine which mechanisms exist for the assimilation of ammonia in *Corynebacterium glutamicum FP6* and to what extent they affect the theoretical lysine yield. The presence of a futile cycle existing around the ammonia transport could not be ruled out. This would explain the difference between the theoretical lysine yield and that obtained routinely during fermentation.

5.3 MATERIALS AND METHODS

5.3.1 Organism

The organism used throughout all fermentations was *Corynebacterium glutamicum* FP6.

5.3.2 Media and culture conditions

A range of fed-batch fermentations were carried out while varying the glucose feed rate during the maturation phase (lysine synthesis phase) and by varying the free NH_4^+ concentration. The culture media and conditions are outlined in Appendix VII. The free NH_4^+ concentration was varied by adding $(NH_4)_2SO_4$ to the base used for pH control. The control of pH during the replication phase was carried out using a 12.5% m/m NH_4OH solution or a 40% m/v H_2SO_4 solution. During the maturation phase however, pH control was carried out using a solution of NH_4OH and $(NH_4)_2SO_4$ in equimolar concentrations relative to the NH_4^+ concentration. This was termed the second base. The glucose feed rate during the replication phase ranged between 2,5 and 3,2g/l/h while that during the maturation phase was varied between approximately 5 and 17g/l/h. The replication phase was taken to be 28 hours, at which time the glucose feed rate was increased. The use of the second base was started at a time ranging from 28 to 38 hours after the start of the fermentation. The longer times were used in an attempt to drive the free NH_4^+

concentration down as a result of its utilization for lysine synthesis and the subsequent association of the lysine in solution with SO_4^- as the counter-ion. Even though no $(NH_4)_2SO_4$ was added to the initial charge, some would arise from the yeast extract and some could arise from the metabolism of amino acids during the replication phase, as a small amount of acid is demanded during this phase.

The inoculum preparation for the fermentations was carried as outlined in section 4.3.2.

5.3.3 Enzyme assays

5.3.3.1 Glutamate dehydrogenase

The activity of glutamate dehydrogenase (L-glutamate:NAD oxidoreductase, deaminating EC 1.4.1.3) was determined on an extract purified as outlined in section 2.3.3. The enzyme precipitated by 60% of saturation $(NH_4)_2SO_4$ was used. This extract was then dialysed for 24 hours against cold 0,01M phosphate buffer containing 0,001M mercaptoethanol with one change in the buffer.

This enzyme extract was used for determining the glutamate dehydrogenase activity by measuring the rate of oxidation of NADPH per minute per mg protein spectrophotometrically at 340nm (Shiio *et al*, 1962). The assay was made up of the following constituents: 20mM NH_4Cl, 0,25mM NADPH and 10mM α-ketoglutarate in 0,1M Tris buffer (pH 6,2). For the determination of the specific activity the protein concentration was determined colorimetrically by the method of Lowry *et al* (1951).

The effect of the ammonium salt concentration on the activity of the enzyme was determined. The ammonium salts used were NH_4Cl, $(NH_4)_2SO_4$ and $(NH_4)_2HPO_4$. Using the dissociation theory as outlined in Chapter 2, a regression analysis was carried out on the effect of the ammonium salt concentration on the concentration of free NH_4^+ in solution (Appendix VIII). This data was then used to determine the effect of the free NH_4^+ concentration on the activity of the enzyme.

5.3.3.2 Glutamine synthetase assay: (Determination of the iso-activity point)

In determining the glutamine synthetase activity in *Corynebacterium glutamicum* the presence of the synthesis and transferase reactions first had to be shown. The possibility of adenylation as the control mechanism of the enzyme also had to be demonstrated. To enable the assay to be carried out, the isoactivity point was determined for the γ-glutamyl transferase activity for both "adenylated" and "deadenylated" enzyme using the modified method of Shapiro and Stadtman (1970) as carried out by Bender *et al* (1977). The cells were prepared by culturing them to mid-exponential growth phase in the presence of glutamate (30mM) and then splitting the culture, one half of the culture being used directly and the other half of the culture being "shocked" by the addition of 15mM $(NH_4)_2SO_4$ and incubated at 30°C for 15 minutes with agitation at 160rpm. The culture media used is outlined in Appendix IX. A volume of 10ml of cetyltrimethylammonium bromide (CTAB)(4,0g/l) was added to 10ml volume of these cultures to give a final concentration of 2,0g/l of CTAB. These solutions were then incubated for 15 minutes before centrifuging and resuspending in 10ml 1% m/m KCl. These cells were then used for the enzyme assay. The composition of the assay mixture is shown in Table 5.6.

The enzyme assays were then run at pH values ranging from pH 6,5 to pH 8,0. The point of intersection of the curves for the "deadenylated" and "adenylated" enzyme was then taken to be the isoactivity point.

The extent of inhibition of the γ-glutamyl transferase activity in the presence of high levels of magnesium was used to approximate the adenylation state of the glutamine synthetase. In the case of *Escherichia coli*, the fully adenylated enzyme is inactive in the presence of magnesium and unadenylated enzyme unchanged in its activity. This ratio of activity in the presence and absence of magnesium therefore gives the degree of deadenylated enzyme and is expressed as a percentage. The concentration of $MgCl_2$ required to give complete inhibition of the γ-glutamyl transferase activity was then determined. This assay was also used during the course of various fermentations to determine the extent of adenylation of the enzyme during fermentation.

5.3.3.3 **Glutamine synthetase: (Determination of the kinetic constants)**

The determination of the kinetic constants for the glutamine synthetase synthesis reaction was carried out using the method of Ertan (1992). *Corynebacterium glutamicum* FP6 was grown in overnight culture of LM media and then transferred to minimal media containing glutamate (Appendix IX) for 24 hours. This was transferred a second time to minimal media containing glutamate and cultured for 24 hours. All cultures were incubated at 30°C on a rotary shaker at 160rpm. The cells were then harvested by centrifugation at 10 000 x g and washed once in cold 1% KCl by centrifugation. This biomass was resuspended in 1% KCl and sonicated for 60 x 30 seconds with 30 second intervals to allow cooling. Sonication was done at 0°C. The ruptured cells were then centrifuged at 10 000 x g and the supernatant dialysed against 0,1M imidazole buffer (pH 7,4). This enzyme extract was then used to assay for the glutamine synthetase synthesis reaction in an assay containing the following components:

Glutamate	concentration varied from 0 to 5mM
$(NH_4)_2SO_4$	concentration varied from 0 to 5mM
ATP	concentration varied from 0 to 5mM
$MgCl_2$	15mM
Imidazole buffer	0,1M (pH 7,4)

The imidazole buffer was used to make up the reaction volume to 300µl. The blank contained no glutamate.

The reaction was started by the addition of the enzyme and incubated at 22°C for 30 minutes. It was stopped using a solution containing 2% v/v H_2SO_4, 0,5% m/v ammonium molybdate and 0,5% m/v SDS. A volume of 20µl of a 10% m/v ascorbic acid solution was then added to each assay. The release of the P_i was determined spectrophotometrically at 750nm. The concentration of P_i was determined using a standard curve. The apparent K_m and V_{max} were determined using regression analysis on double reciprocal plots.

5.3.3.4 **Glutamine synthetase: The effect of ammonia on the extent of adenylation of the enzyme**

The classical experiment to show the effect of ammonia on the glutamine synthetase is carried out by culturing the organism in minimal media containing arginine as the nitrogen source, dividing the culture in two and adding an ammonium salt to the one half and using the other as the control. On monitoring the glutamine synthetase activity in these two cultures over time, it is found that the ammonia shocked culture has a reduction in activity (Wray and Fisher, 1988). As a result of *Corynebacterium glutamicum* FP6 being a methionine, threonine, leucine auxotroph, this experiment could not be run as described above, as the metabolism of threonine leads to the formation of ammonia which affects glutamine synthetase activity. The experiment was therefore run in reverse.

Corynebacterium glutamicum FP6 was grown overnight in 25ml LM media at 30°C with shaking at 160rpm. The culture was aseptically washed by centrifugation at 10 000 x g in 1,0% m/v sterile NaCl and then grown in minimal media (Appendix VIII) plus 10mM $(NH_4)_2SO_4$ and 10mM glutamate (200ml) at 30°C with shaking at 160rpm for 24 hours. The culture was then divided in two. Half was resuspended in minimal media plus ammonia plus glutamate (100ml). The other half was resuspended in minimal media with no amino acids or $(NH_4)_2SO_4$. The activity of the culture was determined over time by harvesting the cells in a 1:1 ratio into 4g/l CTAB. The γ-glutamyl transferase activity in the presence and absence of Mg^{++} was determined as in section 5.3.3.2.

5.3.4 **Analyses**

5.3.4.1 **Biomass**

The biomass during the course of the fermentation was determined gravimetrically on duplicate 10ml samples by centrifugation at 10 000 x g and washing of the sample pellet with 10ml deionised water followed by recentrifugation.

5.3.4.2 L-Lysine

The L-lysine concentration in the culture media after removal of the biomass by centrifugation was determined by HPLC as outlined in section 2.3.5.2.

5.3.4.3 Glucose

The residual glucose concentration in the culture media after removal of the biomass by centrifugation was determined by HPLC as outlined in section 2.3.5.3.

TABLE 5.3 : Composition of the glutamine synthetase assay mixture

ASSAY	VOL (ml)	STOCK SOLUTION	FINAL CONC (mM)
γ-Glutamyl	7,53	Water	
transferase	2,25	1,0M Imidazole.HCl pH 7,70	135
	0,37	0,8M Hydroxylamine.HCl	18
	0,045	0,1M $MnCl_2$	0,27
	1,5	0,28M Potassium arsenate pH 7,70	25
	0,15	40mM Sodium ADP pH 7,70	0,36
	1,5	CTAB (1mg/ml)	90μg/ml
Forward	7,2	Water	
Reaction	2,0	1,0M Imidazole.HCl pH 7,70	94
	1,25	0,8M Hydroxylamine.HCl	47
	0,40	3,0M $MgCl_2$	56
	4,2	0,85M Monosodium L-glutamate	168
	2,0	CTAB (1mg/ml)	94μg/ml

5.3.4.4 **Phosphate**

The residual phosphate concentration was determined in the culture media after centrifugation by ion chromatography, using a Dionex chromatography system with a conductivity detector with 0,1M $NaHCO_3$ as the mobile phase (Dionix Corporation, 1992).

5.3.4.5 **Amino acids**

The free amino acid concentrations in the culture media after centrifugation were determined by the Pico-Tag^c procedure as described by Waters Associates (Inc) (1984).

5.4 RESULTS AND DISCUSSION

5.4.1. Enzymes involved in ammonia assimilation

5.4.1.1 Glutamate dehydrogenase: coenzyme and substrate specificity

The glutamate dehydrogenase from *Corynebacterium glutamicum* was found to be strictly specific for NADPH, as no activity was found to occur when using NADH as the coenzyme. Using NH_4Cl as the source of ammonia the apparent K_m values for NADPH and α-ketoglutarate were obtained by double reciprocal plots of the reaction velocities versus substrate concentration (Table 5.4).

TABLE 5.4 : K_m and V_{max} values for NADPH and α-ketoglutarate

NADP(H)	
K_m (mM)	0,0947
V_{max} (mg/min/mg protein)	0,629
α-Ketoglutarate	
K_m (mM)	1,592
V_{max} (mg/min/mg protein)	0,628

In *Escherichia coli* the affinity constants for α-ketoglutarate and NADPH were found to be 0,64mM and 0,04mM, respectively (Sakamoto *et al*, 1975). In *Brevibacterium flavum* the K_m for α-ketoglutarate was found to be 5,72mM and that for NADPH 0,027mM (Shiio and Ozaki *et al*, 1970).

5.4.1.2 **The effect of the ammonium salt and ammonium ion concentration on the activity of glutamate dehydrogenase**

The apparent affinity of the glutamate dehydrogenase for NH_4^+ was found to be more complex and dependent on the ammonium salt used. Plotting the effect of the total NH_4^+ concentration versus the specific activity it was found that different shape curves were obtained depending on whether NH_4Cl, $(NH_4)_2SO_4$ or $(NH_4)_2HPO_4$ was used (Figure 5.6). Using a regression analysis of the data obtained in Chapter 2 on the effect of the ammonium salt concentration on the free ammonium ion concentration (Appendix VII), the concentration of the free NH_4^+ was calculated for each salt. Plotting the free NH_4^+ ion concentration versus the specific activity there was a slight change in the shape of the curves, however the activities obtained for the equivalent NH_4^+ concentration for each salt were different (Figure 5.7). The Lineweaver-Burk plots of the effect of the total NH_4^+ on the activity indicated a lack of linearity (Figure 5.8). A regression analysis of the data showed that this is in fact the case with the best fit being a cubic fit. The Lineweaver-Burk plot using the free NH_4^+ concentration showed greater similarity in the data (Figure 5.9). As the data fits a non-linear function the Y-intercept (V_{max}) was calculated using a cubic function and was found to be similar in the case of NH_4Cl and $(NH_4)_2HPO_4$ at 2,15mg/min/mg protein. The V_{max} obtained for $(NH_4)_2SO_4$ was 1,58mg/min/mg protein. This was ascribed to the further dissociation of the $(NH_4)_2SO_4$ at the low concentrations to 2 NH_3, 2 H^+ and SO_4^-, with the H^+ acting as a noncompetitive inhibitor of the enzyme. The effect of the further dissociation of the ammonium salt was less in the case of NH_4Cl and more specifically $(NH_4)_2HPO_4$. The dissociation of the proton in NH_4Cl solutions is not as marked as in $(NH_4)_2SO_4$ solutions. In the case of $(NH_4)_2HPO_4$ the proton appeared to reassociate with the HPO_4^- rendering it inactive as an inhibitor. The fact that the data fit is cubic also indicates that at the very low ammonium salt concentrations the glutamate dehydrogenase is unable to assimilate the NH_4^+ as it will all be fully

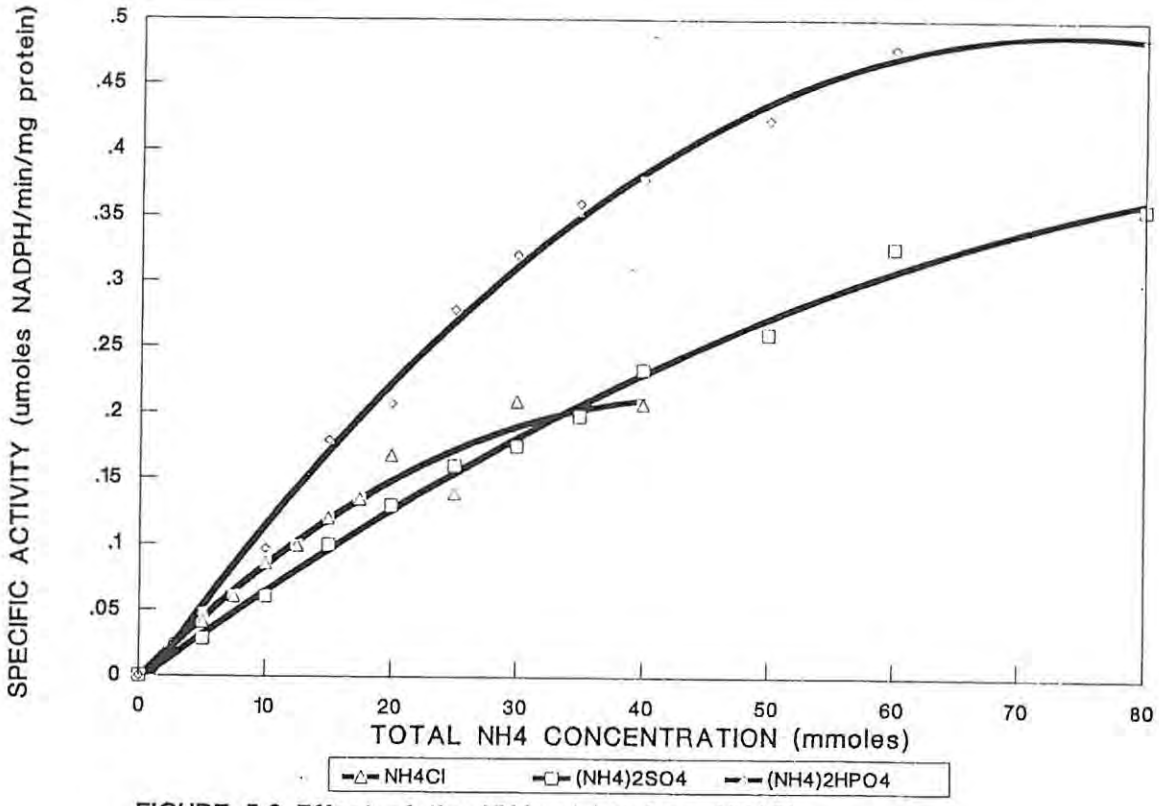

FIGURE 5.6 Effect of the NH4 arising from NH4Cl, (NH4)2SO4 and (NH4)2HPO4 on the specific activity of glutamate dehydrogenase.

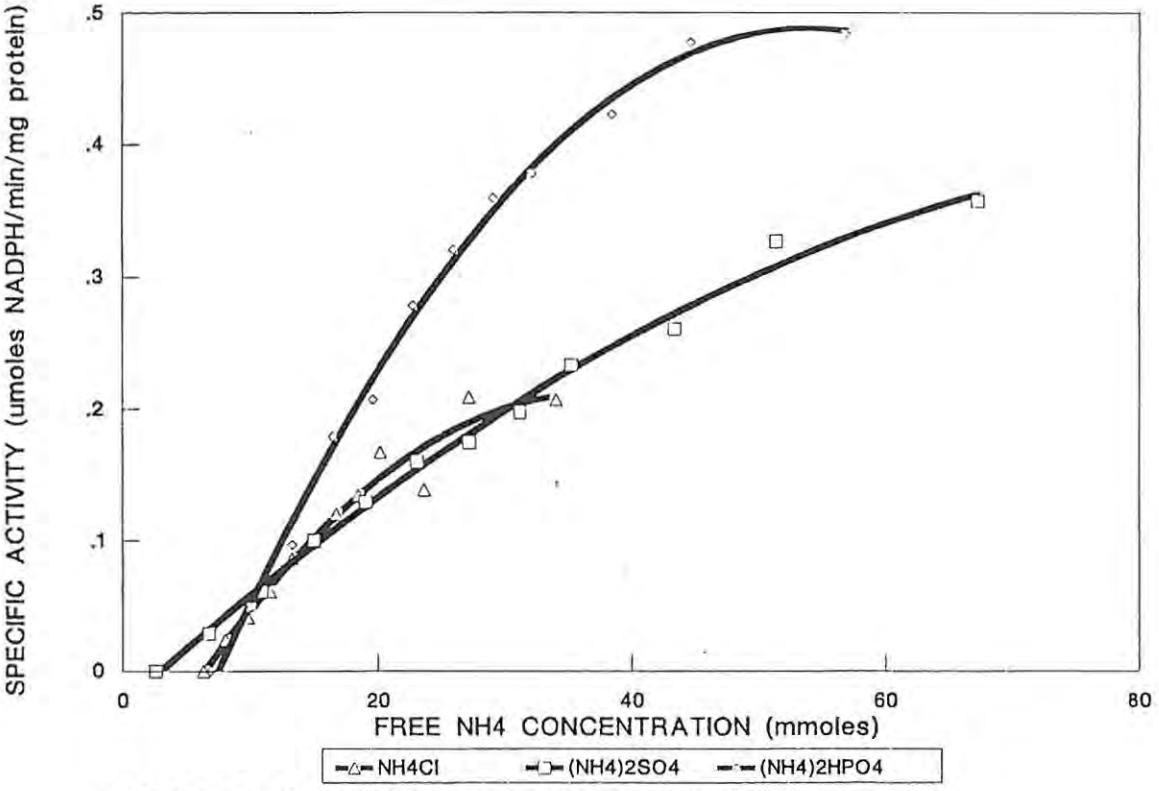

FIGURE 5.7 Effect of the free NH4 concentration arising from NH4Cl, (NH4)2SO4 and (NH4)2HPO4 on the specific activity of glutamate dehydrogenase.

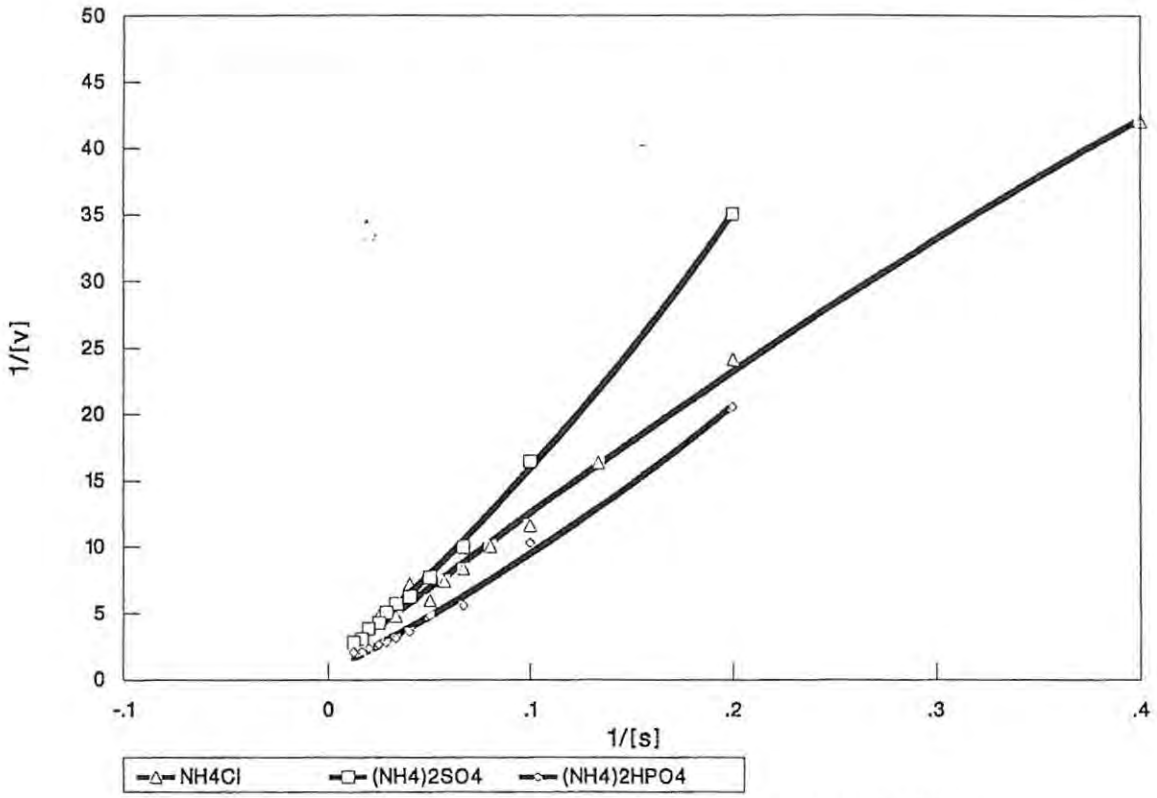

FIGURE 5.8 LineWeaver-Burk plot of the total NH4 concentration versus activity

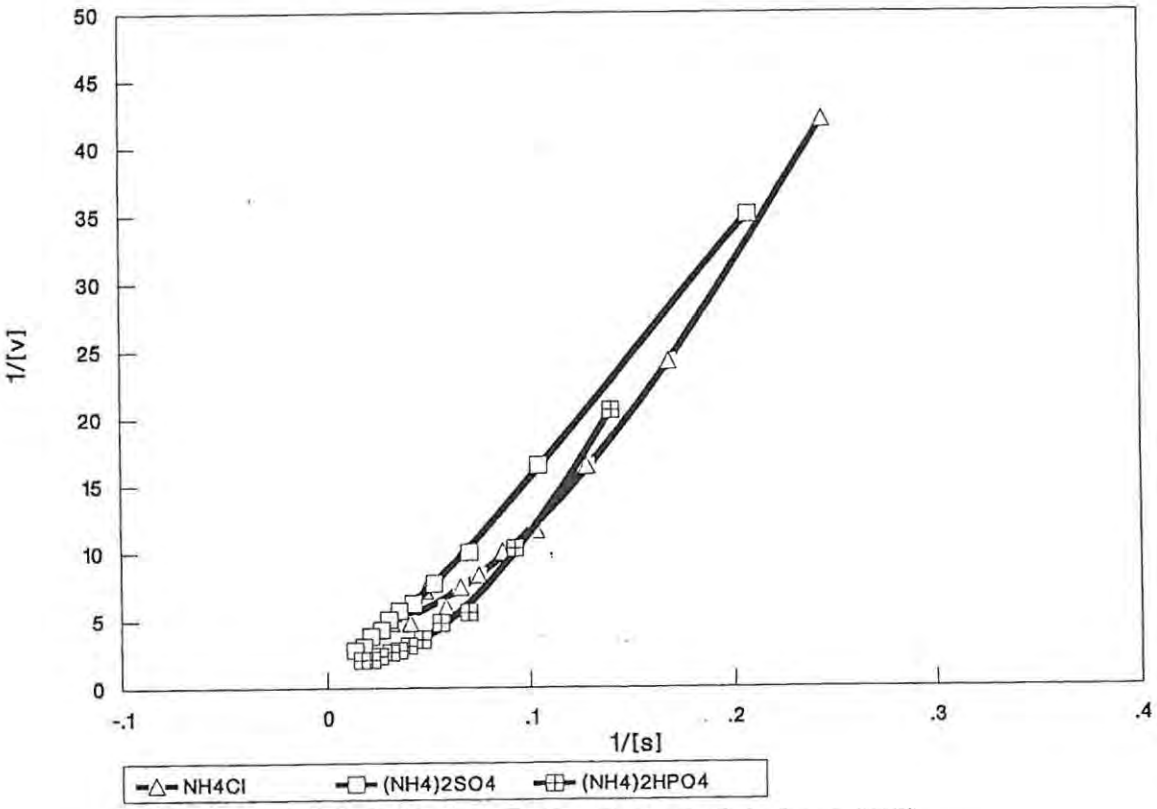

FIGURE 5.9 Lineweaver-Burk plot of the free NH4 concentration versus activity.

dissociated to NH_3 and H^+. The NH_3 therefore appears not to be a substrate for glutamate dehydrogenase. This is indicated by the lack of glutamate dehydrogenase activity at NH_4^+ concentrations below approximately 7mM (Figure 5.7).

5.4.1.3 Glutamine synthetase: γ-glutamyl transferase and synthesis reaction activity

The isoactivity point of the γ-glutamyl transferase reaction and of the synthesis reaction of glutamine synthetase was determined using the whole cell technique of Shapiro and Stadtman (1970). The isoactivity point was found to be pH 7,7 for the glutamine synthetase of *Corynebacterium glutamicum* FP6 (Figure 5.10). This pH was used throughout all the assays.

The Mg^{++} concentration which causes total inhibition of the γ-glutamyl transferase activity was found to be above 48mM (Figure 5.11). In all fermentation experiments where the degree of adenylation of the enzyme was determined using the γ-glutamyl transferase reaction, the total activity of the enzyme was determined (both adenylated and deadenylated) in the absence of Mg^{++} and the contribution that the deadenylated enzyme made to the overall activity was then determined by the addition of $MgCl_2$. The $MgCl_2$ totally inhibits the adenylated enzyme but has no effect on the deadenylated enzyme. The percentage deadenylation to adenylation could then be calculated.

When the cells grown on the glutamate minimal media were split into two cultures, and at zero time the one culture was shocked with $(NH_4)_2SO_4$ and glutamate and the other culture had no additions, and both cultures were monitored for γ-glutamyl transferase activity using the CTAB whole cell technique, the degree of deadenylation of the culture which had been placed in NH_4^+ limitation gradually increased (Figure 5.12).

5.4.1.4 Kinetic constants of glutamine synthetase for its substrates

The kinetic constants of glutamine synthetase for its substrates are outlined in Table 6. The degree of deadenylation as determined using the

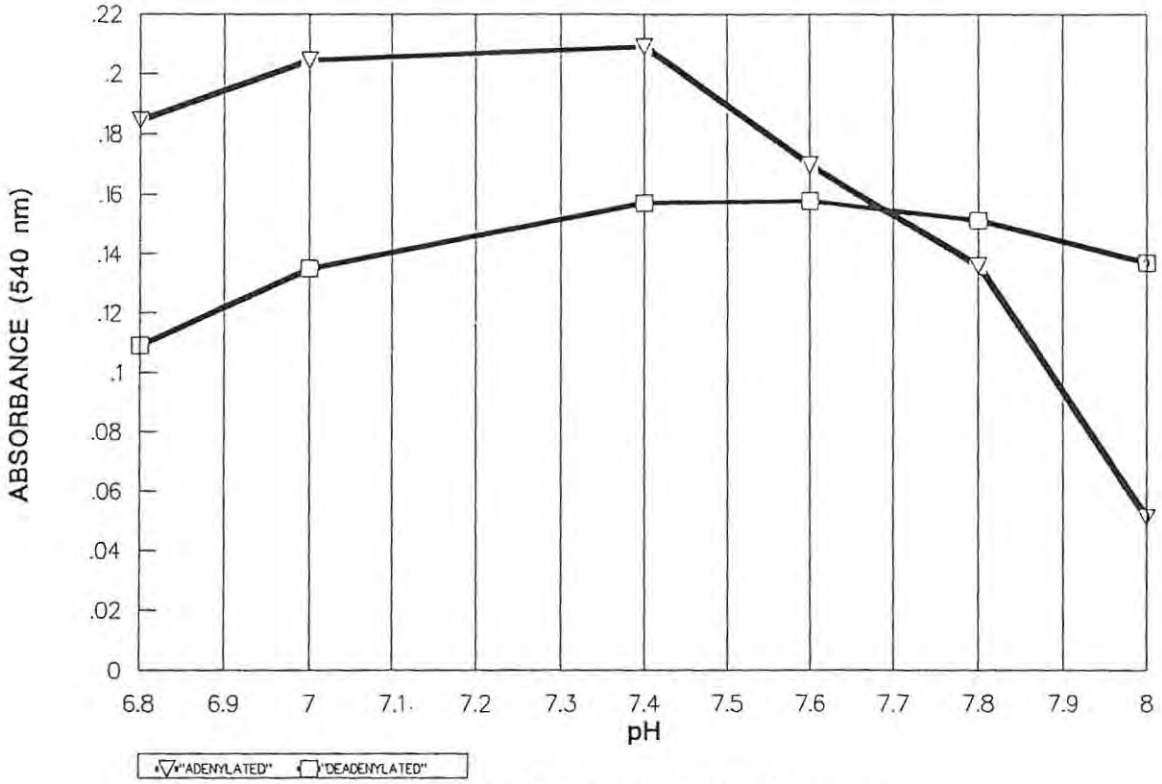

FIGURE 5.10 The isoactivity point of glutamine synthetase

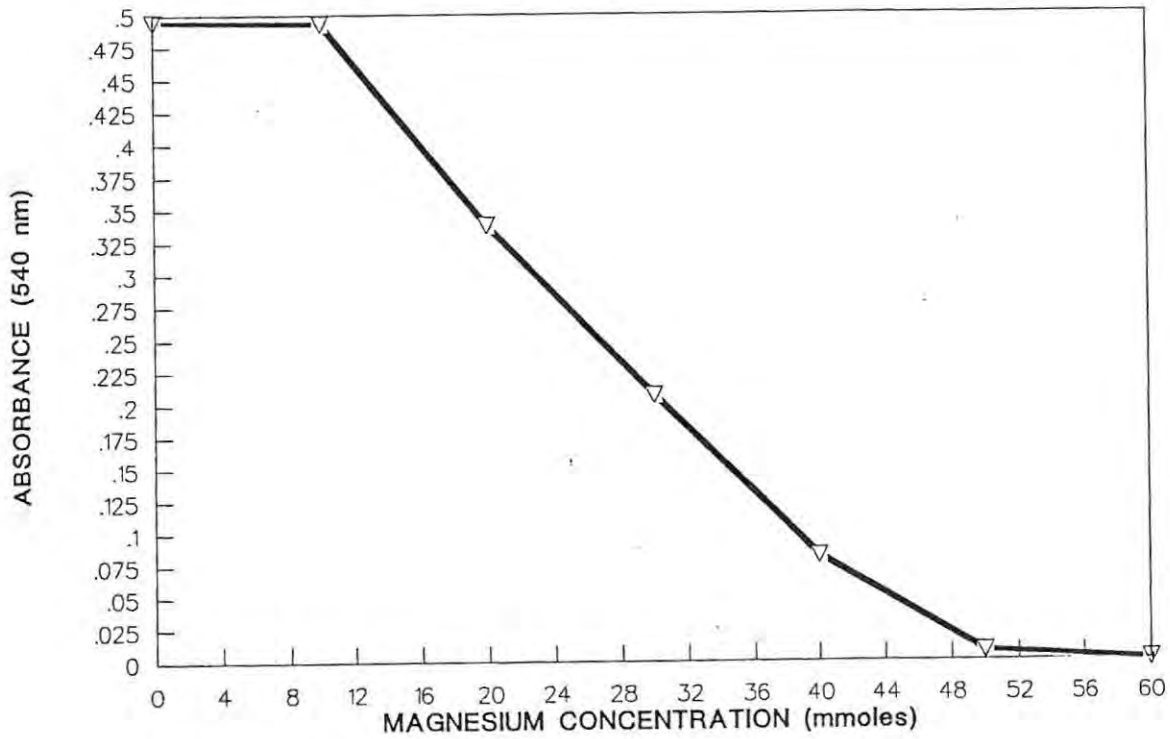

FIGURE 5.11 The inhibition of the glutamyl transferase reaction of glutamine synthetase by magnesium.

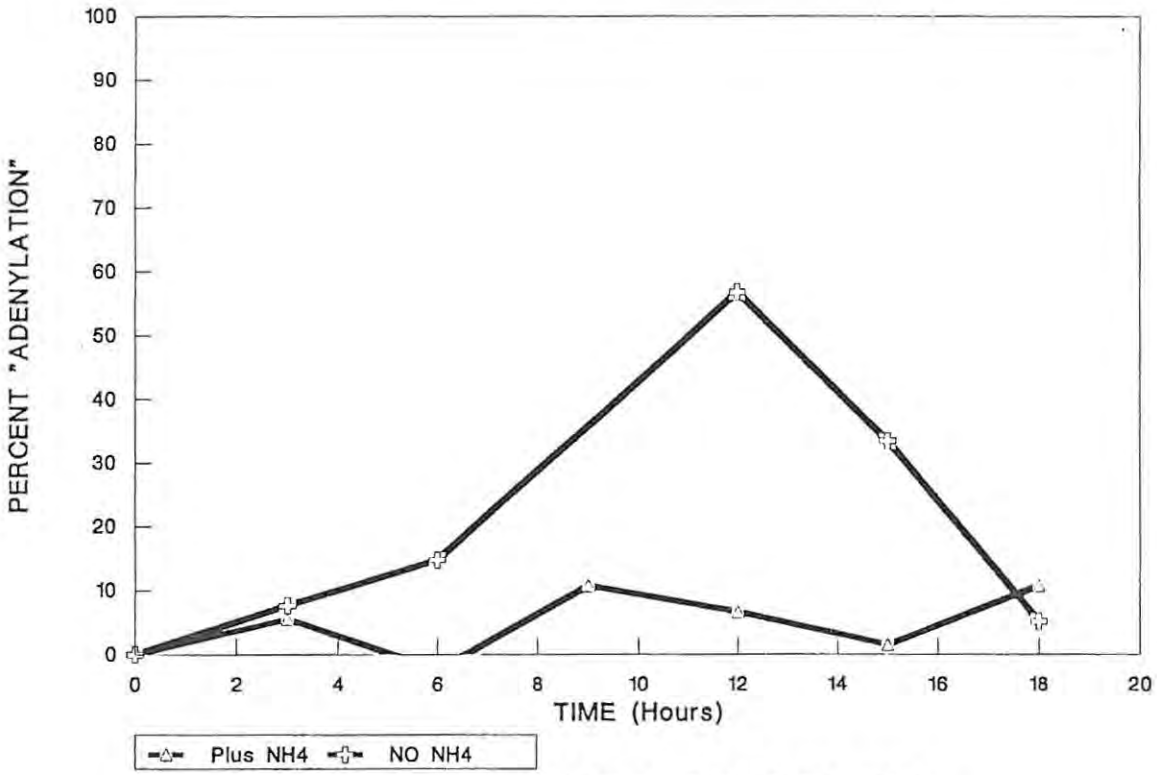

FIGURE 5.12 Activity of glutamine synthetase and its activation by the removal of NH4 in whole cells (Activity = % increase in the adenylation).

γ-glutamyl transferase activity on the cell free extract was 86%.

TABLE 5.5 : Kinetic constants of the glutamine synthetase synthesis reaction

	K_m (mM)	V_{max}
ATP	1,02	
Glutamate	0,46	
NH_3	0,31	0,51

The units of activity are μM P_i/minute/mg protein.

The values of the kinetic constants obtained are comparable with those of *Bacillus sp* (Schreier, 1993) with the affinity for NH_3 being ≃0,5mM. In *Chlorobium vibrioforme* the apparent K_m for glutamate and NH_3 were found to be 2,2mM and 0,2mM respectively (Khanna and Nicholas, 1983). In *Escherichia coli* the apparent K_m for NH_3 was also found to be 0,2mM (Denton and Ginsburg, 1970). The K_m of the glutamine synthetase of *Micrococcus glutamicus (Corynebacterium glutamicum)* for glutamate, NH_3 and ATP were determined to be 7,9, 5,0 and 1,2mM respectively (Tachiki *et al*, 1981). Tachiki *et al* also found that Mg^+ had no effect on the transferase reaction, which is in conflict to the above data. It is believed that in determining the K_m for the NH_3, sufficient care was not taken by Tachiki *et al* in ensuring that the enzyme was in as fully deadenylated form as possible. In *Escherichia coli* the K_m, of the fully adenylated enzyme and the individual subunits for NH_3 range between 10 and 50mM (Reitzer and Magasanik, 1987).

5.4.2 The effect of a limiting free NH_4^+ ion concentration on fermentation and L-lysine synthesis

A range of fermentations were run in media which had no $(NH_4)_2SO_4$ in the initial charge. The requirement for a divalent anionic counter-ion was

fulfilled by using a "second base" for pH control containing NH_4OH and $(NH_4)_2SO_4$ in equimolar concentrations relative to the NH_4^+ concentration. A base case fermentation containing $(NH_4)_2SO_4$ in the initial charge (Appendix III), was run for comparative purposes. To enable the free NH_4^+ concentration to get as low as possible, use of the second base was initiated at varying times. All the fermentations were run in two phases; the first phase (replication phase) was run for 28 hours at a low glucose feed rate (2,0 to 3,8g/l/h) and the second phase (maturation phase) was run from 28 hours into the fermentation until the end of the fermentation at glucose feed rates ranging from 6,0 to 17,4g/l/h. The conditions of the fermentations, the overall lysine yield, maximum lysine productivity, and maximum lysine yield are indicated in Table 5.6. The maximum lysine yield is the maximum yield attainable over a sustained period and is calculated by the lysine formation rate, obtained by linear regression, divided by the glucose utilization rate obtained by linear regression. The r^2 for the linear regressions are also indicated.

The corresponding fermentation profiles are shown in Figures 5.13 to 5.23. Also shown are the lysine yields, instantaneous lysine yields and free NH_4^+ concentrations. The instantaneous lysine yield was calculated as the lysine produced from the utilization of glucose between samples. The free NH_4^+ concentration was calculated as in section 3.3.3. The yields were calculated from the start of the high rate sugar feed and from the start of using the second base pH control.

TABLE 7 : Results of fermentations run at low free NH_4 concentrations

FERMENTATION	GLUCOSE FEED RATE INITIAL (g/l/h)	SECOND (g/l/h)	SECOND BASE [a]TIME (h)	YIELD RANGE (g/g)	OVERALL YIELD (g/g)	[b]MAXIMUM PRODUCTIVITY (g/h)	[c]GLUCOSE UTILIZATION (g/h)	MAXIMUM YIELD (g/g)	LYSINE TITRE (g/l)
A	2,44	6,10	NA	0,30-0,42	0,42	12,5 (0,97) (28-120 h)	33,88 (0,97)	0,42	123,51
B	3,35	8,58	28	-	0,28	9,8 (0,99) (28-70 h)	46,3 (0,99)	0,28	62,19
C	2,49	14,31	32,5	-	0,36	26,5 (0,97) (32-50 h)	65,8 (0,97)	0,40	77,54
D	3,80	9,98	31,5	0,63-0,67	0,34	23,9 (1,0) (31-49 h)	42,8 (0,98)	0,56	65,92
E	3,09	17,37	31,0	0,39-0,40	0,34	12,7 (0,94) (39-71 h)	29,7 (0,80)	0,42	54,90
F	1,95	10,10	29,75	0,32	0,31	15,1 (0,93) (30-69 h)	49,3 (0,97)	0,32	72,64
G	3,30	12,99	32,5	0,50-0,70	0,32	15,6 (0,99) (33-75 h)	26,7 (0,89)	0,58	84,84
H	2,85	5,92	38,0	0,42-0,64	0,32	24,42 (0,99) (42-52 h)	35,11 (1,0)	0,56	57,92
I	2,53	9,08	37,5	0,43-0,68	0,31	22,6 (0,99) (41,5-51,5)	41,32 (1,0)	0,56	73,89
J	2,62	7,48	36,5	0,37-0,63	0,43	12,75 (0,93) (36,0-71,0)	21,33 (0,90)	0,60	79,62

(a) Time at which the use of the "second base" for pH control, was initiated.

(b) () alongside the productivity = r^2
() below the productivity value = time over which the productivity was calculated

(c) () = r^2

FERMENTATION A (Base case) (Figure 5.13)

In the base case fermentation the lysine yield over time remains relatively constant at around 0,35g/g. There are however "spikes" in the instantaneous yield. These are found in all subsequent fermentations and will be discussed in the general discussion. At no stage during this fermentation were there sustained high instantaneous yields. A low second glucose feed rate was maintained at 6,0g/l/h. The free NH_4^+ concentration was maintained at above 300mmoles for 70 hours of the fermentation, at which point it decreased to zero with a concomitant increase in the lysine yield. As this fermentation started with $(NH_4)_2SO_4$ in the initial charge, the calculated free NH_4^+ concentration is believed to be a true reflection of this concentration. The final titre of the lysine was 120g/l.

FERMENTATION B (Figure 5.14)

In fermentation B the second base control was started at 28 hours. The lysine yield was maintained at approximately 0,25g/g with spikes in the instantaneous yield again occurring. The free NH_4^+ concentration rose to approximately 400mmoles (Figure 5.14). This is however believed not to be a true reflection of this concentration as there was a major change in the concentration immediately after the start of using the second base. It is believed if the free NH_4^+ concentration is allowed to drop below a critical value, causing it to dissociate to $NH_3 + H^+$ the teichoic acid in the cell wall loses its associated counter-ions, namely lysine and NH_4^+ (Figure 5.26). Therefore by the end of the replication phase, the NH_4^+ which was bound to the teichoic acid, has possibly been replaced by H^+. This is analogous to the dissociation of $(NH_4)_2HPO_4$ (Chapter 2, Section 2.4.2). The taking up of NH_4^+, by the teichoic acid at the start of lysine synthesis therefore renders some of it "unavailable". It is only the dissociated ions that can act as effectors of the physiology.

A complex set of concentration gradients are possibly set up with lysine, H^+ and NH_4^+ all interacting with the teichoic acid. This becomes better defined in subsequent fermentations. The low yield is possibly due to the organism using both glutamate dehydrogenase and glutamine synthetase

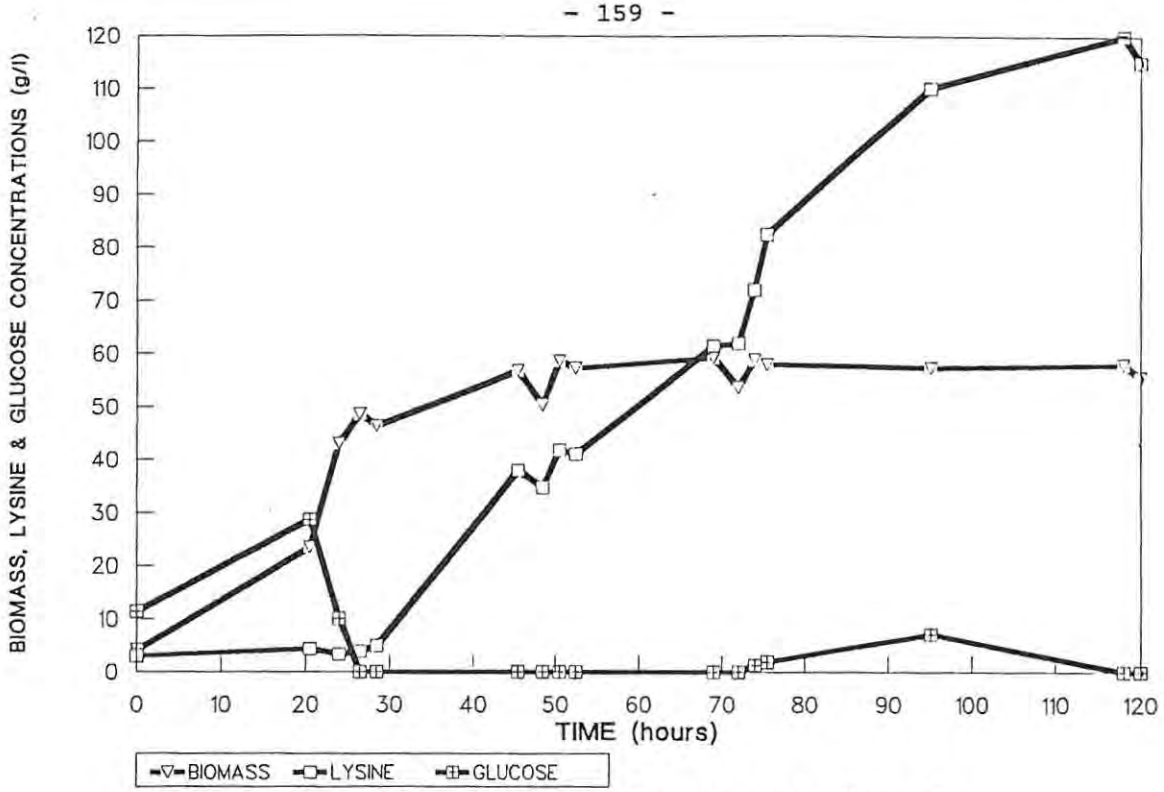

FIGURE 5.13A The change in the concentration of biomass, lysine and glucose during fermentation.

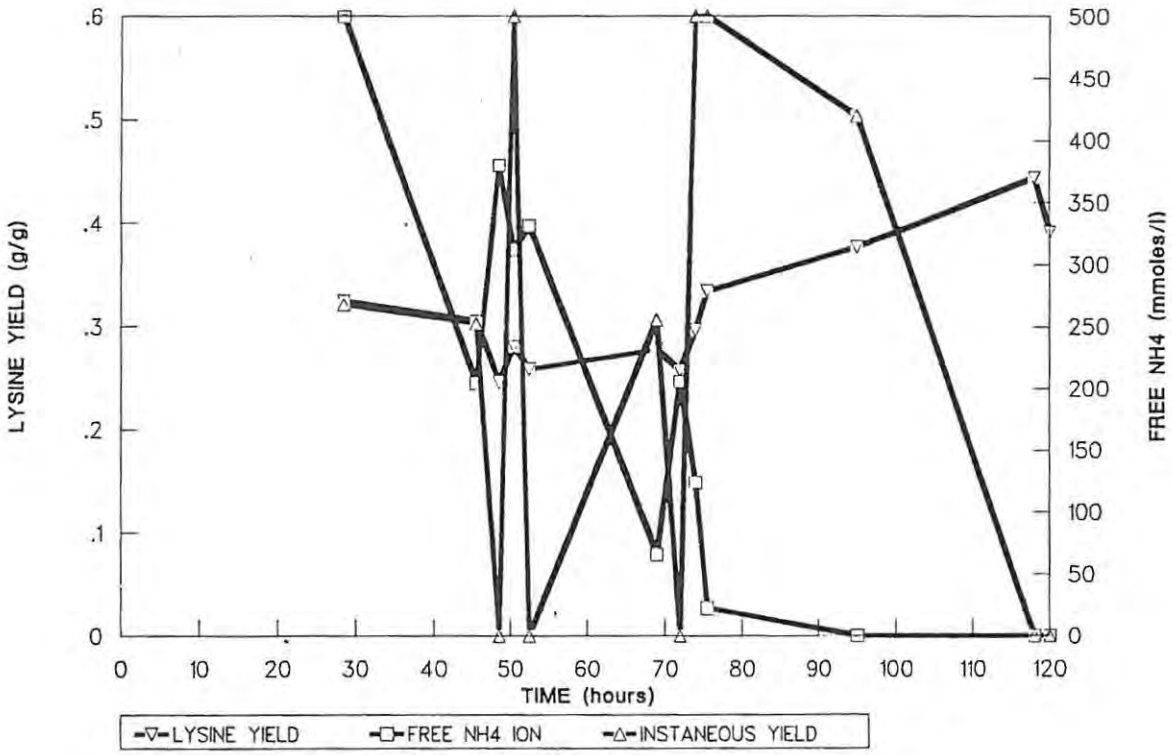

FIGURE 5.13B Change in the lysine yield, the instantaneous yield and the free NH4 concentration taken from the onset of the high glucose feed.

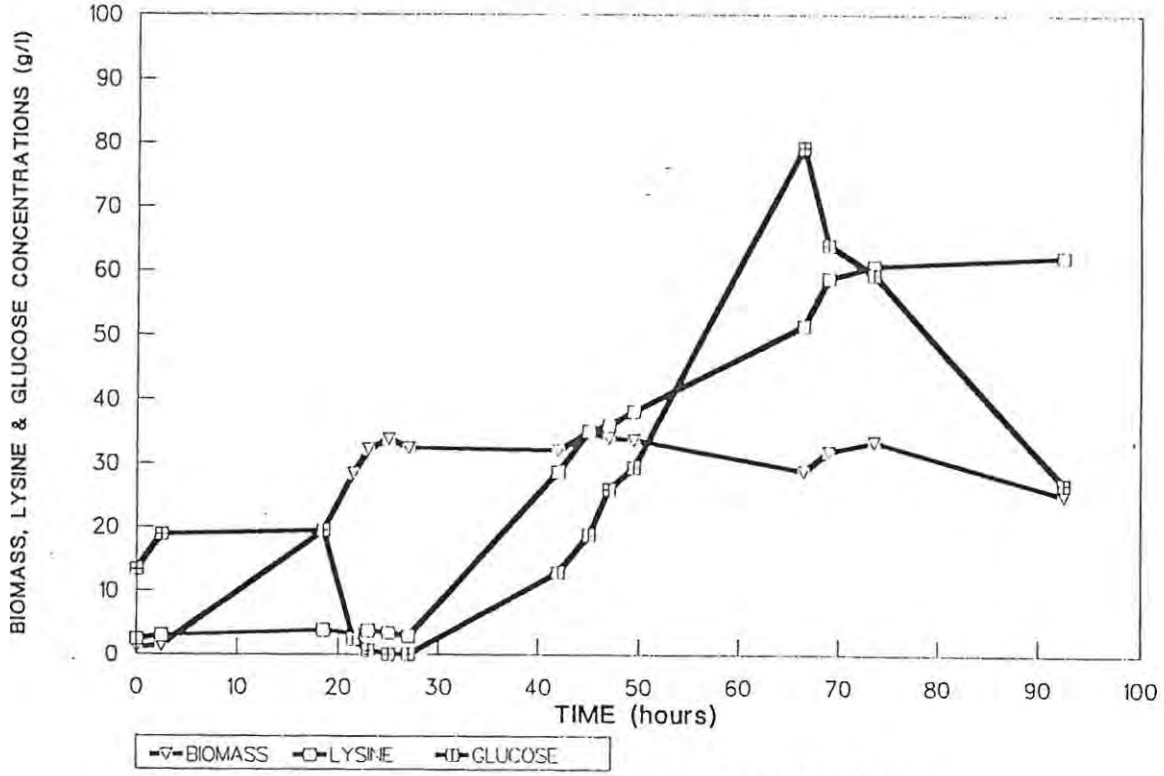

FIGURE 5.14A The change in the concentration of biomass, lysine and glucose during fermentation.

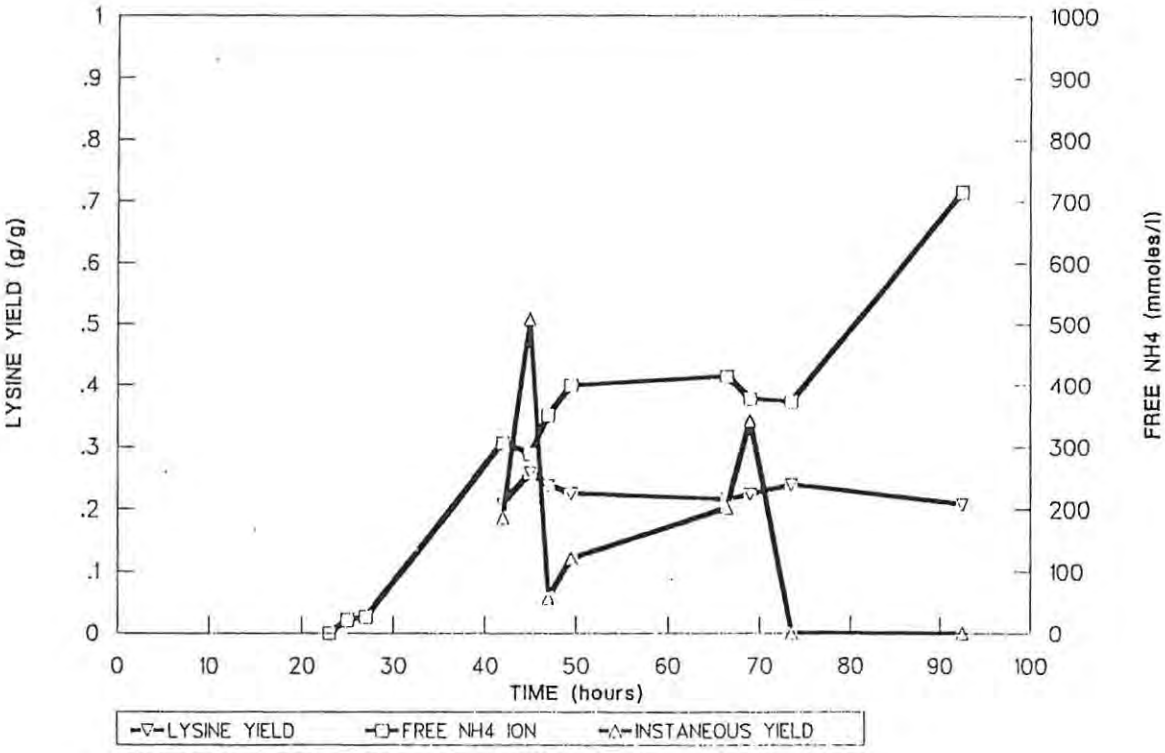

FIGURE 5.14B Change in the lysine yield, the instantaneous yield and the free NH4 concentration taken from the onset of the high glucose feed.

161/...

under sub-optimal conditions. This fermentation also accumulated glucose during lysine synthesis.

FERMENTATION C (Figure 5.15)

In this fermentation the second base feed was started at 32,5 hours. After the start of using the second base there was an increase in the lysine yield. This is probably due to the change in mechanism of assimilating ammonia from glutamate dehydrogenase to glutamine synthetase. There was also a concomitant apparent increase in the free NH_4^+ concentration. The lysine yield then decreased between 42 and 50 hours. As in fermentation B, this is believed to result from the teichoic acid taking up NH_4^+ to fill the sites made vacant by the utilization of the NH_4^+ off the teichoic acid, thereby demanding additional base. Between 40 and 50 hours of fermentation, the yield and the instantaneous yield were higher then in fermentation B. This fermentation started to accumulate glucose at a time towards the end of the high lysine yield period.

FERMENTATION D (Figure 5.16)

The second base was started at 31,5 hours in fermentation D. For a period of 10 hours from this time, a yield of 0,66g/g was maintained. At this point there was an increase in the free NH_4^+ concentration thus decreasing the instantaneous lysine yield. The fermentation had also started to accumulate glucose. An overall lysine yield of 0,34g/g was obtained. It is believed that a higher instantaneous yield was obtained in this fermentation as the maximum glucose utilization rate and the overall glucose utilization rate were lower during lysine synthesis. As a high instantaneous yield was maintained for a longer period then in the previous two fermentations, it is believed not to be the result of the displacement of lysine by NH_4^+ off the teichoic acid.

FERMENTATION E (Figure 5.17)

Fermentation E was run similarly to fermentation C with a high second glucose feed (17,4g/l/h). It accumulated glucose from the onset of this

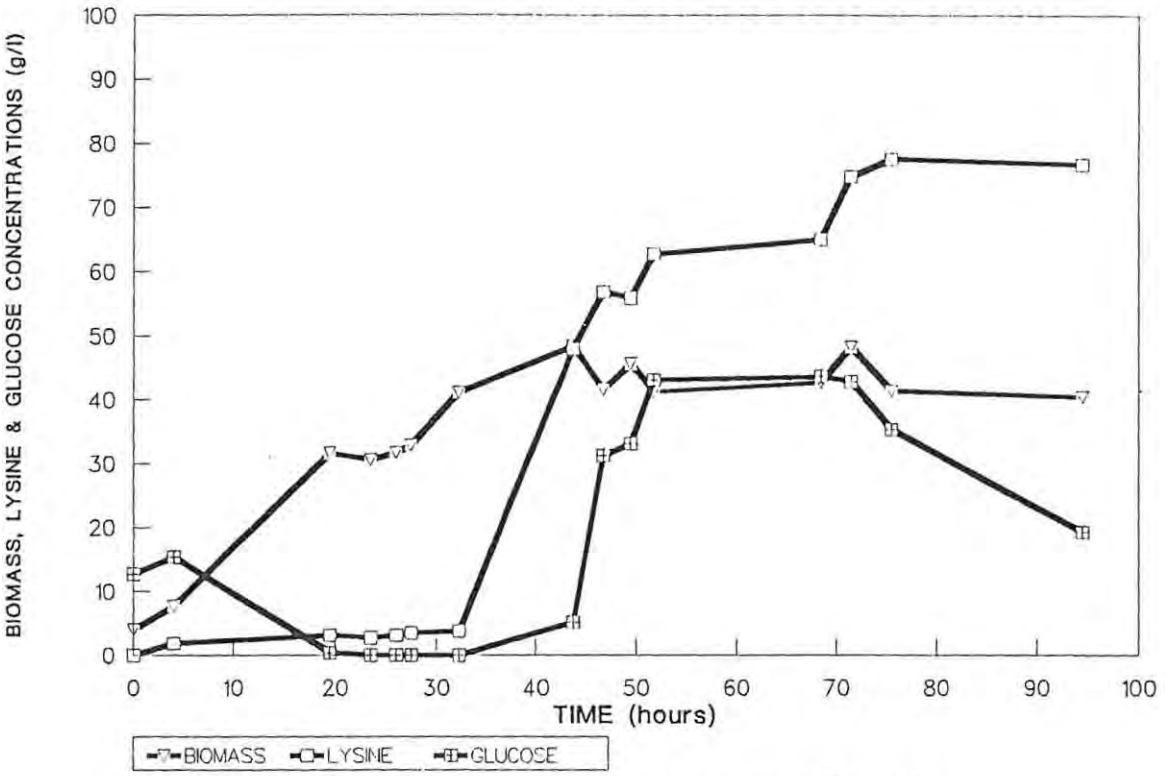

FIGURE 5.15A The change in the concentration of biomass, lysine and glucose during fermentation.

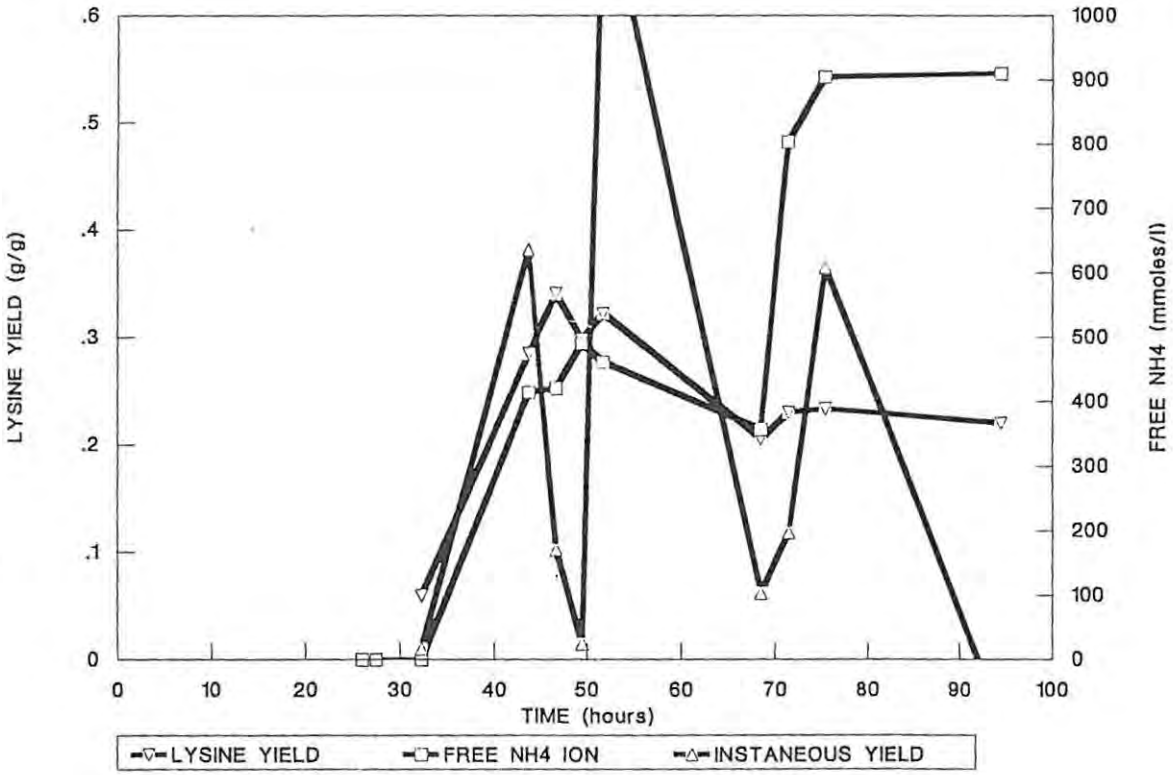

FIGURE 5.15B Change in the lysine yield, the instantaneous yield and the free NH4 concentration taken from the onset of the high glucose feed.

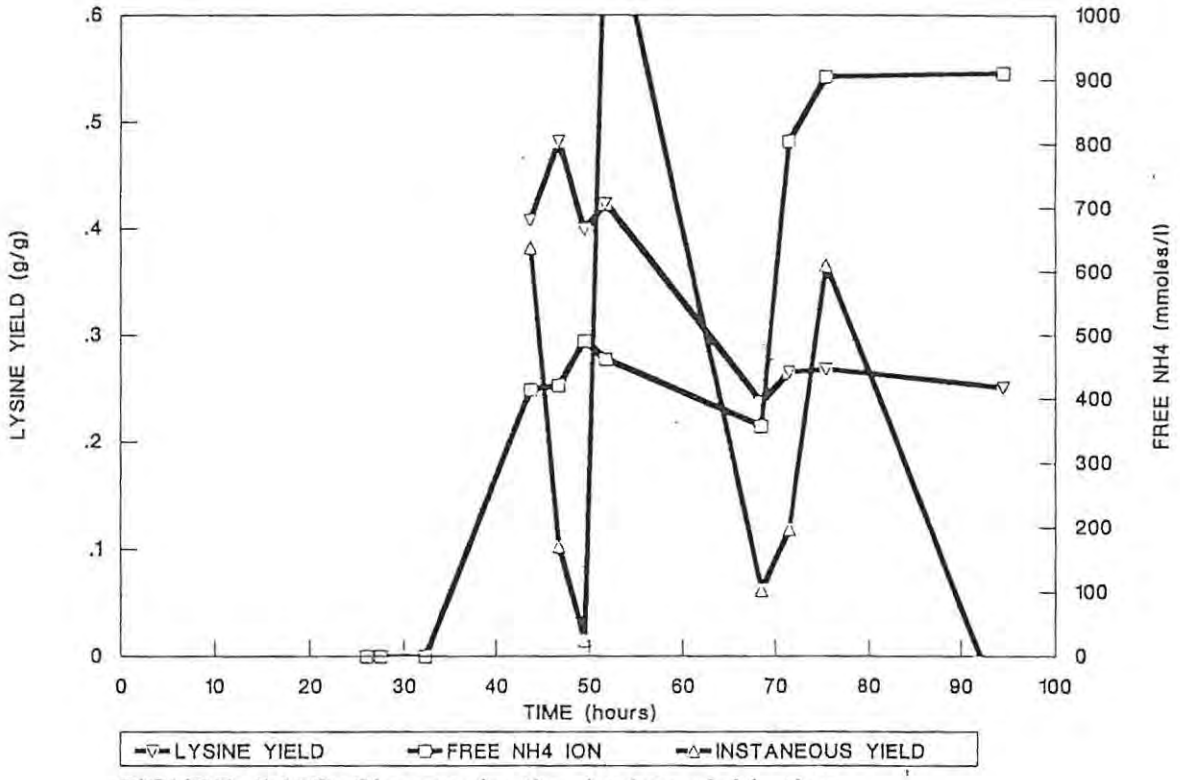

FIGURE 5.15C Change in the lysine yield, the instantaneous yield and the free NH4 concentration taken from the onset of the second base pH control.

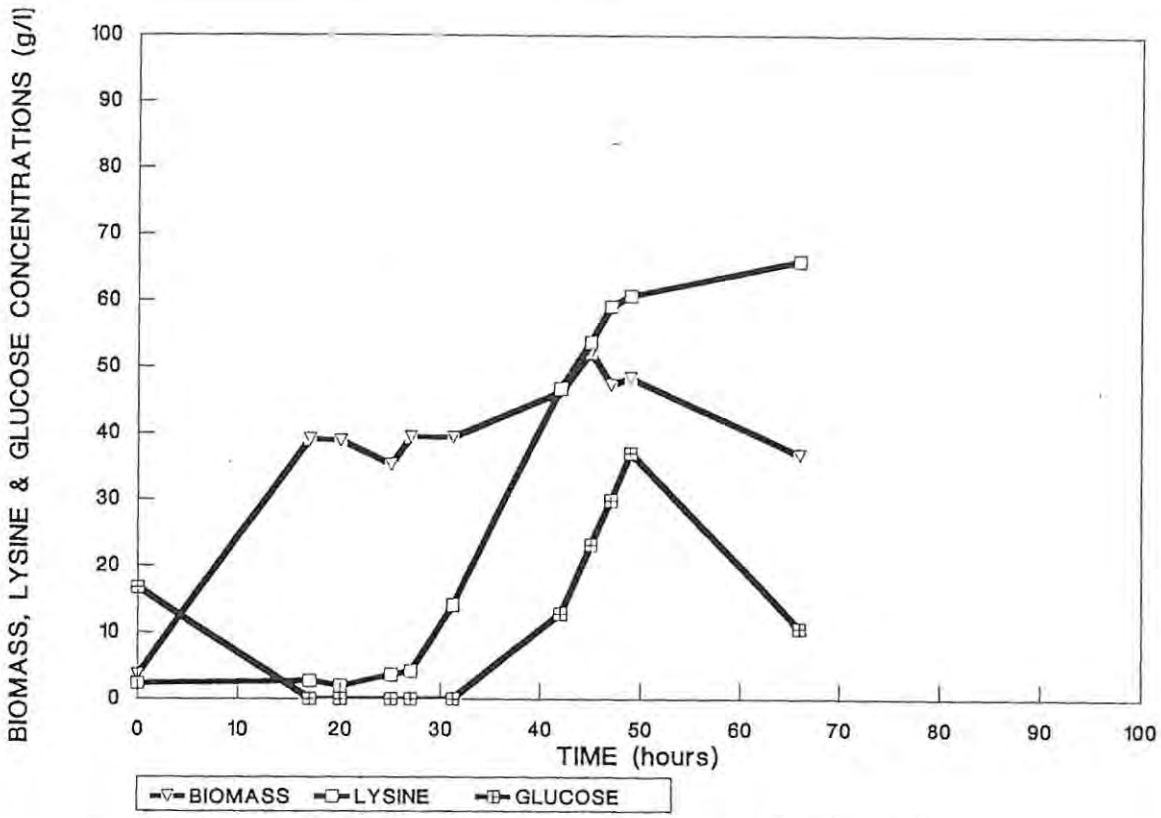

FIGURE 5.16A The change in the concentration of biomass, lysine and glucose during fermentation.

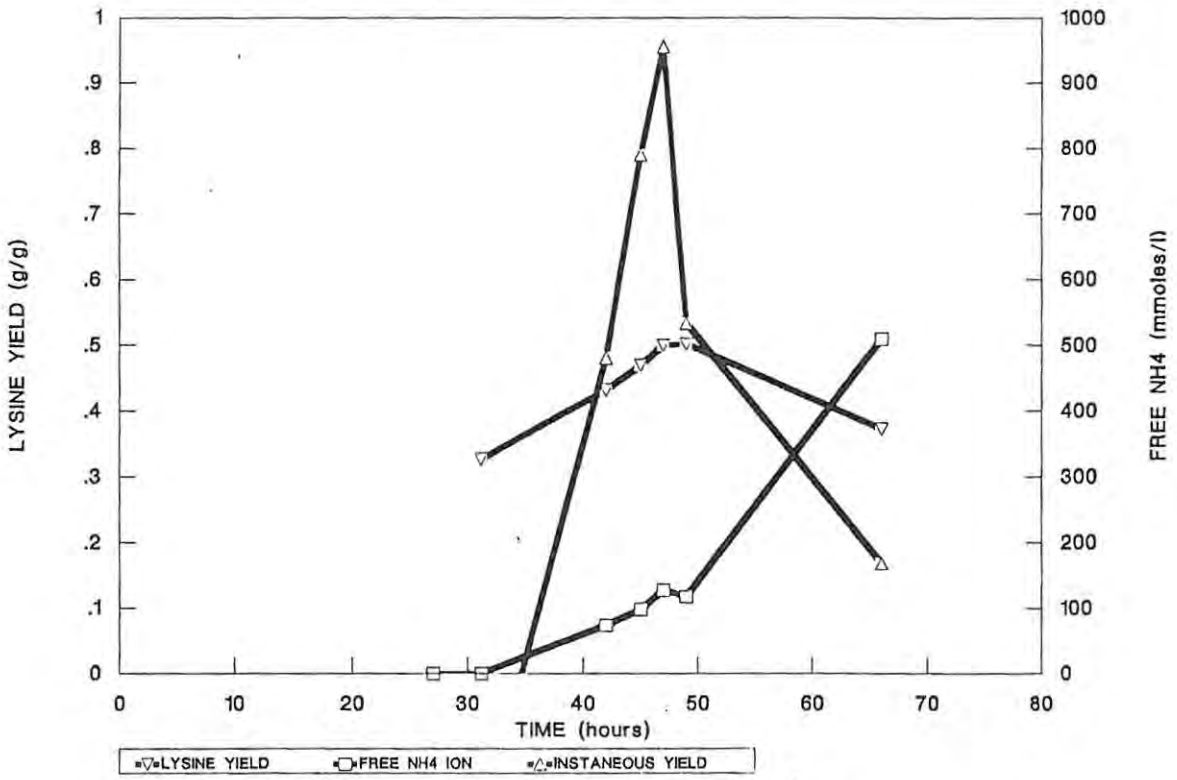

FIGURE 5.16B Change in the lysine yield, the instantaneous yield and the free NH4 concentration taken from the onset of the high glucose feed.

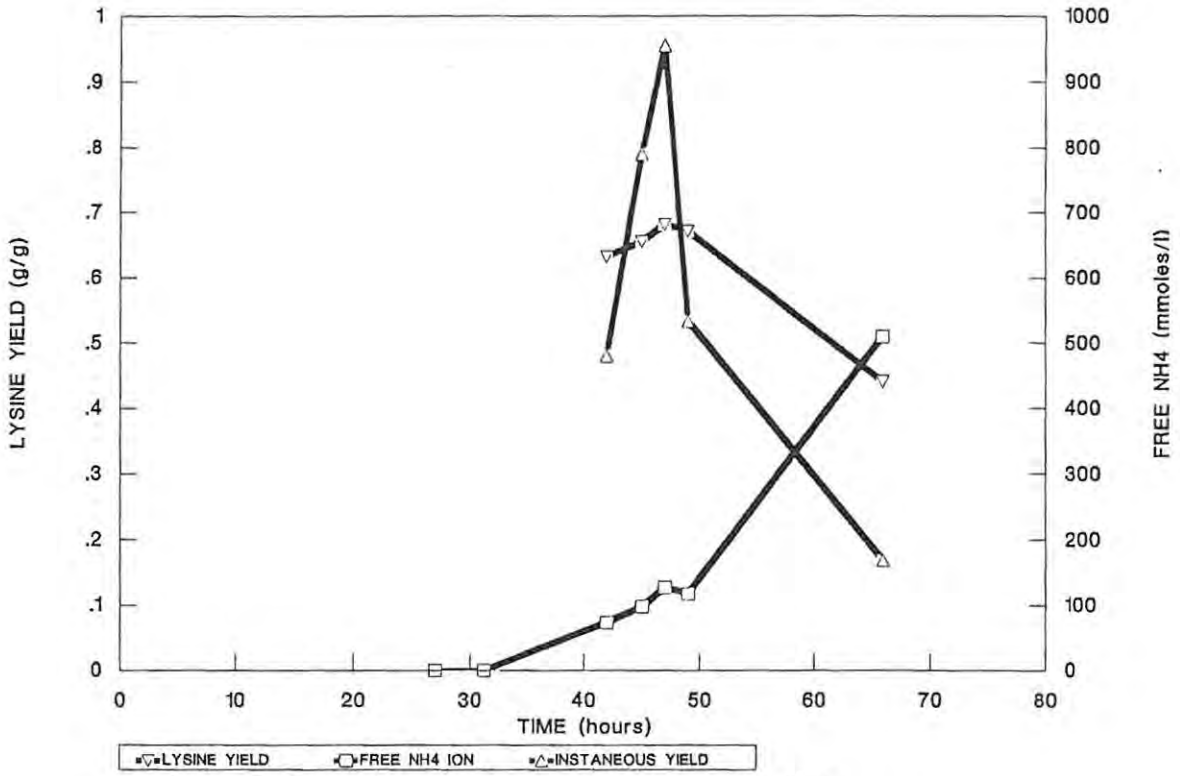

FIGURE 5.16C Change in the lysine yield, the instantaneous yield and the free NH4 concentration taken from the onset of the second base pH control.

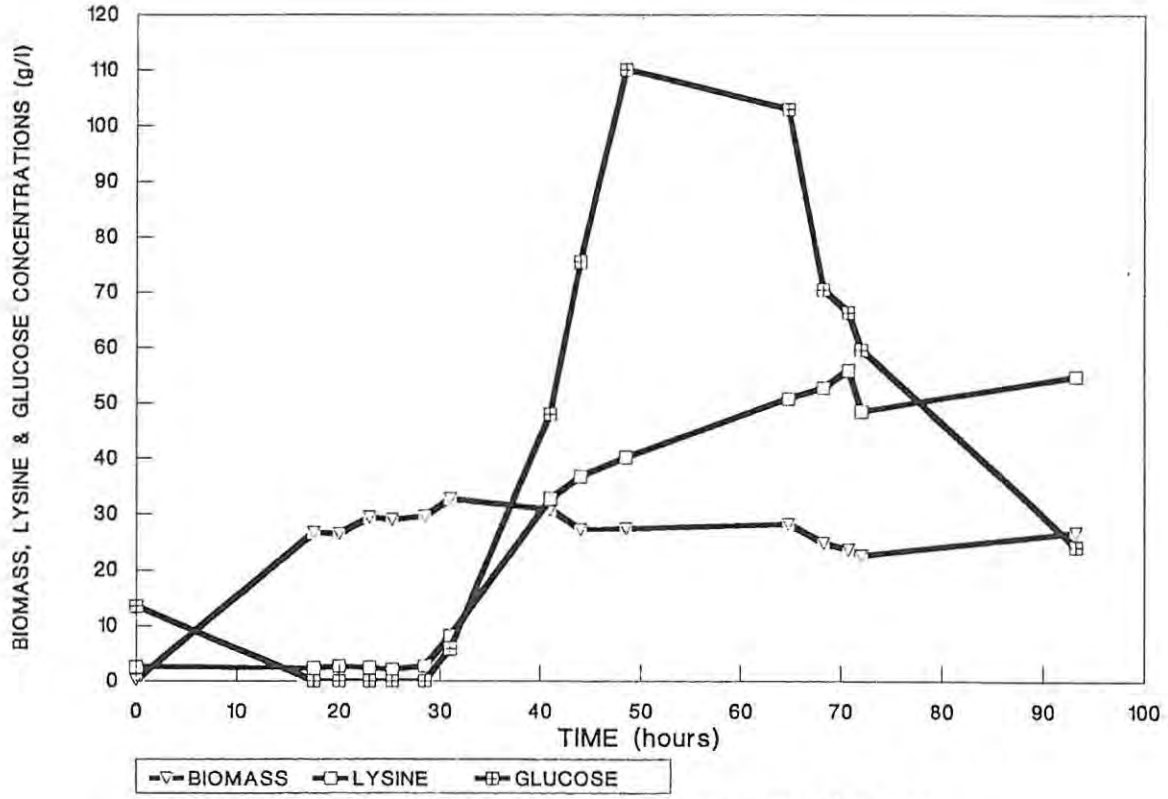

FIGURE 5.17A The change in the concentration of biomass, lysine and glucose during fermentation.

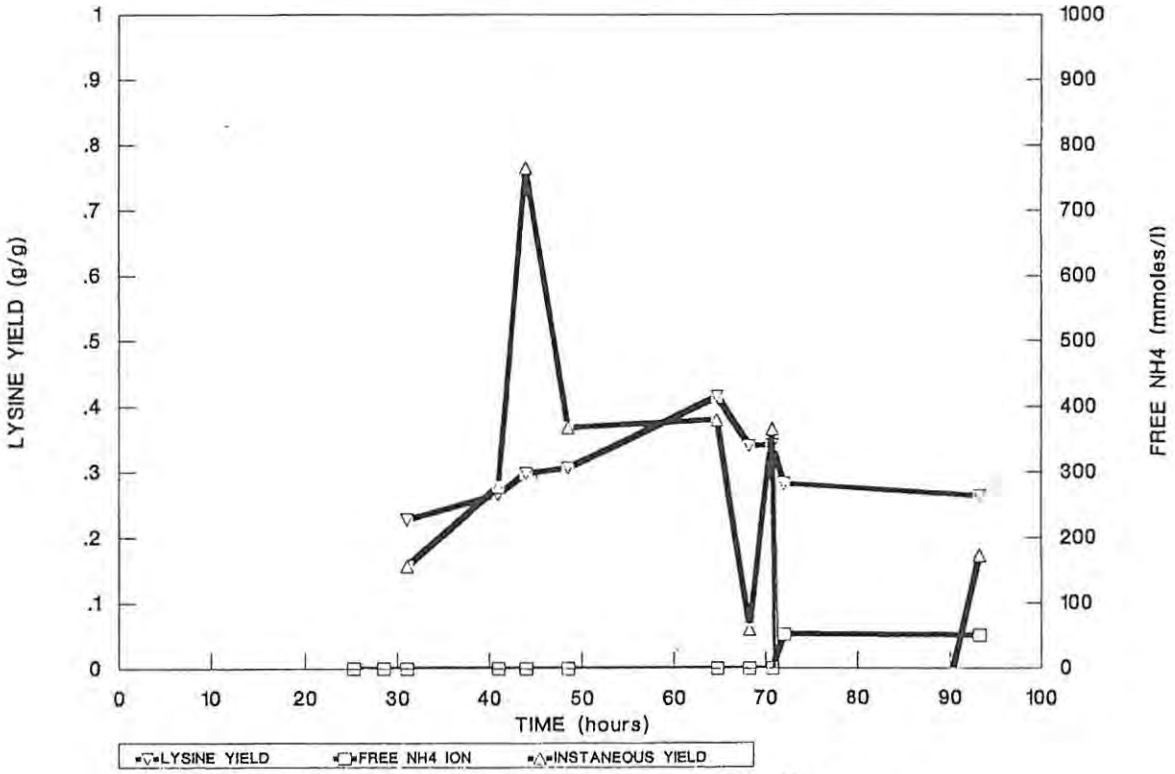

FIGURE 5.17B Change in the lysine yield, the instantaneous yield and the free NH4 concentration taken from the onset of the high glucose feed.

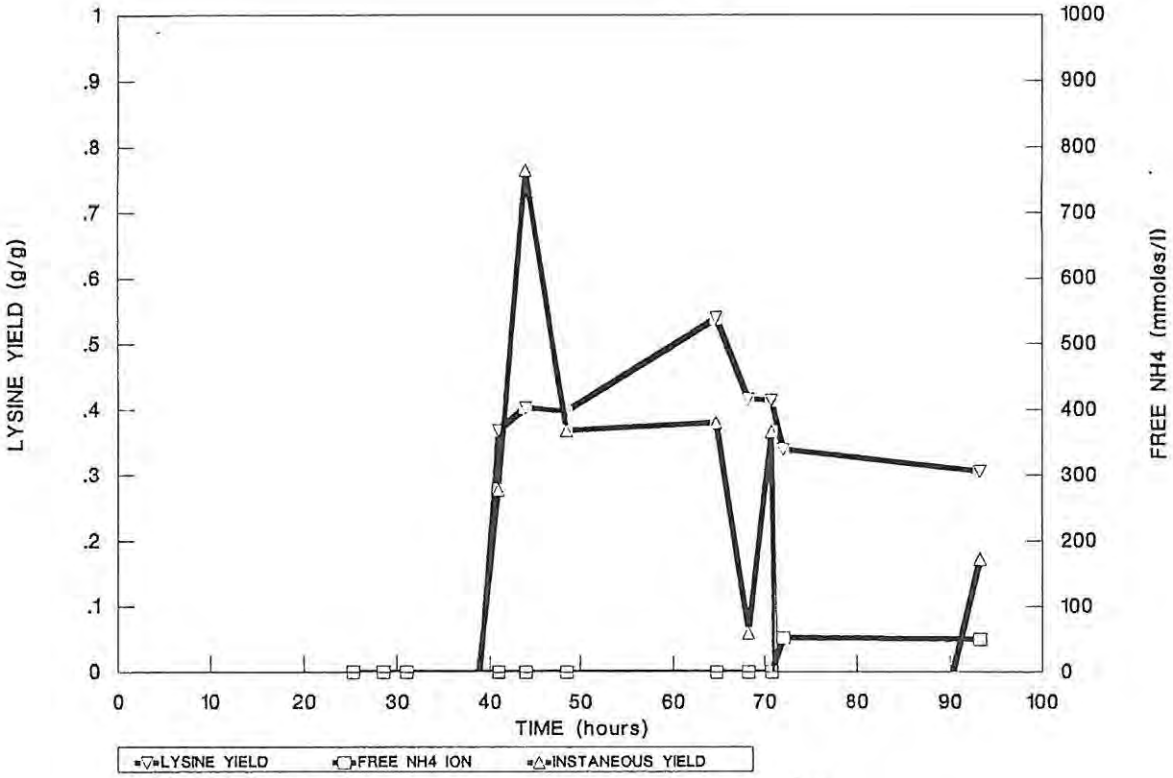

FIGURE 5.17C Change in the lysine yield, the instantaneous yield and the free NH4 concentration taken from the onset of the second base pH control.

feed and the instantaneous lysine yield was lower than in fermentation D, at 0,42g/g.

FERMENTATION F (Figure 5.18)

This fermentation was run at a lower glucose feed rate (10,1g/l/h) however the second base was started at 29,75 hours. As expected, starting the second base earlier brought the lysine yield and the instantaneous yield down to approximately 0,32g/g, as depletion of the NH_4^+ would not occur prior to starting the glucose feed. The reduction in yield is probably due to the ammonia assimilation occurring via both the glutamate dehydrogenase and glutamine synthetase.

FERMENTATION G (Figure 5.19)

The second base pH control was initiated at 32,5 hours in fermentation G and the glucose feed rate was 12,99g/l/h. The lysine yield increased from ≃0,15 to 0,46g/g after initiation of the glucose feed, with final the titre being 82g/l. The increase in yield is again probably due to a change in the mechanism of ammonia assimilation from the low affinity glutamate dehydrogenase to the high affinity glutamine synthetase. The degree of deadenylation of the glutamine synthetase enzyme during the fermentation indicates that this is indeed the case (Figure 5.19D).

FERMENTATION H (Figure 5.20)

Fermentation H was run at a very low second glucose feed rate (≃6g/l/h). During the period 38 to 52 hours, a yield of between 0,45 to 0,58 was maintained. Calculating the lysine yield from the start of the second glucose feed, there was an increase in yield from 0,2 to 0,35g/g. However calculating the yield from the initiation of the second base pH control, the yield decreased from 1,0 to 0,55g/g at 52 hours. The high instantaneous yield at the start of using the second base is believed to be as a result of the desorption of the lysine off the teichoic acid by the NH_4^+. By running the fermentation without counter-ions and NH_4^+ for a long period it is possible that lysine synthesis ceases towards the end of 38 hours as a result of the depletion of the ammonia. The sites on

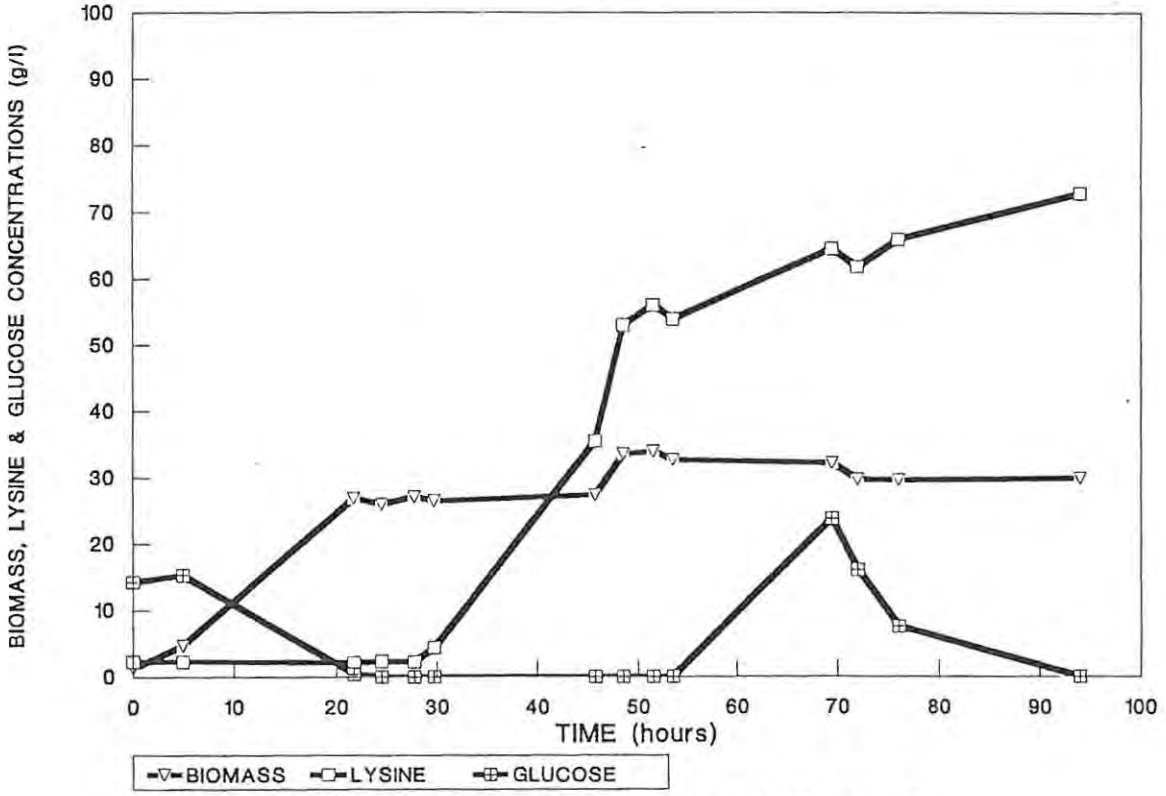

FIGURE 5.18A The change in the concentration of biomass, lysine and glucose during fermentation.

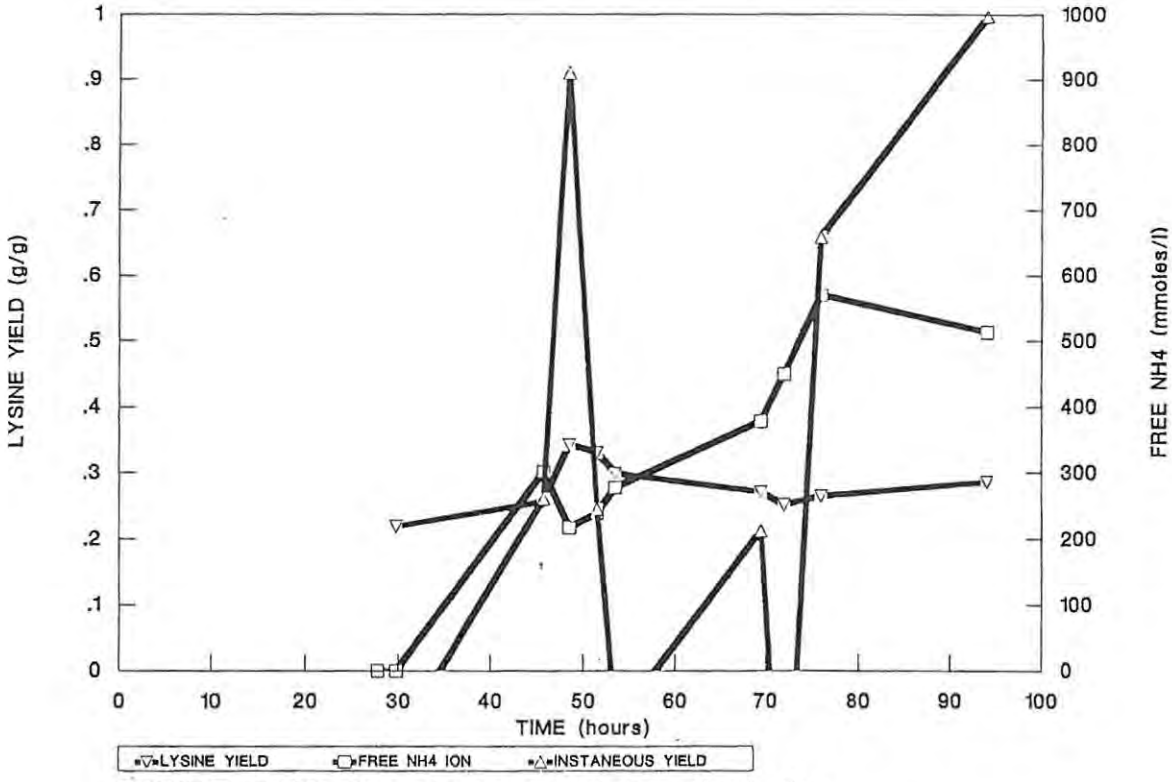

FIGURE 5.18B Change in the lysine yield, the instantaneous yield and the free NH4 concentration taken from the onset of the high glucose feed.

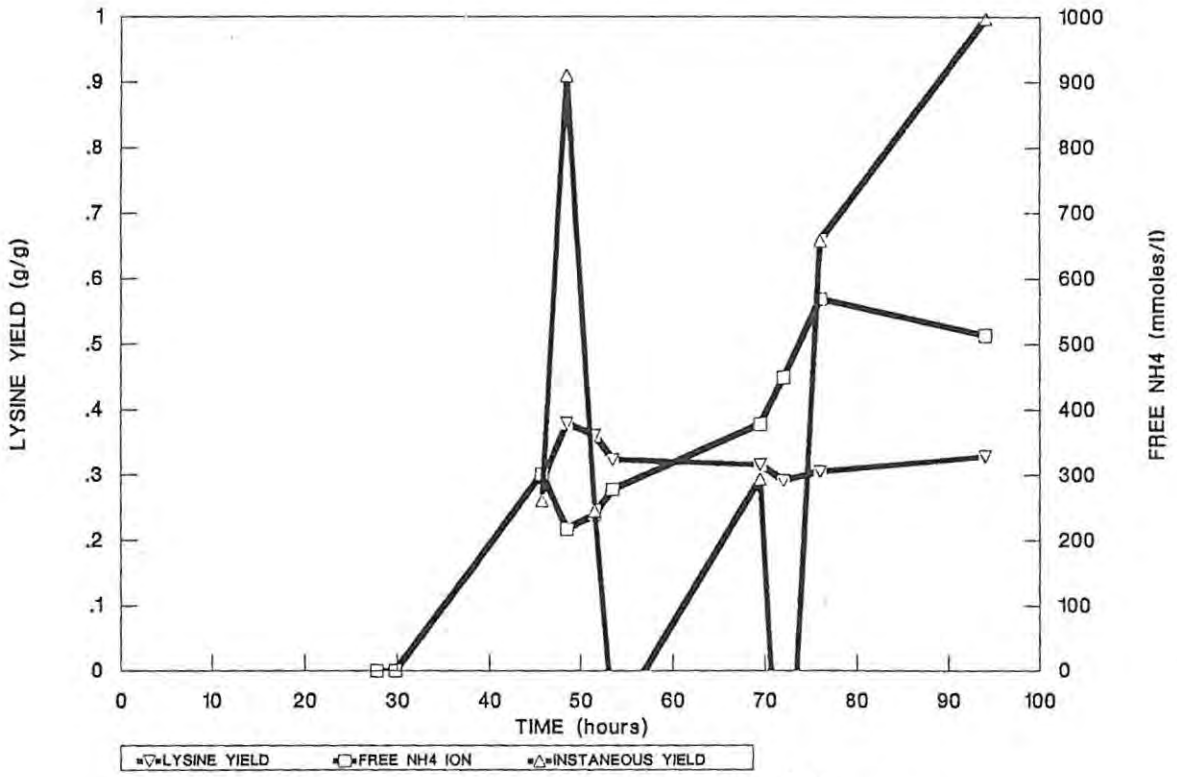

FIGURE 5.18C Change in the lysine yield, the instantaneous yield and the free NH4 concentration taken from the onset of the second base pH control.

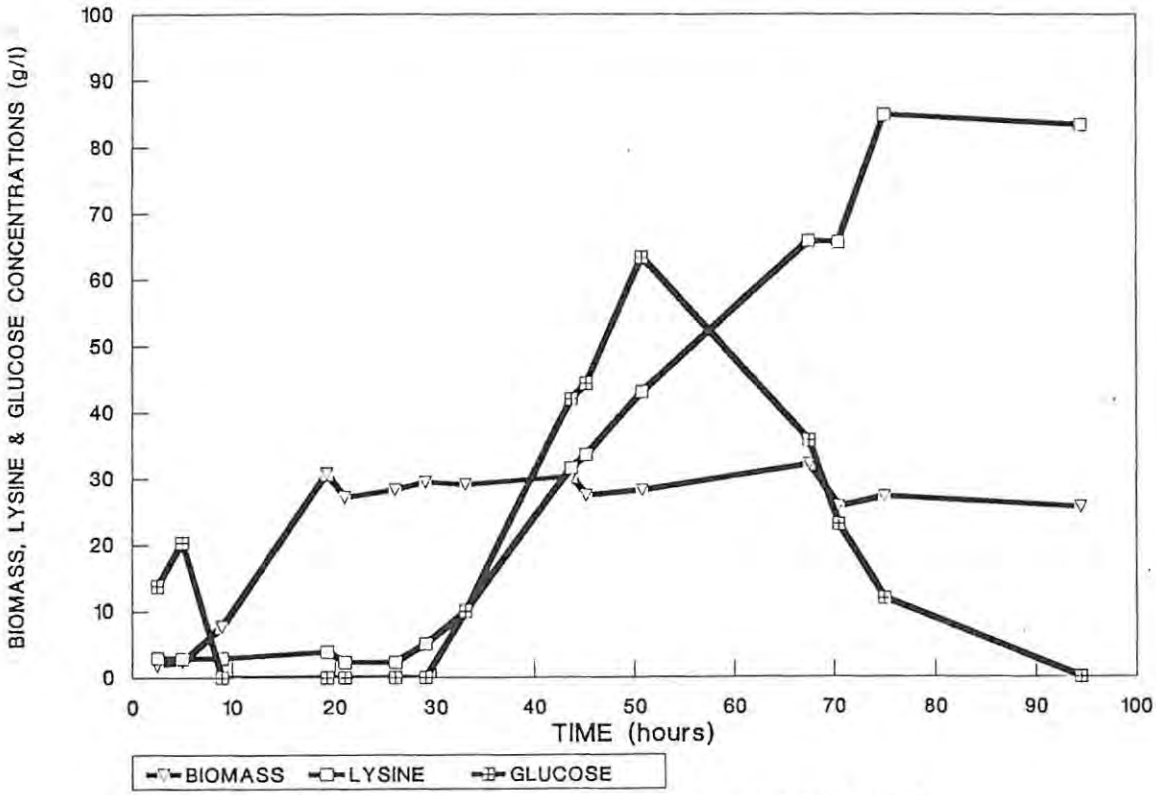

FIGURE 5.19A The change in the concentration of biomass, lysine and glucose during fermentation.

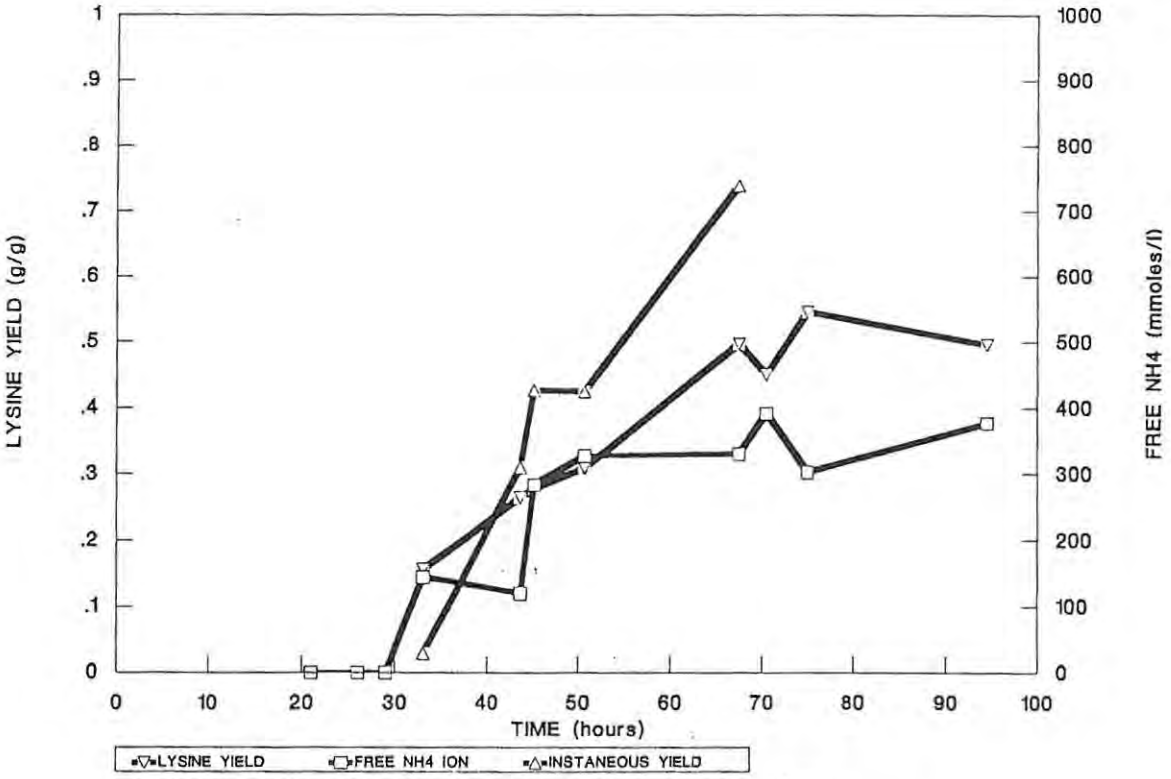

FIGURE 5.19B Change in the lysine yield, the instantaneous yield and the free NH4 concentration taken from the onset of the high glucose feed.

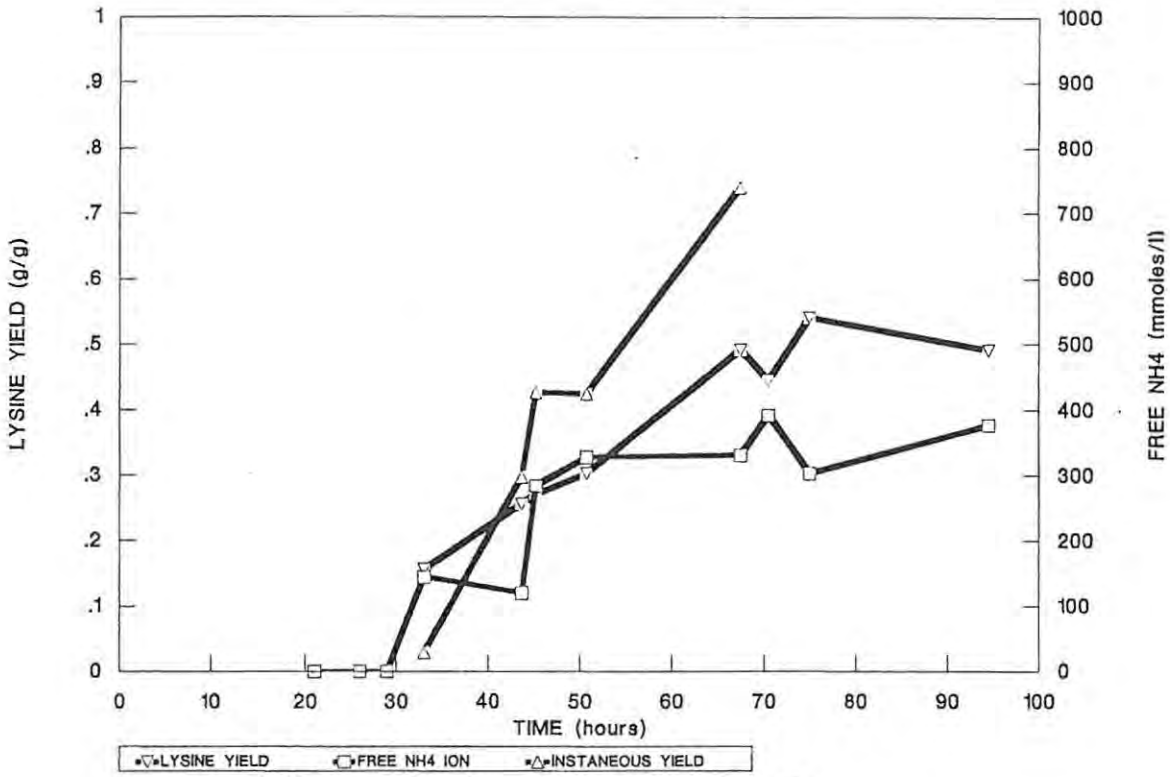

FIGURE 5.19C Change in the lysine yield, the instantaneous yield and the free NH4 concentration taken from the onset of the second base pH control.

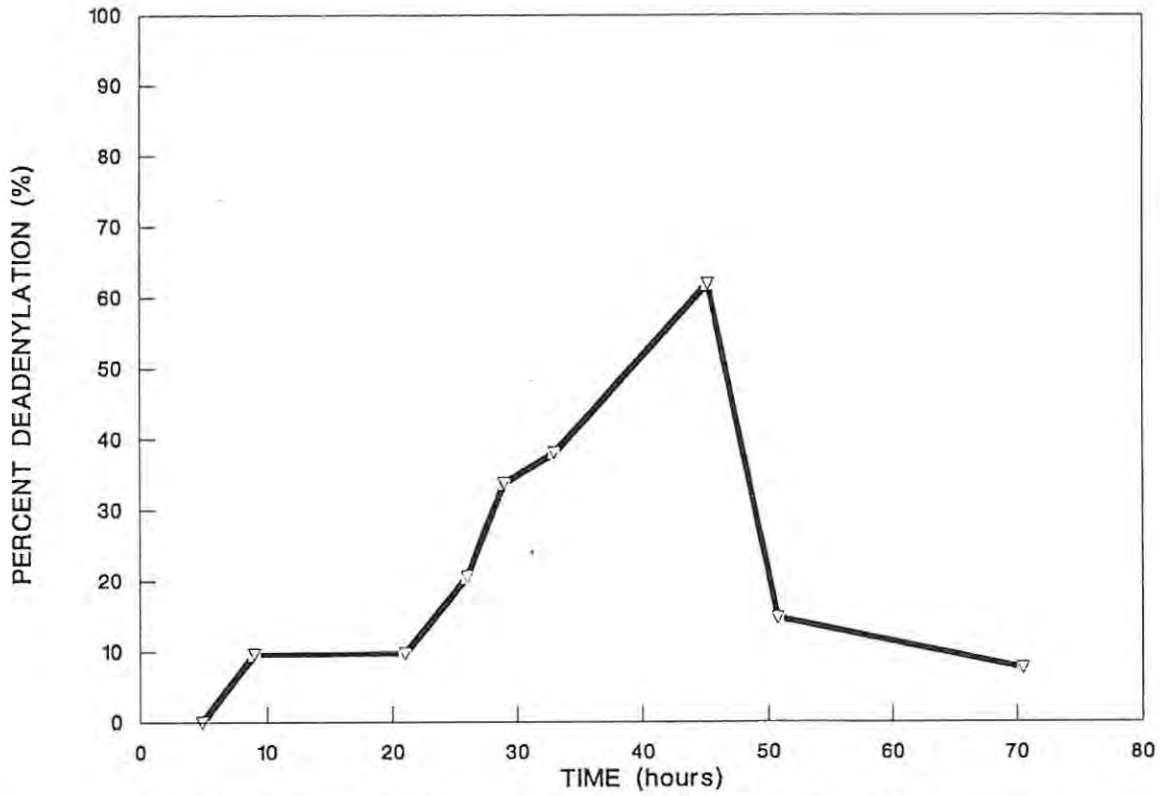

FIGURE 5.19D Change in the percent deadenylation of glutamine synthetase during fermentation.

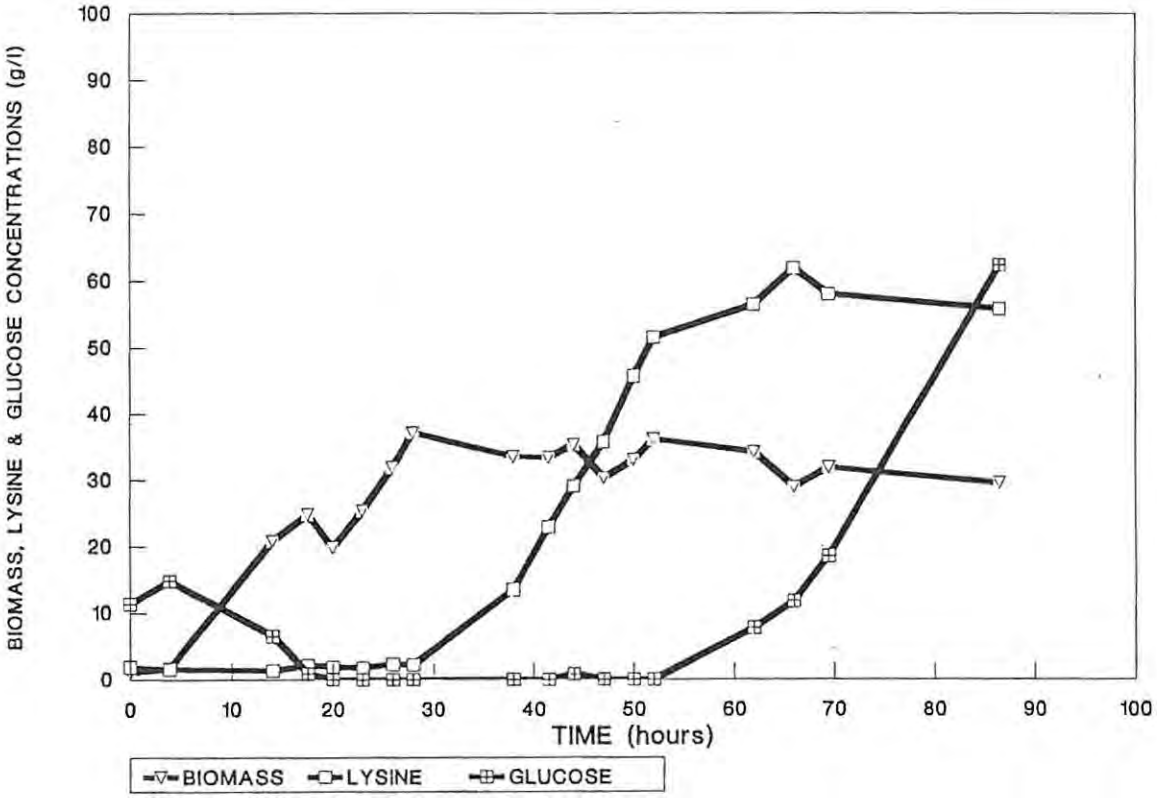

FIGURE 5.20A The change in the concentration of biomass, lysine and glucose during fermentation.

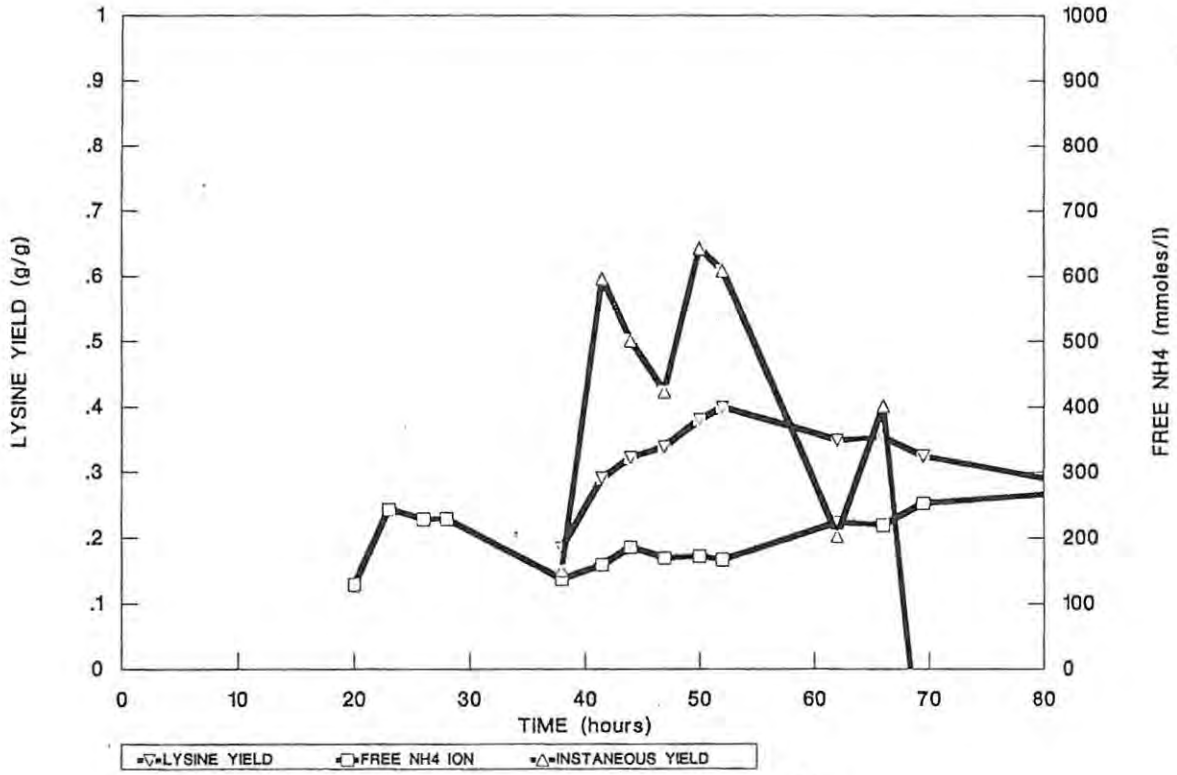

FIGURE 5.20B Change in the lysine yield, the instantaneous yield and the free NH4 concentration taken from the onset of the high glucose feed.

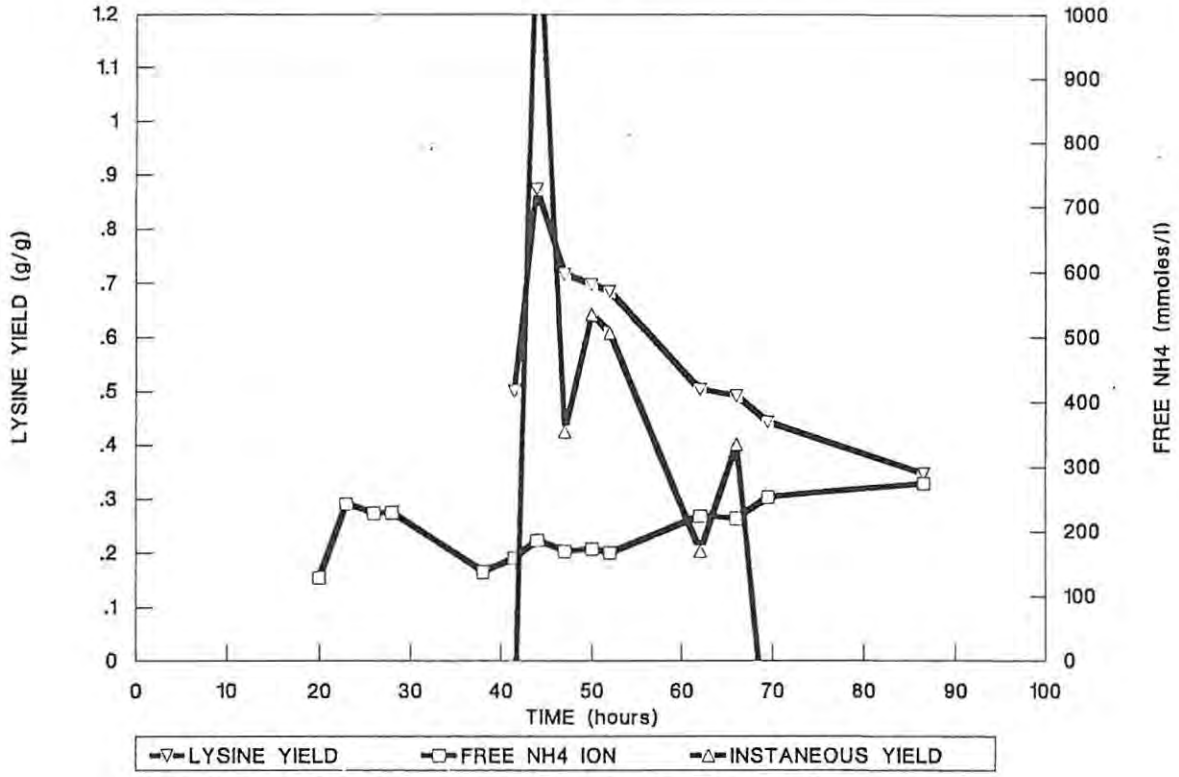

FIGURE 5.20C Change in the lysine yield, the instantaneous yield and the free NH4 concentration taken from the onset of the second base pH control.

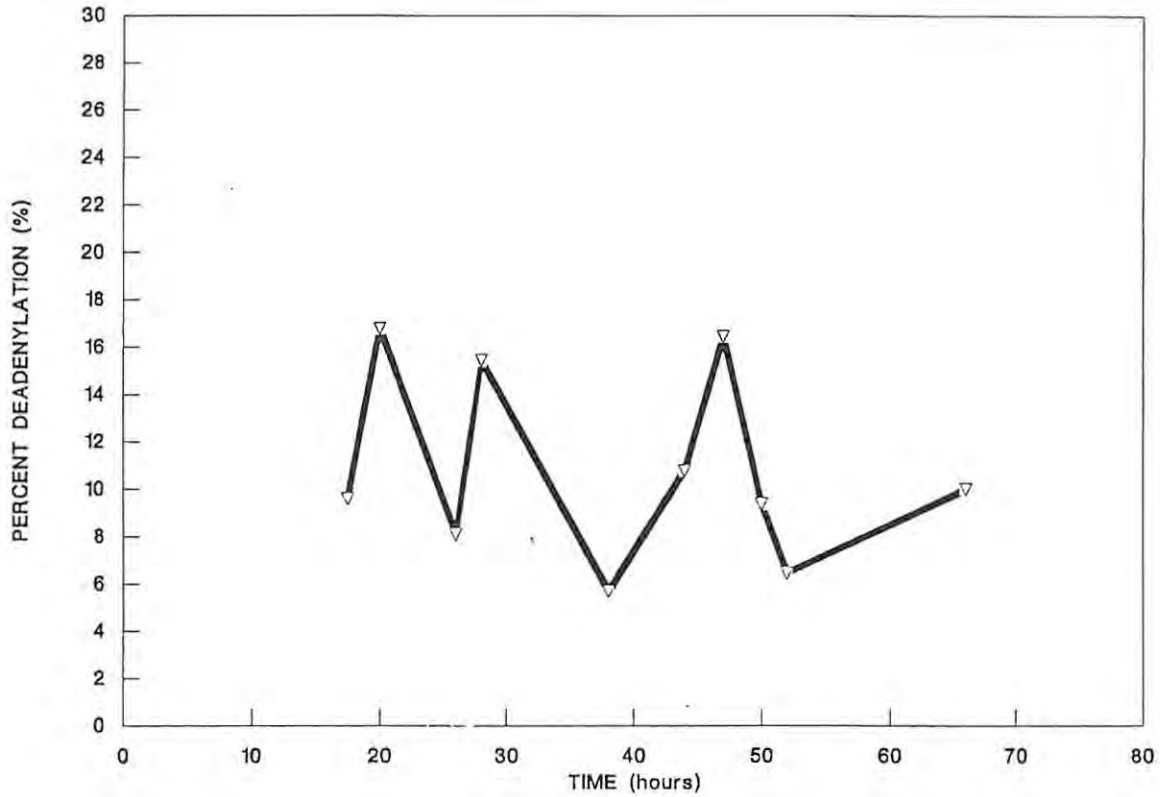

FIGURE 5.20D Change in the percent deadenylation of glutamine synthetase during fermentation.

the phosphate groups of the teichoic acid are the completely filled with lysine. At the start of using the second base this lysine is then eluted off the teichoic acid giving a high instantaneous yield. The overall yield and lysine titre of this fermentation were however low at 0,32g/g and 57,92g/l, respectively. The proline content of this biomass was found to be 7,0% m/m at the end of the fermentation.

FERMENTATION I (Figure 5.21)

Fermentation I was run in the same manner as fermentation H, however the second glucose feed was higher at 9,0g/l/h. Similar results were obtained with high yields ranging between 0,52 and 0,66 being obtained between 41,5 and 51,5 hours (Figure 5.21). The titre in this fermentation was however 73,89g/l. Again there was a gradual reduction in the yield from the start of using the second base. Over this period there is also a concomitant increase in the degree of deadenylation of the glutamine synthetase. The proline content of this biomass was 8,1% m/m at the end of the fermentation. It is believed that the organism is able to control the state of the teichoic acid depending on its nutrient requirements. This would account for the spikes in the lysine yield, via elution of lysine by NH_4^+, and of lysine and NH_4^+, by H^+.

Comparing fermentation H with fermentation I, it appears that during fermentation H the rate of assimilation of glucose and ammonia, in terms of the stoichiometry for lysine synthesis, appear to be equivalent, as there was no accumulation of glucose until the fermentation was 55 hours old. In fermentation I however, there was an accumulation of glucose from as early as 38 hours of fermentation. The proline content of the biomass was however 8,1% m/m compared to 7,0 % m/m in fermentation H. It is conceivable therefore that the stoichiometry for lysine synthesis is based on the concomitant synthesis of glycerol-3-phosphate for teichoic acid provided that the rate of assimilation of ammonia and glucose are balanced. However, if the glucose assimilation rate is greater than the ammonia assimilation rate another compound is produced to balance the nucleotides. This could possibly be proline. As the proline is negatively charged at pH 7,2, this could also act as an intracellular counter-ion to lysine in the same way as has been proposed for glycerol-

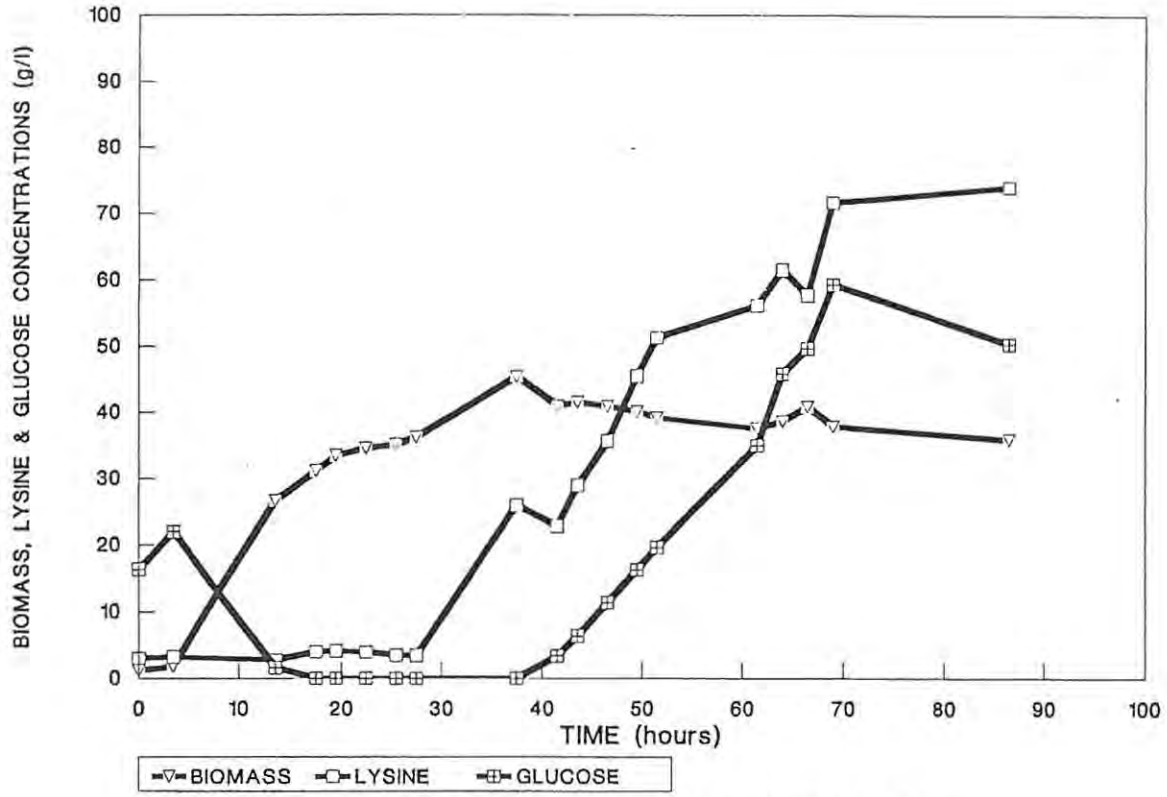

FIGURE 5.21A The change in the concentration of biomass, lysine and glucose during fermentation.

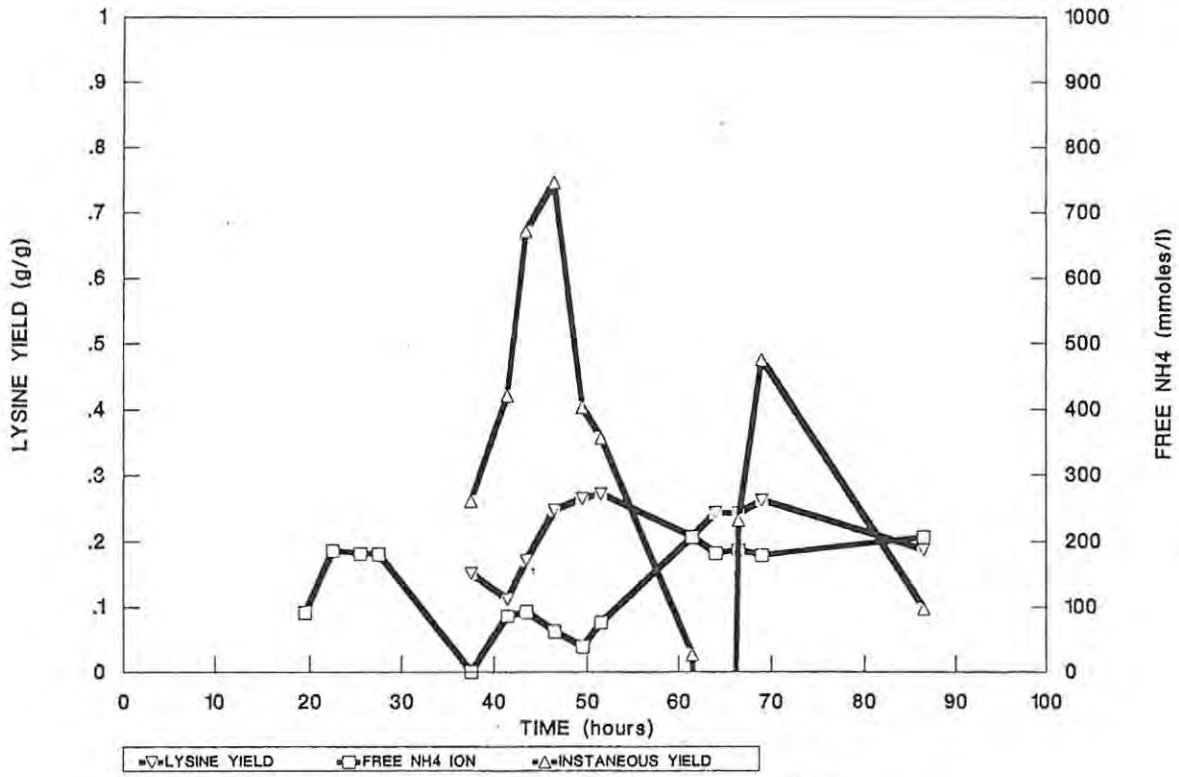

FIGURE 5.21B Change in the lysine yield, the instantaneous yield and the free NH4 concentration taken from the onset of the high glucose feed.

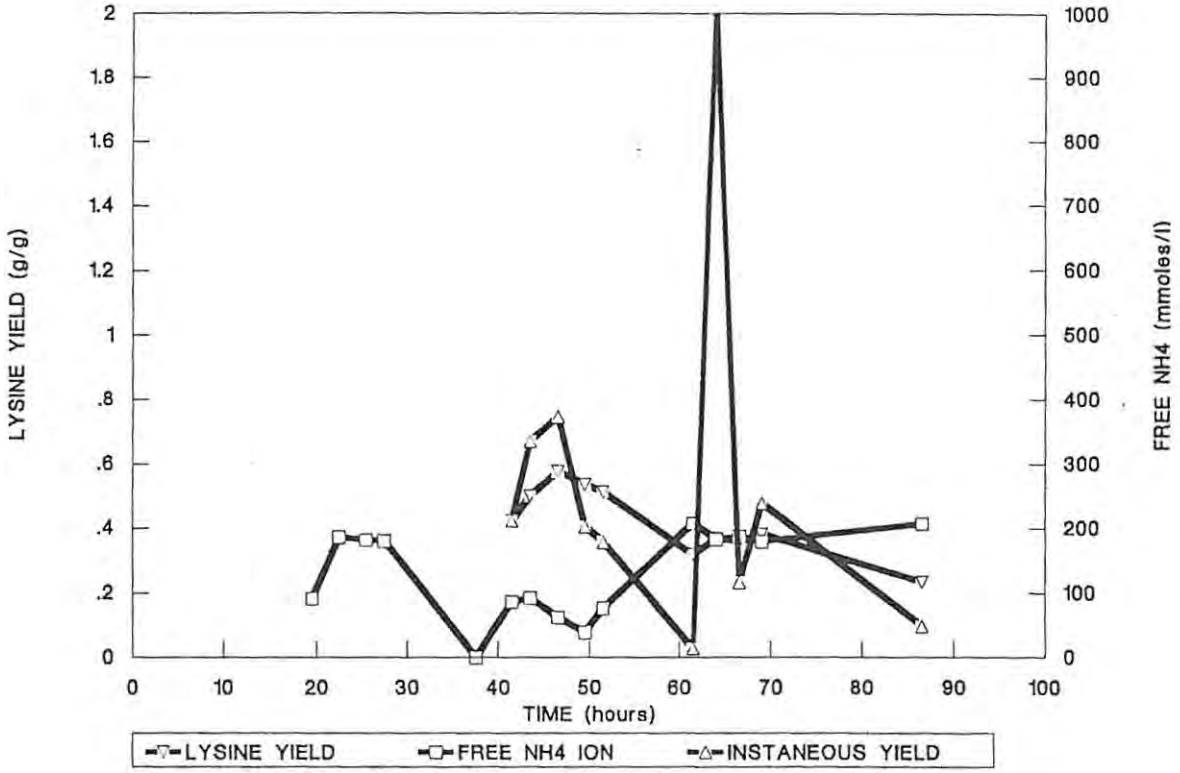

FIGURE 5.21C Change in the lysine yield, the instantaneous yield and the free NH4 concentration taken from the onset of the second base pH control.

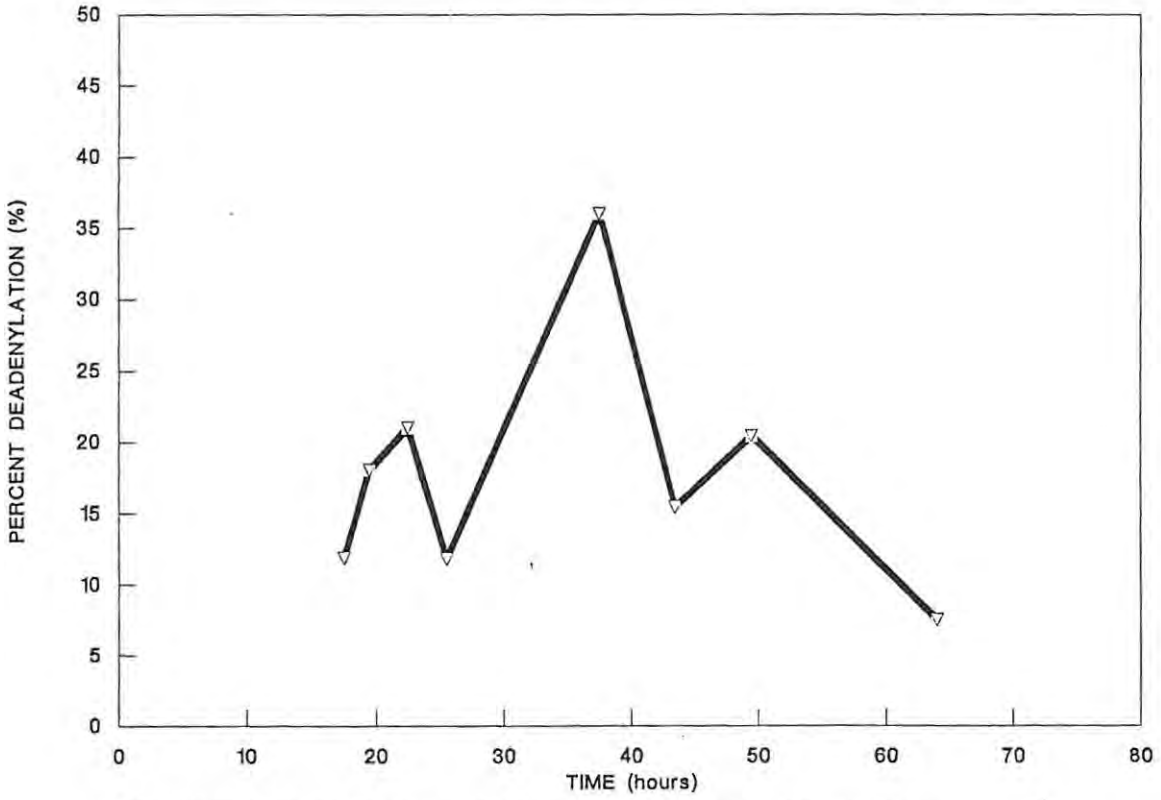

FIGURE 5.21D Change in the percent deadenylation of glutamine synthetase during fermentation.

3-phosphate.

FERMENTATION J (Figure 5.22)

Fermentation J was run in a similar way to fermentation H, however at 54 hours into the fermentation the base for the pH control was changed to contain only NH_4OH to try and extend the time period for which the free NH_4^+ concentration was kept as low as possible (Figure 5.22). This enabled a titre of 79,62g/l at an overall yield of 0,43g/g to be attained for the fermentation. The residual glucose concentration was 115g/l. During the period of high yields the respiratory quotient increased to 3,0 (Figure 5.22 D). This is in keeping with the theoretical mass balance (Chapter 4, Section 4.4.3.3).

5.4.3 The utilization of amino acids during fermentation

The utilization of the amino acids which result from the addition of the yeast extract to the culture media was determined for fermentations H and I (section 5.4.2). In both fermentations the threonine and methionine had been depleted by the end of the replication phase (Figures 5.23 and 5.24). It is also interesting to note that threonine, serine, methionine, and aspartate are all depleted prior to lysine synthesis and all these amino acids produce NH_4^+ in their pathway of entry into the TCA cycle (Table 5.1). Alanine and glycine which also produce NH_4^+ are however not depleted. Alanine could arise from the synthesis of lysine as it is the product of the transamination of pyruvate by glutamate to produce alanine and α-ketoglutarate via glutamate pyruvate transaminase. As glycine may be synthesized from pyruvate, it is feasible that a change during the fermentation causing an accumulation of pyruvate, by deviating carbon flux away from oxaloacetate, would result in the synthesis of glycine and/or alanine.

5.4.4 Phosphate utilization during fermentation

The utilization of phosphate during fermentation to produce lysine is shown in Figure 5.25. A major proportion of the phosphate assimilation occurs during the growth phase with a reduction in the rate of

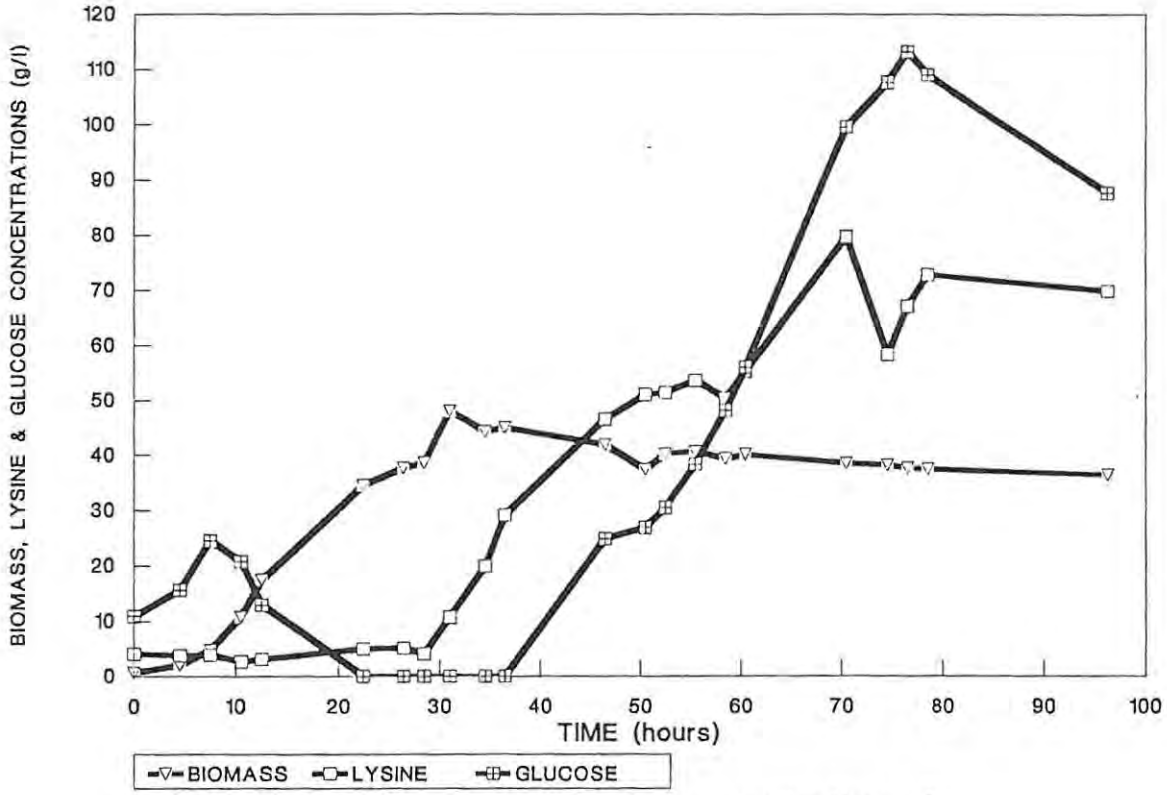

FIGURE 5.22A The change in the concentration of biomass, lysine and glucose during fermentation.

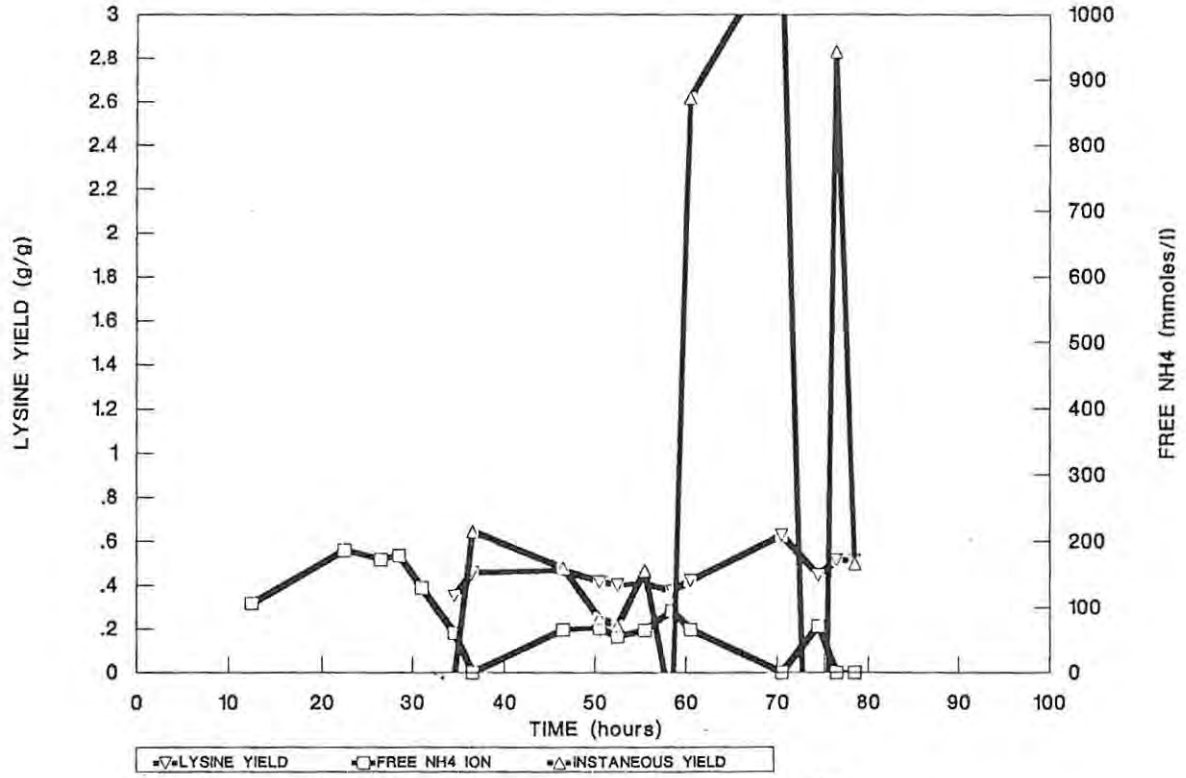

FIGURE 5.22B Change in the lysine yield, the instantaneous yield and the free NH4 concentration taken from the onset of the high glucose feed.

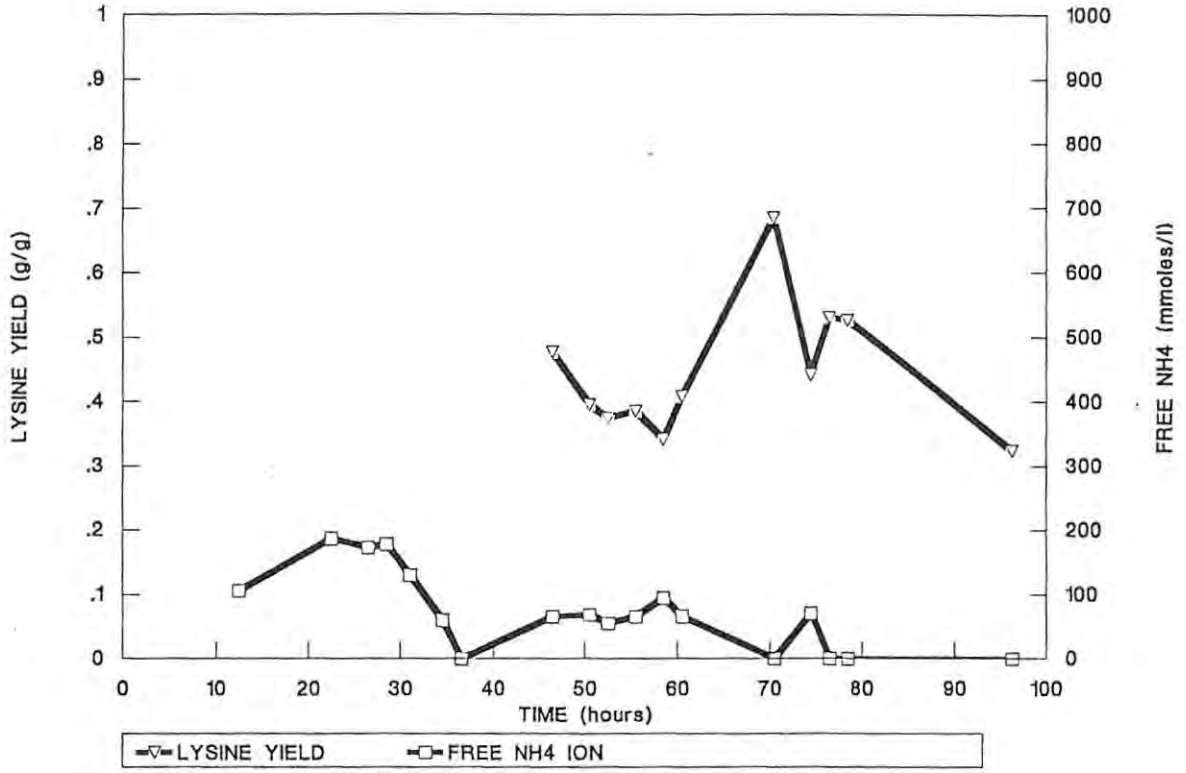

FIGURE 5.22C Change in the lysine yield, the instantaneous yield and the free NH4 concentration taken from the onset of the second base pH control.

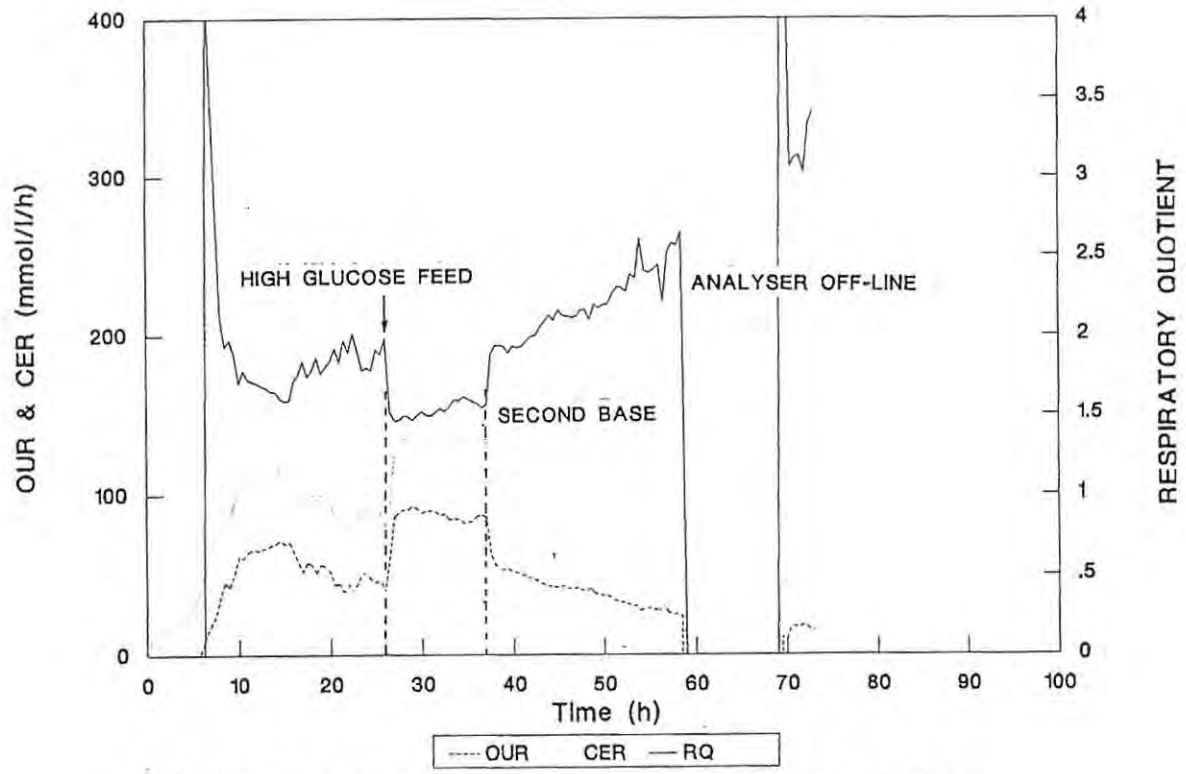

FIGURE 5.22D The change in the oxygen utilization rate, carbon dioxide evolution rate and the respiratory quotient during fermentation.

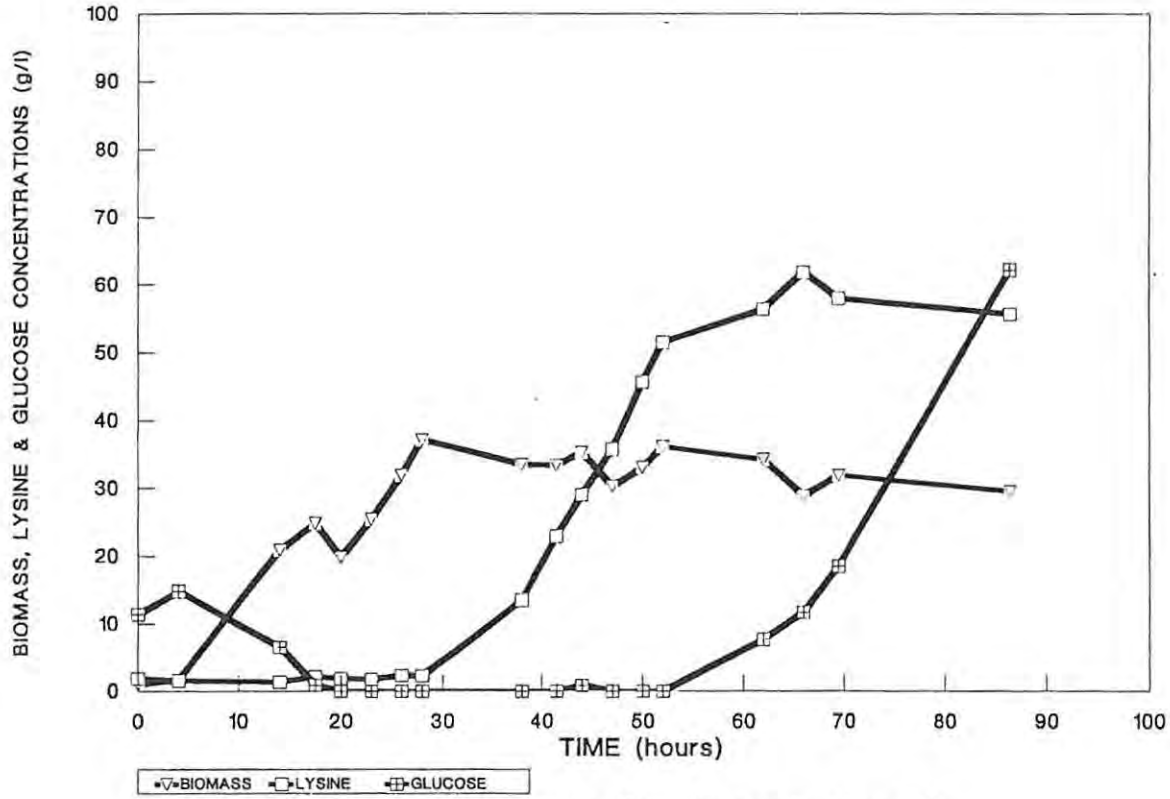

FIGURE 5.23A The change in the concentration of biomass, lysine and glucose during fermentation.

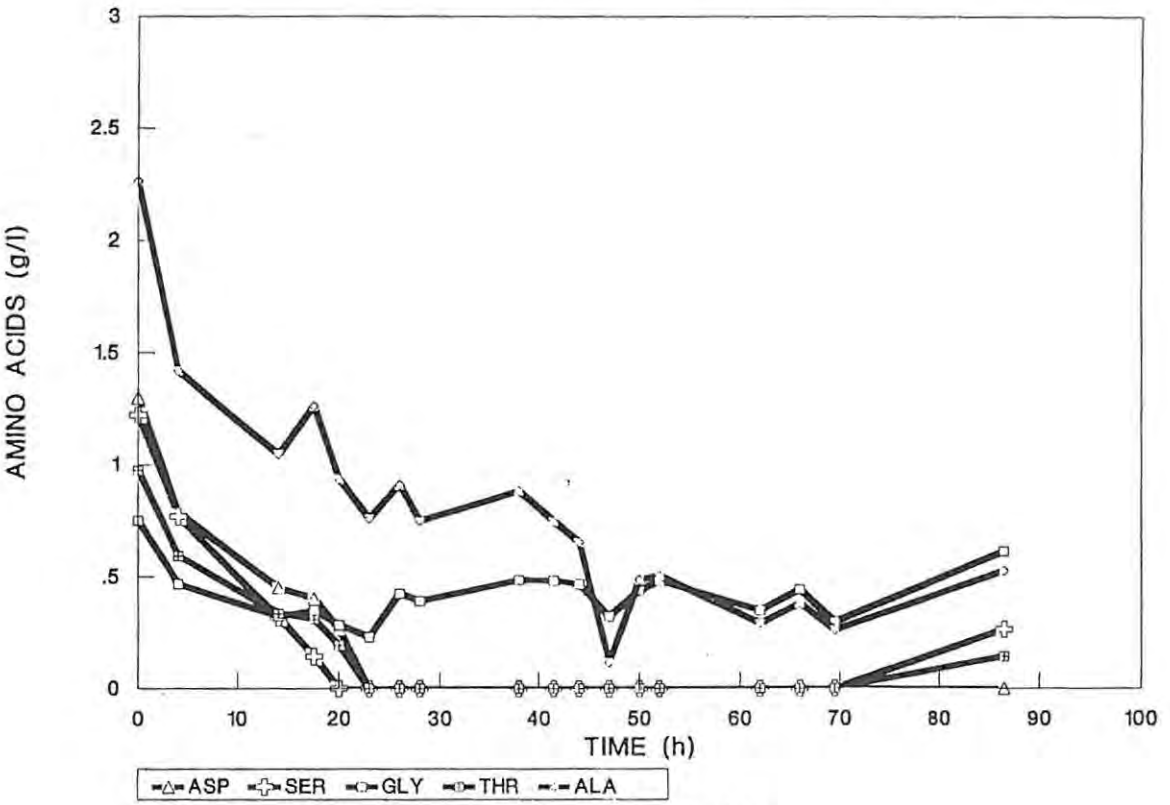

FIGURE 5.23B Amino acid profile during fermentation H.

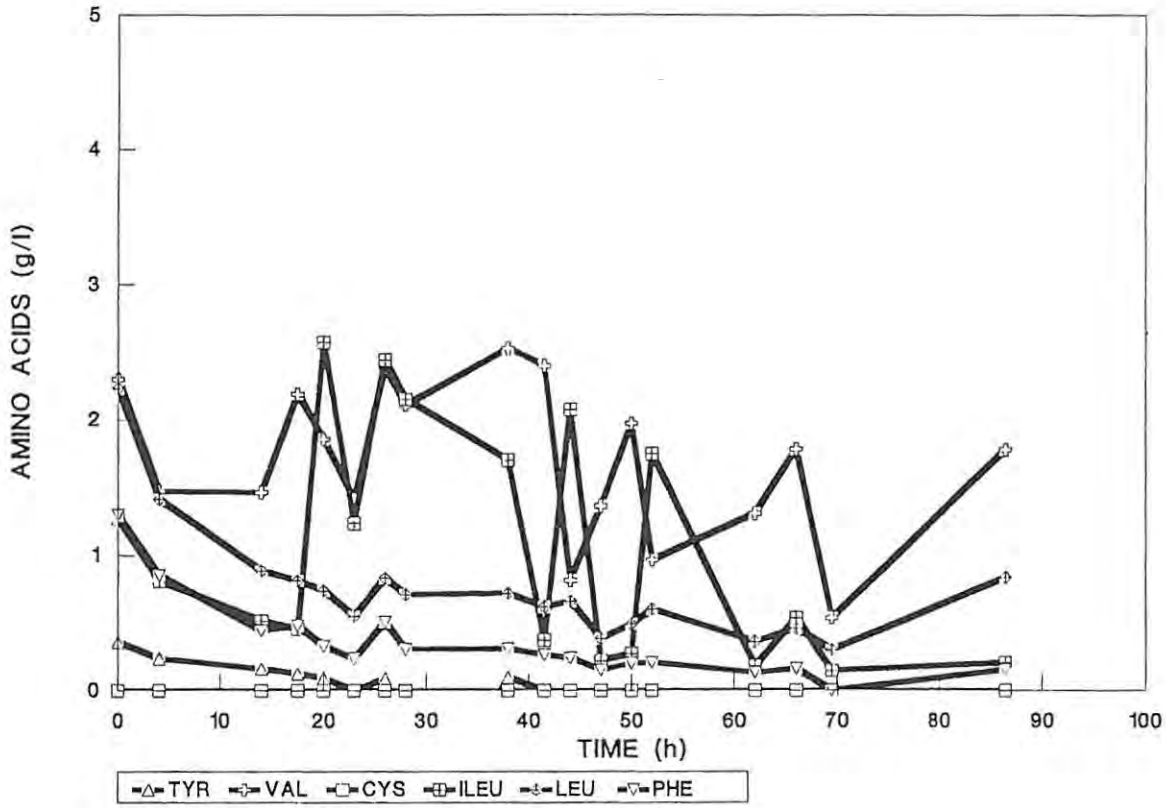

FIGURE 5.23C Amino acid profile during fementatlon H.

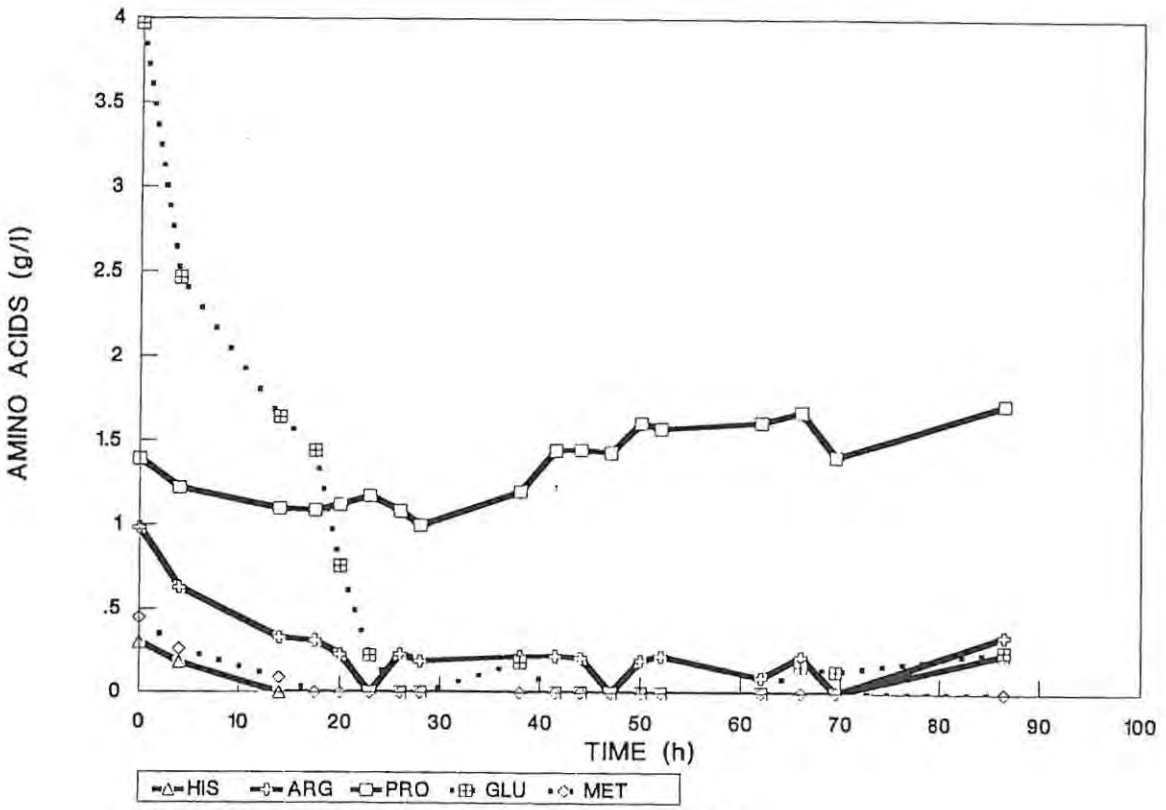

FIGURE 5.23D Amino acid profile during fermentation H.

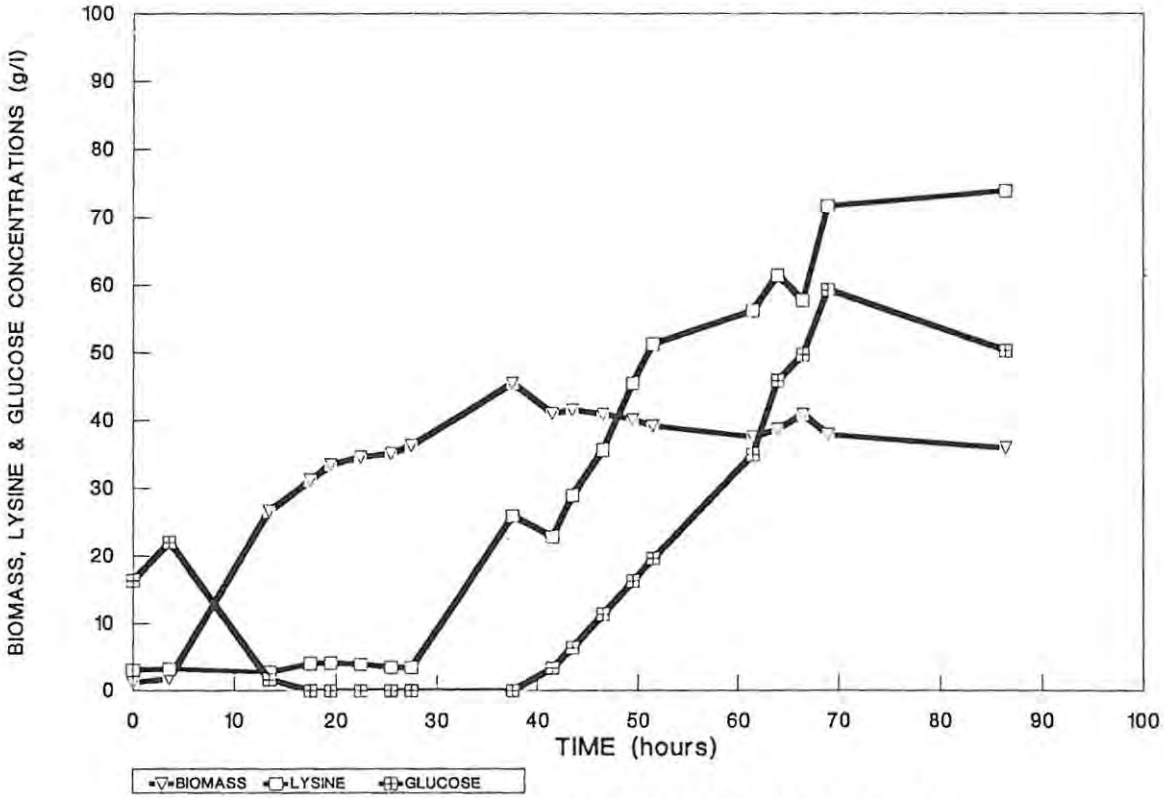

FIGURE 5.24A The change in the concentration of biomass, lysine and glucose during fermentation.

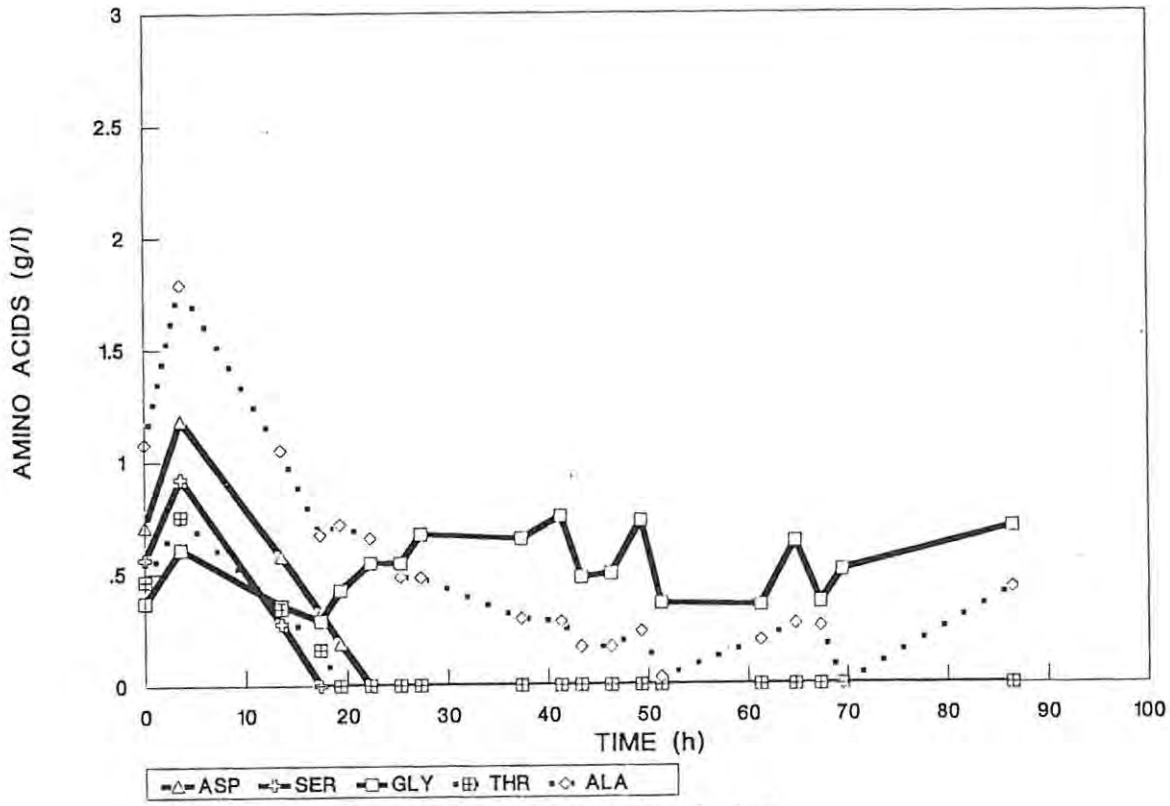

FIGURE 5.24B Amino acid profile during fermentation I.

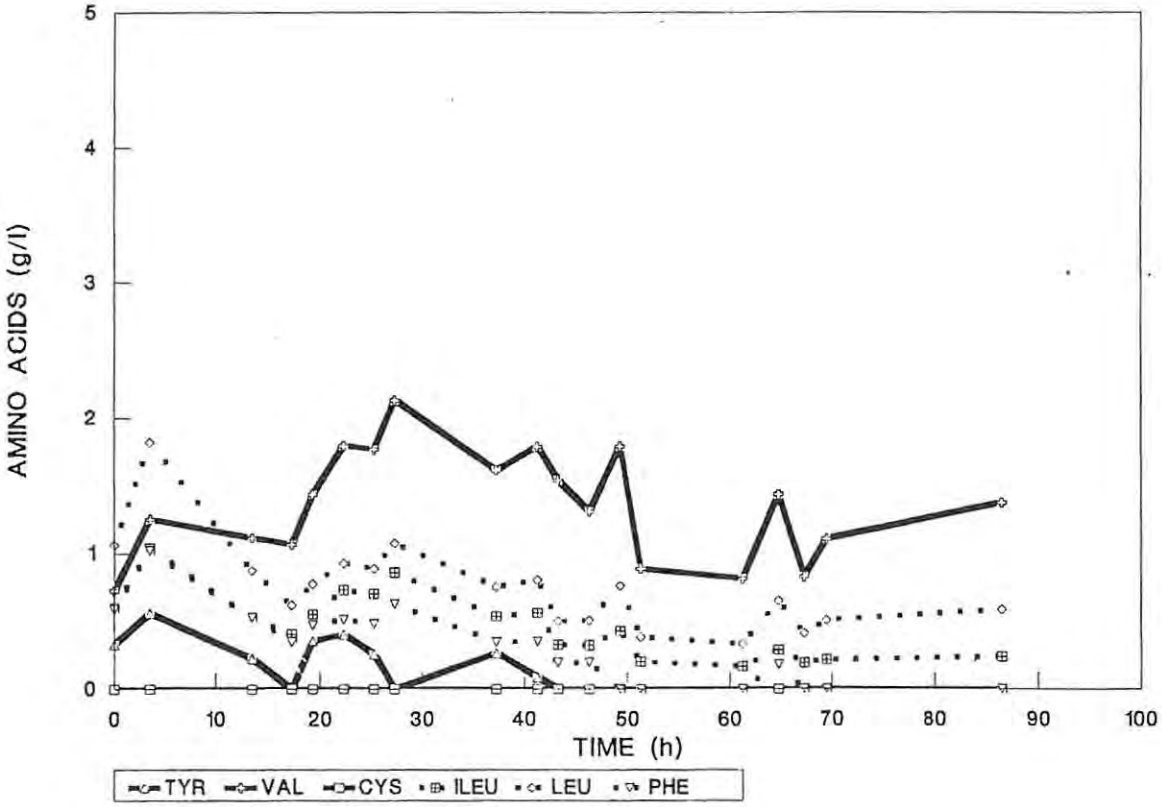

FIGURE 5.24C Amino acid profile during fermentation I.

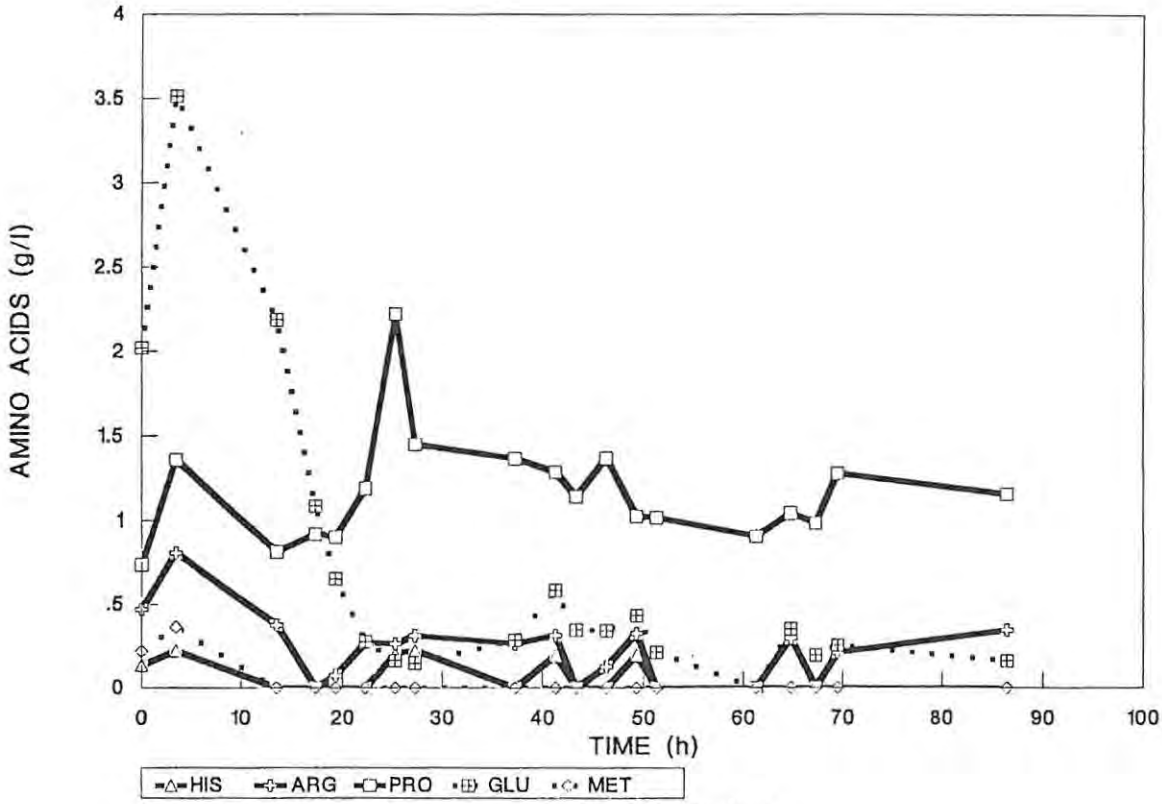

FIGURE 5.24D Amino acid profile during fermentation I.

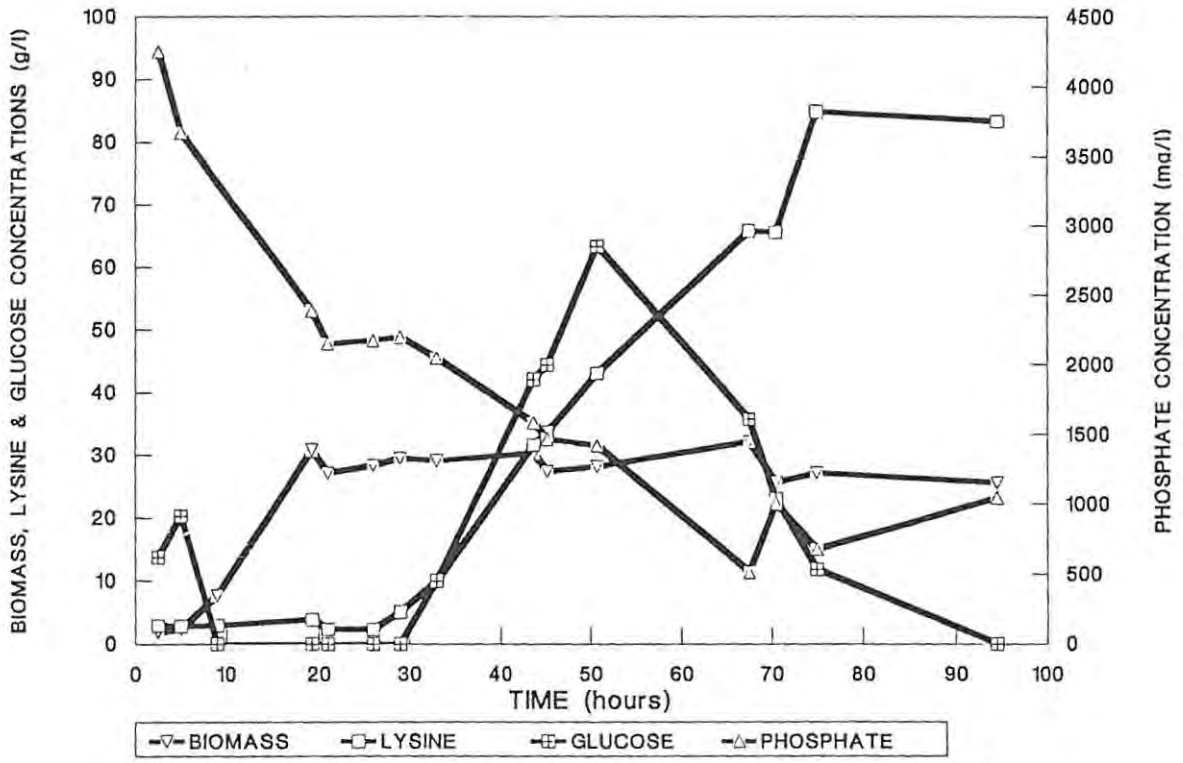

FIGURE 5.25 The change in the concentration of the biomass, lysine, phosphate and glucose during fermentation.

assimilation towards the end of growth. However once lysine synthesis is initiated the assimilation of phosphate continues. This is possibly as a result of the synthesis of glycerol teichoic acid. The assimilation of phosphate and the synthesis of lysine appear to occur simultaneously.

5.5 CONCLUSION

The assimilation of ammonia by *Corynebacterium glutamicum* for the synthesis of lysine occurs by two mechanisms - the low affinity glutamate dehydrogenase and the high affinity glutamine synthetase. The activity of the glutamate dehydrogenase in cell free extract appears to be dependent on the ammonium salt used. At low concentrations the NH_4^+ appears to further dissociate to NH_3 and H^+. The glutamate dehydrogenase cannot use the NH_3 as a substrate, and in the case of $(NH_4)_2SO_4$ where the proton does not re-associate with the anion, as in NH_4Cl and $(NH_4)_2HPO_4$, the proton appears to act as a noncompetitive inhibitor of the enzyme.

The glutamine synthetase of *Corynebacterium glutamicum* appears to be similar to that of *Streptomyces coelicolor*, in that the control occurs via modification similar to the adenylation which is found in enteric organisms (Fisher and Wray, 1989) and not by the mechanism employed by other Gram-positive bacteria such as *Bacillus* (Fisher and Sonenshein, 1991).

The assimilation of glucose and ammonia for the purpose of lysine synthesis appears to linked. The control of the uptake of the ammonia at high free NH_4^+ concentrations is possibly via a complex ion-exchange type reaction, mediated through the teichoic acid in the cell wall and then transported into the cell through an NH_4^+/K^+ antiport active transport system (Figure 5.26). At low free NH_4^+ concentrations, the sites on the teichoic acid are probably filled with lysine or H^+, however as the NH_4^+ is dissociated to NH_3 and H^+, the NH_3 diffuses into the cell and is then assimilated by the glutamine synthetase. Lysine yields of the order of 0,66 are then attainable during the course of ammonia limited fermentations. It is postulated that a futile cycle exists during the glutamate dehydrogenase assimilation of NH_4^+. Once the NH_4^+ has been actively taken up by the cell it dissociates intracellularly allowing the

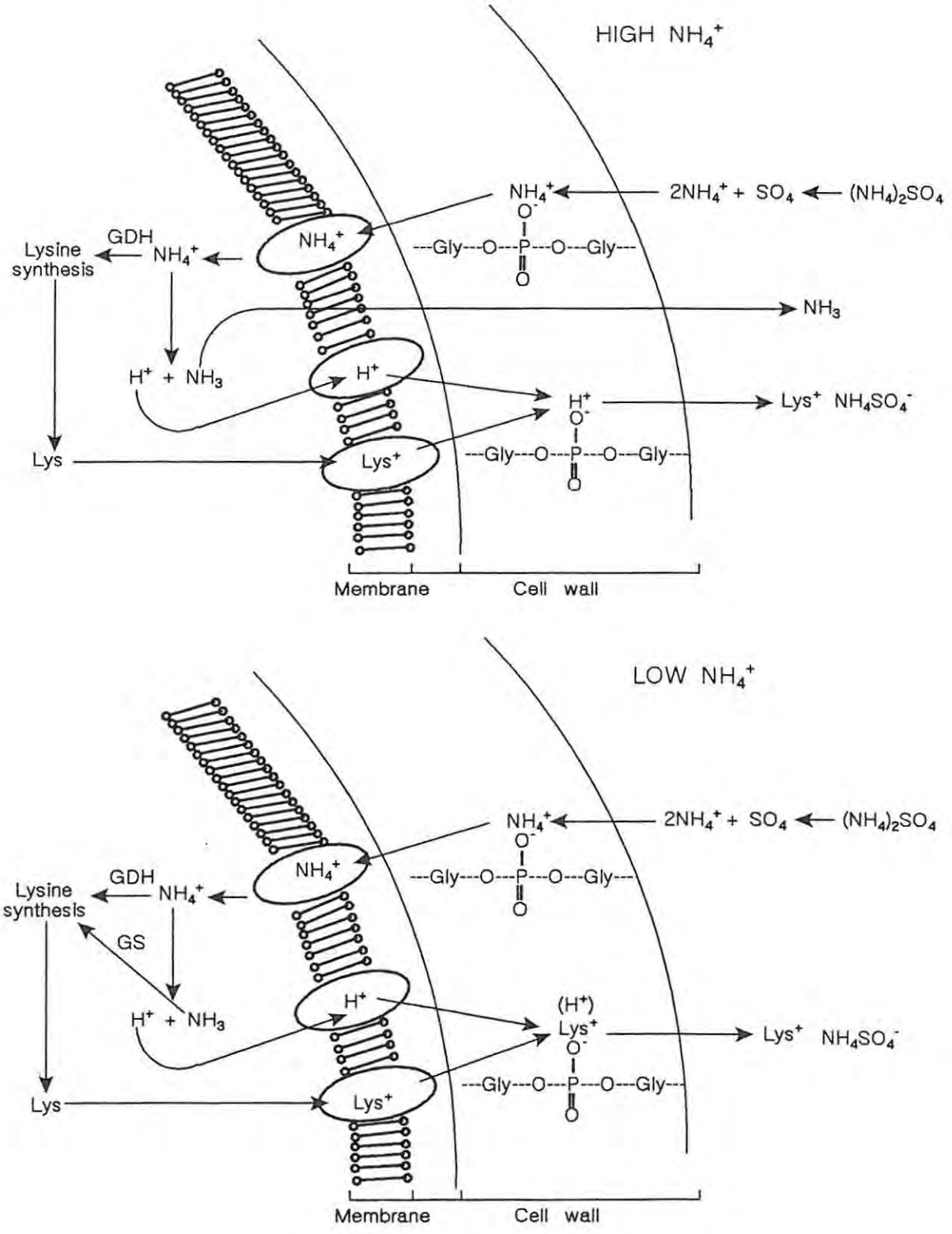

FIGURE 5.26 The effect of the free NH_4^+ concentration on lysine synthesis and subsequent transfer to the culture media.

NH_3 to freely diffuse out of the cell. The cell then wastes energy having to re-transport the NH_4^+ and this is manifested as a low yield and instantaneous yield throughout the fermentation as is obtained in fermentations containing $(NH_4)_2SO_4$ in the initial charge. In fermentations where the free NH_4^+ concentration is allowed to decrease, high yields are sustainable for long periods during the maturation phase. There is also a concomitant increase in the degree of deadenylation in these fermentations.

If the rates of assimilation of NH_4^+ and glucose are balanced in terms of the stoichiometry for lysine synthesis, high yields are obtained when the fermentations are run under NH_4^+ limitation, however there is a reduction in the titre. To attain higher titres it appears that an imbalance in the glucose utilization rate and the NH_4^+ assimilation rate is required. To counter the nucleotide imbalance which possibly occurs another molecule or molecules are possibly produced. The molecule could be proline.

CHAPTER 6

GENERAL DISCUSSION

6.1 GENERAL DISCUSSION

The synthesis of L-lysine by *Corynebacterium glutamicum* FP6 appears to be coupled to the physiology of cell wall synthesis and more specifically the synthesis of glycerol-3-phosphate as the polymer glycerol teichoic acid. A theoretical molecular balance during the lysine synthesis stage is therefore proposed to be as follows:

$$3\ C_6H_{12}O_6 + HPO_4^- + 2\ NH_4^+ + O_2 + 2NH_3 \rightarrow 2\ C_6H_{15}O_2N_2^+ + 3\ CO_2 + [C_3H_7O_5P]_n + 9\ H_2O$$

where n = 1.

The glycerol-3-phosphate is laid down in the cell wall as the polymer glycerol teichoic acid. Due to the highly acidic nature of the glycerol-3-phosphate it will require a counter-ion intra-cellularly. It is proposed that during the "normal" growth of wild type strains of *Corynebacterium glutamicum* this material is synthesised and other metabolites such as amino acids act as the counter-ion. It is reasonable to assume that the amount of teichoic required in the cell wall of a "complete" cell is fixed. The stoichiometry of the synthesis of all these metabolites and their interactions is therefore very strict. However, as a result of the selection of the auxotrophic requirements in this strain, namely threonine, methionine and leucine, the cells are unable to complete the normal synthesis of all the teichoic acid required for completion of the cell wall. If an optimal glucose feed rate is maintained during the replication phase it appears that very little additional biomass (possibly glycerol teichoic acid) is laid down during this phase. If an "excess" of glucose is fed during this phase, the cell cycle is completed prematurely, via the synthesis of other amino acids as counter-ions, with a concomitant reduction in the lysine produced. Part of the problem resulting from the threonine requirement of the organism, is that threonine inhibits lysine synthesis during the replication phase via concerted feedback inhibition of the aspartokinase enzyme. As the optimal feed rate prevents the deposition of teichoic acid during the replication phase, this manifests itself in the mutant strain as two distinct phases, which have been termed the replication phase and the maturation phase. As the organism appears to be unable to complete the synthesis of the cell wall during the replication phase, possibly due to

190/...

the lack of counter-ions for the glycerol-3-phosphate, synthesis of the teichoic acid is minimised. As soon as the threonine has been depleted lysine synthesis can occur, enabling the continued synthesis of the teichoic acid.

However the overall picture appears to be more complex than this during the maturation phase or lysine synthesis stage. Concomitant with the uptake of glucose and the synthesis of lysine and glycerol-3-phosphate is the assimilation of ammonia required for the lysine synthesis. Two distinct mechanisms exist for the assimilation of NH_4^+; the low affinity system mediated through glutamate dehydrogenase and the high affinity system mediated through glutamine synthetase. Both systems exist in *Corynebacterium glutamicum*. Preliminary findings outlined in Chapter 5 would indicate that the glutamine synthetase enzyme is similar to that of the enteric bacteria rather than that of *Bacillus sp*, with the enzyme being modified possibly by adenylation. This has been found to be the case in other Gram-positive bacteria such as *Streptomyces coelicolor* (Fisher and Wray, 1989). The cladistics of these two groups of organisms would indicate that this should be the case relative to the Clostridial (bacillus) lineage, as the Gram-positive bacteria have been separated into two separate lines of descent (Woese, 1987). Using dissociation theory (Chapter 5) it was shown that at the concentrations of the K_m values of the respective enzymes for their ammonium substrate, the glutamate dehydrogenase uses NH_4^+ as its substrate and glutamine synthetase uses NH_3 as its substrate.

It was believed that having a high and low affinity mechanism to assimilate ammonia could be exploited to improve the lysine yield of the fermentation by running the fermentation using only the high affinity mechanism. It appeared that during fermentation the rate of lysine synthesis was affected by the free NH_4^+ concentration. The data on the dissociation of various ammonium salts indicated that at very low concentrations the NH_4^+ actually further dissociated to NH_3 and H^+ (Chapter 2). If under these conditions the glutamine synthetase was in fact not functional or only partially active, the NH_3 would be lost from the cell by diffusion. As energy is required for NH_4^+ transport, the possibility of a futile cycle, which consumes energy to re-transport the

NH_4^+, could therefore exist.

The efficiency of lysine synthesis during the maturation phase was shown to be dependent on the glucose utilised during the replication phase (Chapter 4). A reduction in the lysine yield occurred when the quantity of glucose utilised during the replication phase exceeded a specific threshold. It appeared that the cells were capable of completing a greater proportion of their cell cycle, using a counter-ion other than lysine during this replication phase. As less glycerol-3-phosphate was required to complete the cell cycle, less lysine synthesis was required to complete the nucleotide balance of the cell. As threonine is required for cell replication, the cycle could not be re-initiated. For optimal lysine synthesis therefore, the replication phase has to be effectively separated from the maturation phase with minimal teichoic acid synthesis during the replication phase.

For the synthesis of lysine and teichoic acid a range of reactions have to be balanced (Figure 6.1). The rate of assimilation of ammonia has to be balanced with the rate of synthesis of lysine, which is dependent on whether glutamate dehydrogenase or glutamate synthetase is being used to assimilate the ammonia. If the glucose uptake rate is greater than the ammonia assimilation rate at high NH_4^+ concentrations, it appears that a counter-ion other than lysine is produced. This is possibly alanine, which allows the cell to complete the cell cycle "early". If glucose transport is limiting, the cell responds by taking up additional phosphate for its needs. However under glucose limitation, where the NH_4^+ assimilation rate is greater than the carbon assimilation rate, the cells appear to produce proline, a negatively charged amino acid, to counter the charge from the synthesis of lysine. At low NH_4^+ concentrations similar effects to those under conditions of excess glucose may be seen. Even though high instantaneous yields may be attainable, the overall yield is reduced as a result of the cell having to counter the synthesis of glycerol-3-phosphate by the synthesis of another amino acid. Where the ammonia assimilation rate is greater than the glucose utilization rate proline is produced. If these rates are all balanced, yields of approximately 0,66g/g are attainable. This is believed to be the theoretical maximum yield of lysine on glucose utilised during lysine

192/...

KINETIC CONTROL MODEL OF L-LYSINE SYNTHESIS

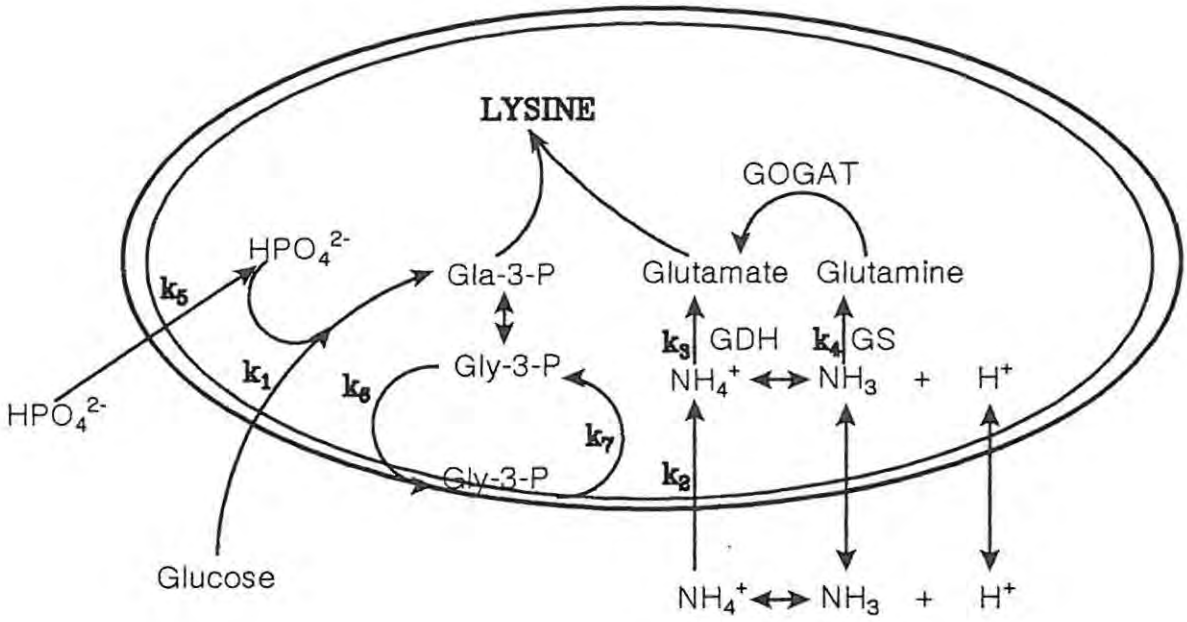

$k_1 > k_3$	Yield reduced and titre reduced as cell completes cycle early. ($k_6 > k_7$ completing the cell cycle)
$k_1 = k_3$	Yield is constant and the titre high.
$k_1 < k_3$	HPO_4^- uptake will increase.
$k_1 < k_4$	HPO_4^- uptake will increase.
$k_1 > k_4$	Yield reduced and titre reduced as cell completes cycle early. ($k_6 > k_7$ completing the cell cycle)
$k_1 = k_4$	Yield is constant however greater than $k_1 = k_3$ due to the lower afinity constant of GS.

Gly-3-P = sn-Glycerol-3-phosphate
Gla-3-P = Glyceraldehyde-3-phosphate
GDH = Glutamate dehydrogenase
GS = Glutamine synthetase
GOGAT = Glutamate synthase

FIGURE 6.1 The model for lysine synthesis.

synthesis. However, if the NH_4^+ assimilation is greater than the glucose utilization rate, proline may be produced to balance the nucleotides, maintaining the yield to 0,66g/g. However, the titre is increased, as more lysine can be produced per mole of teichoic acid laid down in the cell wall.

The assimilation of ammonia does not appear to be as simple as merely running the fermentation at high and low free NH_4^+ concentrations. It is postulated that the teichoic acid in the cell wall acts as an ion-exchange polymer in the selective uptake of NH_4^+ and the export of lysine from the cell (Figure 6.2). The driving force behind the flux of NH_4^+ into the cell appears to be concentration. As the NH_4^+ is assimilated from the periplasmic space by the transport system, it causes the NH_4^+ to continuously move across the cell wall. Acting counter current to this is the accumulation of lysine in the periplasmic space. It is proposed that the lysine is actively transported across the cell membrane, setting up a concentration gradient. There is therefore a counter-current flow of lysine and NH_4^+ across the cell wall. The free NH_4^+ concentration which is perceived within the cell periplasmic space is therefore dependent on the concentration gradient across the cell wall, and also the rate of lysine synthesis, as the lysine fills NH_4^+ binding sites on the teichoic acid. If a high concentration of NH_4^+ is maintained in the periplasmic space, the NH_4^+ is assimilated via glutamate dehydrogenase. Due to the low affinity of this enzyme for its substrate, some dissociation of the NH_4^+ occurs allowing the NH_3 to diffuse out of the cell thereby wasting energy and therefore glucose which could be used for lysine synthesis. However, if the concentration of the NH_4^+ in the periplasmic space is allowed to drop below a "critical" level as a result of the low concentration gradient across the cell wall, the high affinity glutamine synthetase takes over. If the cells are starved of ammonia there appears to be an immediate uptake of NH_4^+ once the ammonia source is reinstated. This uptake is possibly only onto the teichoic acid. Setting up the NH_4^+ gradient then takes time which is seen in the gradual reduction in the lysine yield as a result of the NH_4^+ assimilation changing from the glutamine synthetase back to glutamate dehydrogenase. The fact that the NH_4^+ flux across the cell wall works against the flow of lysine complicates the reinstatement of the concentration gradient. As high

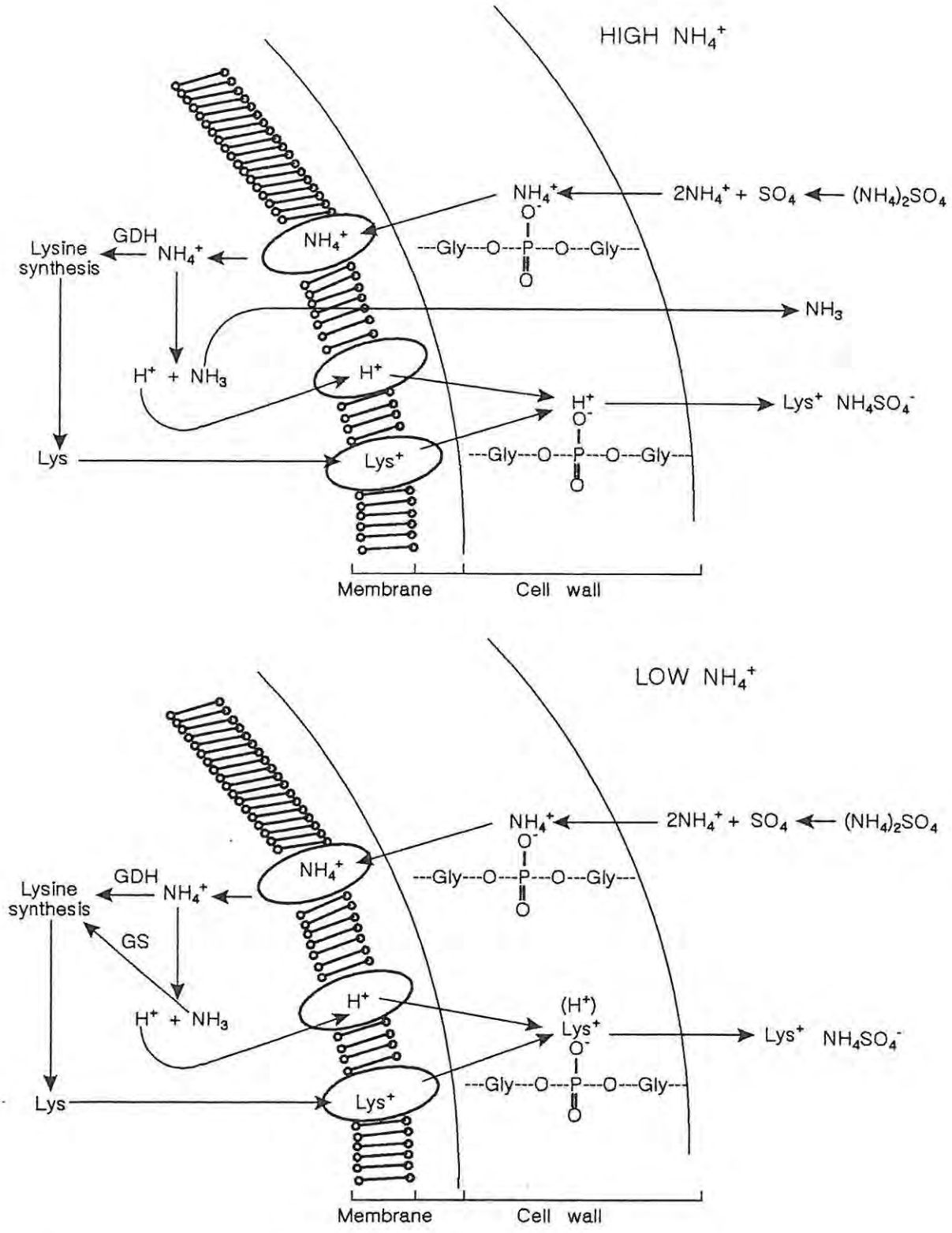

FIGURE 6.2 The effect of the free NH_4^+ concentration on lysine synthesis and subsequent transfer to the culture media.

instantaneous yields are attainable during lysine synthesis upon reinstatement of the $(NH_4)_2SO_4$ supply, these possibly result from the cell being able to control the chemistry of absorption on and elution off the teichoic acid. This may be mediated via the efflux of H^+ from the cell in antiport to NH_4^+. The H^+ then displaces the lysine from the teichoic acid. In fermentations where the free NH_4^+ concentration was allowed to decrease over a long period of time it is believed that all the sites on the teichoic acid would eventually be filled with either lysine or H^+.

When assessing the metabolic flux distribution within the cell, two scenarios may exist depending on whether the organism is assimilating ammonia via the high affinity system or the low affinity system. A continuum of differing flux distribution may exist between the two systems depending on the degree of adenylation of the glutamine synthetase. Therefore under specifically controlled conditions of ammonia and glucose assimilation it is postulated that specific metabolic flux characteristic of that set of conditions will be obtained. This can be seen in the range of lysine yields and instantaneous lysine yields that are obtained depending on the availability of the NH_4^+ in the culture media.

This physiology must, however, be controlled genetically. As the biochemistry of the glutamine synthetase appears to be similar to that of the enteric bacteria, the genetic control will be assumed to be similar to that of *Escherichia coli*. The model of the genetic control is outlined in Figure 6.3. During the growth phase there is repression of the synthesis of the glutamine synthetase structural gene, both as a result of the high NH_4^+ concentration and as a result of the low levels of the cAMP-CAP due to the high levels of glucose. Under conditions of excess glucose the synthesis of the glutamine synthetase structural protein and the ammonium transport protein is not induced if amino acids which form NH_4^+ are present. Under conditions of glucose limitation alone, induction occurs via the cAMP-CAP complex only. When the concentrations of glucose and the amino acids forming NH_4^+ are low there is moderate induction of the glutamine synthetase mediated from the *glnL* and *glnG* gene products. However if the NH_4^+ and the glucose assimilation

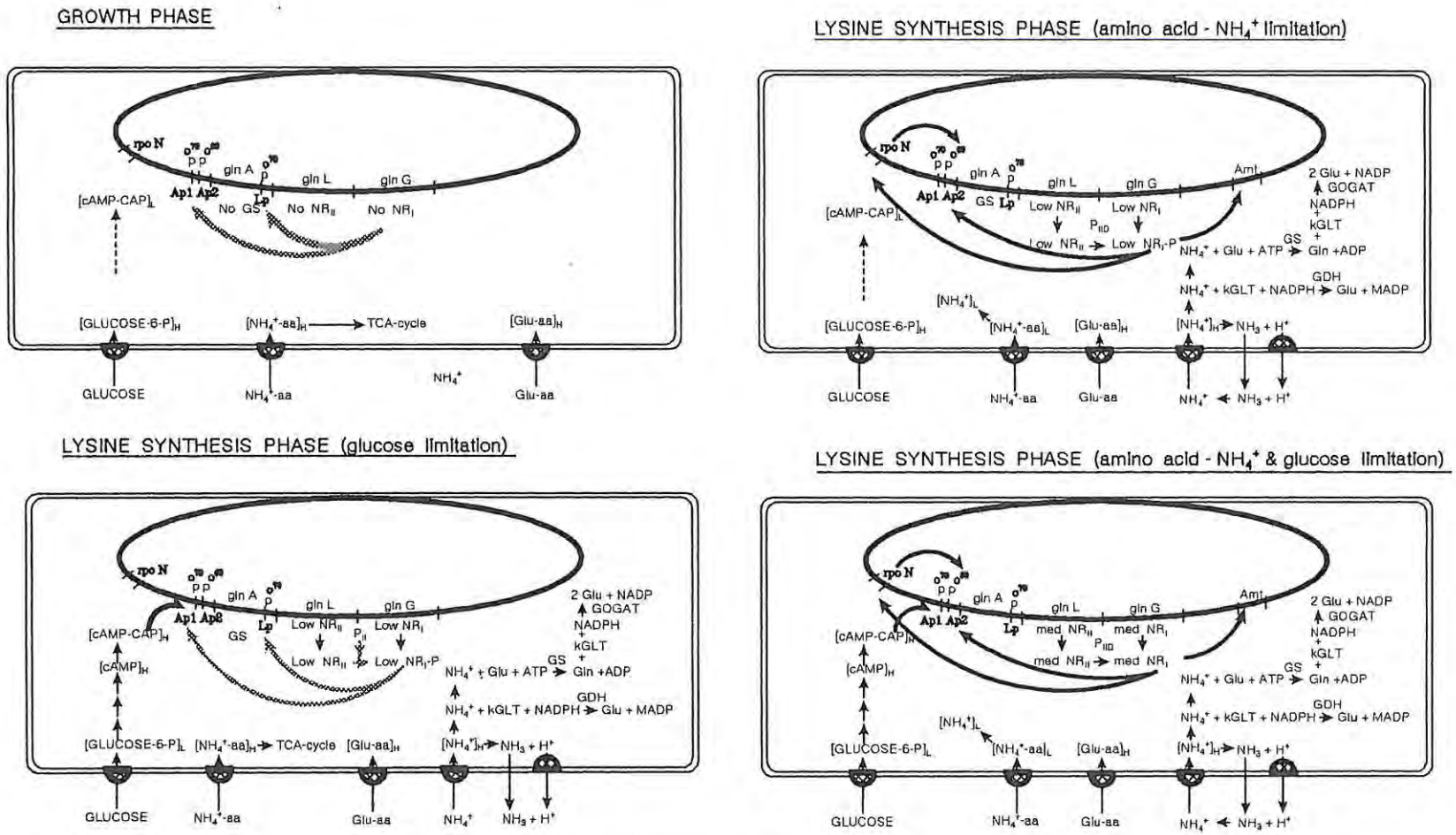

FIGURE 6.3 Model of the induction of glutamine synthetase at various concentrations of NH_4^+ and glucose.

is well regulated there is complete induction of the glutamine synthetase (Figure 6.4).

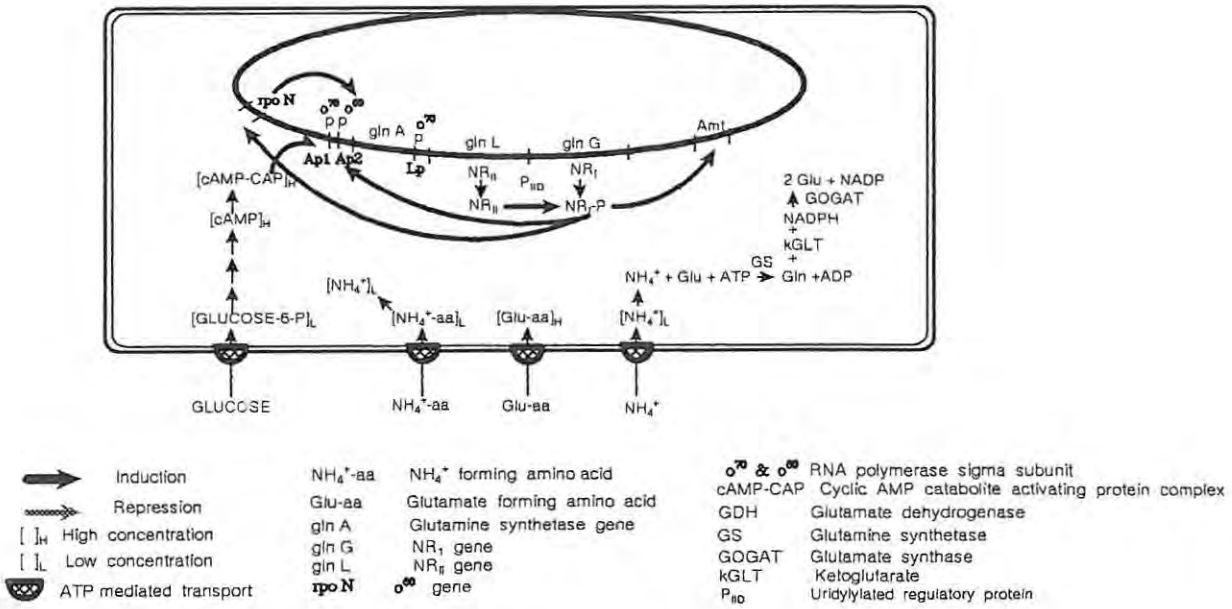

FIGURE 6.4 Model of the induction of glutamine synthetase under conditions of NH_4^+ and glucose limitation.

If this system or a similar system does exist in *Corynebacterium glutamicum* it is believed that it is not only essential to exploit the physiological consequences of using the high affinity glutamine synthetase for maximum lysine yield but also to ensure that as much genetic material as possible has been induced to maximise the productivity of lysine.

4. REFERENCES

Aida, K. (1986). In: "Biotechnology of Amino Acid Production". Aida, K., Chibata, I., Nakayama, K., Takinami, K. and H. Yamada (eds.), *Progress in Industrial Microbiology*, **24**. Kadansha Ltd., Tokyo.

Ames, G. Ferro-Luzzi (1990). Energetics of Periplasmic Transport Systems. In: "The Bacteria. A Treatise on Structure and Function". Krulwich, T. A. (ed., Volume 11, p225-246, Academic Press, New York.

Archibald, A. R., Baddiley, J. and N. L. Blumsom (1968). *Advan. Enzymol.*, 30, 223-253.

Arhibald, A. R., Baddiley, J. and Buchanan, J. G. (1961). *Biochem. J.*, **81**, 124-134.

Archibald, A. R. Baddiley, J. and Button, D. (1965). *Biochem. J.*, **95**, 8c-11c.

Archibald, A. R., Baddiley, J. and Shakat, G. A. (1968). *Biochem. J.*, 110, 583-588.

Archibald, A. R., Hancock, I. C. and Horwood, C. R. (1993). Cell Structure Synthesis and Turnover, 381-410. In: "*Bacillus subtilis* and Other Gram-Positive Bacteria". Sonenshein, A. L., Hoch, J. A. and Losick, R. (eds.), American Society for Microbiology, Washington D.C.

Armstrong, J. J., Baddiley, J. and Buchanan, J. G. (1960). *Biochem. J.*, 76, 610-621.

Asai, T., Aid, K. and Oishi (1957). *Bull. Agr. Chem. Soc. Japan*, **21**, 134-149.

Atkinson, M. R. and Fisher, S. H. (1991). *J. Bacteriol.*, **173**, 1, 23-27.

Baddiley, J. (1968). *Proc. Roy. Soc. B.V.* 1170, 331-348.

Baddiley, J., Buchanan, J. G., Rajbhandasy, U. L. and Sanderson, A. R. (1962). *Biochem. J.*, **82**, 437-449.

Barros, M. E. C., Rawlings, D. E. and Woods, D. R. (1986). *J. Gen. Microbiol.*, **132**, 1989-1995.

Banks, W. H., Righellato, E. C. and Davies, C. W. (1931) *Trans. Faraday. Soc.* **27**, 621-627.

Bender, R. A., Macaluso, R. and Magasanik, B. (1976). *J. Bacteriol.*, **127**, 141-148.

Burger, M. M. and Glaser, L. (1964) *J. Biol. Chem.*, **239**, (10), 3168-3177.

Black, S. and Wright, N. G. (1955). *J. Biol. Chem.*, **213**, 27-38.

Blender, R. A., Jannsen, K. A., Resnick, A. D., Blumenburg, M., Foor, F. and Magasanik, B. (1977). *J. Bacteriol.*, **129**, (2), 1001-1009.

Boyd, R. (1984) (ed). In: "General Microbiology". Times Mirror, Mosby, College Publishing, St Louis, USA.

Bazouklian, H. and Elmerich, C. (1986). *Biochemie*, **68**, 1181-1189.

Brenchley, J. E., Baker, C. A. and Patil, L. G. (1975). *J. Bacteriol.*, **128**, 182-189.

Brill, W. J. (1975). *Ann. Rev. Microbiol.*, **29**, 100-109.

Brown, C. M. (1976) Nitrogen metabolism in bacteria and fungi. In: "*Int. Sym. Contin. Cult. Micro-org.*". Dean, A. C. R., Ellwood, D. C., and Evans, C. G. T. (eds.), 6th, Ellis Harwood, Chester, England.

Brown, C. M., Macdonald-Brown, D. S. and Stanby, S. O. (1973). *Antoine van Leeuwenhoek*, **39**, 89-93.

Castoph, H. and Kleiner, D. (1984). *Arch. Microbiol.*, **139**, 245-247.

Cohen, G. N. (1969). The aspartokinases and homoserine dehydrogenases of *Escherichia coli*, p183-231. In: "Current Topics in Cellular Regulation". Horecker, B. L. and Stadtman, E. L. (eds.), Vol. 1, Academic Press Inc., New York.

Cranston, J. A. and Brown, H. F. (1937). *Trans Faraday Soc.*, **33**, 1455-1458.

Cross, R. J. (1993). Personal communication.

Dawson, R. M. C., Elloitt, D., Elloitt, W. H., and K.M. Jones, (eds.). (1969). "In: Data for Biochemical Research". Oxford University Press, Oxford.

Denton, M. D. and Ginsburg, A. (1970). *Biochemistry*, **9**, 617-632.

Dean, D. R., Hoch, J. A. and Aronson, A. (1977). *J. Bacteriol.*, **131**, 981-987.

Deuel, T. F., Ginsberg, A., Yak, J., Shelton, E. and Stadtman, E. (1970). *J. Biol. Chem.*, **245**, 5195-5205.

Dionex Corporation (1992). Document No.034656.

Ellwood, D. C. and Tempest, D. W. (1967). *Biochem. J.* **104**, 69p.

Ellwood, D. C., Keleman, M. V. and Baddiley, J. (1963). *Biochem. J.*, **86**, 213-225.

Ertan, H. (1992). *Arch. Microbiol.* **158**, 35-41.

Evangelista, A. T., Saha, A., Lechevaher, M. P. and Furness, G. (1978). *Int. J. Syst. Bact.*, **28**, No.3, 344-348.

Fisher, S. H. and Sonenshein, A. L. (1984). *J. Bacteriol.*, **157**, 612-621.

Fisher, S. H. and Sonenshein, A. L. (1991). *Ann. Rev. Microbiol.*, **45**, 107-135.

Fisher, S. H. and Wray, L. V. (1989). *J. Bacteriol.*, **171**, (5), 2378-2383.

Fumanage, V. L., Ayling, P. D., Dendinger, S. M. and Brenchley, J. E. (1978). *J. Bacteriol.*, **136**, (2), 588-596.

Gaillardin, C. M. and Magasanik, B. (1978). *J. Bacteriol.*, **133**, 1329-1388.

Ghuysens, J. M. and Stominger, J. F. (1963). *Biochemistry*, **2**, 1110-1115.

Gilvarg, G. (1963). *143rd Mtg. Am. Chem. Soc. Abstracts.* **46A**, 46-52.

Glaser, L. (1964). *J. Biol. Chem.*, **239**, (1), 3178-3186.

Glasstone, S. and D. Lewis, (eds.). (1978). In: "Elements of Physical Chemistry". The Macmillan Press Ltd, London.

Henderson, P. J. F. (1971). *Ann. Rev. Microbiol.*, **25**, 393-428.

Hulley, S. B., Joergensen, S. B., and Lin, E. C. C. (1963). *Biochim. Biophys. Acta.*, **67**, 219-224.

Ishino, S., Yamaguchi, K., Shirahata, K. and Araki, K. (1984). *Agric. Biol. Chem.*, **48**, (10), 2557-2560.

Jayakumar, A., Epstein, W., and E. M. Barnes (1985). *J. Biol. Chem.*, 260, 7528-7532.

Jayakumar, A., Schulman, I., MacNeil, D. and Barnes, E. M. (1986). *J. Bacteriol.*, **160**, (1), 281-284.

Kashyap, A. K. and Johar, G. (1984). *Mol. Gen. Genet.*, 197, 509-512.

Kato, I. T., Strominger, J. L. and Kotani, S. (1968). *Biochemistry*, **7**, (8), 2762-2773.

Keddie, R. M. and Cure, G. L. (1977). *J. Appl. Bact.*, **42**, 229-252.

202/...

Khanna, S. and Nicholas, D. J. D. (1983). *Arch. Microbiol.*, **134**, 98-103.

Kinoshita, S., Nakayama, K. and Kitada, S. (1958). *J. Gen. Appl. Microbiol.*, **4**, 128-129.

Kinoshita, S., Udaka and Shimono, M. (1957). *J. Gen. Appl. Microbiol.*, **3**, 193-197.

Kleiner, D. (1985). *FEMS Microbiol. Revs.*, **32**, 87-100.

Kleiner, D. (1981). *Biochim. Biophys. Acta*, **639**, 41-52.

Kleiner, D. (1985). *FEMS Micro. Rev.*, **32**, 87-100.

Kubota, K., Tasaka, O., Yoshihara, Y. and Hirose, Y. (1976). Japan Patent 51-19186.

Kutsu, S. G., McFarland, N. C., Hui, S. P., Esmon, B and Ames, G. F. (1979). *J. Bacteriol.*, **138**, (1), 218-234.

Lehninger, A. L. (1977). In: "Biochemistry". Worth Publishers Inc., New York.

Lowry, O. H., Rosebrough, N. J., Farr A. C. and Randall. (1951) *J. Biol. Chem.*, **193**, 265-275.

Magasanik, B. (1982). *Ann. Rev. Genet.*, **16**, 135-168.

Magasanik, B. and F. C. Neidhardt (1987). In: "*Escherichia coli* and *Salmonella typhimurium*". Cellular and Molecular Biology. American Society for Microbiology, Washington DC.

Maloy, S. R. (1990). Sodium-Coupled Cotransport. In: "The Bacteria. A Treatise on Structure and Function". Krulwich, T. A. (ed.), Volume XII, 203-224, Academic Press, New York.

McFarland, N., McCarter, L. Artz, S. and Kurtu, S. (1981). *Proc. Natl. Acad. Sci. USA*, **78**, (4), 2135-2139.

Merck Index (1978).

203/...

Miller, E. R. and Stadtman, E. R. (1972). *J. Biol. Chem.*, **251**, 3300-3305.

Misono, H. and Soda, K. (1980). *J. Biol. Chem.*, **255**, (22), 10599-10605.

Ottaway, J. H. (1988). In: "Regulation of Enzyme Activity". Information Printing Limited, Oxford, England.

Reitzer, L. J. and B. Magasanik (1987). In: "*Escherichia coli* and *Salmonella typhimurium*". Cellular and Molecular Biology. American Society for Microbiology, Washington DC.

Righellato, E. C. and Davies, C. W. (1930). *Trans. Faraday Soc.*, **26**, 592-600.

Robinson, R. A. and R. H. Stokes (eds.). (1970). In: "Electrolyte solutions". Butterworth and Co. Ltd., London.

Rogers, H. J. and Garret, J. A. (1963). *Biochem. J.*, **88**, 6p.

Sakamoto, N., Kotre, A. M. and Savageau, M. A. (1975). *J. Bacteriol.*, **124**, (2), 775-783.

Sano, K. and Shiio, I. (1970). *J. Gen. Appl. Microbiol.*, **16**, 373-391.

Saukkonen, J. J. (1961). *Nature*, **192**, 816.

Schleifer, K. H. and Kandler, O. (1972). *Bacteriology Reviews*, **36**, (4), 407-477.

Schreier, H. J., Brown, S. W., Hirshci, K. D., Nomellini, J. F. and Sonenshein, A. L. (1989). *J. Mol. Biol.*, **210**, 57-63.

Schreier, H. J. (1993). In: "*Bacillus subtilis* and Other Gram Positive Bacteria". Sonenheim, A. L., Hoch, J. A. and R. Losick (eds.), American Society for Microbiology, Washington.

Segal, A., Brown, M. S. and Stadtman, E. R. (1975). *J. Biol. Chem.*, **250**, 6264-6272.

204/...

Senior, P. J. (1975). *J. Bacteriol.*, **123**, (2), 407-418.

Shapiro, B. M. and Stadtman, E. R. (1970). *Methods in Enzymology*, **17A**, 917-922.

Shaw, D. R. D. (1962). *Biochem. J.*, **104**, 297-311.

Shaw, J. F., Funkhauser, J. D., Smith, V. A. and Smith, W. G. (1983). *J. Inorg. Biochem.*, **18**, 49-58.

Shiio, I., Otasaka, S. I. and Tahahashi, M. (1962). *J. Biochem.* **51**, 56-62.

Shiio, I. and Ozaki, H. (1970). *J. Biochem.*, **68**, 633-647.

Shiio, I. and Sano, K. (1969). *J. Gen. Appl. Microbiol.*, **15**, 267-287.

Sonenshein A. L., Hoch, J. A.and Losick, R. (eds.). (1993). In: "*Bacillus subtilis* and other Gram-positive Bacteria. American Society for Microbiology, Washington.

Stanier, R. T., Adelberg, E. A. and Ingraham, J. L. (1976). *J. General Microbiology*. Prentice Hall Inc., Englewood Cliffs, New Jersey, USA.

Stephanopoulos, G. and Vallino, J. J. (1991). *Science*, **252**, 1675-1681.

Stevenson, R. and Silver, S. (1977). *Biochem. Biophys. Res. Commun.*, **52**, 1133-1139.

Stranch, M. A., Aronson, A. I., Brown, S. W., Schreier, H. J. and Sonenshein, A. L. (1988). *Gene*, **71**, 257-265.

Strominger, J. L. and R. H. Threnu (1958). *Biochim. Biophys. Acta*, **33**, 280-295.

Tosaka, O., Enei, H. and Y. Hirose (1983). *Trends in Biotechnology*, **1**, (3), 70-74.

Tosaka, O., Morioka, H. and K. Takinami (1981). U.S. Patent 4275157.

205/...

Tosaka, O., Takinami, K. and Y. Hirosa (1978). *Agric. Biol. Chem.*, **42**, (4) 745-752.

Tosaka, O. and K. Takinami (1978). *Agric. Biol. Chem.*, **42**, 95-103.

Tosaka, O. and K. Takinami (1986). In: "Biotechnology of Amino Acid Production". Aida, K., Chibata, I., Nakayama, K., Takinami, K. and H. Yamada (eds). Progress in Industrial Microbiology, 24, Kadansha Ltd, Tokyo.

Tyler, B. (1978). *Ann. Rev. Biochem.* **47**, 1127-1162.

Usdin, K. P., Zappe, H., Jones, D. T. and D. R. Woods (1986). *Appl. Environ. Microbiol.*, **52**, 413-419.

Véckey, K. and L. F. Zerilli (1991). *Organic Mass Spectrometry*, **26**, 939-944.

Waters Associates Technical Bulletin (1984). Sept/Oct.

Watson, T. (1989). CSIR Summary Report.

Woese, C. R. (1987). *Microbiol. Rev.*, **51**, 221-271.

Wray, L. V. and Fisher, S. H. (1988). *Gene*, 71, 247-256.

Yamada, K. and K. Komagata (1970). *J. Gen. Appl. Microbiol.*, **16**, 103-113.

APPENDIX I

LYSINE CULTURE MAINTENANCE MEDIA

Tryptone	10,0g
Yeast extract	10,0g
NaCl	5,0g
Distilled water	1 000ml
pH	7,0

Agar is added to a concentration of 2,5% m/v when solid media is required.

FERMENTATION MEDIA (TNIY)

Glucose monohydrate	110,0
$(NH_4)_2SO_4$	40,0g
KH_2PO_4	1,0g
$MgSO_4.7H_2O$	0,4g
$FeSO_4.7H_2O$	10,0mg
$MnSO_4.4H_2O$	8,13mg
Thiamine.HCl	200μg
Biotin	200μg
Yeast extract	10,0g
Distilled water	1 000ml
pH (adjusted with NH_4OH)	7,2

The inoculum for fermentation was prepared in 1,0 litre Erlenmeyer flasks at a volume of 200ml. The required number were then pooled to give an inoculum size of 10% of the final fermentation volume. This media was buffered by the addition of 5,0g/l of $CaCO_3$. The inoculum was grown for 18 hours unless otherwise specified.

HIGH TEST MOLASSES FERMENTATION MEDIA

Fermentation culture media using yeast extract and high test molasses for a final sugar concentration of 200g/l:

INITIAL CHARGE	FINAL VOLUME 10 LITRES 40g/l $(NH_4)_2SO_4$	FINAL VOLUME 16 LITRES 30g/l $(NH_4)_2SO_4$
[a]High test molasses (HTM)	718,75	1519g
$MgSO_4.7H_2O$	4,0g	6,4g
$(NH_4)_2SO_4$	300	480g
Yeast extract	57,5	92g
KH_2PO_4	10g	16g
$FeSO_4.7H_2O$	75mg	120mg
$MnSO_4.4H_2O$	45,33mg	75,53mg
Thiamine	1,5mg	2,4mg
Biotin	1,5mg	2,4mg
Antifoam	5,75ml	9,2ml
Water to	5,75 litres	12,0 litres
pH	7,2	7,2

a The concentration of HTM used is determined by the concentration found in each batch.

The HTM is made up to 2,0 litres ((1,5 litres) separately and autoclaved, and the remaining ingredients in 7,2 litres (4,25 litres) are prepared in the fermenter for sterilization.

FIRST FEED		
Yeast extract	146,5	234,4g
Antifoam	1,0ml	1,0ml
Water to	500ml	800ml
pH		
SECOND FEED		
High test molasses	1781,3g	2 850g
$(NH_4)_2SO_4$	100g	-
Antifoam	10ml	25ml
Biotin	700µg	1,0mg
Water to	2,75 litres	4 000
Overall sugar concentration @ 75% m/v sugars in HTM	187,5g/l	192,75g/l

The first feed was started four hours after inoculation and run for 16 hours. At this stage the second feed was started and run for 36 hours.

APPENDIX II

HIGH PERFORMANCE LIQUID CHROMATOGRAPHY ANALYSIS OF L-LYSINE

The basic technique involves the precolumn derivatization of the primary amino acids with o-phthaldehyde (OPA) followed by their determination using reversed phase high performance liquid chromatography with an ultra-violet light detector at a wavelength of 340nm. The amino acids were separated on a Nova-Pak C18 column.

APPARATUS

The equipment used was a Waters Auto-Tag system which consisted of the following units

Gradient pump Model 6000A
Autosampler Model Wisp 710B
Data module Model Maxima 820
Gradient control module Model 680
UV/VIS detector (variable wavelength) Model 450
Column: Nova=Pak C18: 3.9mm x 150 mm id + precolumn
Column heater/temperature control module

REAGENTS

Except where stated all reagents used are analytical reagent grade

A solution of 0,06M KH_2PO_4 and 0,06M K_2HPO_4 is prepared and the pH adjusted to 6,65 with phosphoric acid. This is known as solution A. A second solution (solution B) is prepared containing 182ml acetonitrile, 182ml methanol 182ml isopropanol and 454ml solution A. The mobile phase is then prepared by mixing 800ml solution B and 200ml solution A. The flow rate used for the mobile phase was 1,5 ml/minute.

SAMPLE PREPARATION

The protein in the samples was precipitated by the addition of 5% ethanol and removed by centrifugation. The samples were then suitably diluted in nano-pure water.

HIGH PERFORMANCE LIQUID CHROMATOGRAPHY ANALYSIS OF GLUCOSE

Pump Model 6000A

Autosampler Model Wisp 710B

Data module Model Maxima 820

Detector Dionex Pulsed Amperometric Detector

Column CarboPak PA1

REAGENTS

The mobile phase used is a 150mM solution of NaOH.

SAMPLE PREPARATION

The samples are suitably diluted with nano-pure water and filtered through 0,4 micron filters.

APPENDIX III

EFFECT OF THE TEMPERATURE ON THE LIMITING CONDUCTIVITIES IN WATER

	H	NH4	SO4	Cl
0	225	40.2	41	41
5	250.1			47.5
15	300.6			61.4
18	315	63.9	68.4	66
25	349.8	73.5	80	76.35
35	397	88.7		92.2
45	441.1			108.9

H ION

Regression Output:

Constant		226.9566
Std Err of Y Est		2.144768
R Squared(Adj,Raw)	.9992243	.9993536
No. of Observations		7
Degrees of Freedom		5
Coefficient(s)	4.824500	
Std Err of Coef.	.0548731	

NH4 ION

Regression Output:

Constant		40.22060
Std Err of Y Est		.2463828
R Squared(Adj,Raw)	.9998532	.9999511
No. of Observations		4
Degrees of Freedom		1
Coefficient(s)	1.226150	.0044976
Std Err of Coef.	.0312466	.0008847

SO4 ION

Regression Output:

Constant		41.04646
Std Err of Y Est		.5557138
R Squared(Adj,Raw)	.9994914	.9998305
No. of Observations		4
Degrees of Freedom		1
Coefficient(s)	1.309852	.0106006
Std Err of Coef.	.0704763	.0019953

Cl ION

Regression Output:

Constant		39.66532
Std Err of Y Est		1.121364
R Squared(Adj,Raw)	.9978332	.9981943
No. of Observations		7
Degrees of Freedom		5
Coefficient(s)	1.508341	
Std Err of Coef.	.0286897	

Values calculated from regression data

	TEMP				
	20	21.7	25	28.8	30
HION	323.4466	331.6483	347.5691	365.9022	371.6916
NH4	64.74361	66.82806	70.87436	75.53373	77.00511
SO4	67.24349	69.47024	73.79275	78.77018	80.34201
Cl	69.83214	72.39632	77.37385	83.10554	84.91555

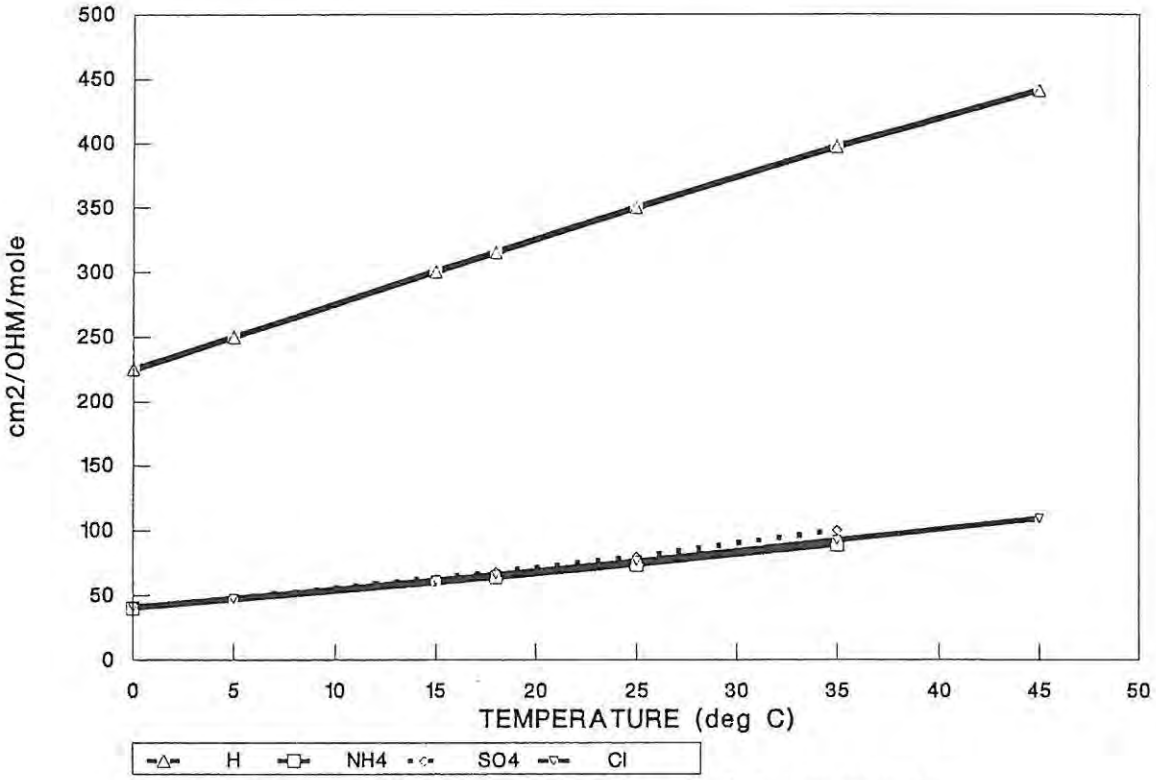

APPENDIX III. FIGURE 1. The effect of temperature on the limiting conductivities of various ions in water.

APPENDIX IV

NH_4Cl FERMENTATION MEDIA

CULTURE MEDIA CONSTITUENTS	FINAL COUNTER ION SALT CONCENTRATION (g/l)	
	9,457	14,91
INITIAL CHARGE		
CSL	266g	73,81
NH_4Cl	36,90g	
$MgSO_4.7H_2O$	4g	
HTM	737,1g	
KH_2PO_4	10g	
$FeSO_4.7H_2O$	75mg	
$MnSO_4.4H_2O$	45,33mg	
Thiamine	1,5µg	
Biotin	1,5µg	
Antifoam	1,0ml	
Water to	5 750ml	
pH	7,2	
FIRST FEED		
CSL	534g	
Antifoam	1,0ml	
Water to	500ml	
pH	7,2	
SECOND FEED		
HTM	1 827g	
Biotin	700µg	
Antifoam	3,0ml	
NH_4Cl	17,61g	35,30
Water to	2 750ml	
INOCULUM CONSTITUENTS		
CSL	25g	
NH_4Cl	6,418g	
$MgSO_4.7H_2O$	0,4g	
HTM	256,4g	
KH_2PO_4	10g	
$FeSO_4.7H_2O$	10mg	
$MnSO_4.4H_2O$	8,1mg	
Thiamine	200µg	
Biotin	200µg	
Antifoam	1,0ml	
Water to	1 000ml	
pH	7,2	

APPENDIX IV

$(NH_4)_2HPO_4$ FERMENTATION MEDIA

CULTURE MEDIA CONSTITUENTS	FINAL COUNTER ION SALT CONCENTRATION (g/l)					
INITIAL CHARGE						
CSL $(NH_4)2HPO_4$ $MgSO_4.7H_2O$ HTM KH_2PO_4 $FeSO_4.7H_2O$ $MnSO_4.4H_2O$ Thiamine Biotin Antifoam Water to pH	266g 0,00g 4g 737,1g 10g 75mg 45,33m 1,5µg 1,5µg 1,0ml 5 750ml 7,2	90,0g	104,0g	141,0g	141,0g	141,0g
FIRST FEED						
CSL Antifoam Water to pH	534g 1,0ml 500ml 7,2					
SECOND FEED						
HTM Biotin Antifoam $(NH_4)2HPO_4$ Water to pH	1 827g 700µg 3,0ml 0,00g 2 750ml 7,2	40,27g	50,60g	64,0g	98,0g	240,00g
INOCULUM CONSTITUENTS						
CSL $(NH_4)2HPO_4$ $MgSO_4.7H_2O$ HTM KH_2PO_4 $FeSO_4.7H_2O$ $MnSO_4.4H_2O$ Thiamine Biotin Antifoam Water to pH	25g 16g 0,4g 256,4g 10g 10mg 8,1mg 200µg 200µg 1,0ml 1 000ml 7,2					

APPENDIX V

YEAST EXTRACT FERMENTATION MEDIA

The following culture media was used to determine the effect of the yeast extract concentration and the initial glucose feed rate on lysine synthesis. The yeast extract concentrations used were 25g/l, 35g/l, 45g/l and 55 g/l. The feed rates used are as outlined in the text.

INITIAL CHARGE	
Yeast extract	varied
$MgSO_4.7H_2O$	3,6g
$(NH_4)_2SO_4$	360g
KH_2PO_4	10,9g
$FeSO_4.7H_2O$	67,5mg
$MnSO_4.4H_2O$	30,9mg
Thiamine	1,35mg
Biotin	1,35mg
Antifoam	5,4ml
Water to	4,5 litres
pH	7,2
GLUCOSE FEED	
Glucose monohydrate	2 890,8g
Biotin	630μg
Antifoam	45ml
Water to	3,6 litres

APPENDIX VI

FERMENTATION CULTURE MEDIA FOR THE 1 800 LITRE PILOT PLANT

INITIAL CHARGE	
Glucose monohydrate	126,5kg
$MgSO_4.7H_2O$	0,8kg
$(NH_4)SO_4$	80kg
Yeast extract	7kg
KH_2PO_4	2,0kg
$FeSO_4.7H_2O$	15g
$MnSO_4.4H_2O$	12g
Thiamine	0,3g
Biotin	0,3g
Antifoam	1 150ml
Water to	1 150 litres
FIRST FEED	
Yeast extract	33kg
Antifoam	100ml
Water to	100 litres
SECOND FEED	
Glucose monohydrate	291,5kg
Biotin	149mg
Antifoam	550ml
Water to	550 litres

The first feed was started 3 hours after inoculation and run for 23 hours.
The second feed was started 26 hours after inoculation and run for 30 hours.

APPENDIX VII

YEAST EXTRACT FERMENTATION MEDIA

The following culture media was used to determine the effect of varying the free NH_4^+ concentration on the lysine synthesis. The feed rates used are as outlined in the text.

Initial charge	
Yeast extract	55,0g
$MgSO_4.7H_2O$	3,6g
$(NH_4)_2SO_4$	360g
KH_2PO_4	10,9g
$FeSO_4.7H_2O$	67,5mg
$MnSO_4.4H_2O$	30,9mg
Thiamine	1,35mg
Biotin	1,35mg
Antifoam	5,4ml
Water to	4,5l
pH	7,2
Glucose feed	
Glucose monohydrate	2 890,8g
Biotin	630µl
Antifoam	45ml
Water to	3,6l

The pH of the fermentations was controlled using either one of the following ammonia solutions:

FIRST BASE	
NH_4OH (32%)	530ml
Distilled H_2O	800ml
SECOND BASE	
NH_4OH	544ml
$(NH_4)_2SO_4$	595g
Distilled water	1 600ml

At the end of the growth phase the first base was used. The time which was allowed between the use of the first and the second base was varied.

APPENDIX VIII

mmoles (NH4)SO4	FRACTION BIVALENT ION ASSOCIATED	mmoles FREE NH4
.757	.734	1.400
7.568	.245	13.276
15.135	.257	26.374
30.271	.305	51.304
60.542	.346	100.082
121.084	.368	197.537
242.167	.561	348.567
484.335	.746	607.265

FREE NH4 vs (NH4)2SO4

Regression Output:

Constant		2.537
Std Err of Y Est		4.532
R Squared(Adj,Raw)	.9995671	1.000
No. of Observations		7.000
Degrees of Freedom		4.000
Degrees of Freedom		
Coefficient(s)	1.653727	-.001
Std Err of Coef.	.0415027	.000

mmoles NH4Cl	FRACTION DISSOCIATED NH4Cl	mmoles FREE NH4
.935	.887	.829
1.869	.907	1.696
18.69	.861	16.097
37.383	.845	31.581
74.766	.826	61.646
149.533	.783	117.057
299.065	.717	214.324
598.131	.730	436.632
1196.262	.695	831.887

FREE NH4 vs NH4Cl

Regression Output:

Constant		2.209
Std Err of Y Est		4.235
R Squared(Adj,Raw)	.9997693	1.000
No. of Observations		9.000
Degrees of Freedom		6.000
Coefficient(s)	.7486462	.000
Std Err of Coef.	.0137510	.000

mmoles (NH4)2HPO4	FRACTION BIVALENT ION ASSOCIATED	mmoles FREE NH4
.7567	.000	1.700
7.567	.095	14.410
15.135	.233	26.740
30.27	.398	48.500
60.54	.569	86.650
121.084	.739	152.660
242.167	.923	260.930
484.335	1.130	421.320

FREE NH4 vs (NH4)2HPO4

Regression Output:

Constant		6.783
Std Err of Y Est		4.861
R Squared(Adj,Raw)	.9989076	.999
No. of Observations		8.000
Degrees of Freedom		5.000
Coefficient(s)	1.288573	-.001
Std Err of Coef.	.0410786	.000

APPENDIX IX

MINIMAL MEDIA

SOLUTION A	
$(NH_4)_2SO_4$	5g
Urea	5g
KH_2PO_4	0,5g
K_2HPO_4	0,5g
MOPS	21g
$MgSO_4.7H_2O$	0,25g
$CaCl_2.H_2O$	10mg
$MnSO_4.7H_2O$	10mg
$FeSO_4.7H_2O$	10mg
$ZnSO_4$	2mg
$CuSO_4$	0,2mg
Dist. H_2O to	900ml
SOLUTION B	
Biotin	0,4mg
Glucose	40g
Dist. H_2O to	100ml

Solution A was heat sterilized at 121°C and 100kpa pressure for 20 minutes. Solution B was filter sterilized and aseptically added to solution A. The amino acids threonine, methionine and leucine were added at concentrations of 150mg/l, 500mg/l and 150mg/l, respectively. When required the $(NH_4)_2SO_4$ and glutamate were both added at a concentration of 10mM, and the urea removed from the broth.